Mitochondria and microRNAs in obesity and after weight loss

Stella Panagio Breininger

Submission for the degree of Doctor of Philosophy

September 2019

Human Nutrition research Centre

Institute of Cellular Medicine

Wellcome Trust Centre for Mitochondrial Research

LLHW Centre for Ageing and Vitality

Fibrosis Research Group

Newcastle University, UK

Abstract

Colorectal cancer (CRC) is the 3rd most common cancer worldwide. CRC is initiated in colonocytes and, with advancing age, colonocytes accumulate mitochondrial mutations which contribute to age-related dysfunction and to increased cancer risk. Obesity, and its lifestyle determinants, physical inactivity and poor diet, also increase CRC risk. However, the effects of weight loss by bariatric surgery on mitochondrial defects in human colonoctyes and on CRC risk are unclear. Epigenetic mechanisms involving microRNAs that lead to dysregulated gene expression may mediate the effects of obesity and weight loss on CRC risk.

I hypothesised that mitochondrial defects and microRNAs are i) elevated and aberrantly expressed in obese individuals compared with healthy non-obese individuals and ii) reduced and modulated by significant weight loss following bariatric surgery, respectively.

Colorectal mucosal biopsies of obese patients listed for bariatric surgery were collected at baseline and six months post-surgery and at baseline only from non-obese Controls. Mitochondrial oxidative phosphorylation proteins complex I and IV and mitochondrial mass were quantified by immunofluorescence. Using Next Generation Sequencing and bioinformatics i) mitochondrial DNA was sequenced and ii) a panel of 8 microRNAs was selected and validated by quantitative PCR in colorectal mucosal biopsies.

Greater adiposity and advancing age resulted in significantly more complex I and IV deficient crypts in the human colorectal mucosa but, at least after 6 months, weight loss following bariatric surgery had no significant effect on these mitochondrial defects. Neither excess adiposity nor significant weight loss resulted in differences in mtDNA mutations between the study groups. Expression of miR-31, miR-215, miR-3196 and miR-4516 was significantly higher in obese than in non-obese individuals. Weight loss reduced expression of miR-31, miR-215 and miR-3196 significantly to expression levels that were comparable with those in Controls. These differentially expressed microRNAs are implicated in pathways linked with inflammation, obesity and cancer.

This research enables the broadening of our knowledge on the mechanistic pathways of obesity related CRC risk and provides novel evidence on the effects of intentional weight loss by bariatric surgery on these biomarkers in the colon.

Dedications

This thesis is dedicated to the most important people in my life.

My Parents, my sister and my son.

And my best friend who feels like family:

Ariadne Tatalia-Aloupi.

Acknowledgements

Table of Contents

Contents

List of Figures

List of Tables

Abbreviation

A	Adenine
A>P	Alanine to Proline
A>T	Alanine to Threonine
A>V	Alanine to Valine
AA	Amino Acid
ADP	Adenosine Diphosphate
Ago	Argonaute
ANCOVA	Analysis of Covariance
ANOVA	Analysis of Variance
APC	Adenomatous Polyposis Coli
ASH1L	ASH1 Like Histone Lysine Methyltransferase
ATF7	Activating Transcription Factor 7
ATP	Adenosine Triphosphate
BAX	BCL2 Associated X
BclxL	B-cell lymphoma-extra large
BFU	BORICC Follow-Up
BMI	Body Mass Index
BMP	Bone Morphogenetic Proteins
BMPR1A	Bone Morphogenetic Protein Receptor Type 1A
BOCABS	Biomarkers Of Colorectal Cancer After Bariatric Surgery
BORICC	Biomarkers Of RIsk of Colorectal Cancer
bp	Base Pair
BRAF	B-Raf
BS	Bariatric Surgery
C	Cytosine
C/EBPα	CCAAT-enhancer-binding protein alpha
C>R	Cysteine to Arginine
C12orf55	Chromosome 12 Open Reading Frame 55
cAMP	cyclic Adenosine Monophosphate
CCND2	Cyclin D2

CDC25A	Cell Division Cycle 25A
cDNA	complementary DNA
ceRNAs	competing endogenous RNAs
CIMP	CpG Island Methylator Phenotype
CIN	Chromosomal Instability
CK20	Cytokeratin 20
COX1	Cyclooxygenase 1
COX-2	Cyclooxygenase-2
CRC	Colorectal Cancer
CRP	C-reactive Protein
Ct	Cycle threshold
CTTNBP2NL	CTTNBP2 N-Terminal Like
CYTB	Cytochrome b
D>G	Aspartic acid to Glycine
D>N	Aspartic acid to Asparagine
D>Y	Aspartic acid to Tyrosine
DANCR	Differentiation Antagonizing Nonprotein Coding RNA
DISC	Dietary Intervention Stem cells and Colorectal cancer
DKK1	Dickkopf WNT signaling pathway inhibitor 1
DNA	Deoxyribonucleic Acid
E>K	Glutamic acid to Lysine
EMT	Epithelial to Mesenchymal Transition
eNOS	Endothelial Nitric Oxide Synthase
F>L	Phenylalanine to Leucine
F>S	Phenylalanine to Serine
FABP4	Fatty Acid Binding Protein 4
FFPE	Formalin Fixed and Paraffin Embedded
FOS	Fos Proto-Oncogene
FTX	Five Prime to Xist
G	Guanine
G>A	Glycine to Alanine
G>D	Glycine to Aspartic acid

G>E	Glycine to Glutamic acid
G>S	Glycine to Serine
G>V	Glycine to Valine
G>W	Glycine to Tryptophan
G0s2	G0/G1 Switch 2
G6PD	Glucose 6 Phosphate Dehydrogenase
gDNA	human genomic control DNA
GLUT	Glucose Transporters
GSK3β	Glycogen Synthase Kinase 3 beta
GTP	Guanosine Triphosphate
H	Hip
H>N	Histidine to Asparagine
H>R	Histidine to Arginine
has	homo sapiens
HbA1c	Haemoglobin A1c
HECTD2	HECT Domain E3 Ubiquitin Protein Ligase 2
HGI	High Glycemic Index
HIC1	HIC ZBTB Transcriptional Repressor 1
HKG	House Keeping Genes
HSP27	Heat Shock Protein 27
I>M	Isoleucine to Methionine
I>T	Isoleucine to Threonine
I>V	Isoleucine to Valine
IDH1	Isocitrate Dehydrogenase 1
IGF-1	Insulin-like Growth Factor 1
IGLL5	Immunoglobulin Lambda Like Polypeptide 5
IL-1β	Interleukin 1 beta
IL-6	Interleukin 6
IL-8	Interleukin 8
iNOS	inducible Nitric Oxide Synthase
IRS-1	Insulin receptor substrate 1
JUN	Fos Proto-Oncogene

KEGG	Kyoto Encyclopedia of Genes and Genomes
KRAS	Kirsten-Ras
L>I	Leucine to Isoleucine
L>M	Leucine to Methionine
L>P	Leucine to Proline
LF	Low Fat
LGI	Low Glycemic Index
lncRNA	long non-coding RNA
LSINCT5	Long Stress-Induced Non-Coding Transcript 5
M>I	Methionine to Isoleucine
M>T	Methionine to Threonine
MAPK	Mitogen Activated Protein Kinase
MED7	Mediator Complex Subunit 7
Mfn2	Mitofusin 2
microRNAs	micro Riboxynucleic Acids
miRNAs	micro Riboxynucleic Acids
MMR	Mismatch Repair
mRNA	messenger RNA
MSI	Microsatellite Instability
MTATP6	Mitochondrially Encoded ATP Synthase Membrane Subunit 6
MTCOI	Cytochrome c oxidase subunit I
mtDNA	mitochondrial DNA
N>K	Asparagine to Lysine
N>S	Asparagine to Serine
N>Y	Asparagine to Tyrosine
NADH	Nicotinamide Adenine Dinucleotide Hydrogen
NCOA1	Nuclear Receptor Coactivator 1
ncRNA	non-coding RNA
ND5	NADH-ubiquinone Oxidoreductase Chain 5
nDNA	nuclear DNA
NDUFB8	NADH:Ubiquinone Oxidoreductase Subunit B8
NGS	Next Generation Sequencing

NRF1	Nuclear Respiratory Factor 1
NRF2	Nuclear Respiratory Factor 2
NTGH	North Tyneside General Hospital
oncomiRs	oncogenic miRNAs
OXA1L	Mitochondrial Inner Membrane Protein
OXPHOS	Oxidative phosphorylation
P>H	Proline to Histidine
P>L	Proline to Leucine
P>Q	Proline to Glutamine
P>S	Proline to Serine
P>T	Proline to Threonine
PANK4	Pantothenate Kinase 4
PARL	Presenilins Associated Rhomboid Like Protein
PCA	Principle Component Analysis
PCBP1	Poly(RC) Binding Protein 1
PCR	Polymerase Chain Reaction
PI3K/AKT	Phosphatidylinositol-3 kinase/Akt
piRNA	piwi RNA
PGC-1α	Proliferator Activated Receptor g Coactivator-1 alpha
PGC-1β	Proliferator Activated Receptor g Coactivator-1 beta
PPARγ2	Peroxisome Proliferator Activated Receptor Gamma 2
PPP3R1	Protein Phosphatase 3 Regulatory Subunit B alpha
PTPN6	Protein Tyrosine Phosphatase Non-Receptor Type 6
PTPN14	Protein Tyrosine Phosphatase Non-receptor Type 14
PUMA	p53 Upregulated Modulator of Apoptosis
Q>K	Glutamine to Lysine
qPCR	quantitative Polymerase Chain Reaction
R>H	Arginine to Histidine
R>L	Arginine to Leucine
R>Q	Arginine to Glutamine
RAB11FIP2	RAB11 Family Interacting Protein 2
RACGAP1	Rac GTPase-activating Protein 1

RIF1	Replication Timing Regulatory Factor 1
RISC	RNA-induced Silencing Complex
RNA	Ribonucleic Acid
RNU6	RNA small nuclear U6
ROS	Reactive Oxygen Species
rRNA	ribosomal Ribonucleic Acid
RYGB	Roux-en-Y Gastric Bypass
S>C	Serine to Cysteine
S>F	Serine to Phenylalanine
S>I	Serine to Isoleucine
S>N	Serine to Asparagine
S>Y	Serine to Tyrosine
SATB2	Special AT-rich Sequence-binding Protein 2
SD	Standard Deviation
SDH	Succinate Dehydrogenase
SF	Subcutaneous Fat
SHOC2	Leucine Rich Repeat Scaffold Protein
siRNA	short interfering RNA
SIRT1	Sirtuin 1
SMA	Smooth Muscle Actin
SMAD3	Mothers Against Decapentaplegic Homolog 3
SMAD4	Mothers Against Decapentaplegic Homolog 4
SNORD68	Small Nucleolar RNA, C/D Box 68
snoRNA	small nucleolar RNA
snRNA	small nuclear RNA
SP	Serrated Pathway
SPRY2	Sprouty Homolog 2
SRPX2	Sushi Repeat Containing Protein X-Linked 2
STAT3	Signal Transducer and Activator of Transcription 3
T	Thymine
T>A	Threonine to Alanine
T>I	Threonine to Isoleucine

T>M	Threonine to Methionine
TAE	Tris Acetate EDTA
TAG	Triacylglyceride
TBX15	T-Box Transcription Factor 15
TCA	Tricarboxylic Acid Cycle
TCF/ LEF	T-cell factor/lymphoid enhancer-binding factor
TCF4	Transcription factor 4
TFAM	Transcription Factor A Mitochondrial
TGFBR2	Type 2 Receptor for TGF-β
TGFBR2	Transforming Growth Factor beta Receptor 2
TGF-β1	Transforming Growth Factor-β 1
TIAM1	T-cell Lymphoma Invasion and Metastasis 1
TNF-α	Tumor Necrosis Factor alpha
TNM	Tumour Node Metastasis
TOMM20	Translocase Of Outer Mitochondrial Membrane 20
TP53	Tumor Protein p53
TRBP	Transactivate Response RNA Binding Protein
tRNA	Transfer Ribonucleic Acid
TSG	Tumour Suppressor Genes
UBE2G1	Ubiquitin Conjugating Enzyme E2 G1
UBE2J1	Ubiquitin-conjugating enzyme E2 J1
UICLM	Upregulated In CRC Liver Metastasis
V>A	Valine to Alanine
V>I	Valine to Isoleucine
V>L	Valine to Leucine
V>M	Valine to Methionine
VF	Visceral Fat
VST	Variance of Stabilising Transformation
W	Waist
W>L	Tryptophan to Leucine
W>R	Tryptophan to Arginine
WBC	White Blood Cells

WHO	World Health Organisation
WNT	Wingless-related Integration Site
Y>C	Tyrosine to Cysteine
ZEB2	Zinc Finger E-Box Binding Homeobox 2
ΔCt	delta Ct
18q LOH	18q Loss of Heterozygosity

1   Introduction

1.1   Colorectal cancer

1.1.1   Epidemiology

Colorectal cancer (CRC) is the 3rd most common cancer worldwide; in 2012 approximately 1.4 million cases were diagnosed (Ferlay et al., 2015) and it is estimated that CRC incidence will increase by 60% with over 2.2 million new cases predicted in 2030 (Arnold et al., 2016). There are wide geographical variations in CRC incidence, with more economically developed regions having a higher prevalence compared with less developed regions (Ferlay et al., 2015). Countries that go through sudden economic and societal changes demonstrate a fast rise in CRC, which is even more predominant in high income countries (Arnold et al., 2016). Studies of migrants from lower to higher risk countries reveal that migrants experience higher CRC risk within one generation, suggesting that this may be due to environmental and lifestyle factors (Kolonel et al., 1985, Flood et al., 2000, Maskarinec and Noh, 2004). Globally, CRC incidence is higher in men than in women and increases with age so that most CRC cases are aged ≥65 years (Douaiher et al., 2017).

1.1.2   Colorectal cancer development

Figure 1-1 shows the normal colonic epithelium including the colonic crypts (blue arrow), surface epithelium (yellow arrow), and goblet cells (red arrow). Most CRC develop sporadically and only 15-30% are due to hereditary factors (Mundade et al., 2014). CRC results from unrepaired genomic damage to stem cells and their progeny located in the crypts of the colorectal mucosa (see Figure 1-2) (Walther et al., 2009). Through a Darwinian process, damage that provides the nascent tumour cell with a competitive advantage results in the development of cell clones with excessive proliferation and, therefore, neoplastic potential and leads to monocryptal adenomas or aberrant crypt foci. Crypt fission may expand such lesions resulting in the appearance of non-malignant lesions known as adenomatous polyps (Humphries and Wright, 2008). With further genetic and epigenetic changes driving hyperplasia, some adenoma develop into malignant adenocarcinoma and, eventually, some metastasise (Mundade et al., 2014).
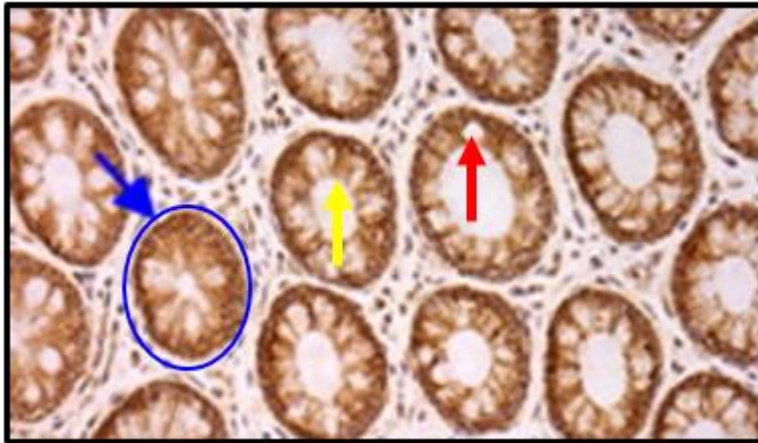
Figure 1-1: Transverse section of human colorectal mucosal biopsy showing normal colonic epithelium including the colonic crypts (blue arrow), surface epithelium (yellow arrow), and goblet cells (red arrow) (Adapted from Greaves et al., 2010) (Copyright: figure is open-access)

Both epigenetic modifications and gene mutations contribute to CRC development by activating oncogenes and oncogenic pathways and by inactivating tumour suppressor genes (TSG) (Fearon, 2011). This genomic damage includes chromosomal defects, mutations in the nuclear DNA (nDNA) and mitochondrial DNA (mtDNA) and epigenetic abnormalities that lead to aberrant gene expression and uncontrolled growth of colonocytes.

On the one hand, inactivating mutations in the tumour suppressor gene *APC* occur early in almost all CRC. Loss of *APC* function results in aberrant activation of the WNT signalling pathway which contributes to increased cell proliferation and polyp development (Lao and Grady, 2011). On the other hand, mutations in the proto-oncogenes *KRAS* or *BRAF* occur in 55-60% of CRC and KRAS signals through BRAF to activate the mitogen-activated protein kinase (MAPK) pathway, which regulates cell proliferation and apoptosis and can cause and progress CRC development (Lao and Grady, 2011); (Slattery et al., 2018). Further mutations in genes, such as in *KRAS* or *TP53,* regulating key pathways including the transforming growth factor-β (TGF-β1) signalling pathway, mediate the transformation from polyps to cancer (Vogelstein et al., 1988, Vazquez et al., 2008, William and Sanford, 2008). It has been found that approximately 30% of CRC comprise mutations in the gene encoding the type 2 receptor for TGF-β (TGFBR2) (Grady et al., 1998). More research has identified additional mutated TGF-β signalling pathway members including *TSP1, RUNX3, SMAD2* and *SMAD4* (Sjoblom et al., 2006, William and Sanford, 2008, Eppert et al., 1996, Takaku et al., 1998, Wood et al., 2007).
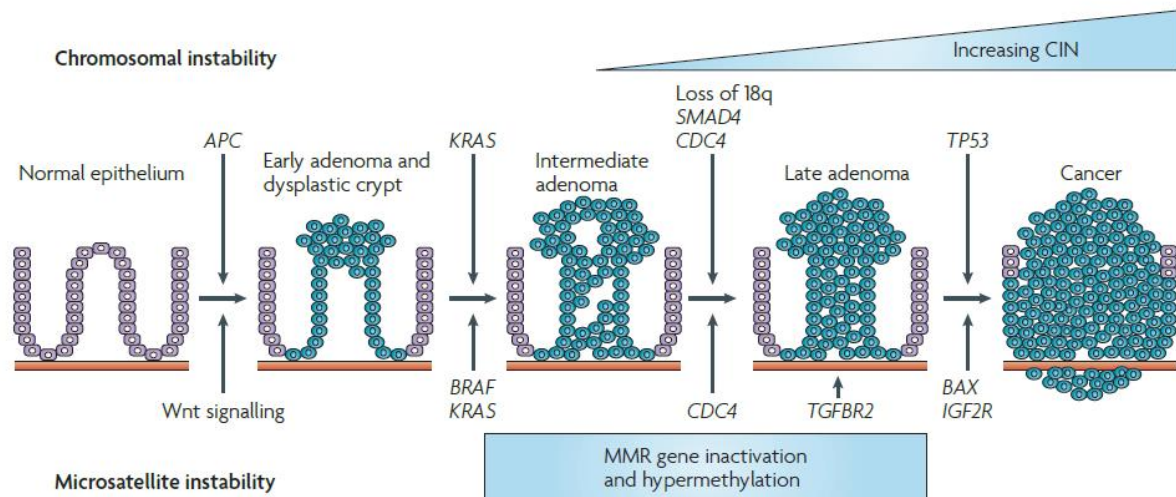
Figure 1-2: Colorectal cancer development (Walther et al., 2009) (Copyright: figure is open-access).

Three main molecular pathways for CRC development have been identified, namely the i) chromosomal instability (CIN), ii) microsatellite instability (MSI) and iii) serrated pathway (SP) (see Figure 1-3).

During the CIN pathway, proto-oncogenes such as *KRAS*, *c-SRC* and *c-MYC* are activated and TSG including *APC, TP53, SMAD4* and *18q LOH* are inactivated (Mundade et al., 2014). Inactivation of the APC gene or its promoter, i.e. by hypermethylation, activates the Wnt/ β-catenin signalling which results in adenoma development (Powell et al., 1992, Esteller et al., 2000). Mutations in the *APC* gene result in a failure to produce a functional APC protein. As a consequence, the absence of APC from the multi-protein complex (which includes axin and GSK3B) means that beta-catenin will not be phosphorylated and, therefore, not targeted for degradation. This leads to an accumulation of β-catenin in the cytoplasm that subsequently translocates into the nucleus, acting as a co-activator of TCF/ LEF transcription factors; this activates genes involved in cell growth and proliferation (Mann et al., 1999). Furthermore, activation of the *KRAS* gene plays a key role in apoptosis, cell division and differentiation through the MEK and ERK pathway (Pruitt and Der, 2001). *KRAS* mutations impair GTPase activity which leads to the accumulation of active KRAS in the GTP-bound conformation activating downstream pro-proliferative signalling and disrupting the RAS signalling pathway (Schubbert et al., 2007). Furthermore, a loss of *SMAD4* leads to tumourigenesis through the TGFβ pathway (Mundade et al., 2014). *TP53* (the guardian of the genome) senses DNA damage and initiates appropriate responses including cell cycle arrest (to allow DNA repair)

and apoptosis when damage is extensive. P53 mutation results in uninhibited cell growth (Vogelstein et al., 1988, Li et al., 2015).

MSI is a result of genetic hyper-mutation due to impaired DNA mismatch repair (MMR). This leads to the accumulation of insertions or deletions in microsatellites and, indeed, throughout the genome. When this unrepaired damage occurs in i) DNA coding regions for TSG and oncogenes, or ii) proteins including APC, TGFβRII and/ or BAX, it leads to CRC (Geiersbach and Samowitz, 2011). MMR genes are inactivated by i) epigenetic silencing due to hypermethylation of the promoter CpG of the *MLH1* gene and by ii) point mutations in MMR genes (Armaghany et al., 2012).

Mutations in proto-oncogene *BRAF* and epigenetic silencing of genes playing a role in cell cycle control, DNA repair and cell differentiation are observed in SP (Jass et al., 2002, Leggett and Whitehall, 2010). BRAF is involved in cell differentiation, division and secretion via the MAPK/ ERK signalling pathway (Rustgi, 2013). BRAF point mutations result in enhanced MAPK/ ERK signalling via impaired negative feedback mechanism (Rustgi, 2013). Subsequently this activates downstream effects such as uncontrolled cell proliferation, angiogenesis through HIF-1α, impaired immune response, vascular endothelial growth factor, tissue invasion, migration, metastasis and apoptosis resistance (Ascierto et al., 2012). Additionally, silencing of TSG, such as *p16* and *TP53*, via promoter hypermethylation has also been shown (Mundade et al., 2014).
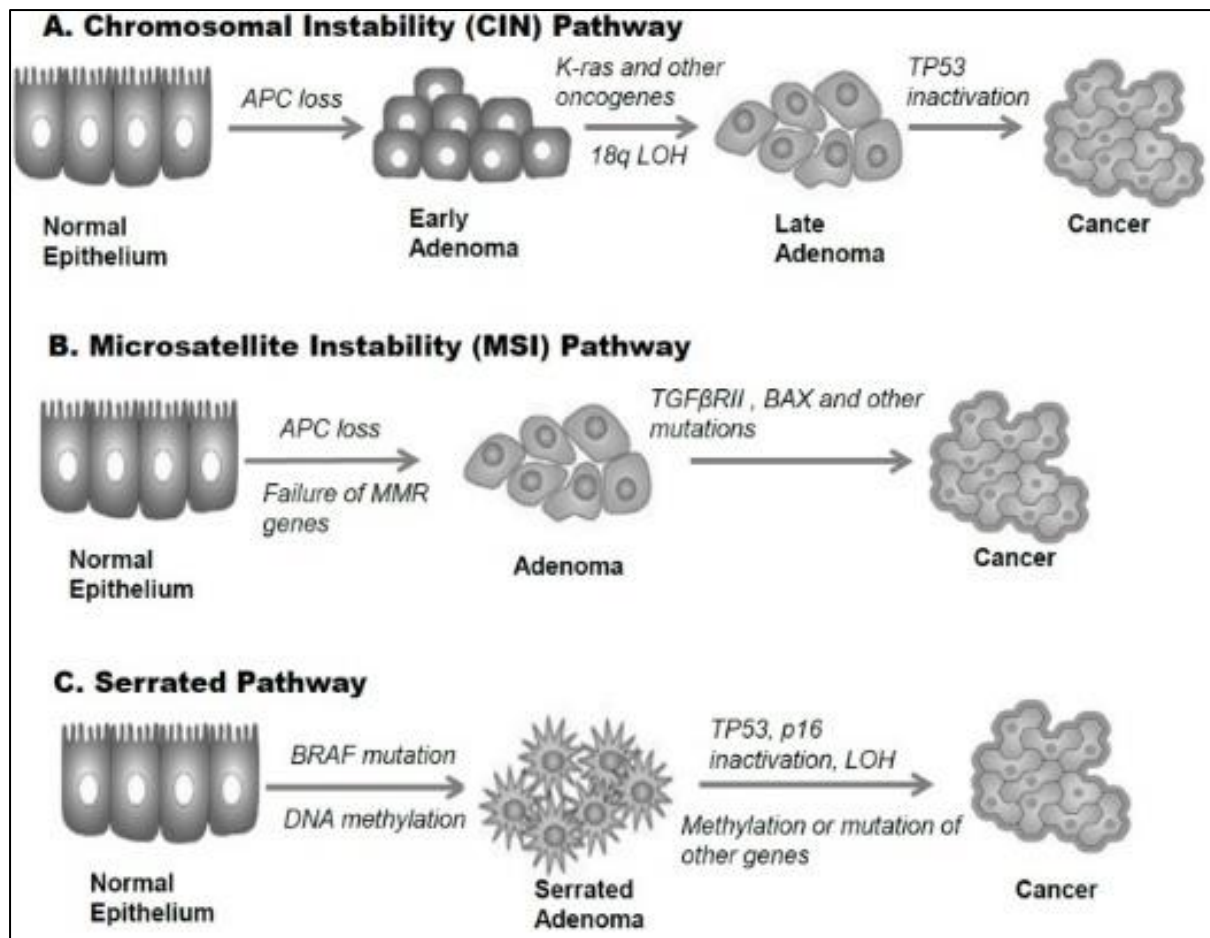
Figure 1-3: Main genetic pathways in CRC development (Mundade et al., 2014) (Copyright: figure is open-access).

1.1.3 Colorectal cancer risk factors

CRC risk increases with age and is further exacerbated by adverse lifestyle factors such as smoking, physical inactivity, poor diet and obesity (World Cancer Research Fund, 2018). These increase CRC risk by increasing the acquisition and decreasing the repair of genomic damage (World Cancer Research Fund, 2018). A population-based study showed that 3.6% of all new cancer cases globally are due to excessive adiposity and that breast and colon cancer account for about two thirds of cancers due to excessive body weight (Arnold et al., 2015).

1.1.3.1 Obesity and CRC risk

Strong evidence demonstrates that obesity increases the risk for CRC. Ning (2010) conducted a systematic review and meta-analysis of data from 56 observational studies on over 7 million people including 93,812 CRC cases which showed that higher BMI was associated with increased CRC risk both in retrospective and prospective studies. The same study also showed

that each 5 kg/m^2 unit increment in BMI increased CRC risk by 18%; this association with BMI was stronger for colonic than for rectal cancer and for males than for females (Ning et al., 2010). Obesity is also a major risk factor for colorectal adenomas (Omata et al., 2013) which indicates that increased adiposity may be a key player at an early stage in colorectal tumourigenesis (Mathers, 2018). A systematic review and meta-analysis including 19 prospective cohort studies and a total of 1,343,560 people of whom 12,837 developed CRC, reported that abdominal obesity, measured by waist circumference and waist-to-hip ratio, was associated with increased colorectal, colon and rectal cancer risk (Dong et al., 2017). A dose-dependent linear relationship has been confirmed between colorectal adenomas and visceral/ abdominal adiposity indicating that accumulation of body fatness within and around visceral organs may explain this positive association seen between risk of colorectal adenomas and CRC and greater BMI, waist and hip circumference (Ma et al., 2013, Keum et al., 2015b). Kantor (2016) reported that a higher BMI of nearly 240,000 16-20 years old Swedish men undergoing military enlistment was associated with significantly greater CRC risk 35 years after. Moreover, a meta-analysis of data from 7 prospective cohort studies on 24,751 females and 18,668 males, aged 63 and 62 years, respectively, showed a positive association between CRC risk and increased BMI, waist and hip circumference and waist to hip ratio, 12 years later (Freisling et al., 2017). These findings suggest that increased adiposity at any time point during the adult life course is a major risk factor for CRC (Mathers, 2018). There is some evidence for a sex-specific effect of weight gain on CRC risk. For example, a meta-analysis of prospective studies demonstrated that weight gain during adulthood is associated with significantly higher CRC risk in males but not in females (Keum et al., 2015a). However, a relatively small number of studies focussing on females was included in the review.

Obesity results in chronic systemic low-level inflammation through secretion of pro-inflammatory cytokines and signal molecules and to increased reactive oxygen species (ROS) which accelerate damage to the genome (Kiraly et al., 2015, Tuo et al., 2016). With higher adiposity, leptin concentrations in plasma rise, leading to increased production of TNF-α, IL-6 and -12 and pro-inflammatory macrophage accumulation (see Figure 1-4) (Tuo et al., 2016). Elevated plasma CRP, TNF-α and IL-6 concentrations in obese individuals are linked to impaired glucose tolerance, insulin resistance, abnormally high concentrations of insulin and insulin-like growth factor 1 (IGF-1), and low levels of IGF binding proteins, all of which may

increase CRC risk (see Figure 1-4) (Wei et al., 2005). Plasma concentration of C-reactive protein (CRP)- a widely-used marker of systemic inflammation- correlates positively with CRC risk (Gunter et al., 2006, Otani et al., 2006, Erlinger et al., 2004). In addition, Poullis (2004) showed that faecal calprotectin concentration (a marker of gut mucosal inflammation) is positively correlated with age, physical inactivity and obesity and inversely correlated with fruit, vegetable and fibre intake. An obesity-induced pro-inflammatory environment triggers a mucosal signalling cascade, involving activation of the transcription factor NF-κB and higher inducible nitric oxide synthase (iNOS) and cyclooxygenase-2 (COX-2) expression (John et al., 2006), that may supress apoptosis (Karin et al., 2002) which is one of the hallmarks of cancer (Hanahan and Weinberg, 2011).
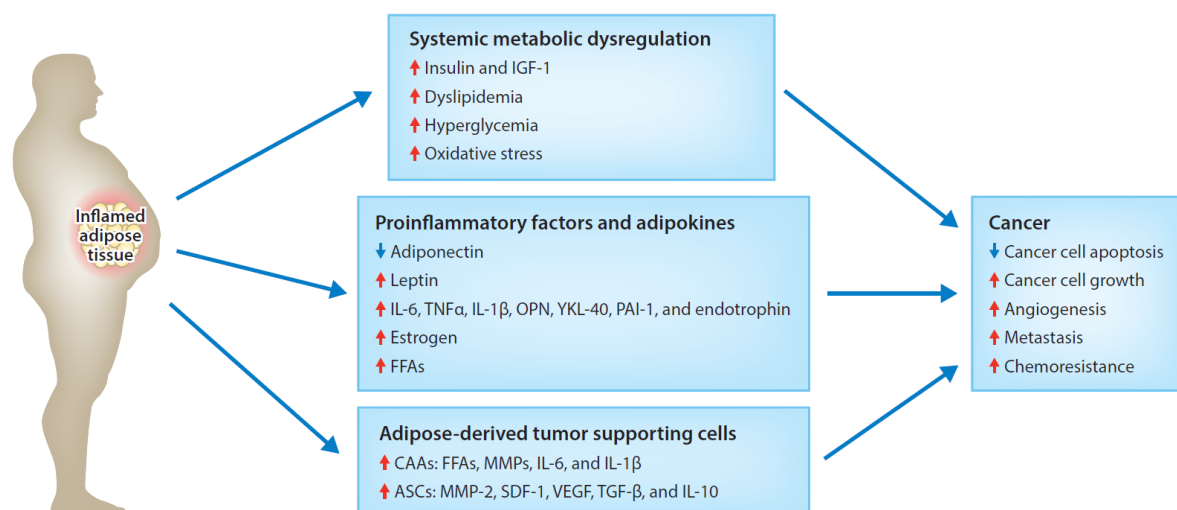
Figure 1-4: Metabolic and inflammatory links between obesity and cancer (Tuo et al., 2016) Reproduced with copyright permission (2019).

1.1.4   Effect of weight loss on biomarkers of colorectal cancer risk

1.1.4.1   *Weight loss via lifestyle based interventions*

In comparison with the wealth of strong and convincing evidence confirming associations between obesity and CRC risk, there are few studies about the effects of weight loss in the obese on CRC risk and, the few studies available to date are equivocal. A meta-analysis of 15 randomised controlled trials including data from 17,186 obese people (approximately equal numbers of males and females; mean age 52 years) showed that intentional weight loss (mean 5.5kg) resulted in a 15% fall in all-cause mortality, however cancer outcomes were not

evaluated in this study (Kritchevsky et al., 2015). A systematic review and meta-analysis of 54 randomised controlled trials investigating the effect of weight loss by lifestyle-based interventions demonstrated significantly reduced all-cause mortality over a two year period but did not detect effects on specific mortality causes such as cancer (Ma et al., 2017). Another systematic review and meta-analysis of data from 13 studies on the effect of weight change on CRC risk reported that weight gain was linked with increased CRC risk but that weight loss showed no effect (Karahalios et al., 2015).

Whilst the effects of lifestyle-based weight loss on CRC risk are unknown, there is evidence of effects of such weight loss on biomarkers of CRC risk e.g. cell proliferation and markers of systemic and tissue specific inflammation (see Table 1-1). In the INTERCEPT Study, 20 obese adults underwent an eight week low-energy liquid diet which resulted in 14% weight loss, reduced expression of Ki-67, which is a cell proliferation marker, in the colorectal mucosa and improved insulin sensitivity (Beeken et al., 2017). As noted above (section 1.1.3.1), increased insulin resistance may play a mechanistic role in obesity-related CRC (Beeken et al., 2017). Weight loss induced by a low-energy diet in obese older individuals (aged over 60 years) reduced pro-inflammatory markers in plasma including CRP, TNF-α and IL-6 and there were no additional benefits of including exercise in the weight loss intervention (Nicklas et al., 2004). Likewise, in middle aged obese women (aged 40 years), a low-energy diet and a low-energy diet plus exercise resulted in decreased IL-6 and TNF-α expression in plasma and subcutaneous adipose tissue. However, women in an exercise-only group who did not lose any fat mass did not show improvements in systemic insulin sensitivity, or in markers of inflammation in adipose tissue or plasma (Lakhdar et al., 2013). Tchernof (2002) demonstrated a positive correlation between plasma CRP concentrations and BMI in obese postmenopausal women (mean age 56 years), and found that a low-energy diet for 13.9 months resulted in mean 14.5kg weight loss and 32.3% lower plasma CRP concentrations.

Although changes in markers of inflammation in plasma and adipose tissue may mirror the change in other tissues, measurements taken from colorectal tissue *per se* are more directly relevant to the present project. Pendyala (Pendyala et al., 2011) found that imposition of a low-energy diet leading to mean 10.1% weight loss reduced the expression of IL-1β, IL-8, TNF-α, monocyte chemotactic protein 1 (markers of inflammation) and of the proto-oncogenes *FOS* and *JUN* in the colorectal mucosa of obese pre-monopausal women. Weight loss (6.4%)

following participation in Slimming World (a community based weight loss programme) resulted in lower faecal calprotectin concentrations only in those overweight and obese individuals who had high concentrations (>50µg/g) at baseline (Kant et al., 2013). Although the weight loss achieved in these studies (see Table 1-1) was relatively modest, ranging from 6.4- 14%, this was sufficient to reduce tissue specific and systemic inflammatory markers.

Study	Tissue	Weight loss intervention	Key Findings
(Tchernof et al., 2002)	Plasma	Low-energy diet	Decreased CRP concentration
(Nicklas et al., 2004)	Plasma	Low-energy diet with/ without exercise	Reduction in pro-inflammatory markers (CRP, TNF-α and IL-6) No additional benefits after exercise
(Pendyala et al., 2011)	Colorectal mucosa	Low-energy diet	Decreased expression of inflammatory markers (IL-1β, IL-8, TNF-α, monocyte chemotactic protein 1) and proto-oncogenes (*FOS* and *JUN*)
(Kant et al., 2013)	Stool	Community based weight loss porgramme by Slimming World	Decreased faecal calprotectin concentration
(Lakhdar et al., 2013)	Plasma and subcutaneous adipose tissue	Low-energy diet with/ without exercise and exercise only	Decreased expression of IL-6 and TNF-α in low-energy diet with/ without exercise groups No change in exercise group

(Beeken et al., 2017)	Colorectal mucosa	8 week low-energy liquid diet	Participants achieved 14% weight loss Ki-67 expression was reduced, Insulin sensitivity was improved

Table 1-1: The effects of lifestyle-based weight loss interventions on tissue specific and systemic inflammatory markers in humans

1.1.4.2   Weight loss via bariatric surgery

In comparison with lifestyle-based interventions, bariatric surgery results in much greater and more sustained body weight loss, which leads to reduced cancer risk after 10 years (Schauer et al., 2017a, Schauer et al., 2017b). A systematic review and meta-analysis of 13 studies including data of 54,257 people investigating the effect of weight loss by bariatric surgery demonstrated a reduction in cancer incidence (Casagrande et al., 2014); and whilst the beneficial effects on total cancer burden are well established, the effects of weight loss following bariatric surgery on cancers at individual sites, including CRC, are less clear and due to the physiological changes in the gut as a result from such surgery, an assumption that any benefits for cancer overall will also apply to CRC should not be made (Mathers, 2018). A systematic review and meta-analysis of studies reporting on 24,321 bariatric surgery patients and 80,866 obese controls showed that bariatric surgery-induced weight loss was linked with 27% reduction in CRC risk (Afshar et al., 2014). An English cohort study comprising more than 1 million obese subjects found no evidence that bariatric surgery modulates CRC risk (Aravani et al., 2018). However, in this study, the number of participants undergoing bariatric surgery and the number of CRC cases were both small; 3.9% of subjects underwent bariatric surgery and only 0.1% of the bariatric surgery group developed CRC (Aravani et al., 2018) so that the power of this study to detect an effect, if it exists, was limited. A recent retrospective cohort study of 22,198 patients undergoing bariatric surgery found a 33% reduced cancer risk, including CRC risk which decreased by 41%, compared with 66,427 nonsurgical subjects at 3.5 years follow-up (Schauer et al., 2019). It is worthwile considering that bariatric surgery is more regularly performed in young patients (Casagrande et al., 2014) though CRC is more frequently observed in older people (Jemal et al., 2010) and hence the long lead time period for CRC appearance might be confounding the links between cancer and bariatric surgery.

Similarly, research on the effect of weight loss by bariatric surgery on biomarkers of CRC risk has yielded apparently conflicting outcomes. Results from the BOCABS Study (carried out in

the Mathers Laboratory and described in detail in Chapter 2) showed that six months post-bariatric surgery, when participants had achieved mean 29kg weight loss, markers of systemic and colorectal mucosal inflammation were reduced, glucose homeostasis was improved and crypt cell proliferation in the colorectal mucosa was reduced (Afshar et al., 2018). In contrast, Sainsbury (2008) found greater expression of the pro-inflammatory genes *COX-1* and *COX-2*, increased mitosis and decreased apoptosis in the mucosal crypts, when BMI had been reduced by 12.6 kg/m^2 units following bariatric surgery. This increased crypt cell proliferation and greater pro-tumourigenic cytokine expression persisted for another 3 years in the patients who had undergone Roux-en-Y gastric bypass (RYGB; one of the most common types of bariatric surgery) (Kant et al., 2011).

The observed differences in the effects of weight loss following bariatric surgery on biomarkers of CRC risk may be due to subtle, but important, differences in the surgical procedures that patients underwent (Afshar et al., 2018, Mathers, 2018). Afshar and colleagues hypothesised that the apparently adverse effects observed by Sainsbury (2008) and Kant (2011), may be a result of resection of a larger amount of the small bowel resection leading to increased malabsorption and, hence, exposure of the large bowel mucosa to luminal agents, for example secondary bile acids, which can harm the colorectal mucosa and are associated with increased CRC risk (Afshar et al., 2018).

The biological mechanisms through which weight loss modulates CRC development are not well understood. It is probable that pathways that are involved in the hallmarks of cancer are associated with the weight loss cancer relationship (Ulrich et al., 2018). These include reduced local and systemic inflammation, reduced angiogenesis, modulated adipokine concentrations and improved immune function, enhanced DNA repair capacity, reduced insulin resistance, and reduced oxidative stress all of which potentially have direct effects on cancer stem cells (Ulrich et al., 2018).

1.2 Mitochondria

1.2.1 Evolutionary origins of mitochondrial

After observing similarities between chloroplasts and free living cyanobacteria, in 1905 Konstantin Sergejewiz Mereschkowsky proposed the endosymbiotic theory, in which he suggested that chromatophores did not arise *de novo*, but were the result of endosymbiosis

(Martin and Kowallik, 1999). This endosymbiotic theory was not accepted until 70 years later. Yang (1985) suggested that the 16S ribosomal RNA sequences from two prokaryotes, namely *Pseudomonas testosteroni* and *Agrobacterium tumefaciens*, defined the origin of the endosymbiont origin which evolved to become the mitochondrion. Mammalian mitochondria include features such as extranuclear DNA, the mtDNA and a double membrane, which are also found in chloroplasts in plants (Embley and Martin, 2006). These features and the similar size of mitochondria and chloroplasts to bacteria suggested that both chloroplasts and mitochondria developed from endosymbiotic events between an archaebacterial host and an α-proteobacterial symbiont (leading to mitochondria) or cyanobacterial symbiont (leading to the chloroplast) approximately one to two billion years ago (Embley and Martin, 2006).

1.2.2 Mitochondrial structure and function

Mitochondria are eukaryotic organelles found in the cytosol and play an important role in many metabolic pathways such as iron-sulfur cluster biogenesis, maintenance of membrane potential, apoptosis, intracellular calcium signalling and adenosine triphosphate (ATP) production via oxidative phosphorylation; the latter being their primary function (Fernandez-Silva et al., 2003, Stewart and Chinnery, 2015).

Each mitochondrion holds multiple copies of a double-stranded, closed, circular mitochondrial DNA genome (mtDNA) which are found in the mitochondrial matrix and are maternally inherited (Case and Wallace, 1981). The human mitochondrial genome is comprised of 16,569 base pairs forming an inner light 'L' (cytosine rich) and an outer heavy 'H' (guanine rich) strand encoding 37 genes in total (Case and Wallace, 1981). These genes code for 22 tRNAs, 13 proteins of the respiratory chain and 2 rRNAs and are specific to the mitochondria as they are necessary for translation of mtDNA genes (Carling et al., 2011). Furthermore the mitochondrial genome contains the non-coding D-loop, which contains the promoters for 'L' and 'H' strand transcription (Shadel and Clayton, 1993). The mtDNA and proteins are wrapped together into mitochondrial nucleoids and each nucleoid comprises 1-2 mtDNA molecules (Case and Wallace, 1981). This mtDNA-protein assembly (nucleoids) ensures that the genetic material of the mitochondria is distributed throughout the mitochondrion and ensures coordination of mtDNA involvement in cell metabolism (Gilkerson et al., 2013).

The mitochondrial respiratory chain is comprised of five complexes (Sousa et al., 2018) and, in humans, mtDNA encodes the following subunits of the mitochondrial respiratory chain complexes: NADH dehydrogenase 1 (MTND1) - MTND6 and MTND4L (complex I), cytochrome b (MTCYB) (complex III), cytochrome c oxidase I (MTCO1) - MTCO3 (complex IV), ATP synthase 6 (MTATP6) and MTATP8 (complex V) (Anderson et al., 1981). The remaining subunits of complex I and III-V are nuclear DNA (nDNA) encoded and complex II is completely nDNA encoded (Anderson et al., 1981). Figure 1-5 shows the five complexes of the mitochondrial respiratory chain which are located in the inner membrane. Electrons are transported from complex I to complex IV creating a proton gradient across the inner membrane, which is used by complex V for ATP production (Ross, 2011). In Figure 1-5, the red hexagons illustrate mtDNA encoded subunits, whereas the white hexagons demonstrate nDNA encoded subunits (Ross, 2011).

The majority of mitochondrial proteins needed for mitochondrial structure and function are transcribed from nuclear genes and translated within the cytosol before being transported across the mitochondrial membrane (Larsson and Clayton, 1995). A mutation in the nDNA encoding a subunit of the respiratory chain complex affects all mitochondria within that cell, whereas a mutation in the mtDNA encoding a subunit of the respiratory chain complex affects that specific mitochondrion (Ross, 2011). Optimal function of mitochondria depends on both genetic systems (nuclear and mitochondrial) (Larsson and Clayton, 1995).
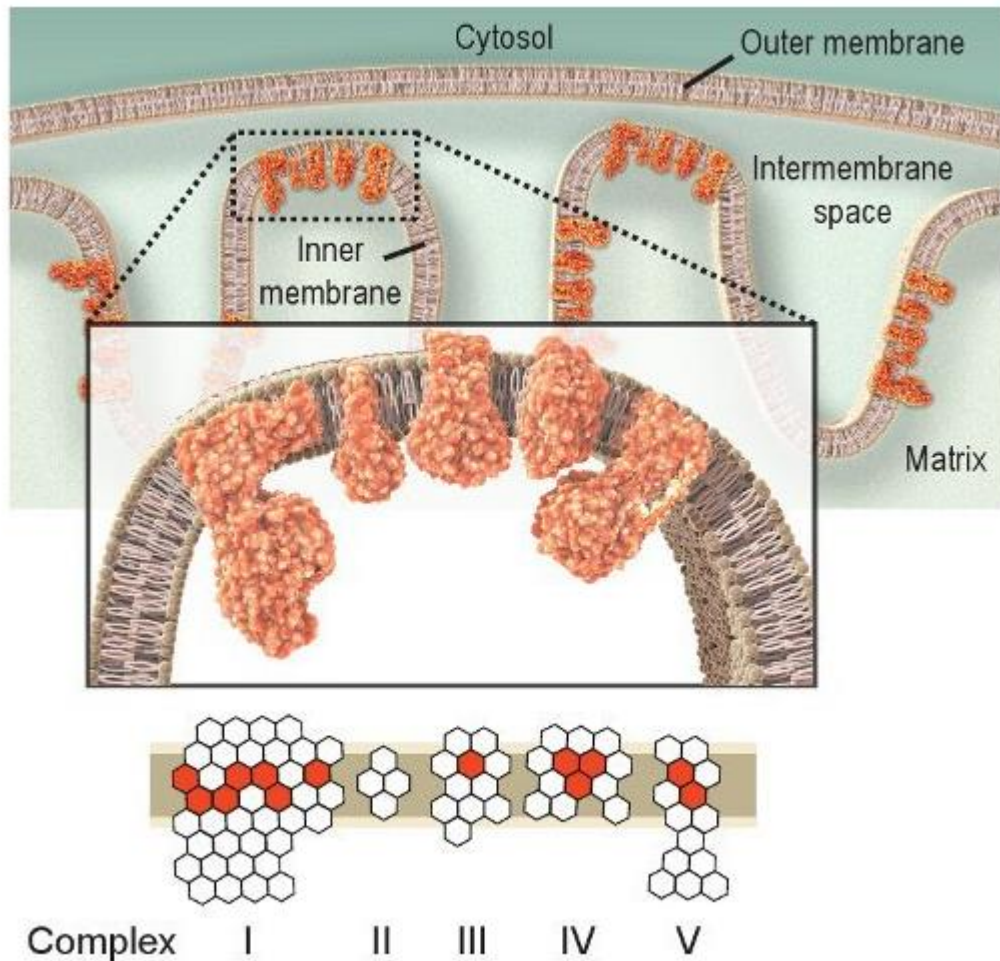
Figure 1-5: Complexes I- V of the mitochondrial respiratory chain are embedded in the inner membrane. Red hexagons and white hexagons show mtDNA and nDNA encoded subunits of the complexes respectively (Ross, 2011) *Reproduced with copyright permission (2019).*

1.2.3 Mitochondrial DNA damage and energy metabolism in mitochondria

As every cell comprises multiple mtDNA copies, mutations can affect all mtDNA molecules (homoplasmy) or only a proportion (heteroplasmy) of the mtDNA in a cell (Larsson and Clayton, 1995, Stewart and Chinnery, 2015). Heteroplasmy can vary from 1% to 99% between cells in the same organ or tissue, across various organs and tissues in the same individual and between people in the same family (Johns, 1995, Stewart and Chinnery, 2015). Mutations of the mtDNA can present in various ways, i.e. there can be point mutations (usually maternally inherited), single large-scale deletions (rarely inherited and never homoplasmic), or acquired somatic mutations (because of ageing and errors in replication) (Gorman et al., 2016). Other studies have also shown that mutations can arise from environmental exposures such as tobacco use (Prior et al., 2006, Tan et al., 2008), viruses and bacteria (Machado et al., 2010) and ultraviolet light (Birch-Machin and Swalwell, 2010, Stewart and Chinnery, 2015). A

14

pathogenic homoplasmic mtDNA point mutation usually leads to a relatively mild biochemical defect affecting only one organ or tissue, but exceptions have been described (Gorman et al., 2016). Contrarily, a heteroplasmic mutation can affect several organs and the degree of heteroplasmy is correlated with the extent of organ involvement and hence with the level of severity of the clinical phenotype (the biochemical defect usually presenting severely in affected tissues) (DiMauro et al., 2013, Gorman et al., 2016). The level of heteroplasmic mtDNA mutations needs to surpass a critical threshold (approximately 60-80%) before the biochemical defect can be detected as altered function (King and Attardi, 1989, Boulet et al., 1992).

Glycolysis and β-oxidation of fatty acids both occur within the cytoplasm. However, the majority of ATP is generated from catabolism of dietary fats and carbohydrates and occurs after the common intermediate acetyl CoA comes into the mitochondrion and undergoes oxidative phosphorylation and the citric acid cycle (Chen et al., 2003, Gao et al., 2010). Reactions involving the electron transport chain yield as a by-product ROS, with complex I and complex III being the main ROS production sites (Chen et al., 2003, Gao et al., 2010). ROS can react with all of the cell's macromolecules i.e. proteins, lipids and nucleic acids, which can lead to reversible or irreversible oxidative alterations of these macromolecules and, thereafter, to dysfunction of the cell and organ (Gao et al., 2010). ROS production due to other environmental and dietary exposures, for example tobacco use or alcohol intake, can also trigger mtDNA adduct development (as well as nDNA adduct development) via covalent binding of polycyclic aromatic molecules to the DNA (Gao et al., 2010). MtDNA repair mechanisms are much less prominent and effective compared with those acting on nDNA (Zinovkina, 2018). To date, there is only evidence on mammalian mtDNA repair systems like base excision repair and micro-homology mediated end joining, as opposed to the nDNA repair system which consists of base and nucleotide excision repair, mismatch repair, homologous recombination and non-homologous end joining (Zinovkina, 2018). A few essential factors involved in nDNA mismatch repair have been identified in mitochondria but their functional role is yet to be defined (Zinovkina, 2018). Hence, ROS affect mtDNA more adversely and can initiate development of diseases (Allen and Coombs, 1980, King and Attardi, 1989, Cakir et al., 2007).

1.2.4 Mitochondrial defects in colorectal cancer

The 'Warburg Effect' describes as a shift from oxidative metabolism to glycolysis and occurs in cancer cells (Warburg, 1956). However, the functions of the Warburg Effect in enabling tumour cell proliferation and malignancy remain unknown (Liberti and Locasale, 2016). A recent review by Fang (2016) reported overexpression of glycolytic enzymes (i.e. pyruvate kinase, hexokinase and lactate dehydrogynase) and glucose transporters (GLUT) in human CRC indicating increased glycolysis. Additionally, a study using a CRC cell line with *KRAS* and *BRAF* mutations showed that *GLUT1* was consistently upregulated, also showing increased potential to transport glucose (Yun et al., 2009).

The role of mitochondrial dysfunction in the aetiology of cancer, including CRC, remains to be discovered. MtDNA mutations have been found in tumour and metastatic tissue of mice. A cytoplasm from both the parental species with or without a pathogenic homoplasmic point mutation at 8993 or 9176 nucleotide position in the *MTATP6* gene were transplanted into nude mice (Shidara et al., 2005). When the cybrids contained mutations in the *MTATP6* gene, they grew faster in culture than the wild type cybrids and, in mice, they conferred a competitive advantage in the early stages of tumour growth, possibly related to reduced mitochondrial respiration (Shidara et al., 2005). Later, another study in mice also using cybrids demonstrated an acquired metastatic potential after transferring mtDNA mutations into the gene coding for NADH, which resulted in deficient complex I activity and overproduction of ROS (Ishikawa et al., 2008). Human CRC tissue showed a lower frequency of random/ non-clonal single base substitutions in mtDNA relative to the adjacent non-tumour tissue (Ericson et al., 2012). In the same study, this lower mtDNA mutation frequency, which was due to a reduction in C:G to T:A transitions which is commonly coupled with oxidative damage, was associated with the Warburg Effect (Ericson et al., 2012). Ericson (2012) concluded that mtDNA integrity is increased in CRC due to reduced ROS mediated mtDNA damage. Somatic mtDNA mutations are found commonly in human CRC and it has been claimed that they contribute to cancer development and to metastatic spread (Polyak et al., 1998, He et al., 2010).

Older individuals have higher rates of somatic mtDNA mutations (see Figure 1-6), but it is unclear if this increased mtDNA mutation load contributes to age-related CRC risk or is a non-causal age-associated phenomenon (Greaves et al., 2014). When mtDNA mutations are

present at high frequencies they compromise mtDNA-encoded respiratory chain subunits, as well as cytochrome c oxidase activity, resulting in dysfunction of mitochondria (see Figure 1-6) and may be a marker of epithelial damage (Greaves et al., 2010). For example, colorectal mucosal crypts with mtDNA mutations show small but significant changes in cell proliferation and apoptosis (Nooteboom et al., 2010). It has been shown that ageing and carcinogenesis generate mutations randomly across the mitochondrial genome (Polyak et al., 1998, Taylor et al., 2003) followed by subsequent mutations throughout the genome as cancer progresses (Taylor et al., 2003, Yoneyama et al., 2005, Lee et al., 2005). Furthermore, there is convincing evidence from cell and animal models, as well as more limited evidence from human studies, that over-feeding and obesity result in mitochondrial dysfunction (this is described in detail in section 1.4.2) (Breininger et al., 2019) which may increase the risk of CRC development.
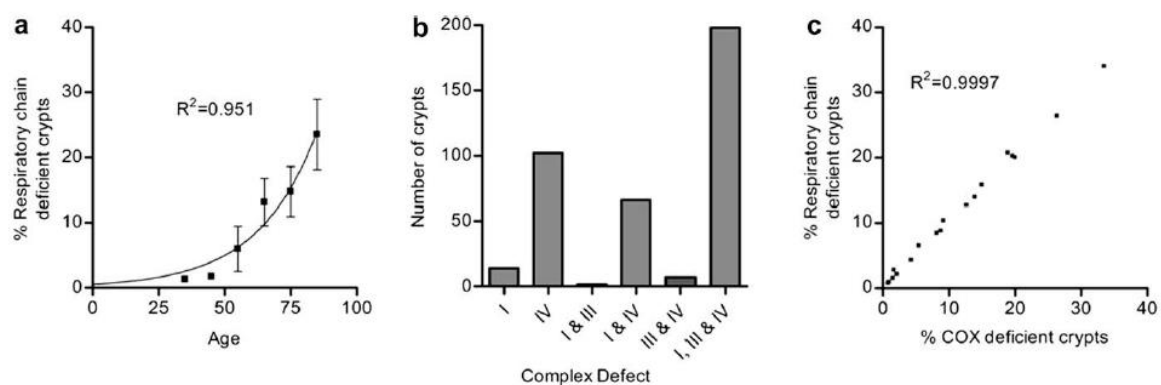
Figure 1-6: a) Rate of percentage respiratory chain deficiency in the aging human colon b) Frequency of specific respiratory chain defects in individual human crypts c) Correlation between total respiratory chain and COX deficiency (Greaves et al., 2010) (Copyright: figure is open-access).

1.3 Epigenetic marks and molecules

1.3.1 The concept of epigenetics

Epigenetics comprises heritable changes to marks on the genome and the associated cellular machinery without involving changes to the primary DNA sequence (Dupont et al., 2009). The totality of such marks on the genome is described as the epigenome, and encompasses three closely interacting epigenetic mechanisms including histone modifications, DNA methylation and non-coding micro riboxynucleic acids (microRNAs) which are key regulators of gene expression (Goldberg et al., 2007, Link et al., 2010, Hardy and Tollefsbol, 2011, Park et al.,

2012). Post-translational modification of histone proteins including phosphorylation, methylation, acetylation, ubiquitylation and sumoylation at specific amino acid residues in the histone tails alters the structure of chromatin (Dupont et al., 2009). DNA methylation is catalysed by a family of enzymes called DNA methyl transferases which add a methyl group to the 5' position on the cytosine residues where the cytosine is followed by a guanine residue, namely a CpG dinucleotide (Dupont et al., 2009). In CRC, tumours with distinctly different patterns of DNA methylation have been identified. Those with simultaneous hypermethylation of numerous CpG islands in the promoter regions of multiple genes (including TSG) have been described as the CpG Island Methylator Phenotype (CIMP), and those tumours have distinct genetic and clinical features (Hinoue et al., 2012). For example, CIMP-high tumours were characterised by *MLH1* DNA hypermethylation and mutation of *BRAF^V600E* (Hinoue et al., 2012). In contrast, CIMP-low tumours had mutations in the *KRAS* gene and DNA hypermethylation outside CpG islands (Hinoue et al., 2012). The combination of these epigenetic mechanisms and, miRNAs specifically, are responsible for the regulation of gene expression both early in life during cellular and tissue differentiation and throughout the life course (Reik, 2007, McKay and Mathers, 2011). Although each nucleated cell within a given organism contains the same nuclear genome, only a fraction of all the encoded genes is expressed in a given cell type. In addition to house-keeping genes that are expressed in all cells, each cell type expresses a characteristic constellation of genes that enable that cell type to carry out its particular functions (Jaenisch and Bird, 2003). In addition, cells need to sense their environments and to up- or down-regulate specific genes to enable them to respond appropriately to the changing environment (Malcomson and Mathers, 2017). Further, cells need to repress harmful sequences, derived largely from viruses, which became integrated in the genome during evolution and this is achieved by DNA methylation of the relevant sequences (Jaenisch and Bird, 2003). Epigenetic related non-coding RNA (ncRNA) is a large family comprising long non-coding RNA (lncRNA), piwi RNA (piRNA), short interfering RNA (siRNA) and microRNAs (miRNAs).

1.3.2 MicroRNA structure, biogenesis and function

MiRNAs are small single stranded non-coding RNA molecules, which are approximately 18-25 (typically 22) nucleotides long and are expressed in all nucleated cells. An overview of the complex process of miRNA biogenesis, of the standard and alternative pathway, which

includes several stages can be seen in Figure 1-7 (Ameres and Zamore, 2013). Primary miRNA transcripts are processed by Drosha in the nucleus and by Dicer in the cytoplasm and then transcribed by RNA polymerase II in the standard pathway (Ameres and Zamore, 2013). More specifically, Exportin-5 exports the pre-miRNAs into the cytoplasm where Dicer and transactivate response RNA binding protein (TRBP) lead pre-miRNAs into mature miRNAs (comprised of 20-24 nucleotides) creating the RNA-induced silencing complex (RISC) (Ding et al., 2018). However, in the alternative pathway, the primary miRNA is generated from a branched mirtron structure which undergoes a process called lariat debranching (Ameres and Zamore, 2013).

Most miRNAs derive from independent genomic transcription units (Mendell and Olson, 2012). A third of known miRNAs can be found in introns of genes coding for proteins and are co-transcribed along with the host gene, resulting in regulated synchronised expression of proteins and miRNAs (Mendell and Olson, 2012). MiRNAs regulate gene expression at the transcriptional or post-transcriptional levels (Heneghan et al., 2010). MiRNAs do this primarily by binding in a sequence-specific manner to the complementary region in the 3' – untranslated mRNA regions which subsequently regulates the translation of mRNAs to proteins (Lai, 2002) including transcription factors to RNA binding proteins and signalling proteins (Ding et al., 2018). MiRNAs couple with proteins forming a RISC that enables regulation of gene expression which is sequence-specific to their complementary mRNAs (Jonas and Izaurralde, 2015). This is achieved by suppressing the translation of target mRNAs or cleavage of target mRNAs to initiate their 5' to 3' mRNA decapping, degradation and de-adenylation, via defective coupling with the target mRNAs (Jonas and Izaurralde, 2015). The mature miRNA region of nucleotide 2-7 has been reported as the locus for target mRNA recognition via base pair complementary (Ding et al., 2018). The effects of miRNAs can be either temporary, for example when they temporarily bind a mRNA suppressing translation, or permanent when they degrade a mRNA strand respectively (Saxena et al., 2003). Completely processed miRNAs work together with the Argonaute (Ago) family of proteins inside the RISC and direct the Ago proteins to target mRNAs through interactions with imperfect complementary sites (Mendell and Olson, 2012). Every miRNA is able to target multiple mRNAs and every mRNA can be targeted by multiple miRNAs (Huntzinger and Izaurralde, 2011).
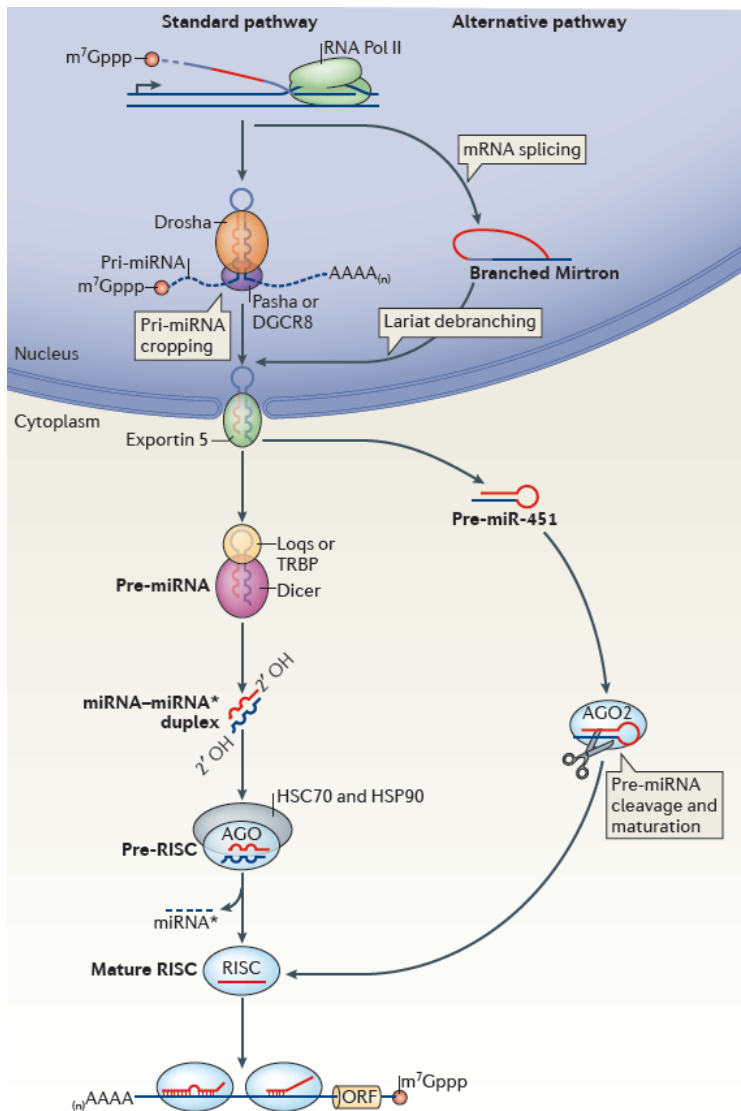
Figure 1-7: The biogenesis of miRNA by the standard and alternative pathways (Ameres and Zamore, 2013) Reproduced with copyright permission (2019).

1.3.3 Aberrant expression of microRNAs in colorectal cancer

MiRNAs play an important role in multiple biological pathways and their expression is dysregulated in many pathological mechanisms (Heneghan et al., 2010). In 2003, for the first time, Cordes (2009) identified the link between miRNAs and CRC and since then numerous studies have revealed a role for miRNAs in CRC. Aberrant patterns of miRNA expression are involved in the initiation and progression of oncogenesis, including CRC, due to their role as tumour suppressors and oncogenes (Ding et al., 2018). For example, oncomiRs (oncogenic miRNAs) target and prevent the expression of endogenous TSG and, in addition, can activate pathways associated with CRC, such as the Wnt signalling pathway (Ding et al., 2018).

A recent review by Ding (2018) identified numerous oncogenes which are significantly upregulated during CRC, including miR-21, miR-31, miR-92a, miR-96, miR-135a/b, miR-155, miR-182/503, miR-200c, miR-210, miR-214, miR-224 and miR-301a. These aberrantly expressed miRNAs regulate multiple functional roles in tumourigenesis and its management including inflammation, genome instability, cell growth, proliferation, angiogenesis, metastasis, invasion, migration, apoptosis, chemoradiosensitivity and drug resistance. For example, miR-21 represses multiple TSG such as T-cell lymphoma invasion and metastasis 1 (*TIAM1*), *PDCD4*, *PTEN*, *hMSH2*, sprouty homolog 2 (*SPRY2*), cell division cycle 25A (*CDC25A*) and transforming growth factor beta receptor II (*TGFBR2*), all of which play a key role during apoptosis, migration, invasion, proliferation, cancer stem cell maintenance, metastasis and chemotherapy resistance (Asangani et al., 2008, Valeri et al., 2010, Xiong et al., 2013, Thomas et al., 2015). Moreover, lncRNA can also be targeted by miRNAs. For example miR-143-3p targets the lncRNA AK094401 (overexpressed in CRC, OECC) which led to downregulation of NF-κB and p38 mitogen-activated protein kinase and promoted CRC cell growth in BALB/C nude mice (Huang et al., 2018). Further, miR-577 targeted and led to overexpression of lncRNA differentiation antagonizing nonprotein coding RNA (DANCR) and heat shock protein 27 (HSP27) which accelerated proliferation and metastasis of CRC (Wang et al., 2018).

The same recent review by Ding (2018) also identified several tumour suppressive miRNAs that are downregulated during CRC including let-7, miR-7, miR-18a-3p, miR-26b, miR-27b, miR-34a, miR-101, miR-126, miR-143/145, miR-144, miR-149, miR-194, miR-320a, miR-330 and miR-455 with their functional role being proliferation, apoptosis, invasion, migration, angiogenesis, colony formation, anchorage independent-growth, metastasis, chemoresistance and hematopoiesis (Ding et al., 2018). For example, let-7, a highly conserved miRNA family consisting of let-7a-1/2/3, -7b, -7c, -7d, -7e, -7f-1/2, -7g, -7i, and miR-98 participate during epithelial-to-mesenchymal transition (EMT) and is significantly downregulated in CRC when compared with adjacent normal tissue (Takahashi et al., 2012). During EMT, let-7 represses numerous oncogenes including *c-Myc, RAS, CDK6, CDC34, CDC25A, LIN28, LIN28B* and *HMGA2* (Takahashi et al., 2012). In addition, let-7 expression in intra-tumour tissue was associated with improved survival in CRC patients (Saridaki et al., 2014). Cappuzzo (2014) and Eslamizadeh (2018) reported that let-7 (plus the cluster miR-99a/let-7c/miR-125b) was associated with clinical outcomes of CRC and regulated response

to anti-EGFR targeting therapy. Furthermore, downregulated miR-194 in CRC was associated with tumour size, tumour node metastasis, overall patients' survival and was correlated with advanced colorectal adenoma after polypectomy; miR-194 was proposed as an independent predictor for recurrence of adenomas (Zhao et al., 2014, Wang et al., 2015). In contrast, miR-194 overexpression targeted the oncogenic transcriptional regulator HMGA2 which is involved in reducing and attenuating cell proliferation and migration, suppressing EMT, reducing xenograft growth and increasing sensitivity to anticancer drugs used in CRC (Chang et al., 2017). In summary, multiple miRNAs play a major role in CRC development which are context dependent role (some can act either as oncogenes or as tumour-suppressors).

1.4 Obesity

1.4.1 Epidemiology

In 2014, the World Health Organisation estimated that more than 1.9 billion and 600 million adults, equivalent to 39% and 13%, are overweight and obese, respectively (Organisation, 2015). The prevalence of obesity has risen unrelentingly in the past 4 decades in all age groups and, if current trends continue, there will be more than one billion obese adults globally by 2025 (World Obesity Day, 2015).

Obesity is a major public health problem caused by a sustained positive imbalance between dietary energy intake and energy expenditure (in basal metabolic rate and physical activity) (World Health Organization, 2015). Numerous other factors including a genetic predisposition, epigenetic factors (Memedi et al., 2013), maternal overweight/ obesity, gestational weight gain (Kaar et al., 2014), short length of breastfeeding (Jing et al., 2014) and lack of sleep which may influence appetite regulatory hormones such as leptin (Boeke et al., 2014) also contribute to the development of obesity. Furthermore, environmental factors such as cultural background, socioeconomic status, and access to healthy foods influence obesity risk (Matthiessen et al., 2014).

1.4.2 Effects of obesity on mitochondrial structure and function

Evidence from cell and animal models, as well as human studies, shows that over-feeding and obesity result in mitochondrial dysfunction (Breininger et al., 2019).

Table 1-2 summarises findings from human studies that have shown that a high fat diet or obesity leads to mitochondrial defects and are discussed in more detail below.

Feeding a high fat diet for 3 days led to lower expression of PGC-1α and PCG-1β mRNA, reduced concentrations of cytochrome C and PGC-1α and downregulation of genes coding for oxidative phosphorylation proteins including complex I-IV in vastus lateralis and gastrocnemius muscle of healthy men (Sparks et al., 2005). As the duration of the intervention was short, it is impossible to conclude if the observed effects on biomarkers of mitochondrial function are because of modifications in adiposity, as distinct from changes in macronutrient intake. Further studies demonstrated that excess intake of energy-yielding nutrients may result in reduced size and number of mitochondria and lower oxidative phosphorylation in extopic brown adipose tissue (Bournat and Brown, 2010). Lower expression of genes coding for oxidative phosphorylation proteins and reduced oxygen consumption was seen in obese individuals, suggestive of a decline in mitochondrial function (Bournat and Brown, 2010). Obese individuals showed reduced mitochondrial oxidative activity in adipocytes, potentially being due to overall adiposity as opposed to hypertrophy of adipocytes or cell size differences between obese and non-obese (Yin et al., 2014). Heinonen (2015) reported reduced mtDNA content and, that 96 out of 130 CpG sites of mitochondria-associated transcripts and upstream regulators were hypermethylated in subcutaneous adipose tissue of obese monozygotic twins. The same study also reported lower mtDNA-encoded transcripts (including 12S rRNA, 16S rRNA, COX1, ND5, CYTB) and OXPHOS subunit proteins complex III-V levels. A more recent study revealed that differential expression of 41 and 73 proteins in inter-myofibrillar and subsarcolemmal mitochondria, respectively, in skeletal muscle (Kras et al., 2018). In the same study, proteins forming complex II and the TCA cycle were increased whereas proteins forming complexes I and III and ATP synthase were reduced in inter-myofibrillar mitochondria of obese individuals (Kras et al., 2018). The mitochondrial phenotype of adipose-derived stromal stem cells was disturbed in obese (altered network, higher number and smaller shape) when compared with lean individuals (Ejarque et al., 2018). Additionally, TBX15, a negative regulator of mitochondrial mass, was hypomethylated and its protein concentration was increased in adipocytes of obese people (Ejarque et al., 2018).

Study	Tissue	Investigation	Key Findings

(Semple et al., 2004)	Adipocytes	Obesity	Reduced PGC-1α concentration
(Sparks et al., 2005)	Male vastus lateralis and gastrocnemius muscle	High fat diet	No changes in mtDNA content, *TFAM*, or *NRF1* Reduced concentrations of PGC-1α mRNA, lower activity of cytochrome C oxidase and Citrate synthase
(Yin et al., 2014)	Adipocytes	Obesity	Reduced mtDNA content, oxygen consumption and citrate synthase activity
(Heinonen et al., 2015)	Subcutaneous adipocytes	Obesity	Reduced mtDNA content, 96 out of 130 CpG sites of mitochondria related transcripts and upstream regulators were hypermethylated, reduced mtDNA-encoded transcripts (12S rRNA, 16S rRNA, COX1, ND5, CYTB) and OXPHOS subunit proteins (complex III-IV)
(Ejarque et al., 2018)	Adipose derived stromal stem cells	Obesity	Altered DNA methylation: *TBX15* was one of the most differentially hypomethylated genes
(Kras et al., 2018)	Skeletal muscle	Obesity	Increased expression of proteins of the TCA cycle and complex II and, decreased expression of proteins forming ATP synthase and complexes I and III

Table 1-2: The effects of over-feeding and obesity on mitochondrial structure and function in humans (Breininger et al., 2019)

There is consistent and strong evidence, in cell and animal models, as well as human studies that both over-feeding and obesity lead to dysfunction of mitochondria (Breininger et al., 2019). PGC-1α downregulation has been seen consistently in studies using cells, animals and

humans. Reductions in complex IV and cytochrome c expression, as well as lower mitochondrial content are reported in animal and human research, but the effects on other measures including β-oxidation and mitochondrial enzyme and protein concentrations are less consistent (Breininger et al., 2019).

1.4.3 Possible underlying mechanisms of the effects of obesity on mitochondrial dysfunction

In vitro and animal studies have provided insight on possible mechanisms underlying the effects of obesity on mitochondrial dysfunction, whereas data from human studies are much more limited. Moreover, these mechanistic studies have been carried out predominantly in various cell types and tissues, with relatively limited studies in colonocytes. Obesity and subsequent obesity-induced inflammation result in reduced β-oxidation and excess ROS causing mitochondrial dysfunction in liver, muscle and adipose tissue (Rogge, 2009, de Mello et al., 2018). During these processes, dysfunctional mitochondria can trigger a vicious cycle of lower mitochondrial β-oxidation and biogenesis and reduced mtDNA content (Rogge, 2009). In addition, impaired β-oxidation leads to increased synthesis of TAG and ectopic lipid deposits. Through increased ROS production, this may result in oxidative stress and cellular dysfunction, higher formation of ceramide, increased concentrations of nitric oxide synthase, increased lipid peroxidation by-products and increased production of inflammatory cytokines (Rogge, 2009). Excessive ROS, such as hydroxyl radicals, perioxynitrite, hydrogen peroxide and superoxide anions, damage proteins (particularly OXPHOS enzymes), lipid membranes and both mitochondrial and nuclear nucleic acids (Rogge, 2009). Accumulation of fatty acids in the cytosol activates β-oxidation in peroxisomes and ω-oxidation in microsomes (Rogge, 2009). Such ω-oxidation can damage mitochondria via uncoupling oxidative phosphorylation and disturbance of the mitochondrial membrane proton gradient (Rogge, 2009). Additionally, in obesity, mitochondria are overloaded with excess fatty acids and glucose, which leads to a greater production of acetyl-CoA and subsequently to increased NADH concentrations formed by the Krebs cycle (de Mello et al., 2018). This increases the availability of electrons to the mitochondrial respiratory chain complexes and production of ROS, which results in the activation of transcription factors, i.e. NFκB, which regulate the inflammatory response (de Mello et al., 2018).

25

1.4.4 Effects of weight loss on mitochondrial structure and function

Evidence from animal models and human studies demonstrates that nutrient and energy restriction and/ or weight loss improve capacity, integrity, biogenesis and function of mitochondria (Breininger et al., 2019).

Findings from human studies which report effects of energy depletion and weight loss on structure and function of mitochondria are summarised in Table 1-3 and discussed in more detail below.

A negative energy balance of 25% (induced either by dietary energy restriction or dietary restriction plus increased energy expenditure via exercise) leads to increased gene expression (*TFAM, PPARGC1A, PARL, eNOS* and *SIRT1*- all of which are involved in mitochondrial function), higher mtDNA content, but did not affect the enzyme activity of mitochondria (β-hydroxyacyl-CoA dehydrogenase for β-oxidation, citrate synthase for TCA cycle and cytochrome c oxidase II for the electron transport chain) in muscle of 36 young overweight people (Civitarese et al., 2007). A mean 8.5kg weight loss following a diet plus exercise intervention improved mitochondrial content, aerobic capacity and reduced the size of mitochondria in skeletal muscle, however the diet only intervention, which achieved a 10.6kg weight loss, showed no effects (Toledo et al., 2008). The observed effects on mitochondria following the diet plus exercise intervention might not be a result of weight loss *per se* but due to the independent and synergistic effects of exercise on mitochondria as opposed to reduction in dietary energy only (Toledo et al., 2008).

The following human studies describe the effects of weight loss following bariatric surgery. Expression of a vital mitochondrial fusion protein which enables the integrity of the mitochondrial network, namely Mfn2, was reduced in skeletal muscle of obese subjects (Bach et al., 2005). A significant increase in Mfn2 expression was observed after a 25 kg/m^2 unit fall in BMI (leading to a mean BMI of 31 kg/m^2) following bilio-pancreatic diversion surgery two years post-operatively, which is indicative of Mfn2 expression being inversely proportional to body weight (Bach et al., 2005). 101 RYGB patients were assigned either to a health education control or exercise intervention; a mean 23.6kg weight loss was achieved by RYGB plus the exercise intervention at 6 months follow-up, which resulted in improved respiration of mitochondria in vastus lateralis muscle (Coen et al., 2015). Even though the other intervention arm (RYGB plus health education) resulted in a comparable weight loss of mean 22.1kg (to

the RYGB plus exercise intervention), it did not affect respiration of mitochondria (Coen et al., 2015). Interestingly, neither intervention arm demonstrated a modification in OXPHOS content and all participants continued to be obese with a mean BMI of 30.4 kg/m^2 at follow-up (Coen et al., 2015); it remains to be discovered if the effects were due to weight loss *per se.* Another study reported that a mean 25.5kg weight loss following RYGB increased coupled respiration in vastus lateralis muscle in 11 obese females 6 months post-operatively (Fernstrom et al., 2016). Nevertheless, no effects on uncoupled respiration (oxygen consumption without ADP phosphorylation) and respiratory control index (a quality measure of isolated mitochondria) were seen and, even though participants accomplished a significant weight loss, they stayed overweight after surgery (mean BMI 29.6 kg/m^2) (Fernstrom et al., 2016). This research reveals that significant and sustained weight loss by bariatric surgery leads to higher levels of the mitochondrial fusion protein Mfn2 and improved coupled respiration of mitochondria in muscle (Bach et al., 2005, Civitarese et al., 2007, Toledo et al., 2008, Coen et al., 2015, Jahansouz et al., 2015, Moreno-Castellanos et al., 2016, Fernstrom et al., 2016).

A 7.5-day short term effect of RYGB in 8 patients and adjustable gastric banding in 8 patients was studied (Jahansouz et al., 2015). Even though the weight loss achieved, a mean 0.9 kg/m^2 decline in BMI, was non-significant and small, an increase in *TFAM, CYT C, eNOS, NRF1* and *PGC-1α* expression was detected (Jahansouz et al., 2015). These genes are involved in biogenesis of mitochondria and protein carbonylation, an indicator of oxidative stress, and were found to be reduced in adipose tissue (Jahansouz et al., 2015). These changes were revealed after RYGB but not seen after adjustable gastric banding (Jahansouz et al., 2015). Bariatric surgery results in prompt and enhanced glycemic control, even before weight loss occurs, being indicative that the reported changes in the expression of genes may be a result of metabolic changes associated with bariatric surgery as opposed to weight loss alone (Breininger et al., 2019). 18 obese women were assigned to either an insulin resistant or a normoglycemic group prior to bariatric surgery. Later, at 13 months follow-up, a reduction in PGC-1α and mitofilin concentrations was found in the adipose tissue of the normoglycemic group, which had achieved a 14.2 kg/m^2 unit reduction in BMI, while a modification in the opposite trend for PGC-1α and mitofilin concentrations was revealed in the insulin resistant group, which attained a 17.5 kg/m^2 unit reduction in BMI (Moreno-Castellanos et al., 2016).

It is therefore possible to conclude that the effects of weight loss following surgery on function of mitochondria may be dependent on the original metabolic status (Moreno-Castellanos et al., 2016). Another study reported increased numbers of mitochondria and smaller adipocytes in 19 obese individuals who attained a mean 33% weight loss following RYGB one year post-operatively (Camastra et al., 2017). Many studies demonstrate that sustained and significant weight loss achieved by bariatric surgery leads to upregulated expression of genes coding for function, biogenesis and dynamic of mitochondria, a higher number of mitochondria and a decline in oxidative stress (Jahansouz et al., 2015, Moreno-Castellanos et al., 2016, Fernstrom et al., 2016, Camastra et al., 2017, Martinez de la Escalera et al., 2017).

Study	Tissue	Weight-loss Intervention	Key Findings
(Bach et al., 2005)	Skeletal muscle	Bilio-pancreatic diversion	Increased Mfn2 expression
(Civitarese et al., 2007)	Muscle	Dietary energy restriction with/ without increased physical activity	Increased expression of *PARGC1A, TFAM, eNOS, SIRT1* and *PARL* and increased mtDNA content
(Toledo and Goodpaster, 2013)	Skeletal muscle	Dietary energy restriction with/ without increased	No change in diet-only group Increased mtDNA and NADH-oxidase activity, improvement in aerobic capacity and mitochondrial content in the diet plus exercise group

		physical activity	
(Coen et al., 2015)	Vastus lateralis muscle	RYGB with exercise intervention or health education	Increased OXPHOS proteins, NADH oxidase, citrate synthase, creatine kinase and cardiolipin in the RYGB with exercise intervention
(Jahansouz et al., 2015)	Subcutaneous adipose tissue	RYGB	Improved mitochondrial biogenesis via increased concentrations of *PGC-1α, NRF1, CYT C, TFAM* and *eNOS*; reduced protein carbonylation
(Moreno-Castellanos et al., 2016)	Subcutaneous adipose tissue	Bariatric surgery	No effect in normoglycemic women, increased PGC-1α and reduced mitofilin in initially insulin resistant women
(Fernstrom et al., 2016)	Vastus lateralis muscle	RYGB	Increased coupled and uncoupled respiration, oxidative phosphorylation ratio and citrate synthase activity
(Camastra et al., 2017)	Muscle and adipose tissue	RYGB	Adipocytes became smaller and richer in mitochondria

Table 1-3: The effects of weight loss on mitochondrial structure and function in obese individuals (Breininger et al., 2019)

Studies researching the effect of weight loss following bariatric surgery to date, have merely concentrated on effects in adipose and muscle tissue, and more investigations in other tissues are required (Breininger et al., 2019). The above investigations differed in the type of bariatric surgery procedure, length of follow-up (7.5 days to 13 months) and weight loss or decline in BMI attained (11.6kg to 25.5kg and, 0.9-25 kg/m^2 unit fall in BMI, respectively) and these variations in study design could clarify the lack of results' consistency on function and structure of mitochondria seen (Breininger et al., 2019). All participants of the earlier discussed studies continued to be overweight and/ or obese post-operatively and evidence of the effect of weight loss resulting in patient's normal weight on measured mitochondrial outcomes is missing, which is an important limitation (Breininger et al., 2019). In addition, exercise might provide further mitochondrial benefits, besides those seen by weight loss *per*

se, however this is beyond the scope of this thesis and will not be elaborated here. Evidence of weight loss either by dietary intervention or bariatric surgery, resulting in increased PGC-1α and fusion protein concentrations and reduced oxidative stress, is consistent and convincing (Breininger et al., 2019). An increase in *eNOS* and *TFAM* expression following an exercise and dietary intervention, as well as RYGB in human individuals, was detected, suggesting enhanced capacity of mitochondria (Breininger et al., 2019). An increase in gene expression of proteins coding for the respiratory transport chain following weight loss was reported, but there is a lack of evidence on the effects of enzyme activity (Breininger et al., 2019). The effects of bariatric surgery have been predominantly studied in females and established differential mitochondrial gene expression and increased mitochondrial respiration resulting in enhanced function of mitochondria (Breininger et al., 2019). I am unaware of investigations on the effects of weight loss on already existing mtDNA damage. The evidence on higher mtDNA content following weight loss is limited in both animal and human studies (Breininger et al., 2019). Overall, some evidence of weight loss leading to enhanced mitochondrial function and structure exists, however more investigations are warranted to reach strong and consistent conclusions on to date's limited findings.

1.4.5 Possible mechanisms underlying the effects of weight loss on mitochondrial function

There is evidence that dietary energy and nutrient restriction (either through fasting, dietary energy restriction or greater exercise levels) result in an increase of cAMP concentrations and AMP:ATP ration which then initiates the AMPK, PKA/CREB and SIRT1 signalling pathways, and hence lead to PGC-1α activation (Handschin and Spiegelman, 2006, Cheng and Almeida, 2014a). The key mitochondrial biogenesis regulator, namely PGC-1α, initiates downstream targets like *NRF1*, *NRF2* and *TFAM* leading subsequently to the upregulation of mitochondrial biogenesis and activity (Cheng and Almeida, 2014a).

1.4.6 Effects of microRNAs on adipogenesis

Many studies recognise the potential functional role of miRNAs in obesity, metabolism and energy homeostasis. Adipogenesis is a complex process tightly regulated by multiple extracellular hormones and transcription factors, however the precise mechanism remains unknown (Heneghan et al., 2010). MiRNAs have been proposed to play a vital role during the process of adipogenesis, predominantly due to their ability to simultaneously regulate numerous target genes via one single miRNA (Heneghan et al., 2010). Data derived mainly

from mouse models showed that miRNAs affect adipocyte differentiation and hence the pathological development of obesity (Esau et al., 2004, Lin et al., 2009, Xie et al., 2009). For example, miR-103 expression was induced about 9-fold during adipogenesis in an adipose-like cell line (3T3-L1), which was accompanied by an increased expression of transcription factors and regulatory molecules, including PPARγ2, G0s2, GLUT4, FABP4 and adiponectin (Xie et al., 2009). Furthermore, computational target prediction has shown that miR-103 targets many mRNAs in pathways involved in cellular lipid metabolism and acetyl-CoA (Heneghan et al., 2010). Kloting (2009) studied whether the expression of miRNAs in human adipocytes is fat-depot specific, subcutaneous or intra-abdominal omental, and whether it is linked with metabolic parameters of obesity, by profiling global miRNA gene expression in 15 individuals with normal glucose tolerance (n=9) or type 2 diabetes (n=6). Out of a panel of 155 miRNAs, 106 (68%) miRNAs were identified in both the subcutaneous and omental adipose tissue, and no miRNA was solely expressed in either fat depot, suggesting mutual developmental origin and miR-17-5p, miR-99a, miR-132, miR-134, miR-145, miR-181a and miR-197 expression were significantly correlated with morphology of the adipose tissue and metabolic parameters of obesity (such as fasting plasma glucose, HbA(1c) and circulating adiponectin, leptin and IL-6) (Kloting et al., 2009). MiR-143 has also been identified to play a key role in adipocyte differentiation (Heneghan et al., 2010). An inverse pattern of miRNA expression in differentiating adipocytes and obese tissue has been observed, showing that obesity can result in a loss of miRNAs that describe fully metabolically active and differentiated adipocytes (Heneghan et al., 2010). It is believed that these modifications occur due to chronic inflammation present in obese adipose tissue (Heneghan et al., 2010). MiR-145 targets the 3'-UTR of *IRS1* gene in human colon cancer cells, causing the downregulation of the IRS-1 protein, leading to the inhibition of cancer cell growth (Shi et al., 2007). The observed inverse miRNA expression patterns during the differentiation of adipocytes and in the adipose tissue suggest that adiposity results in a loss of miRNAs, which characterise completely differentiated and metabolically active adipocytes, which may be due to the chronic inflammatory environment induced by obesity (Heneghan et al., 2010).

A review by Heneghan (2010) identified various miRNAs whose expression was altered during obesity including miR-9, miR-17-5p, miR-29a/ b, miR-99a, miR-103, miR-122, miR-124a, miR-132, miR-133, miR-143, miR-145, miR-192 and miR-375 with their functional role being

adipocyte differentiation, proliferation, growth, clonal expansion, glucose transport, insulin resistance, fatty acid and amino acid metabolism, cholesterol biogenesis, cellular stress, pancreatic islet development and their main target tissue being adipose, liver and pancreas. A more recent review, identified a vast list of adipogenesis promoting miRNAs including miR-17, miR-21, miR-26b, miR-30, miR-103, miR-143, miR-146b, miR-148a, miR-181, miR-199a, miR-204, miR-210, miR-320, miR-371, miR-375, miR-378 and miR-637 and miRNAs that interfere with adipocyte differentiation including let-7, miR-15a, miR-22, miR-27a/b, miR-31, miR-33b, miR-93, miR-125a, miR-130, miR-138, miR-145, miR-155, miR-193a/b, miR-194, miR-221, miR-222, miR-224, miR-344, miR-363, miR-365, miR-369, miR-448 and miR-709 (Iacomino and Siani, 2017). In association with adipogenesis, miR-130 and miR-143 are widely studied; miR-143 is a positive regulator during differentiation of adipocytes and acts through the ERK5 signalling pathway and its increased expression prevented insulin-stimulated AKT activation and homeostasis of glucose (Iacomino and Siani, 2017). MiR-130a, together with miR-27a, have demonstrated to impair adipocyte differentiation via downregulation of PPARγ (Iacomino and Siani, 2017). The polycistronic miR-17-92 cluster, encoding for miR-17, miR-18a, miR-19a, miR-20a, miR-19b-1 and miR-92a, has been reported to be overexpressed during the clonal expansion of adipocytes and represses the RB family Rb2/p130, hence regulating the RB-E2F pathway (Iacomino and Siani, 2017). MiR-363 has also been reported to regulate the same pathway and impair differentiation of adipocytes through E2F and downregulation of PPARγ and C/EBPα (Chen et al., 2014a). Additionally, adipogenesis is negatively regulated by let-7, which controls high-mobility group AT-hook2 expression (Iacomino and Siani, 2017). In the 3T3-L1 cell line model of adipogenesis, let 7 has been found to be upregulated and, reduced the clonal expansion and terminal differentiation, indicating its anti-adipogenic properties (Sun et al., 2009). Additionally, a mouse model demonstrated that let-7 is involved in insulin resistance and glucose metabolism targeting molecules affecting the insulin/IGF-1R pathway (Zhu et al., 2011). Also, miR-375 promotes 3T3-L1 adipocyte differentiation by increasing C/EBPα and PPARγ mRNA concentrations and by promoting accumulation of triglycerides and adipocyte fatty acid-binding protein and contrarily has been found to suppress ERK1/2 phosphorylation in 3T3-L1 cells (Ling et al., 2011). Recently, Thomou (2017) indicated the adipose being the major source of circulating miRNAs and its potential mechanistic implications of cell-cross talk, for example by regulating gene expression in remote organs. However, as miRNAs may modulate numerous pathways

and genes simultaneously, more research is warranted to define the precise mechanism by which miRNAs modulate obesity and its potential role in therapeutic strategies of the latter.

1.4.7 Effects of weight loss on microRNA expression

Multiple studies have investigated the effect of weight loss, either by lifestyle interventions or bariatric surgery, on miRNA expression and found a modulated profile of miRNA expression. There is some evidence that significant and sustained weight loss by bariatric surgery improved and recovered miRNA expression.

The following human studies describe the effects of weight loss following a diet and/ or exercise intervention on miRNA expression. To date, the majority of studies looked at the effect of weight loss on miRNAs in blood. An 8-week dietary energy restriction (provision of 800-880 kcal/d) found differential baseline miRNA in non-responders (<5% of initial body weight loss achieved, n=5) and responders (>5% of initial body weight loss achieved, n=5) namely, miR-935 and miR-4772 were upregulated and miR-223, miR-224 and miR-376b were downregulated in peripheral blood mononuclear cells in 10 obese females; baseline miR-935 and miR-4772 was associated with the magnitude of weight loss achieved (Milagro et al., 2013). Another study investigated the reproducibility of miRNAs on the effect of diet-induced weight loss on a panel of miRNAs initially identified in a cohort following weight loss by bariatric surgery, and found that mean 17% of initial body weight loss (5.7 kg/m^2 unit fall in BMI) showed no significant associations with circulating miR-15a, miR-126, miR-520c-3p, miR-590-5p, miR-625 and miR-636 in 9 obese individuals, who had a mean baseline BMI of 34.4 kg/m^2 (Ortega et al., 2013). Marques-Rocha (2016) studied the effect of weight loss following an 8-week dietary intervention on a selected panel of 9 inflammatory miRNAs in white blood cells (WBC) of 40 obese subjects (mean BMI 35.4 kg/m^2). Although participants remained obese, a mean 7.1kg weight loss following a 30% energy restriction based on the Mediterranean dietary pattern significantly decreased WBC levels of miR-155-3p and increased let-7b (Marques-Rocha et al., 2016). A 12-week dietary intervention, comparing a high protein diet and normal protein diet, 30% and 20% protein of energy, respectively, investigated the effect of weight loss on HDL-associated miRNAs in serum, namely miR-16, miR-17, miR-126, miR-222 and miR-223 in 47 obese subjects (mean BMI 32.7 kg/m^2) (Tabet et al., 2016); the high protein diet resulted in a mean 9kg weight loss and significant

downregulation of miR-223, which was also positively correlated with modulation in body weight (Tabet et al., 2016). Another study by Parr (2016) investigated the effect of a 16-week weight loss intervention (reduction of 250kcal/ day by dietary energy restriction + 250kcal reduction by exercise) on circulating miRNAs in low (n=18, mean baseline BMI 33.6 kg/m^2, mean 3kg weight loss) and high (n=22, mean baseline BMI 31.9 kg/m^2, mean 11kg weight loss) responders; miR-935 expression was higher in low responders compared with high responders at baseline and follow-up, by 47% and 100%, respectively. Furthermore, miR-140 was upregulated by 23% following weight loss in low responders only, miR-221-3p and miR-223-3p were upregulated post-intervention in both groups (Parr et al., 2016). Following a 1 week weight maintenance eucaloric diet, Margolis (2017) studied the effect of a 28 day 30% dietary energy restriction which attained a mean 1.4 kg/m^2 unit fall in BMI on a selected panel of miRNAs (miR-1, miR-133a-3p, miR-133b and miR-206) and found that circulating miR-133a and miR133b were upregulated in 16 older overweight men. Another intervention study investigating the effect of weight loss on plasma miR-146a-5p and miR-126 in 31 obese patients, mean BMI 35.6 kg/m^2, whose miR-146a-5p expression levels were significantly upregulated compared with lean controls (n=37), showed that a 3-month physical activity program (90min aerobic and endurance training administered twice a week) resulting in a 4.2kg weight loss and 1.6 kg/m^2 unit fall in BMI, subsequently significantly downregulated miR-146a-5p in 2/3 of the participants; miR-146a-5p post-intervention expression levels were comparable to those of the lean controls (Russo et al., 2018). Recently, Giardina (2019) studied the effect of 3 dietary energy restrictions including i) moderate-carbohydrate and low glycemic index (LGI), ii) moderate-carbohydrate and high glycemic index (HGI) and iii) low-fat and high glycemic index (LF) on circulating miRNAs in 103 participants before and after the dietary intervention. Data demonstrated that circulating miR-361 expression was lower in the LGI (mean 7.2kg weight loss achieved) compared with the HGI group (mean 7.1kg weight loss achieved), and that miR-139 and miR-340 were downregulated following the HGI, but miR-139, miR-423 and miR-432 were downregulated following the LF (mean 4.3kg weight loss achieved) (Giardina et al., 2019).

To date, only one study looked at the effect of weight loss by a lifestyle intervention on miRNA expression in the adipose tissue. A 15-week weight loss intervention consisting of a hypocaloric diet and moderate daily exercise, resulted in a mean 17kg weight loss and 5.6 kg/m^2 unit fall in BMI, which upregulated miR-29a-3p and -5p and, downregulated miR-20b-

5p in subcutaneous adipose tissue of 19 obese individuals whose mean baseline BMI was 47.1 kg/m^2 (Kristensen et al., 2017).

The following human studies describe the effects of weight loss following bariatric surgery. A retrospective study demonstrated that, in 21 morbidly obese who underwent bariatric surgery, miR-181a, miR-181b and miR-181d quantified in monocytes were significantly downregulated compared with lean controls and normalised following weight loss 3 months post-operatively (mean 8 kg/m^2 unit fall in BMI) (Hulsmans et al., 2012). Ortega (2013) revealed that a mean 30% weight loss (of initial body weight, 37.4kg reduction and 14 kg/m^2 unit fall in BMI) by bariatric surgery significantly downregulated circulating miR-16-1, miR-19b-1, miR-122, miR-125b, miR-140-5p, miR-142-3p, miR-199a-3p and miR-483-5p and, upregulated miR-21, miR-146a, miR-221, miR-130b and miR-423-5p one year post-operatively in 22 morbidly obese patients. Lirun (2015) investigated the effect of RYGB on serum miRNAs in 15 type 2 diabetic patients with low BMI (≤30 kg/m^2 n=7) and high BMI (≥30 kg/m^2 n=8) using an Affymetrix GeneChip miRNA Array. A vast list of serum miRNAs were significantly modulated following weight loss by RYGB after 2 months, out of which 39 miRNAs showed a fold change of ≥1.5 or ≤2/3. More specifically, in both the low and high BMI group, where a 4.4 kg/m^2 and 6.5 kg/m^2 unit fall in BMI was achieved, respectively, let-7, miR-23a/b, miR-24, miR-26a, miR-93, miR-103a, miR-146a, miR-151-3p, miR151-5p and miR-425 were downregulated and miR-1281, miR-1825 and miR-4787-5p upregulated (Lirun et al., 2015). Global miRNA profile analysis was performed in 6 obese African-American females (mean BMI 51.2 kg/m^2) who underwent gastric bypass and achieved a mean 49.5kg weight loss and 18.6 kg/m^2 unit fall in BMI one year post-operatively. This study revealed 168 differentially expressed miRNAs in circulating adipocyte derived exosomes, whose top predicted targeted pathways were the Wnt-β catenin pathway and the insulin receptor signalling pathway (Hubal et al., 2017). Another study researched the effect of an exercise intervention following RYGB on plasma miRNAs in 22 severely obese subjects, who were recruited 1-3 months post-surgery an allocated to either an intervention arm with an exercise program (n=11, mean baseline BMI 39.5 kg/m^2) or without one (n=11, mean baseline BMI 40.8 kg/m^2) and followed-up 6-months later (Nunez Lopez et al., 2017). This study showed that 27.7kg weight loss and 10.2 kg/m^2 unit fall in BMI by RYGB only, significantly upregulated miR-7, miR-15a and miR-106 and downregulated miR-34a, miR-122 and miR-221. In contrast, a 25kg weight loss and 9.3 kg/m^2

unit fall in BMI by RYGB plus the exercise intervention significantly upregulated miR-15a and miR-149 and downregulated miR-34a, miR-122, miR-135b, miR-144 and miR-206 (Nunez Lopez et al., 2017). Alkandari (2018) studied the effect of weight loss following RYGB on circulating plasma miRNA expression at 1 month, 3 months, 6 months, 9 months and 1 year in 9 obese (mean baseline BMI 49 kg/m^2 and mean BMI at 1y follow-up 30.7 kg/m^2) and found that expression of 48 miRNAs, involved in pathways of regulation and rescue from metabolic dysfunction which were correlated with BMI, was modulated in a time dependent manner. Out of a panel of 7 miRNAs only miR-10a-5p was significantly upregulated in circulating mononuclear cells following a 46kg weight loss and 16 kg/m^2 unit fall in BMI by RYGB at 2 year follow-up in 58 morbidly obese patients (Hohensinner et al., 2018).RYGB induced weight loss resulting in a 13.9 /m^2 unit fall in BMI 2 years post-operatively revealed differential expression of 15 miRNAs in adipose tissue of 16 morbidly obese (mean baseline BMI 43.1 kg/m^2) when compared with 26 age-matched lean females (BMI 24.2 kg/m^2), more specifically miR-130b, miR-155, miR-221 and miR-339 were significantly downregulated post-surgery and significantly different when compared to lean controls whose expression levels of those miRNAs was even lower (Ortega et al., 2015a). Another study found that miR-155, miR-221 and miR-222 were significantly downregulated 2 years post-bariatric surgery in subcutaneous adipocytes of 9 obese females (Ortega et al., 2015b). In three obese females, weight loss by laparoscopic adjustable gastric banding (mean baseline BMI 42.9 kg/m^2, 10.9 kg/m^2 unit fall in BMI) upregulated miR-370 and miR-487a and downregulated miR-212, miR-229-5p, miR-519d and miR-671-3p in subcutaneous adipose tissue 3 years post-operatively compared with two lean controls (mean BMI 21.5 kg/m^2) (Nardelli et al., 2017). Another study investigated the baseline miRNA signature in visceral fat (VF) and subcutaneous fat (SF) of the adipose tissue in 20 bariatric-surgery patients (mean BMI 42.4 kg/m^2) and 8 non-obese (mean BMI 24.6 kg/m^2) and showed differential miRNA profiles in obese SF and VF; more specifically miR-122 showed significantly higher expression in VF of obese, which was correlated with % excess body weight loss at 6-month and 1-year post bariatric surgery (Liao et al., 2018).

Studies researching the effect of weight loss on miRNA expression following lifestyle interventions to date, have merely concentrated on effects in the blood, only one study has researched the adipose tissue and, I am unaware of any human studies in the colon, and more investigations in other tissues are required. Weight loss in all discussed studies modulated the expression of a wide range of miRNAs, and two studies found that miR-223 was

downregulated (Milagro et al., 2013, Tabet et al., 2016) and one found that it was upregulated (Parr et al., 2016). The above studies differed in lifestyle intervention type, length of follow-up (28 days- 16 weeks) and weight loss and decline in BMI achieved (which ranged between 3-11kg and a 1.4-5.7 kg/m^2 unit fall in BMI, respectively). These variations in study design could clarify the lack of results' consistency on miRNA expression.

Whereas studies investigating the effect of weight loss on miRNA expression following bariatric surgery to date, have merely concentrated on effects in the blood and adipose tissue and, I am unaware of any human studies in the colon, and once more investigations in other tissues are warranted. Weight loss in all discussed studies modulated the expression of a wide range of miRNAs, and found some consistent and some conflicting results for specific miRNAs. More specifically, two studies found that weight loss downregulated miR-122 (Ortega et al., 2013, Nunez Lopez et al., 2017) and contrarily one study found that it was correlated with excess body weight (Liao et al., 2018). Similarly, one study revealed that weight loss upregulated miR-146a (Ortega et al., 2013), whereas another found it to be downregulated (Lirun et al., 2015). Finally, one study demonstrated that weight loss resulted in the upregulation of miR-221 (Ortega et al., 2013), but in contrast 3 other studies revealed the opposite direction of miR-221 expression (Nunez Lopez et al., 2017, Ortega et al., 2015a, Ortega et al., 2015b). Once again, the above studies differed in bariatric surgery type, length of follow-up (6 months- 3 years) and decline in BMI attained (10.9- 13.9 kg/m^2 unit fall). These variations in study design could explain the lack of consistency in the data on miRNA expression, although, compared with the studies investigating lifestyle intervention, a trend for more consistent miRNA expression could be seen (miR-122, miR-146a and miR-221) which might be due to the fact that bariatric surgery is the most successful intervention in achieving sustained weight loss.

Furthermore, all participants of the earlier discussed studies continued to be overweight and/ or obese following both lifestyle interventions and bariatric surgery studies and evidence of the effect of weight loss resulting in participants returning to their normal weight on miRNA expression is missing, which is an important limitation.

The level of miRNA expression differs considerably between studies. Reason for this variation may include the different miRNA quantification methods used and the different tissue of interest in which the miRNA expression was measured. Across these studies, 6 different

miRNA quantification methods were used including a microarray (Hulsmans et al., 2012), TaqMan low-density array and qRT-PCR (Ortega et al., 2013, Ortega et al., 2015b, Nardelli et al., 2017), Real time PCR (Nunez Lopez et al., 2017), Affymetrix GeneChip miRNA Array (Lirun et al., 2015, Hubal et al., 2017, Ortega et al., 2015a), Exiqon miRCURY locked nucleic acid and PCR (Alkandari et al., 2018) and RT-qPCR (Hohensinner et al., 2018). The issues of interest in which miRNA expression was measured included monocytes (Hulsmans et al., 2012), surrogate such as plasma and serum (Ortega et al., 2013, Nunez Lopez et al., 2017, Lirun et al., 2015, Alkandari et al., 2018, Hubal et al., 2017, Hohensinner et al., 2018) and adipose tissue (Ortega et al., 2015a, Ortega et al., 2015b, Nardelli et al., 2017). These between study differences (i.e. in assay used and tissue specificity) are a potential limitation when comparing studies.

1.5 Links between adiposity, mitochondria, microRNAs and colorectal cancer risk

Obesity affects mitochondrial biogenesis, function and dynamics via epigenetic mechanisms (see Figure 1-8) (Cheng and Almeida, 2014b) and, in particular, miRNAs regulate the function and dynamics of mitochondria in the obese (Sun et al., 2011, Bolmeson et al., 2011, Zhang et al., 2013). For example, Sun (2011) demonstrated that miR-15a promoted the synthesis and secretion of insulin by targeting and silencing the mitochondrial uncoupling protein UCP2, which in turn increased oxygen consumption and reduced ATP production. MiR-106b is greatly over-expressed in the skeletal muscle of obese diabetic patients (Gallagher et al., 2010). The 3'-UTR of Mfn2, a mitochondrial dynamic and network regulator, has binding sites for miR-106b (Zhang et al., 2013) and binding of the miRNA suppresses Mfn2 expression which impairs mitochondrial function. In contrast, downregulation of miR-106b enhances mitochondrial function and sensitivity to insulin (Zhang et al., 2013). Further, miR-184, which regulates insulin secretion, may do that by repressing Slc25a22, which is a mitochondrial glutamate carrier controlling cytosolic glutamate and insulin granule activity as well as the activity of secretory vesicles during exocytosis of insulin (Bolmeson et al., 2011).
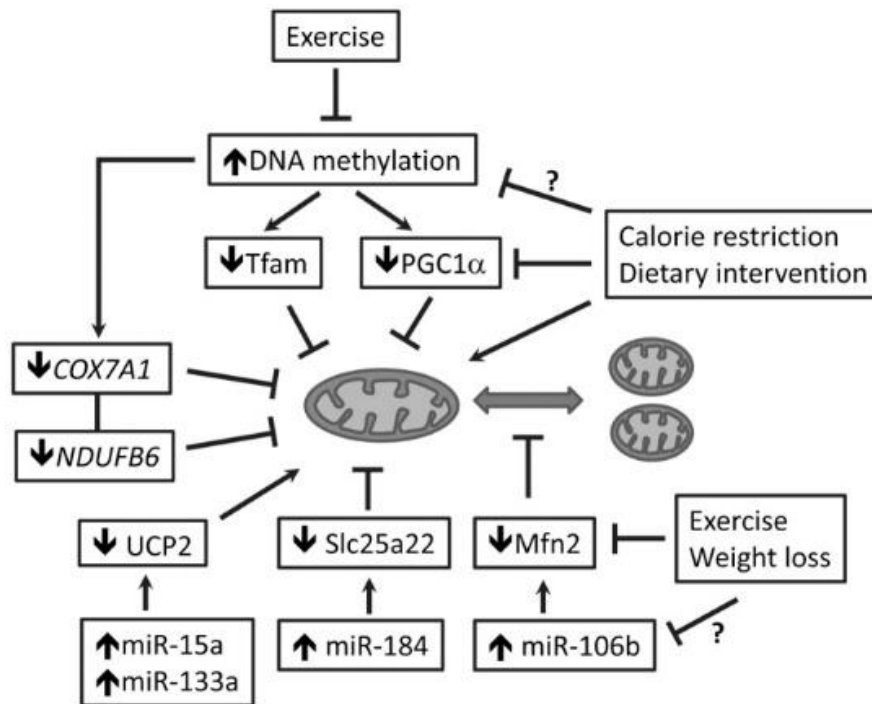
Figure 1-8: Epigenetic mechanisms affecting mitochondrial function in people with obesity (Cheng and Almeida, 2014b) (Copyright: figure is open-access).

As summarised earlier in this chapter (section 1.1.3), obesity is a major risk factor for CRC. There is evidence that obesity modulates CRC risk via epigenetic effects, and that these epigenetic changes are improved or even reversed following weight loss. Furthermore, there is evidence that obesity results in dysfunctional mitochondria. However it remains to be discovered if obesity modulates CRC risk via effects on the mitochondria; or whether dysfunctional mitochondria are a result of CRC itself. More research is warranted to clarify whether i) epigenetic regulation via miRNAs, can affect the expression of mitochondrial genes and generation of mitochondrial proteins (i.e. OXPHOS proteins) and ii) if such an epigenetic regulation will affect the morphology, respiration and function of mitochondria. Furthermore, more research is required to establish whether an interaction between miRNAs and mitochondria during obesity plays a role in the development of CRC (Figure 1-9). Additionally, more studies are needed to uncover epigenetic mechanisms responsible for regulating networking, biogenesis and function of mitochondria. And finally, if the latter is the case, there is a need to discover whether lifestyle modification and behavioural interventions leading to sustained weight loss reverse or prevent epigenetic dysregulation of mitochondrial metabolism and function and, in so doing, reduce CRC risk.
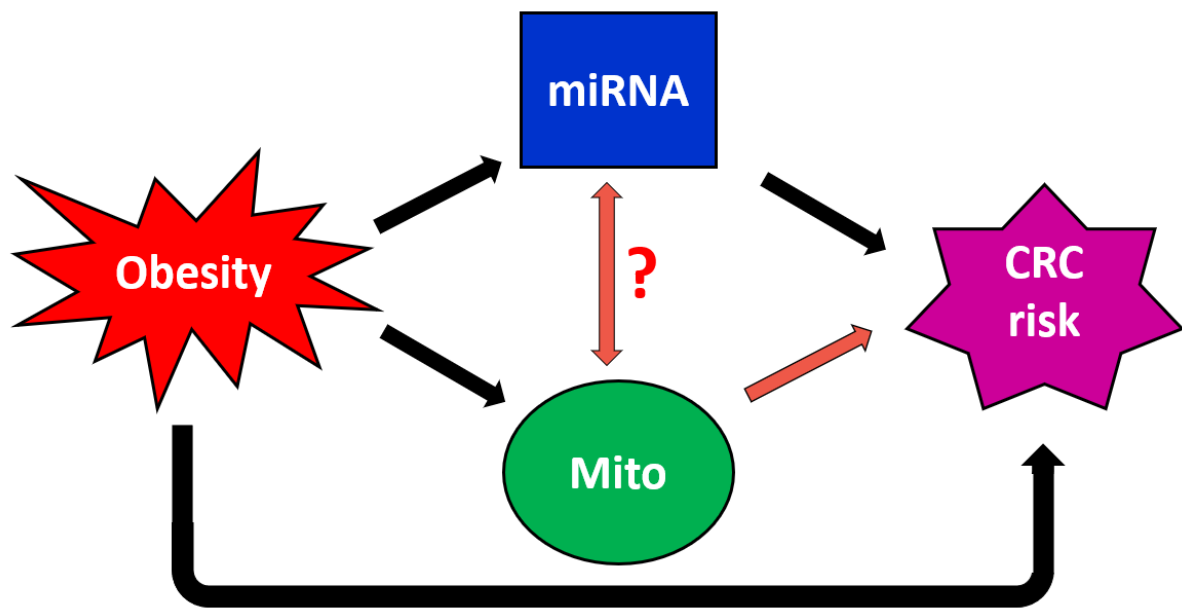
Figure 1-9: Conceptual hypothesis for effects of obesity on CRC risk illustrating the potential epigenetic link and interactions between miRNA regulation and mitochondrial function

1.6 Hypotheses, Aims and Objectives

I hypothesise that i) biomarkers of CRC risk are elevated in obese compared with normal weight participants; and ii) weight loss in the obese has beneficial effects on these biomarkers of CRC risk. I also hypothesise that these obesity-related biomarkers of CRC risk are exacerbated by ageing.

My project aims to test these hypotheses by addressing the following objectives:

1st Objective: To investigate the links between obesity, mitochondrial oxidative phosphorylation proteins and mitochondrial DNA mutations in the colorectal mucosa and to investigate the effects of surgically-induced weight loss in the obese on these associations using samples and data from the Biomarkers Of Colorectal cancer After Bariatric Surgery (BOCABS) Study.

2nd Objective: To investigate the links between obesity and epigenetic markers, namely miRNA expression, in the colorectal mucosa and to investigate the effects of surgically-induced weight loss in the obese on these associations using samples and data from BOCABS Study.

3rd Objective: To investigate the links between adiposity, ageing and epigenetic markers, namely microRNA expression, in the colorectal mucosa of aged participants, by performing a 12+ year follow-up in the participants from the Biomarkers Of RIsk of Colorectal Cancer (BORICC) Study, namely BORICC Follow-Up (BFU) Study.

4th Objective: To investigate the links between obesity, weight loss, epigenetic regulation, namely miRNA expression, and mitochondrial function or dysfunction in the colorectal mucosa using the samples and data from BOCABS Study.

2   Methods

All procedures were carried out by myself, unless stated otherwise.

2.1   Human Studies

2.1.1   Overview of Biomarkers of Colorectal Cancer after Bariatric Surgery (BOCABS) Study

2.1.1.1   *Participant recruitment and sample collection*

The Biomarkers Of Colorectal cancer After Bariatric Surgery (BOCABS) Study was an observational study investigating biomarkers of CRC risk after bariatric surgery in a prospective cohort of obese adults listed for a bariatric surgery at the North Tyneside General Hospital (NTGH). In addition, healthy non-obese participants were recruited as a control group from patients listed for a rigid sigmoidoscopy or colonoscopy at NTGH. The BOCABS Study was conducted by Dr Sorena Afshar under the supervision of Prof John Mathers. Participants were checked for suitability (exclusion criteria are shown in Appendix A) and written informed consent was obtained. Obese participants underwent bariatric surgery and colorectal mucosal biopsies, anthropometric and body composition measurements were collected at baseline and, again, at six months post-surgery. Additional biological samples including duodenal biopsies, urine, stool and blood and other data including Food Frequency Questionnaire, Lifestyle Questionnaire, Bowel Habit Diary, physical activity by both questionnaire and accelerometry were also collected, but these samples and data were not utilised in the present project.

Ethical approval was obtained from the NRES Committee, North East - Newcastle and North Tyneside 2 (13/NE/0204) and the project was recorded on the ISRCTN register under the following code: ISRCTN95459522. As the BOCABS participants had consented for usage of their samples for future research studies, no further ethical approval was required.

Additionally, questionnaire and anthropometric data and rectal biopsies from a further eight non-obese healthy participants who had been recruited to The Dietary Intervention, Stem cells and Colorectal cancer (DISC) Study (registered under NCT01075893) were used to increase the sample size of the control group for the BOCABS Study. Inclusion and exclusion criteria were very similar and collection of biopsies were in exactly the same manner in the DISC Study and the BOCABS Study. DISC Study participants had consented for usage of their

data and samples for future research studies and no further ethical approval was required. Figure 2-1 shows the overall BOCABS Study design and the subsets of participants used for subsequent analysis of mitochondrial markers and microRNA expression. Justification for the subsets of participants used can be found in the relevant chapters, i.e. Chapter 3 for mitochondrial investigations and Chapter 4 for microRNA investigations. The key inclusion criterion for the non-obese (Control) group was that their BMI was less than 30 kg/m^2. All participants in the Control group fulfilled this criterion. The non-obese Controls used in Chapter 3 had a mean BMI of 25.5 kg/m^2.

BOCABS Study
n=29 pre-surgery
n=29 post-surgery
n=20 non-obese Controls
(n=12 non- obese recruited to
the BOCABS Study + 8 non-obese
recruited to the DISC Study)

Subset of BOCABS Study used for mitochondrial work
n=26 pre-surgery
n=26 post-surgery
n=16 non-obese Controls
(n=9 non- obese recruited to the
BOCABS Study + 7 non-obese recruited
to the DISC Study)

Subset of BOCABS Study used for microRNA work
n=22 pre-surgery
n=22 post-surgery
n=20 non-obese Controls
(n=12 non- obese recruited to the
BOCABS Study + 8 non-obese recruited
to the DISC Study)

Figure 2-1: Overall BOACBS Study design and subsets of participants used for mitochondrial and microRNA work conducted for this thesis

2.1.1.2   Non-laboratory methods

All measurements were made and samples were collected by Dr Sorena Afshar in the presence of a chaperone using standardised protocols, in order to minimise researcher related variability. Further details of relevant methods are presented in (Afshar, 2016b, Afshar et al., 2016, Afshar et al., 2017, Afshar et al., 2018).

2.1.1.2.1 Anthropometric measurements

Anthropometric measurements were taken in the morning after a six hour fast. Participants were requested to wear light indoor clothing, remove shoes and belts and empty their pockets.

Using a stadiometer, height was measured with the head in the Frankfurt horizontal plane. The circumference of the waist was measured at the midpoint between the top of the iliac crest and the lower margin of the palpable rib in the mid axillary line. In obese participants, this anatomical position can be difficult to identify, so participants were asked to find the bottom of their ribs and top of their hips and the midpoint was used for the waist measurement. The hip circumference was measured at the largest gluteal (buttock) muscles when individuals were standing with their feet were slightly parted.

Measurements were recorded in duplicate to the closest millimetre and, if they were not within one centimetre of each other, measurements were repeated. The mean value of duplicates was used.

2.1.1.2.2 Body composition measurements

Body weight and fat percentage were measured using a bioimpedance instrument (*Tanita TBF-300MA Body composition analyser*) and body weight was recorded to the nearest 0.1kg. Body mass index (BMI) was calculated by dividing weight by height squared (kg/m^2).

2.1.1.2.3 Collection of colorectal mucosal biopsies

No bowel preparation was performed before collection of samples, but using a rigid sigmoidoscopy (Sigmolux, Evexar Medical Ltd., UK) the rectum was examined. Ten 2.2mm colorectal mucosal pinch biopsies were collected using Sarratt Disposable Biopsy Forceps (Stericom) in a circumferential manner at 10cm from the anal margin. Seven biopsies were wrapped immediately in aluminium foil straight, snap frozen in liquid nitrogen and subsequently stored at -80°C. The remaining three biopsies processed as follows:

- One biopsy was placed in 10% formalin and subsequently paraffin embedded;
- One biopsy was placed in RNA later and subsequently stored at -80°C;

- One biopsy was placed Carnoy's solution (70% ethanol and 30% acetic acid) for 2-12 hours and then transferred to 70% ethanol and stored at 4°C.

2.1.2 Overview of Biomarkers of Risk of Colon Cancer (BORICC) Study

2.1.2.1 *Participant recruitment and sample collection*

The BORICC Study was conducted by Professor John Mathers and colleagues in 2005- 2009. It was a project designed to develop and validate biomarkers of CRC risk and to investigate their relationships with dietary exposure and nutritional status. Specifically, BORICC1 recruited 268 healthy participants, who were neoplasia-free, had no signs of colonic inflammation or diverticulae and no familial susceptibility to CRC at endoscopy. In addition, a further 100 participants at higher CRC risk, because they had adenomatous polyps, were recruited to the BORICC2 Study. All participants were recruited from the gastroenterology outpatients clinics at Wansbeck General Hospital in Ashington, Northumberland. The participants were phenotyped extensively by recording anthropometric measurements, physical activity, medical history, smoking behaviour and habitual diet and by collecting colorectal mucosal biopsies, buccal swabs, blood and urine samples.

Table 2-1 summarises the participant characteristics of the BORICC1 and BORICC2 groups. Further details of the BORICC Study procedures and findings are reported by (Mathers, 2009, Greaves et al., 2010, Nooteboom et al., 2010, Greaves et al., 2014).

Characteristics	BORICC1 (n=268)	BORICC2 (n=100)
Age (years)	50 (13.5)	58.5 (11.5)
Males (%)	44.8	65
Females (%)	55.2	35
BMI (kg/m^2)	28.3 (5.7)	28.9 (6.6)
Waist (cm)	93.4 (14.9)	95.7 (15.7)
Hip (cm)	104.8 (11.8)	102.5 (14)
W:H ratio	0.9 (0.09)	0.93 (0.08)

Table 2-1: Characteristics of BORICC1 and BORICC2 participants, Mean (SD) (Mathers, 2009)

2.1.3   The BORICC Follow-Up (BFU) Study

2.1.3.1   Participant recruitment and sample and data collection

The BORICC Follow-Up (BFU) study is a 12+ year follow-up of participants recruited to the BORICC Study. The primary aim of the BFU Study is to investigate links between dietary and other lifestyle factors and markers of colorectal health and ageing. In addition, the BFU Study is investigating the effects of change in lifestyle factors, 12+ years later, on markers of healthy ageing, large bowel health and CRC risk. This is an observational and longitudinal study. The BORICC Study had two sub-studies and follow-up participants to the BORICC1 and BORICC2 were called BFU1 and BFU2, respectively.

I was part of the BFU Study Team and was actively involved during recruitment, ethical amendments, showcase events and study visits. My specific role is specified in more detail below.

Figure 2-2 shows the overall BORICC and BFU Study designs and the subsets of participants used for subsequent analysis of microRNA expression. Justification for the subset of participants used can be found in the relevant chapter, i.e. Chapter 5.
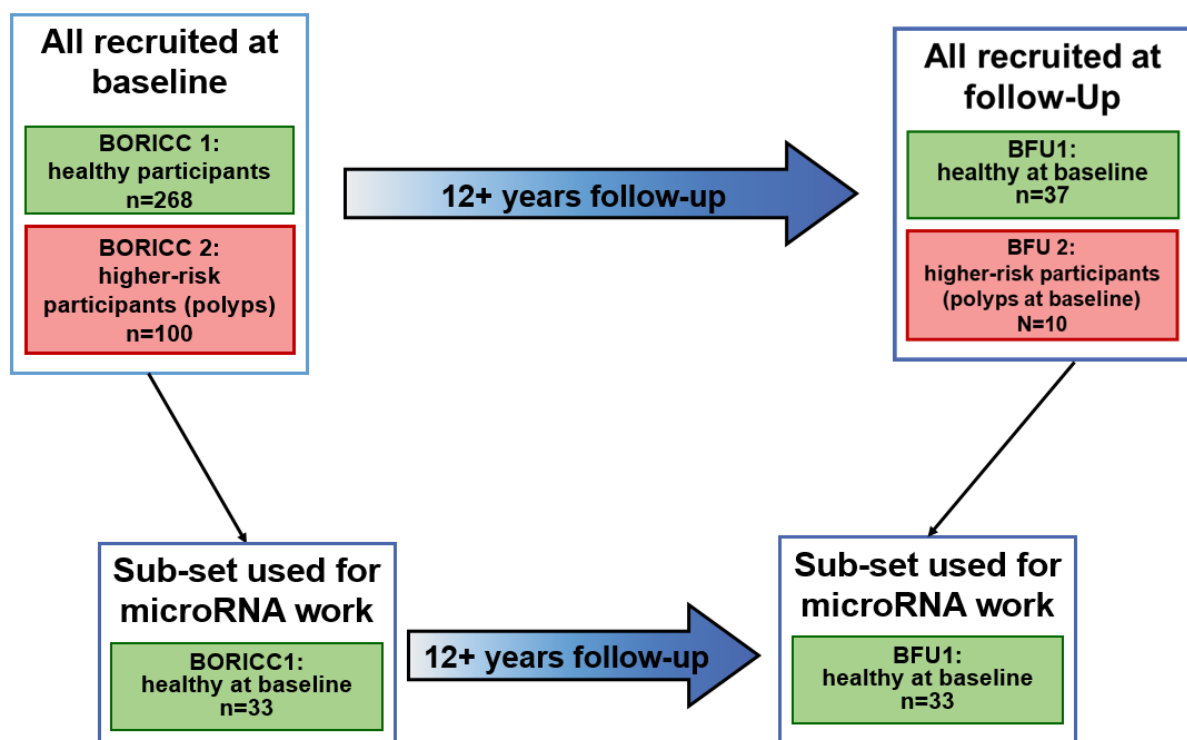
Figure 2-2: Overall BORICC and BFU Study designs and subsets of participants used for microRNA work conducted for this thesis

2.1.3.1.1   Ethics approval

Ethical approval was obtained from the NRES Committee, West Midlands - Coventry and Warwickshire Research Ethics Committee (16/WM/0424) on 29th of November 2016 and the IRAS project ID was listed under the following code: 207081 (see Appendix B). An application for a substantial amendment was submitted the ethics committee on 19th April 2017 and approval was obtained on 23 May 2017 for changes to the recruitment protocol including use of a response card, invitation of potential participants to a showcase event and the addition of participant bone densitometry measurement (see Appendix C). Another application for amendment to the study protocol to call participants to check if they had received their study invitation letter and to invite them to return their response cards was submitted to the ethics committee on 17th of November 2017 and approval was obtained in 15 December 2017 (see Appendix D).

2.1.3.1.2   Recruitment strategy

Identification of potentially eligible participants: The medical records of BORICC Study participants were checked by the BFU Study Team using Northumbria Healthcare NHS Foundation Trust's 'Single View' to identify those who were deceased and those who met the exclusion criteria. Exclusion criteria included potential dementia (limiting capacity to provide informed consent), unable to travel to attend the hospital study visit and use of anti-blood clotting medication. The latter individuals were invited to participate in all elements of the study except for the collection of colorectal mucosal biopsies, as a rigid sigmoidoscopy may increase the risk of bleeding. A total of 291 potential recruits who met the inclusion criteria for the BFU Study were identified, 227 and 64 for BFU1 and BFU2 respectively.

Recruitment protocol: BFU Study invitation letters (see Appendix E), participant information sheets (see Appendix F), a flyer for the BFU Study showcase event (see Appendix G) and a response card (see Appendix H) with a pre-stamped and addressed envelope were sent to potential recruits in batches of 60. If potential recruits did not contact the study team within 3 weeks, a second invitation was sent. If no contact was made, an attempt was made to contact the individual by telephone. When contact was made by telephone, email or post,

the study was discussed and participants were invited to take part in a showcase event or directly in the study without participation in a showcase event after signing a consent form (see Figure 2-3).

Data and sample collection by participants at home: After consent was obtained an appointment for the hospital visit at North Tyneside General Hospital, UK was arranged and a study pack was sent out 10 days prior to the hospital visit. The study pack included:

- Study pack instructions
- Consent forms
- Hospital study visit instructions and directions
- A lifestyle questionnaire
- A food frequency questionnaire
- A sunlight exposure questionnaire
- Accelerometer instructions
- Record sheet and sleep log
- Stool collection instructions
- Urine collection instructions
- At-home sample and questionnaire collection record sheet
- Accelerometer (GENEActiv^{TM}) to record physical activity for 7 days
- Stool collection pot (Fecotainer®)
- Cool bag and cool block for transportation of samples
- Urine collection pots (x2) and
- Urine vacutainers (x8) separated into two zip lock bags.
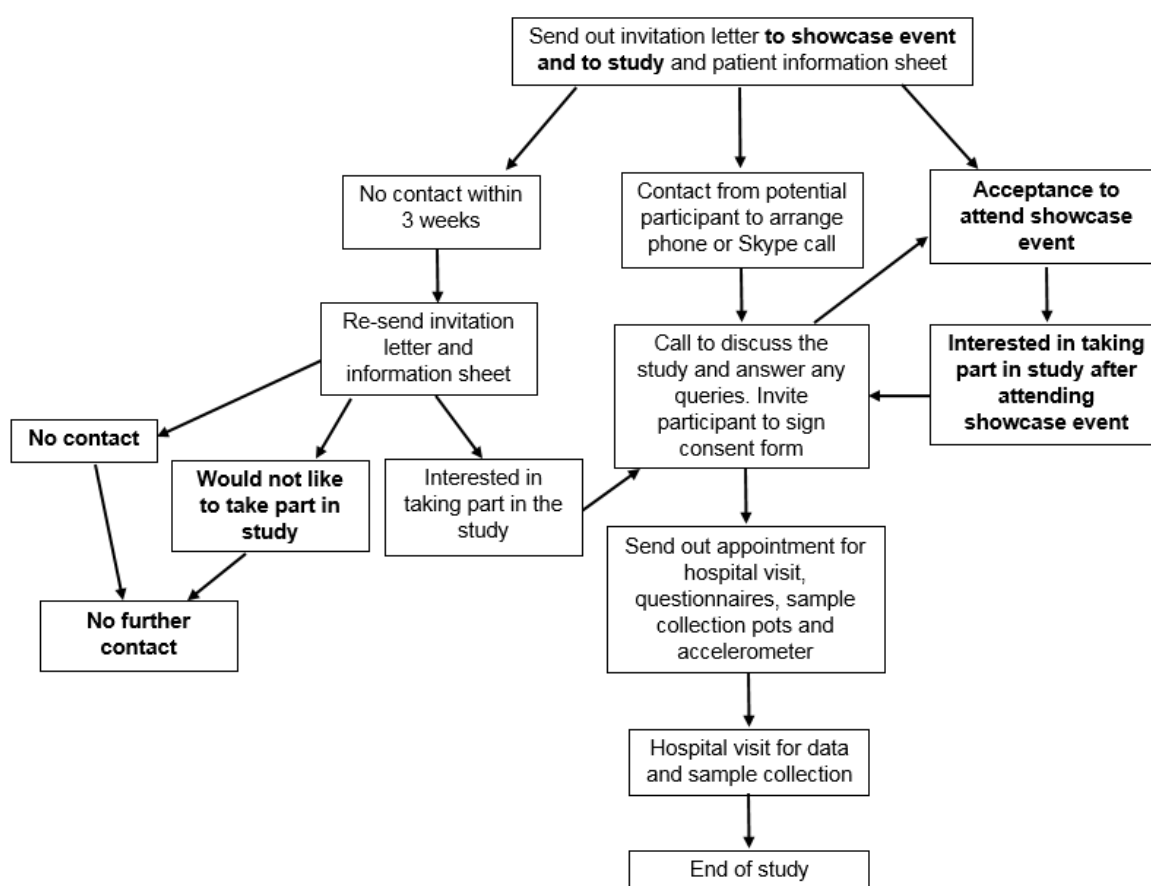
Figure 2-3: Protocol for participant recruitment

2.1.3.1.3   Showcase events

Showcase events took place on both week and weekend days at North Tyneside General Hospital Education Centre, UK. During the showcase events potential participants watched a presentation delivered by a BFU Study team member about the BORICC Study outcomes and the hypothesis, aims and objectives for the BFU Study. In addition, the procedures for the BFU Study hospital visit, sample and data collection were explained. Attendees had a chance to experience the protocol for assessment of handgrip strength and weight (on Tanita scales) and it was my responsibility to conduct these assessments during the showcase event. Participants had ample opportunity to ask questions and to discuss aspects of BFU Study throughout the showcase event. At the end of the session, attendees were invited to contact the research team by telephone, post or email if they had any further questions or wanted to sign up for the study. A total of 7 showcase events were held.

2.1.3.1.4   Study visit at North Tyneside General Hospital

During the study visit, which lasted about 45min, I was responsible for checking each participant's questionnaires for missing data and for counter-signing consent forms. A medical and health history record was obtained by a clinically-qualified member of the BFU Study team. The urine and stool samples that had been collected at home were received, processed and archived. I was also responsible for undertaking anthropometric measurements including weight (Tanita scales), height measurements in the Frankfurt horizontal plane (Leicester height measure) and waist and hip circumference (measuring tape). Another BFU team member measured heel bone density (Achilles EXPII bone ultrasonometer) and muscle function measurements including time up and go, and hand grip strength. Biological samples including blood samples (I was responsible for blood centrifugation and for separating plasma, serum and white blood cells), buccal cells and rectal biopsies were collected, processed and subsequently stored at -80°C (except for buccal cells which were stored at room temperature).

2.1.3.1.5   Non-biological sample collection

Anthropometric and body composition measurements were collected in the exact same manner as described in 2.1.1.2.1 and 2.1.1.2.2 respectively with the exception that participants did not attend the study visit after a standardised fast.

2.1.3.1.6   Biological sample collection

Colorectal mucosal pinch biopsies were collected as described in 2.1.1.2.3

2.2   Laboratory Methods

2.2.1   Assessment of mitochondrial dysfunction in colorectal mucosal biopsies

2.2.1.1   Sectioning of formalin fixed and paraffin embedded colorectal mucosal biopsies

Miss Anna Smith (laboratory technician) sectioned the formalin fixed and paraffin embedded (FFPE) blocks containing colorectal mucosal biopsies. The blocks were placed on ice for 30min before cutting 4μm thick sections on a HM325 microtome. The cut sections were placed carefully on a 37°C deionised water flotation bath for a few minutes to stretch and flatten the tissue sections. Subsequently, the sections were placed on glass slides (Superfrost Ultra Plus), labelled with participant ID and incubated at 37°C for 24 hours to fix the sections on the glass slides. The prepared slides were stored at 4°C.

Immunofluorescence staining for mitochondrial respiratory chain proteins in the cut sections of FFPE colorectal mucosal biopsies was carried out using a protocol optimised by the Mitochondrial Research Group, Newcastle University. This protocol was carried out over two days.

2.2.1.2.1   Procedures undertaken on Day 1

One biopsy section from each participant was labelled as 'primary' (primary antibodies were applied to that slide) whilst another slide from the same participant was labelled 'no primary' (primary antibodies were omitted on that slide) and the slides were incubated in a 60°C oven for one hour. The sections were deparaffinised in Histoclear and rehydrated through a graded series of ethanol (in the order: '100% ethanol 1 dewaxing', '100% ethanol 2 dewaxing', '95% ethanol dewaxing' and '70% ethanol dewaxing'). Then the sections were placed in an EDTA-containing buffer at pH 8 and antigens were retrieved by heating in a pressure cooker for 40min. The sections were washed in running tap water and blocked with 10% normal goat serum (Sigma- Aldrich, Poole, UK) for one hour and endogenous avidin and biotin were blocked by incubating the slides in avidin and biotin blockers (Vector Laboratories, UK) for 15min each. Sections labelled 'primary' were incubated at 4 °C with primary antibodies (see Table 2-2) in the dark.

2.2.1.2.2   Procedures undertaken on Day 2

Sections were washed three times for 5min in TBST (TBS + 1:100 Tween® 20, pH 7.4) and incubated for two hours with an IgG specific secondary antibody (see Table 2-2) at room temperature in the dark. Then sections were washed three times for 5min in TBST and incubated for two hours with the appropriate tertiary antibody (see Table 2-2) at room temperature in the dark. Subsequently, sections were washed three times for 5min in TBST and incubated for 15min in Hoescht, a nuclear counterstain, at room temperature in the dark. Finally, sections were washed three times for 5min in TBST and mounted in ProLong™ Gold antifade reagent (Thermo Fischer Scientific) using a coverslip. Sections were stored in the -20 °C freezer until ready to be viewed under the confocal microscope.

Primary Antibody	Ms mAb* to NDUFB8 (Abcam)	Ms mAb* to MTCO1 (Abcam)	Rb mAb** to TOMM20 (Abcam)
Function under investigation	Complex 1	Complex 4	Mitochondrial mass marker
Antibody subtype	IgG1	IgG2a	IgG1
Concentration	1:50	1:100	1:100
Secondary antibody	Biotinylated anti mouse IgG1	N/A	N/A
Tertiary antibody	Streptavidin conjugated 647	Goat anti rabbit 488	Goat anti mouse IgG2a 546

Table 2-2: Antibodies used to quantify complex 1 (NDUFB8), complex 4 (MTCO1) and mitochondrial mass (TOMM20) by immunofluorescence
*Mouse monoclonal Antibody
**Rabbit monoclonal Antibody

2.2.1.3   Image capture using Confocal Microscopy

Stained colorectal mucosal sections were viewed and imaged under the Nikon A1 confocal (upright) microscope in the Bio-Imaging Unit, Newcastle University within 10 days of immunofluorescence staining. Channels Alexa 647, Alexa 488 and Alexa 546 were used for the antibodies NDUFB8, MTCO1 and TOMM20 respectively. Initially, the 'primary' sections were viewed and laser power, detector sensitivity and offset/ signal cutoff were set to optimise visibility of the antibodies within the crypts of the biopsies; this required a pixel value of around 3000 and up to 3500. The 'no primary' slides were viewed using exactly the same settings. The crypts within the 'no primary' biopsy were expected to be barely visible, with a pixel value close to zero. However, if the crypts were visible and the pixel value above 50 the settings were adjusted so that the crypts would be barely visible and the pixel value close to zero, and these adjusted settings were used for imaging of both the 'primary' and 'no primary' sections. A snap shot (single image) and a tile (a collection of snap shots stitched together which results in an image of the whole biopsy) from both the 'no primary' and 'primary' sections were taken. For imaging, a laser application time per pixel of 1.1 was used at resolution size 1024.

2.2.1.4 *Data processing of images from colorectal mucosal biopsies immunofluorescence stained for mitochondrial respiratory chain proteins*

All images obtained from the confocal microscopy were processed using ImageJ. Using the 'polygon selection', individual crypts were selected and a boundary drawn around them. This process was carried out for 20 crypts from the 'no primary' sections and for all crypts present in a biopsy from the 'primary' sections. The expression levels for each individual antibody were measured using 'Region of Interest Manager' in the selected crypts and recorded. Subsequently, the recorded data were uploaded online to the 'Oxphos quadruple immunofluorescence analyser', which was developed in-house by the Mitochondrial Research Group at Newcastle University (https://research.ncl.ac.uk/mitoresearch/). This software normalises the data for each antibody measured as follows: first the average 'no primary' antibody expression level of the crypt was subtracted from the 'primary' one. Then the natural logarithm was taken for each antibody. After transforming the values of the antibodies to their natural logarithm, values for MTCO1 and NDUFB8 were divided by the value for TOMM20 and a mean value and standard deviation for all crypts in the biopsy was calculated. Z-scores were calculated by subtracting the obtained mean expression value per antibody measured from the individual expression value of the crypt for that specific antibody and dividing it by the standard deviation obtained previously. Based on the value of the z-score, each respiratory chain protein measured within a crypt was designated as overexpressed ($z > 2$), normal ($z < 2$), slightly deficient ($z < -2$), very deficient ($z < -3$) or depleted ($z < -4$) (Rocha et al., 2015). The percentage of crypts showing overexpressed, normal, slightly deficient, very deficient and depleted for each respiratory chain protein measured within each biopsy were calculated and recorded.

2.2.2 Sequencing the mitochondrial genome in human colonic crypts of colorectal mucosal biopsies

2.2.2.1 *Cryostat sectioning of frozen colorectal biopsies*

Colorectal mucosal biopsies stored at -80°C were transported in liquid nitrogen to the cryostat and 20µm thick sections were cut at -20°C. Care was taken to ensure that the tissue temperature did not deviate from that target because if it is too cold the section may curl and if it is too warm it may stick to the cutting knife (Ross, 2011). Subsequently, the sections were

placed on 1mm PEN-membrane slides, labelled with participant ID, left to fix by air drying at room temperature for 1.5 hours, and then stored in a plastic container at -80°C.

2.2.2.2 Succinate Dehydrogenase (SDH) staining of section from frozen colorectal biopsies

Succinate Dehydrogenase (SDH) staining of sections from frozen colorectal mucosal biopsies was carried out using a protocol optimised by the Mitochondrial Research Group, Newcastle University. Fresh tissue, frozen initially in liquid nitrogen, was used for SDH staining because, unlike FFPE, this avoids freezing artifacts, optimises morphology and ensures that the enzyme activity is retained (Ross, 2011).

Sections were thawed at room temperature for 30min in the storage plastic container followed by 30min air drying. Sections were incubated in the SDH incubation medium (1.5mM Nitroblue tetrazolium, 130mM sodium succinate, 0.2mM phenazine methosulphate and 1mM sodium azide) for 50min at 37°C in the dark. Sections were washed gently twice for 30sec in phosphate buffered saline (Oxoid™ ThermoFisher Scientific). The sections were dehydrated through a graded series of ethanol (in the order: '70% for 2min', '95% for 2min' and '100% for 12min') and then stored in a plastic container at -80°C.

2.2.2.3 Laser microdissection and lysing of SDH stained crypts from frozen colorectal mucosal biopsies

SDH staining made the crypts in the colorectal mucosal biopsies visible under the PALM MicroBeam Laser Capture Microdissection microscope (ZEISS). Between 300 and 500 crypts per sample were cut from the stained PEN membrane slides into sterile 0.5mL PCR tubes into 15µL of cell lysis buffer (50mM Tris-HCl pH8.5, 1% Tween-20, 20mg/mL proteinase K and distilled water, which was prepared on ice under the UV hood to minimise contamination) using the PALM MicroBeam Laser Capture Microdissection microscope (ZEISS). The collected isolated crypts were centrifuged at 14,000rpm for 15min and lysed at 55°C for two hours followed by 95°C for 10min (to denature proteinase K). The crypt lysates were stored in the freezer at -20°C.

2.2.2.4 Mitochondrial DNA amplification by long range PCR

The obtained crypt lysates were utilised as DNA templates to enrich/amplify two overlapping fragments of the mtDNA genome to ensure complete coverage of the whole mitochondrial genome (see Table 2-3). A long range PCR, using Takara PrimeSTAR GXL DNA polymerase

(Takara Bio Europe, France) and primers pair detailed in Table 2-3, was prepared in a DNA-free, UV-sterilised PCR cabinet to minimise contamination.

MtDNA fragment	Fragment length (bp)	Primer sequence forward 5'-3'	Primer sequence reverse 5'-3'
A: m.6222-m.16153	9932	CCCTCTCTCCTACTCCTG	CAGGTGGTCAAGTATTTATGG
B: m.15295-m7791	9066	CATCTTGCCCTTCATTATTGC	GGCAGGATAGTTCAGACGG

Table 2-3: Forward and reverse primer sequences used for mtDNA fragment amplification

The master-mix used for the long range PCR contained:

- 5ul 5xPrimeSTAR GXL Buffer (Mg2+ plus)

- 2ul dNTP Mix (2.5mM)

- 0.5ul For Primer (10uM)

- 0.5ul Rev Primer (10uM)

- 0.5ul PrimeSTAR GXL DNA Pol (1.25U/ul)

- 2ul DNA lysate.

Controls were set up with each new mastermix including lysis buffer only (without cells), human genomic control DNA (positive control) and water only (negative control). Reactions were amplified on an Applied Biosystems Veriti 96-wel thermal cycler (ThermoFisher Scientific) with the cycling conditions shown in Table 2-4.

Step	Time	Temperature	Number of cycles
Initial activation step	5min	94°C	1
Denaturing	10sec	98°C	30
Annealing	15min	68°C	

Extension	10min	72°C	1
Hold	∞	4°C	

Table 2-4: Long range PCR cycling conditions

2.2.2.5 Agarose gel electrophoresis of products from long range PCR

Following amplification by the long range PCR, 5μL of the PCR product, 7.5μL orange G loading dye (50% glycerol and 50% dH$_2$O plus a little orange G powder) and 5μL 1kb Gene Ruler Plus DNA ladder (ThermoFisher Scientific) were loaded onto a 0.8% agarose gel (0.8% agarose (Bioline) in 100mL 1x Tris Acetate EDTA (TAE) buffer (Formedium) and 4μL SYBRSafe gel stain (Invitrogen). In brief, a flask containing TAE buffer and agarose was heated for 2min in a microwave (stirred a few times during heating) and the flask was cooled with running tap water. After adding the SYBRSafe gel stain, the gel was poured, any bubbles present were removed and the gel was left to set for 15min. All samples were prepared on parafilm and loaded into individual wells of the gel. Samples included the long range PCR product, the lysis buffer only (without cells), human genomic control DNA (gDNA) (Promega) and a negative control containing water only. SYBRSafe gel stain was added to enable visualisation of the PCR products. The gel was electrophoresed at 60 volts for 45min in 1x TAE buffer to separate products and a digital image was obtained using the BioRad Imager and ImageLab software® (see Figure 2-4).
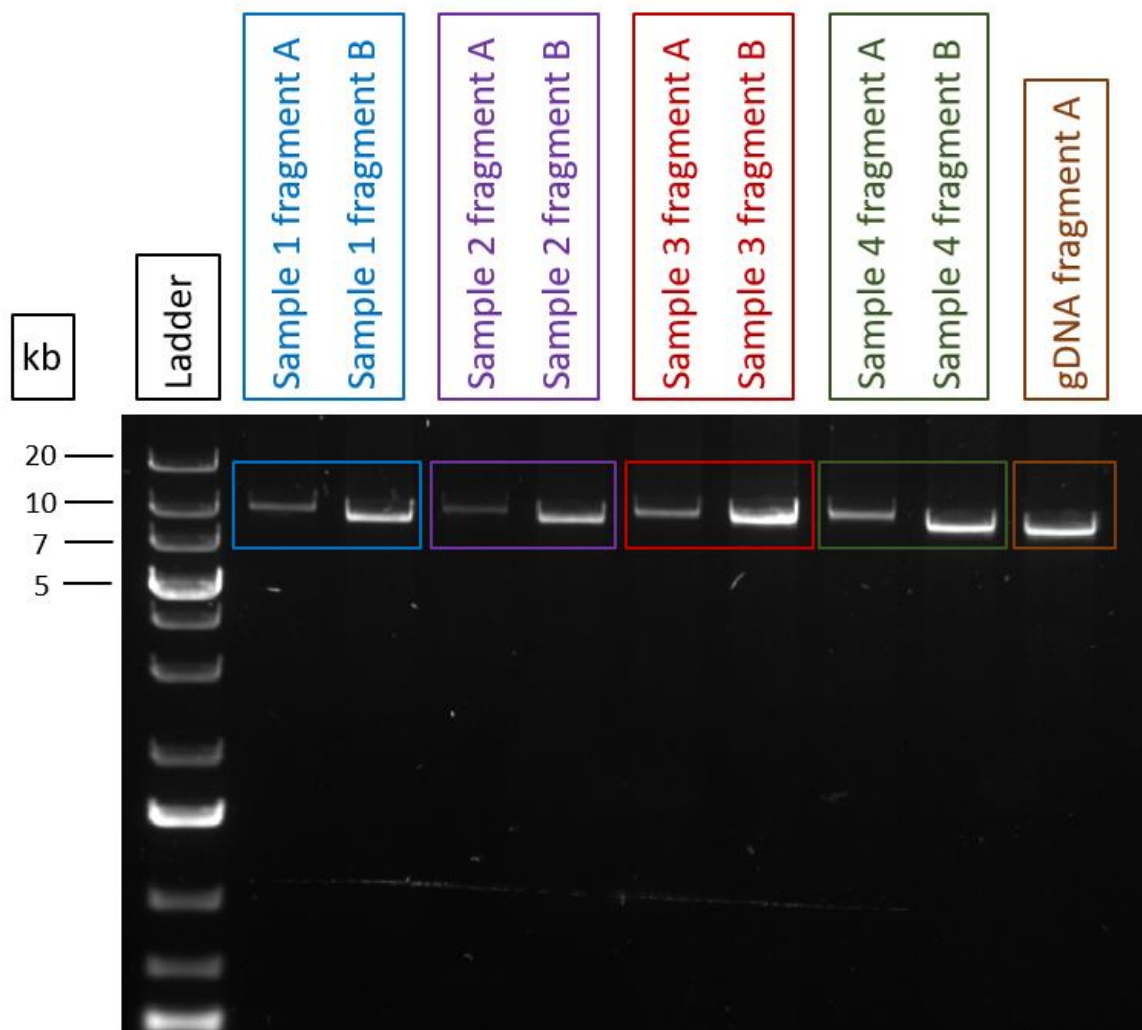
Figure 2-4: Agarose gel electrophoresis image of ladder, amplified mtDNA product (fragment A and B for each sample) and human genomic control DNA by long range PCR

2.2.2.6   Purification and quantification mtDNA concentration

Following gel electrophoresis, the mtDNA from the long range PCR product was purified using AgenCourt AMPure XP bead technology (Beckman Coulter). AMPure XP beads were resuspended by vortexing until the suspension appeared to have a homogeneous colour.

Then 36μL Agencourt AMPure XP and 20μL PCR product were added to a reaction plate (a 1.8μL bead:1 μL product ratio according to the manufacturer's instructions), mixed by pipetting 10 times and incubated for 5min at room temperature. During this step, the mtDNA fragments bound to the magnetic beads. Then the reaction plate was placed on the Agencourt SPRIPlate 96 Super Magnet Plate for 2min to separate the beads from the solution. With the reaction plate still on the Agencourt SPRIPlate 96 Super Magnet Plate, the clear solution/ supernatant was removed from the reaction plate (leaving 5μL of solution behind to prevent

beads being removed) and discarded. Next, a wash was performed by adding 200μL of 70% ethanol to each sample and incubated for 30sec at room temperature, and then the ethanol was removed from the reaction plate and discarded. As the beads were not drawn out easily when in ethanol, it was not necessary to leave supernatant behind in this step. The wash was performed twice and samples were air dried for 4-5min to remove all ethanol. Afterwards, the reaction plate was removed from the magnetic plate, samples were eluted in 20μL nuclease-free water and mixed by pipetting 10 times followed by a 2min incubation at room temperature. Finally, the reaction plate was placed once more onto the Agencourt SPRIPlate 96 Super Magnet Plate for 1min to allow separation of the beads from the solution and the eluate was transferred onto a new 96-well PCR plate.

The concentrations of DNA in the samples and controls (standard 1 and standard 2- provided by the kit) were estimated by Qubit quantification, (Qubit® dsDNA BR Assay kit (Life Technologies)). The Qubit® working solution was prepared by diluting the Qubit® dsDNA BR reagent (fluorescent dye) 1:200 in Qubit® dsDNA BR buffer. In a Qubit® assay tube, 190μL of Qubit® working solution was mixed with 10μL of standard and 198μL of Qubit® working solution was mixed with 2μL of sample (the final volume in each tube was 200μL), vortexed for 2-3 seconds and then incubated for 2min at room temperature. In order to calibrate the Qubit® dsDNA BR assay, first standard 1 and then standard 2 were measured on the instrument. Following the calibration, the mtDNA concentration of the samples was calculated and quantified. A minimum mtDNA concentration of 1ng/μL was required for the next step of the protocol. If samples had a concentration below 1ng/μL, the previously obtained lysate (see 2.2.2.3) was re-amplified (see 2.2.2.4), re-purified and re-measured. If the mtDNA concentration of the repeated samples was ≥ 1ng/μL they were included and if ≤1ng/μL excluded from the following steps in the procedure. Fragments A and B for each sample were pooled together to produce a 10ng pool. This was prepared in a 96-well Eppendorf TwinTec PCR plate. Pooled samples were stored at -20°C.

2.2.2.7 Nextera XT DNA Library Preparation and MiSeq

Pooled samples from Section 2.2.2.6 were further diluted to 0.2ng/ul. Libraries were prepared using the Nextera XT DNA Library Prep Kit (Illumina®) according to the manufacturer's instructions (see Appendix I for protocol) by Dr Angela Pyle, at the Institute of Genetic Medicine, Newcastle University. The procedure was performed through the following 5 steps:

1. Tagmentation of genomic DNA

2. Amplification of Libraries

3. Clean up of Libraries

4. Quantification and manual normalisation of libraries

5. Pooling of Libraries.

Briefly, pooled DNA samples were tagmented and then amplified using the Nextera XT Index Kit v2 Set A (Illumina). Each library was cleaned using AMPure XP beads (see Section 2.2.2.6). Library size was verified using the Agilent High Sensitivity D5000 Screen Tape assay and Agilent 2200 TapeStation. Analysis was performed in Agilent TapeStation software. Each library should have a broad size distribution between 200bp and 1.5 kb.The concentration of each library was also measured using the Qubit® dsDNA BR assay (see Section 2.2.2.6). Using these measurements, libraries were manually normalised to 4nM, pooled and sequenced using the MiSeq Reagent Kit V3 600 cycles and the Illumina MiSeq v3.0 sequencing platform in paired-end, 250bp reads (Mr Rafiqul Hussain, Genomics Core Facility, Institute of Genetic Medicine, Newcastle University).

2.2.2.8 Bioinformatic analysis

An established bioinformatic pipeline was applied to the post-run FASTQ files (carried out by Dr Gavin Hudson, Institute of Genetic Medicine, Newcastle University). In summary, reads were aligned to Hg19 using BWA v0.7.10 invoking –mem (Li and Durbin, 2009). Aligned reads were sorted and indexed using Samtools v0.1.18 (Li et al., 2009), duplicate reads were removed using Picard v1.85 (http://broadinstitute.github.io/picard/). Variant calling was performed using VarScan v2.3.8 (minimum depth =1000bp, support reads = 10, base-quality = >30, mapping quality = >30 and variant threshold = 0.01) (Koboldt et al., 2009). Variants were annotated with ANNOVAR v529 (Wang et al., 2010). Heteroplasmic variants are defined as >1% minor allele frequency.

Bioinformatic analysis Post-run FASTQ files were analysed using an established in-house bioinformatics pipeline. Briefly, reads were aligned to the Hg19 using BWA v0.7.10 invoking (Li and Durbin, 2009). Aligned reads were sorted and indexed using Samtools v0.1.18 (Li and Durbin, 2009) and duplicate reads were removed using Picard v1.85 (http://broadinstitute.github.io/picard/). Variant calling was performed using VarScan v2.3.8

(minimum depth =100bp, support reads = 10, base-quality = >30, mapping quality = >10 and variant threshold = 0.05) (Koboldt et al., 2009). Variants were annotated with ANNOVAR v529 (Wang et al., 2010). Heteroplasmic variants are defined as >1% minor allele frequency.

2.2.3 Quantification of microRNA expression in colorectal mucosal biopsies

2.2.3.1 *RNA extraction of frozen colorectal mucosal biopsies and measurements of RNA purity and concentration using spectrophotometry*

RNA was extracted from frozen colorectal mucosal biopsies using the Qiagen miRNeasy Mini Kit according to the manufacturer's instructions. All steps were carried out at room temperature. In brief, a whole biopsy was put in a 2mL tube where it was homogenised with 350μL Buffer RLT TissueLyser (which lyses the tissue, inhibits RNases and removes genomic DNA and proteins from the lysate) using sterile homogenisation pestles (BIOQUOTE, UK) until the biopsy was completely disrupted and invisible to the naked eye. Then one volume of 70% ethanol was mixed to the lysate, and transferred to an RNeasy Mini spin column which was placed into a 2mL collection tube and centrifuged for 15sec at 13,000 rpm. Ethanol enabled binding of the RNA molecules, from 18 nucleotides upwards, to the membrane of the spin column, ensuring that total RNA was bound to the membrane and other contaminants were washed away during the following series of washes with buffers. The flow-through was discarded and 700μL Buffer RW1 was added to the spin column and centrifuged for 15sec at 13,000 rpm. The flow-through was discarded again and 500μL Buffer RPE was added to the spin column and centrifuged for 15sec at 13,000 rpm. The flow-through was discarded and the last buffer step was repeated and centrifuged for 2min at 13,000 rpm. Then the RNeasy spin column was put in a new collection tube and centrifuged at full speed for 1min to dry the membrane and reduce the risk of buffer carry-over. Once more, the RNeasy spin column was put in a new collection tube and 30μL RNase free water was added directly to the spin column membrane and centrifuged for 1min at 13,000 rpm to elute the RNA. Straight after the RNA extraction procedure, RNA was put on ice and its concentration (ng/μL) and its purity were measured on the NanoDrop 1000 spectrophotometer (Thermo Scientific) and then stored at -20°C. The NanoDrop was used to measure RNA at specific wavelengths (260nm and 280nm) and the ratio of absorbance (260/ 280 ratio) was used to evaluate RNA purity. RNA concentrations (ng/μL) were recorded in order to calculate the required concentration

(~200ng) for the procedure of the generation of small RNA libraries. A value between 1.8 to 2.1 for the 260/280 ratio was considered as adequate for further analysis, as ratios outside of that range were indicative of protein, phenol or other contaminants present. Table 2-5 shows the mean RNA concentrations and the A 260/280 ratios of pre- and post-surgery and control participants used for further procedures and analysis.

	Pre-surgery (N=22)	Post-surgery (N=22)	Controls (N=20)
RNA concentration ng/µL	92.2 (31.5)	65.8 (31.6)	57.0 (20.0)
A260/ 280	2.06 (0.04)	2.05 (0.04)	2.06 (0.04)

Table 2-5: RNA concentrations and A260/280 ratios of pre- and post-surgery and control participants, Mean (SD)

2.2.3.2   Quality control check for extracted RNA

Miss Amber Knox (laboratory technician) carried out a quality control check for extracted RNA from colorectal mucosal biopsies, according to the manufacturer's instructions (see Appendix J for protocol), using the Aglient RNA 6000 Pico Kit which allowed to test for reproducible characterisation of total RNA and its quality.

2.2.3.3   Generation of the Library from extracted RNA of colorectal mucosal biopsies (Procedures undertaken on Day 1)

Small RNA transcripts were converted into barcoded cDNA libraries for next-generation sequencing using the Illumina platform. Libraries were generated from extracted RNA of frozen colorectal mucosal biopsies using the NEBNext® Multiplex Small RNA Library Prep Set for Illumina® (Set 1 and Set 2, New England BioLabs). The volume of components and reagents was used as demonstrated in Table 2-6 for a single reaction. This platform enabled elimination of the adapter-dimer formation during the construction of small RNA libraries by transforming single-stranded adapters into double-stranded forms (NewEngland Biolabs, 2019).

Ligation of the 3' SR Adaptor: Input RNA (1-6µL) was calculated to reach a RNA amount of ~200ng/µL for each sample (if needed, the remaining volume was made up with nuclease-free water) and for each reaction 1µL 3' SR Adaptor for Illumina was added to a sterile nuclease-free PCR tube and mixed. The tube was incubated in a preheated thermal cycler for 2min at 70°C and transferred to ice. Then 10µL 3' Ligation Reaction Buffer (2X) and 3µL 3'

Ligation Enzyme Mix were added to each reaction, mixed and incubated in a preheated thermal cycler for 1h at 25°C.

Hybridizing the Reverse transcription Primer: 4.5μL of nuclease-free water and 1μL of SR RT Primer for Illumina were added to the Ligation mix, mixed and heated for 5min at 75°C, followed by 15min at 37°C and transferred for 15min at 25°C in the thermal cycler.

Ligation of the 5' SR Adaptor: With 5min remaining before the end of the hybridization step from the thermal cycler, the 5' SR Adaptor for Illumina was denatured for 2min at 70°C and the tube was immediately placed on ice. The denatured adaptor needed to be used within 30min of denaturation. Then 1μL of the denatured 5' SR Adaptor for Illumina, 1μL 5' Ligation Reaction Buffer and 2.5μL Ligation Enzyme Mix were added and mixed to the Hybridization mix. This was incubated in the thermal cycler for 1h at 25°C.

Reverse transcription: To the mixture obtained from the ligation of the 5' SR Adaptor step, 8μL First Strand Synthesis Reaction Buffer, 1μL Murine RNase Inhibitor and 1μL ProtoScript II Reverse Transcriptase were added, mixed and incubated for 1h at 50°C in the thermal cycler.

PCR Amplification: For the performance of PCR amplification, 50μL LongAmp Taq 2X Master Mix, 2.5μL SR Primer for Illumina, 2.5μL Index (X) Primer and 5μL nuclease free water were added to the obtained reaction mix from the reverse transcription. For each reaction/ sample only one of the available 24 Index (X) Primers was used in the PCR amplification. Table 2-7 shows the PCR amplification cycling conditions applied. Table 2-9 shows the index primer sequences for Illumina used, which produced barcoded libraries.

Component	Volume per reaction (μL)
RNA	1-6
3' SR Adaptor for Illumina	1
3' Ligation Reaction Buffer (2X)	10
3' Ligation Enzyme Mix	3
Nuclease-free water	4.5
SR RT Primer for Illumina	1
5' SR Adaptor for Illumina (denatured)	1
5' Ligation Reaction Buffer (10X)	1

5' Ligation Enzyme Mix	2.5
First Strand Synthesis Reaction Buffer	8
Murine RNase Inhibitor	1
ProtoScript II Reverse Transcriptase	1
LongAmp Taq 2X Master Mix	50
SR Primer for Illumina	2.5
Index (X) Primer	2.5
Nuclease free water	5

Table 2-6: NEBNext® Multiplex Small RNA Library Prep Set for Illumina® volume of components for a single reaction

Step	Time	Temperature	Number of cycles
Initial denaturation	30sec	94°C	1
Denaturing	15sec	94°C	15
Annealing	30sec	62°C	
Extension	15sec	70°C	
Final extension	5min	70°C	1
Hold	∞	4°C	

Table 2-7: PCR amplification cycling conditions

Finally, in order to remove impurities, enzymes, primers and nucleotides from the sample, the obtained amplified PCR product was purified using the QIAquick® PCR Purification Kit (Qiagen) according to the manufacturer's instructions. In brief, 5 volumes of PB buffer and one volume of the obtained PCR reaction mix were placed in a QIAquick column and centrifuged for 45sec at 13,000 rpm (centrifuge model: *Thermo SCIENTIFIC Heraeus PICO17*). The flow-through was discarded and centrifuged once more for 1min at 13,000 rpm to allow removal of residual wash buffer. The QIAquick column was placed in a clean 1.5mL clear-view Snap-Cap microtube (Sigma-Aldrich) and 26.5µL RNase free water was added directly to the spin column membrane, it was left to set for 3min, and then centrifuged for 1min at 13,000 rpm to elute the RNA, which was stored at -20°C.

2.2.3.4 Generation of the Library from extracted RNA of colorectal mucosal biopsies (Procedures undertaken on Day 2)

RNA samples obtained from procedures undertaken on day 1 were removed from the -20°C freezer and put on ice until ready to be added to the acrylamide gel for size selection of the small RNA. For one gel 12mL molecular water, 781.2µL Tris/Borate/EDTA, 2.8mL acrylamide (40%), 95µL ammonium persulfate and 15µL tetramethylethylenediamine were mixed in a falcon tube. The mixture was filled to the top between the space of the gel plates and the green combs were placed carefully between the plates avoiding the formation of bubbles, any bubbles were popped with the tip of a 10µL pipette tip. Whilst the gel was allowed to polymerise for 15-20min, the samples were prepared by adding 10µL loading dye (NEBNext® Multiplex Small RNA Library Prep Set for Illumina®) to 25µL RNA. Once the gel solidified, the combs were removed carefully, the plates placed on the electrode holder and the space filled with 10x TBE buffer. The ladder and samples (in duplicates) were loaded into the wells of the gel (see Figure 2-5) and electrophoresed at 120 volts for 1 hour.
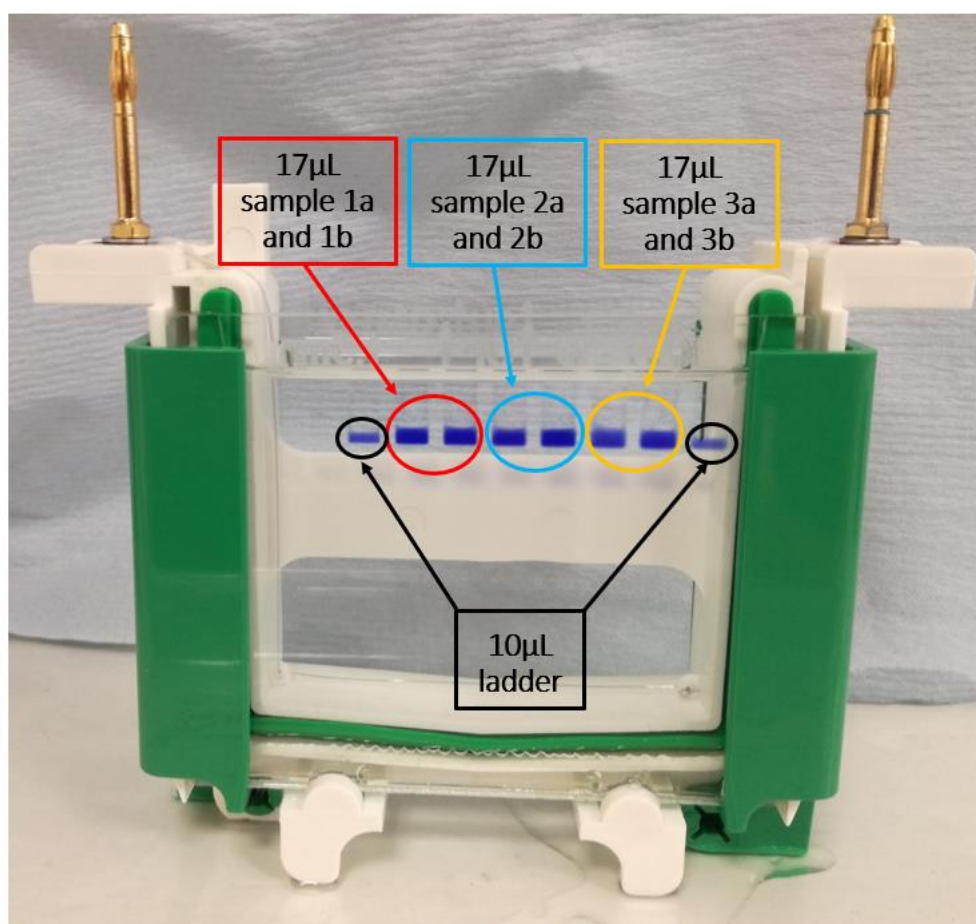
Figure 2-5: Example of allocation of the BOCABS samples and ladder into the wells for the acrylamide gel

Next, the fluorescent mixture for the gel was prepared by adding 5µL SYBR Green for nucleic acid gel stain (Invitrogen, ThermoFisher Scientific) to 50mL TBE buffer (per gel). Using a spatula, the gel was carefully placed into an ethanol cleaned box containing the prepared fluorescent mixture and was incubated for 10min at room temperature in the dark on the rotator/ shaker platform. The SYBR Green became incorporated into the RNA, giving it the fluorescence which enabled visualisation of the band products and band size selection later in the gel. In the meantime, the dark reader, its equipment and bench were prepared and cleaned with 70% ethanol. The dark reader was covered with cling film, avoiding bubbles, and the gel was placed carefully on it in a dark room. The UV light of the dark reader stimulated the SYBR Green and made the bands of the RNA libraries on the gel visible (see Figure 2-6). The 140-150bp bands corresponded to the microRNAs (21nt) (NewEngland Biolabs, 2019) and were cut using a scalpel and put in a labelled Eppendorf tube. More specifically, a primary and a secondary cut were made to the band of interest, where the primary cut contained exactly the band and the secondary cut its surroundings (Figure 2-7). The secondary cut was stored at -20°C and the procedure was continued using the primary cut. The rest of the gel was discarded.
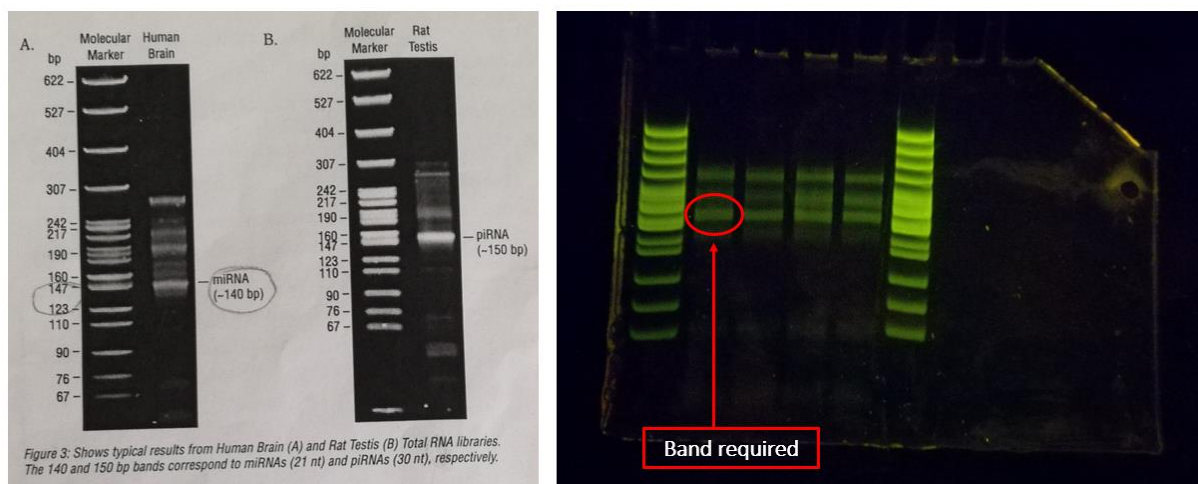
Figure 2-6: Band required to cut i) image from protocol (NewEngland Biolabs, 2019) reproduced with copyright permission (2019) and ii) image taken of BOCABS samples
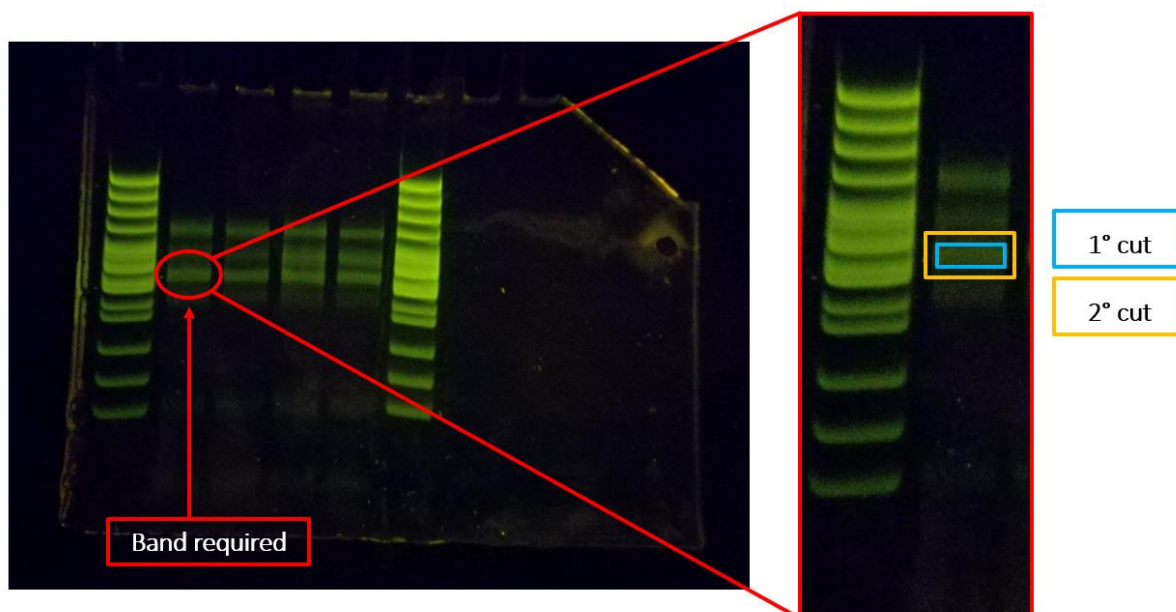
Figure 2-7: Primary and secondary cut made to the band of interest in BOCABS samples

250µL DNA Gel Elution buffer (1X) (NEBNext® Multiplex Small RNA Library Prep Set for Illumina®) was added to the tube containing the primary gel slice and was homogenised using sterile homogenisation pestles. The tube was placed on an end-to-end rotator for 3 hours at room temperature. Then, the gel debris and eluate were transferred to a gel filtration column (Invitrogen, ThermoFischer Scientific) which was placed into a 1.5mL clear-view Snap-Cap microtube, and were centrifuged at 13, 200rpm for 2min in order to remove the remaining gel (centrifuge model: *Thermo SCIENTIFIC Heraeus PICO17)*. The eluate was recovered and 1µL Linear Acrylamide, 25µL 3M sodium acetate (pH 5.5) and 750µL of 100% ethanol were added, vortexed well and incubated at -80°C overnight.

2.2.3.5 *Generation of the Library from extracted RNA of colorectal mucosal biopsies (Procedures undertaken on Day 3)*

The eluate obtained from the procedures undertaken on day 2 were transferred from the -80°C freezer to a microcentrifuge where they were span at 4°C at 14,000rpm for 30min (centrifuge model: *Thermo SCIENTIFIC SORVALL legend micro 17R*). Then the supernatant was removed very carefully without disturbing the pellet. Afterwards, the pellet was washed with 80% ethanol by vigorous vortexing and centrifuged once more in the microcentrifuge at 4°C at 14,000rpm for 30min. The pellet was air dried for 10min at room temperature to eliminate residual ethanol and re-suspended in 12µL RNase free water.

Next, a quality control step was carried out using the Agilent 2100 Bioanalyser High Sensitivity DNA Kit which allowed to test for sizing, quantification and analysis of fragments, for example libraries between 35- 5,000bp. Each DNA chip comprised a set of interconnected micro-channels which separated nucleic acid fragments based on their size while they were driven through electrophoretically. In brief, 9µL gel-dye mix, 5µL green marker, 1µL high sensitivity DNA ladder and up to 11 samples (1µL per sample), otherwise one additional 1µL of the green marker for the unused wells, were loaded onto the High Sensitivity DNA chip according to the manufacturer's instructions. The chip was vortexed horizontally at 2,400rpm for 1min and run in the Agilent 2100 Bioanalyzer instrument within 5min of preparation of the chip. When the run finished, the size, purity and concentration of the sample were checked and the length of the library recorded (see Table 2-8). An example of the sample's electropherogram is shown in Figure 2-8.

Overall Results for sample 1 : _sample 1_

Number of peaks found:	1	Corr. Area 1:	17.6
Noise:	0.4		

Peak table for sample 1 : _sample 1_

Peak		Size [bp]	Conc. [pg/µl]	Molarity [pmol/l]	Observations
1	◀	35	125.00	5,411.3	Lower Marker
2		155	272.70	2,663.4	
3	▶	10,380	75.00	10.9	Upper Marker
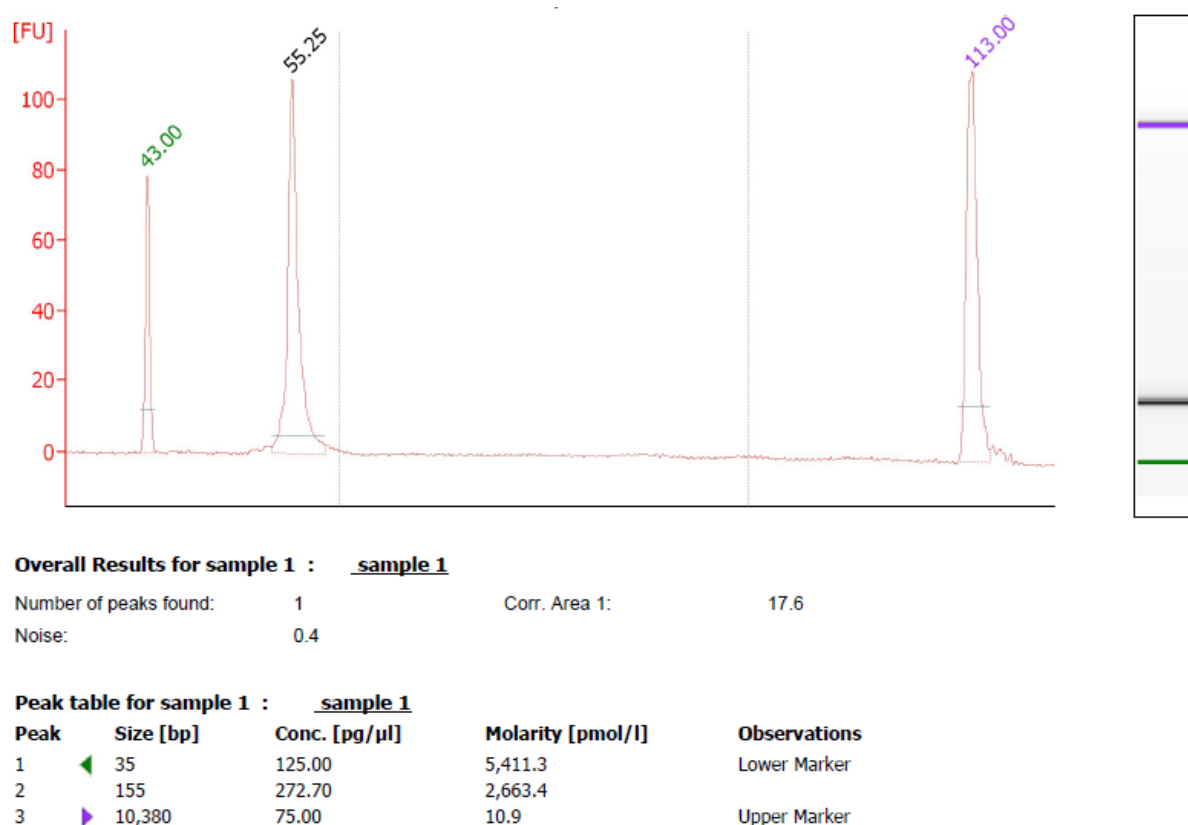
Figure 2-8: Electropherogram of the gel (band cut) size, from total RNA of the selected purified library from colorectal BOCABS sample; sample is 155bp length of library and has a concentration of 272.7 pg/µL

	Pre-surgery (N=22)	Post-surgery (N=22)	Controls (N=20)
Library length bp	152.6 (10.5)	155.5 (11.1)	155.6 (1.8)
Library concentration ng/µL	0.7121 (0.5)	0.9128 (0.6)	0.6607 (0.4)

Table 2-8: Bp length and concentration of library for gel band cut of pre- and post-surgery and control participants, Mean (SD)

2.2.3.6 Next generation sequencing of microRNAs of colorectal mucosal biopsies

The purity and concentrations of the samples and controls (standard 1 and standard 2- provided by the kit) were estimated by Qubit quantification, (Qubit® dsDNA HS Assay kit (Invitrogen, Thermo Fisher Scientific). The Qubit® working solution was prepared by diluting the Qubit®dsDNA HS reagent (fluorescent dye) 1:200 in Qubit® dsDNA HS buffer. In a Qubit® assay tube, 190µL of Qubit® working solution was mixed with 10µL of standard and 198µL of Qubit® working solution was mixed with 2µL of sample (the final volume in each tube was 200µL), vortexed for 2-3 seconds and then incubated for 2min at room temperature. In order to calibrate the Qubit® dsDNA HS assay, first standard 1 and then standard 2 were measured on the instrument. Following the calibration, the concentration of the samples was calculated and quantified. Then the total nM of library was calculated for each sample as follows:

(Sample's library concentration (ng/µL) * 1,000,000) / (650 MM bp * length of sample's library fragment).

Then the sample's volume needed to reach 4nM and was calculated in preparation for the sequencing. If the samples' volume was below 4nM, the number of reads by the sequencer were lower, hence these samples were repeated until the number of reads were similar to that of the samples with 4nM.

The MiSeq Reagent Kit v3 was used for sequencing on the Illumina MiSeq sequencer instrument generating roughly 22 million reads per run. A standard normalisation method for 4nM library was carried out according to the manufacturer's instructions. In brief, a 1mL of 0.2 N NaOH was prepared and the HT1 was removed from the -20°C freezer and thawed at room temperature. Then a 4nM library was denatured by adding 5µL 4nM library and 5µL 0.2 N NaOH into a microcentrifuge tube, which was vortexed briefly and centrifuged at 280rpm for 1min and left to incubate for 5min at room temperature. Then 990µL pre-chilled HT1 were

added to the denatured library resulting in 1mL of 20pM denatured library and no further dilution was required. The 600μL of the denatured 20pM library (600μL 20pM library and 0μL pre-chilled HT1) was loaded onto the reagent cartridge and the sequencing run was set up according to the index sequences used with the samples (see Table 2-9). The run was finished about 1.5 days later. Miss Laura Sabater assisted in setting up and conducting the MiSeq runs.

Index Primer for Illumina	Index Primer Sequence	Expected Index Primer Sequence Read
NEBNext Index 1	5´-CAAGCAGAAGACGGCATACGAGATCGTGATG-TGACTGGAGTTCAGACGTGTGCTCTTCCGATC-s-T-3´	ATCACG
NEBNext Index 2	5´-CAAGCAGAAGACGGCATACGAGATACATCGGT-GACTGGAGTTCAGACGTGTGCTCTTCCGATC-s-T-3´	CGATGT
NEBNext Index 3	5´-CAAGCAGAAGACGGCATACGAGATGCCTAAG-TGACTGGAGTTCAGACGTGTGCTCTTCCGATC-s-T-3´	TTAGGC
NEBNext Index 4	5´-CAAGCAGAAGACGGCATACGAGATTGGTCAGT-GACTGGAGTTCAGACGTGTGCTCTTCCGATC-s-T-3´	TGACCA
NEBNext Index 5	5´-CAAGCAGAAGACGGCATACGAGATCACTGTGTG-ACTGGAGTTCAGACGTGTGCTCTTCCGATC-s-T-3´	ACAGTG
NEBNext Index 6	5´-CAAGCAGAAGACGGCATACGAGATATTGGCGTG-ACTGGAGTTCAGACGTGTGCTCTTCCGATC-s-T-3´	GCCAAT
NEBNext Index 7	5´-CAAGCAGAAGACGGCATACGAGATGATCTGGTG-ACTGGAGTTCAGACGTGTGCTCTTCCGATC-s-T-3´	CAGATC
NEBNext Index 8	5´-CAAGCAGAAGACGGCATACGAGATTCAAGTGT-GACTGGAGTTCAGACGTGTGCTCTTCCGATC-s-T-3´	ACTTGA
NEBNext Index 9	5´-CAAGCAGAAGACGGCATACGAGATCTGATCGT-GACTGGAGTTCAGACGTGTGCTCTTCCGATC-s-T-3´	GATCAG
NEBNext Index 10	5´-CAAGCAGAAGACGGCATACGAGATAAGCTAG-TGACTGGAGTTCAGACGTGTGCTCTTCCGATC-s-T-3´	TAGCTT

NEBNext Index 11	5´-CAAGCAGAAGACGGCATACGAGATGTAGCCG-TGACTGGAGTTCAGACGTGTGCTCTTCCGATC-s-T-3´	GGCTAC
NEBNext Index 12	5´-CAAGCAGAAGACGGCATACGAGATTACAAGGT-GACTGGAGTTCAGACGTGTGCTCTTCCGATC-s-T-3´	CTTGTA
NEBNext Index 13	5´-CAAGCAGAAGACGGCATACGAGATTTGACTGT GACTGGAGTTCAGACGTGTGCTCTTCCGATC-s-T-3´	AGTCAA
NEBNext Index 14	5´-CAAGCAGAAGACGGCATACGAGATGGAACTGT GACTGGAGTTCAGACGTGTGCTCTTCCGATC-s-T-3´	AGTTCC
NEBNext Index 15	5´-CAAGCAGAAGACGGCATACGAGATTGACATGT GACTGGAGTTCAGACGTGTGCTCTTCCGATC-s-T-3´	ATGTCA
NEBNext Index 16	5´-CAAGCAGAAGACGGCATACGAGATGGACGGGT GACTGGAGTTCAGACGTGTGCTCTTCCGATC-s-T-3´	CCGTCC
NEBNext Index 17	5´-CAAGCAGAAGACGGCATACGAGATCTCTACGT GACTGGAGTTCAGACGTGTGCTCTTCCGATC-s-T-3´	GTAGAG
NEBNext Index 18	5´-CAAGCAGAAGACGGCATACGAGATGCGGACGT GACTGGAGTTCAGACGTGTGCTCTTCCGATC-s-T-3´	GTCCGC
NEBNext Index 19	5´-CAAGCAGAAGACGGCATACGAGATTTTTCACGT GACTGGAGTTCAGACGTGTGCTCTTCCGATC-s-T-3´	GTGAAA
NEBNext Index 20	5´-CAAGCAGAAGACGGCATACGAGATGGCCACGT GACTGGAGTTCAGACGTGTGCTCTTCCGATC-s-T-3´	GTGGCC
NEBNext Index 21	5´-CAAGCAGAAGACGGCATACGAGATCGAAACGT GACTGGAGTTCAGACGTGTGCTCTTCCGATC-s-T-3´	GTTTCG
NEBNext Index 22	5´-CAAGCAGAAGACGGCATACGAGATCGTACGGT GACTGGAGTTCAGACGTGTGCTCTTCCGATC-s-T-3´	CGTACG
NEBNext Index 23	5´-CAAGCAGAAGACGGCATACGAGATCCACTCGT GACTGGAGTTCAGACGTGTGCTCTTCCGATC-s-T-3´	GAGTGG
NEBNext Index 24	5´-CAAGCAGAAGACGGCATACGAGATGCTACCGT GACTGGAGTTCAGACGTGTGCTCTTCCGATC-s-T-3´	GGTAGC

Table 2-9: 24 Index Primers for Illumina used producing barcoded libraries (NewEngland Biolabs, 2019)
Where -s- indicates phosphorothioate bond.

Quality control checks were performed to ensure that the raw sequencing data did not contain any problems or biases. The sequencing quality was assessed by the online FastQC software available at: http://www.bioinformatics.babraham.ac.uk/projects/fastqc/ . FastQ files, containing the raw sequencing data (containing the adapter and/ or barcode stripped small RNA sequencing data) obtained from the MiSeq sequencer were uploaded to the online tool on the EMBL- EBI European Bioinformatics Institute website on Chimira '*Analysis of small RNA Sequencing data and microRNA modifications'* (http://wwwdev.ebi.ac.uk/enright-dev/chimira/). Furthermore, *homo sapiens* (hsa) was selected for the species option and the standard adaptor sequence, which was attached to the samples during the procedures undertaken, was specified as 'AGATCGGAAGAGC' when uploading the raw sequencing data. The sequences were trimmed using the specified standard adaptor sequence ('AGATCGGAAGAGC'), afterwards mapped against the human microRNA hairpin sequences from miRBase and finally a count-based microRNA expression data was extracted from Chimira. More specifically, the online tool removed the adaptor sequence from the reads of the samples and checked that the remaining sequence was big enough, i.e. minimum 17-20bp fragment. If the sequence was too short, it would lead to a bias in the data set, hence a too short sequence was discarded. Additionally, Chimira compared the sequences of the samples to a standardised human reference genome, allowing up to two mismatches (Enright and Vitsios, 2015). Input sequences were mapped against all known hairpin precursors of the selected genome allowing for identification of non-template sequences (Enright and Vitsios, 2015). Modifications such as 3p- and 5p- modifications and internal modifications (ADAR edits and SNPs) were identified (Enright and Vitsios, 2015). After these processes, a '*plain counts for file'* containing all the counts for all microRNAs identified in the samples, was downloaded from the online tool which was normalised in R Studio software using the DESeq2 package. In brief, the variance mean dependence in count data from high throughput sequencing assays was estimated and differential expression based on a model using the negative binominal distribution was tested for (Love et al., 2014). This adjusted the read counts by scaling a normalised factor in all libraries and assessed the differential expression of the different time course points (Love et al., 2014). The Benjamini and Hochberg method was used to correct the p-values (Benjamini and Hochberg, 1995) and the level of expression was considered

significant at a p-value adjusted < 0.05 and log2 fold change of >1 minimising false positive errors. The plots were created using 'gplots' in R package (Warnes, 2019).

Using the RT II Reverse Transcription Kit (Qiagen, UK), cDNA was synthesised according to the manufacturers' instructions. In brief, after thawing the extracted RNA from the colorectal mucosal biopsies the reverse-transcription master mix (see Table 2-10) was added, gently mixed and briefly centrifuged and incubated for 1 hour at 37°C followed by 5min at 95°C in the thermal cycler (centrifuge model: *Grant-bio LMC-3000*). The generated cDNA was stored at -20°C.

Component	Volume per reaction (µL)
5x miScript HiSpec Buffer	4
10x miScript Nucleics Mix	2
RNase-free water*	Variable
miScript Reverse Transcriptase Mix	2
Template RNA*	Variable

Table 2-10: Reverse-transcription master mix components and volume for a single reaction
*Volume was calculated to reach 500ng of RNA

2.2.3.9   Selection of microRNA panel and quantification by qPCR in colorectal mucosal biopsies

Bioinformatics analysis revealed extensive lists of significantly differentially expressed miRNAs and their fold change between the pre- and post-surgery group and the control group. The top 4 up- and top 4 down-regulated miRNAs with the greatest and significant fold change between pre- and post-surgery for which validated miScript primer assays were available at Qiagen, were selected for validation by qPCR (see Table 2-11) and which had not been picked up by a miRNome array conducted previously by Dr Sorena Afshar in these samples (Afshar, 2016a).

MiRNA	Fold Change	p-value	miScript Primer Assay	Mature miRNA sequence

mir-4516	-2.73827	0.002303	Hs_miR-4516_1	5'GGGAGAAGGGUCGGGGC
mir-1247-3p	-2.70697	0.008032	Hs_miR-1247-3p_1	5'CCCCGGGAACGUCGAGACUGGAGC
mir-3196	-2.41925	0.037441	Hs_miR-3196_2	5'CGGGGCGGCAGGGGCCUC
mir-671-5p	-1.06421	0.014619	Hs_miR-671-5p_3	5'AGGAAGCCCUGGAGGGCUGGAG
mir-204-3p	2.901349	0.02518	Hs_miR-204-3p_1	5'GCUGGGAAGGCAAAGGGACGU
mir-892c-3p	3.011725	0.006114	Hs_miR-892c-3p_1	5'CACUGUUUCCUUUCUGAGUGGA
mir-215-3p	3.149555	2.39E-08	Hs_miR-215-3p_1	5'UCUGUCAUUUCUUUAGGCCAAUA
mir-31-3p	4.796959	6.20E-05	Hs_miR-31*_1	5'UGCUAUGCCAACAUAUUGCCAU
SNORD68 (control)*			Hs_SNORD68_11	
RNU6-2 (control)*			Hs_RNU6-2_11	

Table 2-11: Top 4 up- and down-regulated microRNAs identified from bioinformatics analysis and housekeeping genes: their fold change, p-value miScript Primer Assay, mature miRNA sequence
*Qiagen UK does not provide mature miRNA sequences for reference genes

MiScript Primer Assays were received lypophilised at room temperature and reconstituted in 550µl TE Buffer (Sigma-Aldrich) and pH 8.0 according to the manufacturers' instructions, aliquoted and stored at -20˚C.

The plates for the qPCR were designed in the StepOne 7500 Software version 2.0.6. Two reference/ housekeeping genes, namely the small nucleolar RNA (snoRNA) SNORD68 and the small nuclear RNA (snRNA) RNU6, were quantified alongside each target miRNA on all plates for each sample. The cDNA samples were run in duplicates for each miRNA and housekeeping

gene on the 96 well plate. In order to eliminate any batch effect the following rules were applied during plate design:

- Samples derived from the same participant coming from different time points, i.e. pre- and post- surgery, were run on the same plate

- Samples from obese and non-obese participants were allocated evenly across the plates

- A 'no template control' was included for each miRNA (instead of cDNA, RNase-free water was added)

For the qPCR, the cDNA, miScript primer assays and the SYBR Green Kit (Qiagen, UK) were thawed and a master mix prepared as shown in Table 2-12 for each of the eight miScript primers and two housekeeping genes. The reactions required were prepared plus two extra reactions in excess.

Component	Volume per reaction (µL)
2x QuantiTect SYBR Green PCR Master Mix	12.5
10x miScript Universal Primer	2.5
10x miScript Primer Assay	2.5
RNase-free water	5

Table 2-12: SYBR Green PCR master mix components and volume for a single reaction for detection of mature miRNA

22.5µL of master mix was dispensed into each well of the 96 well plate and 2.5µL of cDNA was added to yield a total reaction volume of 25µL. The plate was carefully and tightly sealed using an optical adhesive film (Xtra-Clear Advanced Polyolefin StarSeal qPCR, StarLab) and centrifuged for 1min at 1000 x g at room temperature. The plate was put into the Applied Biosystems® StepOnePlus real time PCR machine and the cycling conditions were programmed as demonstrated in Table 2-13 to quantify microRNA expression.

Step	Time	Temperature	Number of cycles
Initial activation	15min	95°C	1
Denaturing	15sec	94°C	40

| Annealing | 30sec | 55°C | |
| Extension | 30sec | 70°C | |

Table 2-13: qPCR cycling conditions

2.2.3.10 Processing of data from qPCR to quantify microRNA expression in colorectal mucosal biopsies

Prior to qPCR data analysis, the melt curves were examined to confirm that a single PCR product had been produced during the qPCR (see Figure 2-9). If more than one peak was present it was an indication of primer dimer formation or lack of specificity of the assay (Dorak, 2006). If a poor melt curve was identified it was used as a criterion for repeating the procedure.
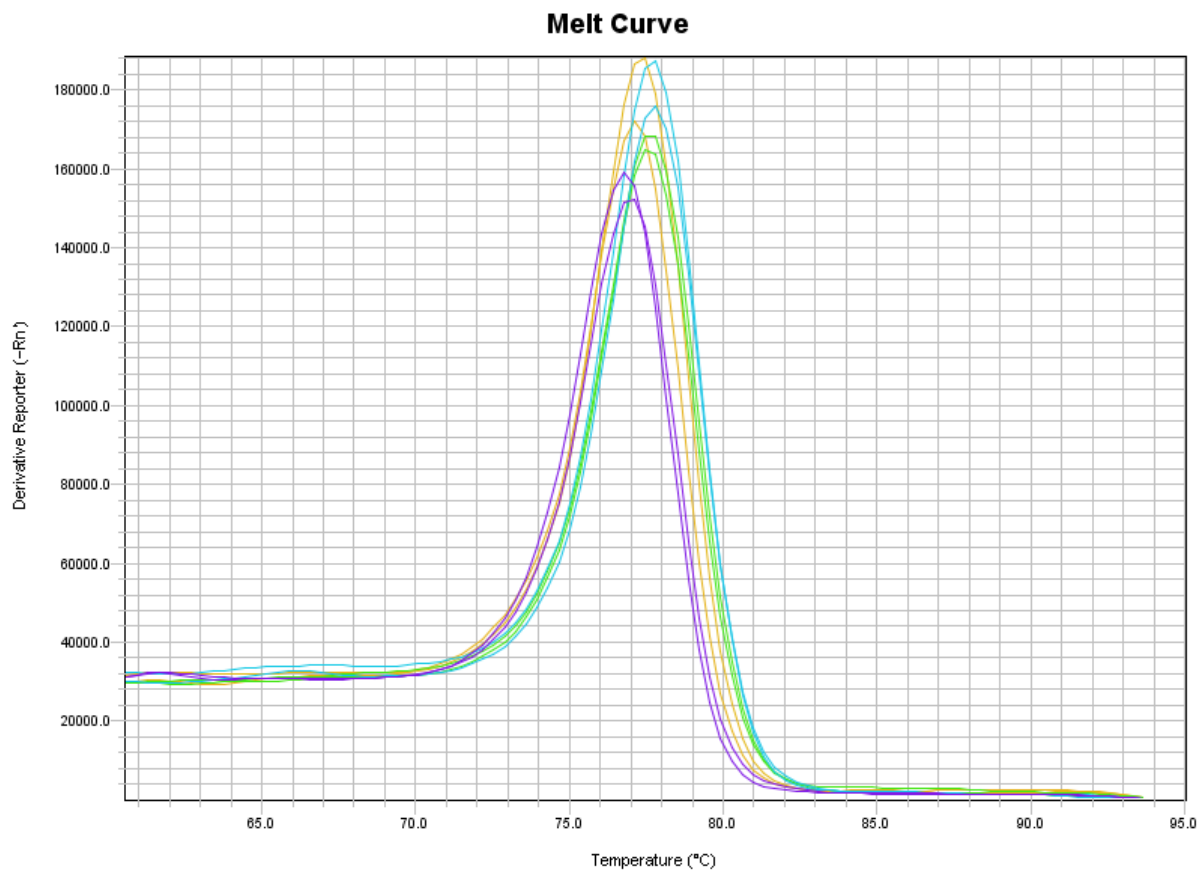
Figure 2-9: qPCR melt curve analysis of miR-3196

Next the baseline was set for all plates. The baseline was considered the 'noise' during the early qPCR cycles where any fluorescence was improbable because of PCR product generation (Qiagen, 2016). The baseline was defined to start at cycle 2 and finish at cycle 13. The upper

limit was defined after examination of all plates for the earliest PCR cycle where amplification was seen and subtracting 2 from it.

Afterwards, a cycle threshold was defined for each miRNA and housekeeping gene across all plates. The threshold value was defined at the highest precision of the duplicates of the procedure, which was usually towards the middle of the geometric phase and/ or lower as proposed by the Qiagen guidelines (Qiagen, 2016). Then an average threshold value for each miRNA and housekeeping gene was calculated for all the samples (see Table 2-14) which was then applied in the analysis settings of all plates. Any subsequent repeat analyses were processed and analysed using this calculated threshold value. The Ct values of duplicates from all samples were recorded and further analysed in Microsoft Excel.

miScript primer	Threshold values
Hs_miR-4516_1	18031.8
Hs_miR-1247-3p_1	14427.9
Hs_miR-3196_2	16334.9
Hs_miR-671-5p_3	19839.6
Hs_miR-204-3p_1	15471.8
Hs_miR-892c-3p_1	16503.0
Hs_miR-215-3p_1	18483.0
Hs_miR-31*_1	16227.6
Hs_SNORD68_11	14933.3
Hs_RNU6-2_11	14634.3

Table 2-14: Calculated average cycle threshold value for each miScript primer

Samples were included if both of the following conditions were met:

- Duplicates within one Ct value
- Melt curves comprising a single peak

If either one of the housekeeping genes did not fulfil the above conditions, the whole sample was repeated (including all miScript primers and housekeeping genes).

Next the delta Ct (ΔCt) method was applied. ΔCt is the ratio of expression of the miRNA of interest to that of the housekeeping gene. Housekeeping genes are consistently expressed in all samples. The geometric mean of the housekeeping genes for each sample was applied to normalise miRNA expression. For each miRNA for each sample the ΔCt value was calculated. The mean Ct value of the geometric mean of the housekeeping genes was subtracted from the mean Ct value of the duplicates for the miRNAs investigated.

For example: ΔCt= Ct (of miRNA) – Ct (of geometric mean of housekeeping genes, SNORD68 and RNU6).

Then the relative copies for each miRNA was calculated.

For example: relative copies = $2^{-\Delta Ct}$

Relative copies were then multiplied by a 1000 (a constant factor) to obtain the adjusted copies.

For example: adjusted copies = relative copies x 1000.

Furthermore, the ΔΔCt was calculated for each miRNA across the pre- and post-surgery group, so the fold change was calculated as the $2^{-\Delta \Delta Ct}$. To calculate the fold regulation 1 was divided by the ΔΔCt and, values >1 were considered as a fold up-regulation and for values <1, the negative inverse of the result was considered as a fold down-regulation.

For example: ΔΔCt= ΔCt post-surgery – ΔCt pre-surgery

Fold regulation= 1/ ΔΔCt

2.3   Statistical analysis

All statistical analyses were performed in IBM® SPSS® Statistics Version 21. A $p < 0.05$ was considered statistically significant. Data were reported as Mean ± Standard Deviation (SD).

Normality of the distribution of the variables was tested by the Shapiro-Wilk test.

Normally distributed data were analysed using paired sample or independent sample t-tests as appropriate. A Wilcoxon-signed-rank and a Mann-Whitney-U test was used for analysis of not normally distributed variables as appropriate. A cross-tabulation was undertaken using a

Chi square test. Linear regression analyses were used to investigate correlation between variables and outcomes of interest. An analysis of variance (ANOVA) was used to investigate the effects of covariates on outcomes of interest between groups and a Kruskal-Wallis H test was used instead where data were not normally distributed.

3 Effects of adiposity, weight loss and ageing on mitochondria in the colorectal mucosa (The BOCABS Study)

3.1 General introduction

A detailed description of the structure and functions of mitochondria can be found in the introductory chapter (see section 1.2).

In brief, mitochondria are eukaryotic organelles found in the cytosol which play a vital role in many metabolic pathways including iron-sulfur cluster biogenesis, maintenance of membrane potential, apoptosis, intracellular calcium signalling and adenosine triphosphate (ATP) production via oxidative phosphorylation; the latter being their primary function (Fernandez-Silva et al., 2003, Stewart and Chinnery, 2015).

The specific role of mitochondrial dysfunction in the aetiology of cancer, including CRC, remains to be discovered. Greaves (2014) detected that older individuals have a higher prevalence of somatic mtDNA mutations, but it is unclear if this increased mtDNA mutation load contributes to age-related CRC risk or is a non-causal age-associated phenomenon. There is evidence that during ageing and carcinogenesis mutations are generated randomly across the mitochondrial genome (Polyak et al., 1998, Taylor et al., 2003), followed by mutations throughout both the nuclear and mitochondrial genome (although the prevalence of nDNA mutations is lower than of mtDNA mutations due to the protection provided by histones, more effective DNA repair mechanisms and lower exposure to ROS) as cancer progresses (Taylor et al., 2003, Yoneyama et al., 2005, Lee et al., 2005).

Obesity is a major risk factor for CRC and mitochondrial dysfunction has been observed during over-feeding and in those with obesity (Breininger et al., 2019) (see section 1.4.2). Deliberate weight loss in the obese appears to lower CRC risk (Afshar et al., 2018, Schauer et al., 2019) and leads to improved capacity, integrity, biogenesis and function of mitochondria in muscle and adipose tissue (Breininger et al., 2019) (see section 1.4.4). If dysfunction of mitochondria in obesity is causal for CRC risk, then one would anticipate that weight loss would "improve" mitochondrial markers and/or reduce the prevalence of mtDNA mutations in this tissue. However, there have been no previous studies on the effects of weight loss following bariatric surgery on mitochondria in the colorectal mucosa of humans.

3.1.1 Hypotheses

The hypotheses for this study were:

- Mitochondrial oxidative phosphorylation (OXPHOS) proteins in the colorectal mucosa are less abundant in obese compared with non-obese adults.

- Weight loss following bariatric surgery in initially obese adults alters OXPHOS protein abundance in the colorectal mucosa.

- OXPHOS proteins in the colorectal mucosa present at lower levels and/ or are deficient in older compared with younger adults.

- Mitochondrial DNA mutations in the colorectal mucosa are elevated in obese compared with non-obese adults.

- Weight loss following bariatric surgery in initially obese adults reduces/ slows down the clonal expansion of mutated mtDNA in the colorectal mucosa.

3.1.2 Aims

The aims of this study were:

- To test the above hypotheses. To do so, patterns of OXPHOS proteins abundance and mtDNA mutations were measured in the colorectal mucosa of i) matched groups of obese and non-obese adults, ii) obese adults before and after bariatric surgery, iii) non-obese adults and adults post-bariatric surgery and iv) younger and older adults.

3.1.3 Objectives

The objectives of this study were:

- To use biological samples (mucosal biopsies) and data from the BOCABS Study (Afshar et al., 2018) to investigate the effects of obesity and of deliberate weight loss on the patterns of OXPHOS protein abundance (complex I and IV and mitochondrial mass) and mtDNA mutation load in the human colorectal mucosa.

- To use immunofluorescent labelling to provide robust quantification of complex I and IV, and mitochondrial mass in colorectal mucosal biopsies.

- To use Next Generation Sequencing (NGS) to provide global, unbiased, quantification of patterns and total load of mtDNA mutations in crypts obtained from colorectal mucosal biopsies.

3.1.4 Overview of methods

A detailed description of the experimental procedures and methods for quantifying OXPHOS protein expression and for sequencing mtDNA can be found in the Methods chapter sections 2.2.1 and 2.2.2, respectively.

In the BOCABS Study, initially obese participants (n=29) underwent RYGB, sleeve gastrectomy or gastric balloon surgery. In this study, I used samples and data from participants for whom matched (before and after surgery) formalin fixed and paraffin embedded mucosal biopsies were available for OXPHOS protein abundance assay by immunofluorescence (n=26). In addition, matched before and after frozen mucosal biopsies from the same participants (n=26) and from matched non-obese individuals were utilised for NGS.

In brief, colorectal mucosal biopsies that were formalin fixed and paraffin embedded were sectioned (see section 2.2.1.1) and labelled for mitochondrial respiratory chain complex I and IV protein subunits and a marker of mitochondrial mass using immunofluorescence (see section 2.2.1.2). The labelled colorectal mucosal biopsies were imaged using confocal microscopy (see section 2.2.1.3) and data were processed using ImageJ (see section 2.2.1.4). Statistical analyses were performed using IBM® SPSS® Statistic Version 21. The Shapiro-Wilk test showed that the data were not normally distributed, and consequently the Mann-Whitney-U test was used to compare OXPHOS protein abundance between the obese and non-obese groups and the Wilcoxon-signed-rank test was used to examine OXPHOS protein abundance in initially obese individuals pre- and post-surgery. Furthermore, data of initially obese (pre-surgery group) and non-obese individuals were dichotomised at the median age (48 years) and, as data were not normally distributed, the Mann-Whitney-U test was used to examine OXPHOS protein abundance between younger and older individuals.

To sequence mtDNA, frozen colorectal mucosal biopsies were sectioned on the cryostat (see section 2.2.2.1) and then SDH stained (see section 2.2.2.2). Crypts were collected from stained sections using laser microdissection, and then lysed (see section 2.2.2.3). The mtDNA of the lysed crypts was amplified using long range PCR (see section 2.2.2.4), products were

separated and visualised by agarose gel electrophoresis (see section 2.2.2.5). Afterwards mtDNA was purified and quantified (see section 2.2.2.6) and libraries were constructed and mtDNA was sequenced (see section 2.2.2.7). Finally, data were analysed using standard bioinformatics approaches (see section 2.2.2.8). Statistical analyses were performed using IBM® SPSS® Statistic Version 21. The Shapiro-Wilk test showed that the data were not normally distributed. Consequently, the Mann-Whitney U test was used to compare mtDNA mutations between the obese and non-obese groups and the Wilcoxon signed rank test was used to examine mtDNA mutations in initially obese individuals pre- and post-bariatric surgery. Where appropriate, data were transformed to the Log(10) scale (Bland and Altman, 1996) to ensure homogeneity of variance in all treatment groups and, the test for normality was repeated to determine the application of the appropriate statistical test. Since Log(10) values for individuals with no mutations cannot be computed, for display purposes a zero value is included in relevant figures. A cross-tabulation using the Chi square test was used to examine differences in the location of mtDNA mutations by gene type. A one-way ANOVA and the Kruskal-Wallis H test were used to determine differences in mtDNA mutations between the participants pre- and post-bariatric surgery and for comparisons with the non-obese Controls. Finally, linear regression analyses were used to examine the effects of BMI and age on patterns of mtDNA mutations.

3.1.5   Participant characteristics

A total of 38 patients were recruited to the BOCABS Study, of whom 4 did not undergo bariatric surgery, resulting in 34 participants eligible for follow-up at six months post-surgery. Of these 34 patients, 3 did not participate in the follow-up, leaving 31 participants who completed the study (91% completion rate). Table 3-1 summaries characteristics at baseline and follow-up for initially obese participants and at baseline only for the non-obese Control group (see Appendix J for un-pooled data of the non-obese Controls, recruited to the BOCABS and DISC Studies). Two participants experienced severe post-surgery complications which meant that they were unlikely to be in equilibrium at follow up and these participants were excluded. There were no statistically significant differences in baseline characteristics between the 'recruited' (n=38) and 'included' (n=29) groups of participants (p-value > 0.05). Participants were predominantly Caucasian (White British) with a mean age of 46 years (range 30.9 to 65.2 years) and more females (n=30; 79%) than males (n=8; 21%) who took part in the

BOCABS Study. At baseline, the obese participants had a mean BMI of 41.9 kg/m^2, body fat of 49% and waist: hip ratio of 0.9, which dropped to 32.5 kg/m^2, 37.9% and 0.9, respectively, at six months follow-up.

The Control group consisted of 20 non-obese and otherwise healthy adults, all of whom were Caucasian (British White) with a mean age of 46 (range 21- 61) years. The group had more females (60%; n=12) than males (4%; n=8) with mean BMI of 25.4 kg/m2 (range 20- 30 kg/m^2), mean body fat 30.3% (range 21.2- 36.2%) and mean waist: hip ratio of 0.87 (range 0.74- 0.99).

	Obese participants at baseline		Non-obese Controls	Obese participants at follow-up	Obese participants P-value	
	Recruited n=38	Included n=29	n=20	n=29	Baseline *recruited vs included**	Baseline vs Follow-up†
Age (years)	46.0 (1.0)	46.4 (1.5)	46.0 (2.6)	-	0.87	0.74
Male	8	6	8	-	1‡	N/A
Female	30	23	12	-		N/A
British White	37	28	19	-	1‡	N/A
Black African	1	1	1	-		N/A
BMI (kg/m^2)	42.7 (1.2)	41.9 (1.1)	25.4 (0.5)	32.5 (1.0)	0.62	**<0.001**
Body fat (%)	48.9 (0.9)	49.0 (1.0)	30.3 (1.3)	37.9 (1.4)	0.91	**<0.001**
Waist (W; cm)	124 (2.2)	123 (2.4)	88.5 (2.3)	99 (3.0)	0.78	**<0.001**
Hip (H; cm)	133 (1.8)	133 (1.7)	102.3 (1.6)	113 (3.2)	0.99	**<0.001**
W:H ratio	0.94 (0.02)	0.93 (0.02)	0.87 (0.02)	0.88 (0.02)	N/A	N/A

Table 3-1: Characteristics of initially obese participants pre- and post-bariatric surgery and of non-obese Controls
Data presented as mean (SEM) unless otherwise stated.
*Two sample t-test
†Paired t-test
‡Chi-Square test, exact significance reported

For the study of quantification of OXPHOS protein abundance in the colorectal mucosa, a subset of participants only from the BOCABS Study was used due to sample availability. Table 3-2 summarises participants' characteristics and anthropometric measurements included for quantification of OXPHOS proteins and sequencing of mtDNA in colorectal mucosal biopsies of pre- and post-bariatric surgery, and of non-obese Control participants (see Appendix L for un-pooled data of the non-obese Controls, recruited to the BOCABS and DISC Studies and Appendix M for the full characteristics of each participant of the 3 groups, pre- and post-surgery and non-obese Controls, included in the subset). For this analysis, 26 paired pre- and post-bariatric surgery samples were used. The characteristics of the pre-surgery group included in this analysis (n=26) did not differ significantly from those recruited (n=38) to the BOCABS Study. The participants included had a mean age of 47.5 years (range 31.7 to 65.2 years) and this study group was comprised of more females (n=19; 73%) than males (n=7; 27%). They had a mean BMI of 41.3 kg/m^2 and body fat of 47.9%, which dropped significantly to 31.7 kg/m^2 and 36.5% respectively at six months follow-up. Their waist:hip ratio was 0.94 which declined to 0.9 at six months follow-up.

The non-obese Control group consisted of 16 participants who had a mean age of 44 (range 21- 59) years. The group had more females (56%; n=9) than males (44%; n=7) with mean BMI of 25.5 kg/m^2 (range 20-30 kg/m^2), mean body fat 30.4% (range 21.2- 36.2%) and mean waist: hip ratio of 0.86 (range 0.74- 0.99).

Figure 3-1 and Figure 3-2 illustrate measures of adiposity, including BMI, body fat percentage and circumference of the waist and the hip, in obese participants before and 6 months after bariatric surgery and in Controls. Although bariatric surgery induced a significant weight loss of mean 27kg, participants remained obese at 6 months follow-up.

	Obese participants at baseline		Non-obese Controls	Obese participants at follow-up	Obese participants P-value	
	Recruited n=38	Included n=26	n=16	n=26	Baseline *recruited* vs *included**	Baseline vs Follow-up†
Age (years)	46.0 (1.0)	47.5 (1.5)	45.6 (2.7)	-	0.52	0.48
Male	8	7	7	-	1‡	N/A
Female	30	19	9	-		N/A
British White	37	26	15	-	1‡	N/A
Black African	1	0	1	-		N/A
BMI (kg/m^2)	42.7 (1.2)	41.3 (1.0)	25.5 (2.3)	31.7 (0.9)	0.49	**<0.001**
Body fat (%)	48.9 (0.9)	47.9 (1.2)	30.4 (1.5)	36.5 (1.6)	0.97	**<0.001**
Waist (W; cm)	124 (2.2)	122.6 (2.3)	88.5 (2.3)	98.5 (3.3)	0.31	**<0.001**
Hip (H; cm)	133 (1.8)	127.6 (2.9)	102.3 (1.6)	109.5 (2.8)	0.58	**<0.001**
W:H ratio	0.94 (0.02)	0.94 (0.02)	0.86 (0.03)	0.90 (0.02)	N/A	N/A

Table 3-2: Characteristics of initially obese participants pre- and post-bariatric surgery and of non-obese Controls for whom analysis of OXPHOS protein quantification and sequencing of the mtDNA in the colorectal mucosa was conducted
Data presented as mean (SEM) unless otherwise stated.
*Two sample t-test
†Paired t-test
‡Chi-Square test, exact significance reported
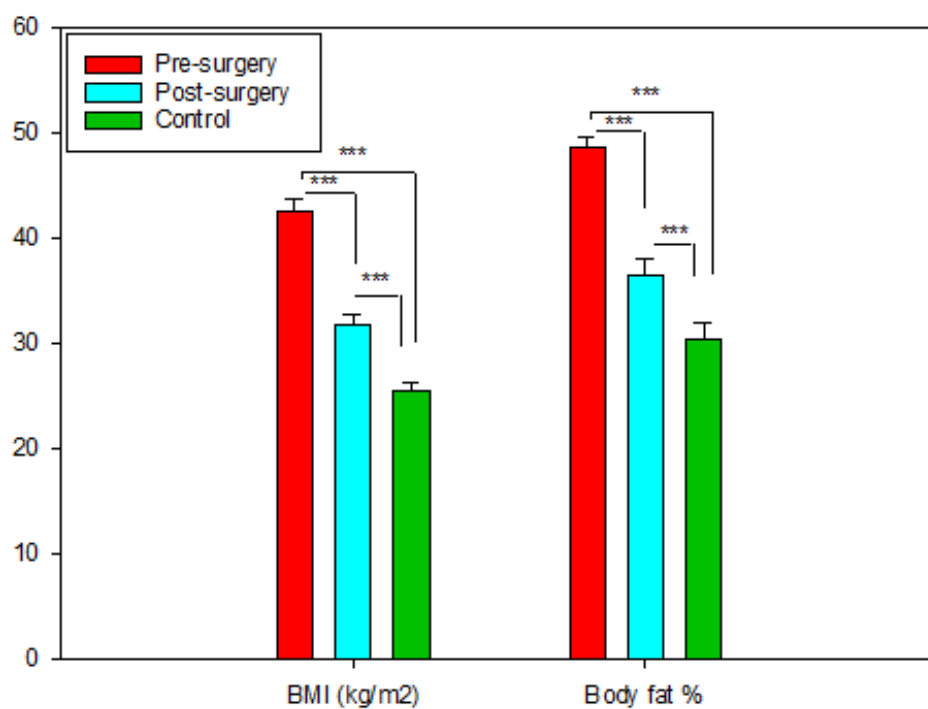
Figure 3-1: BMI and body fat percentage in obese participants before and 6 months after bariatric surgery and in non-obese Controls
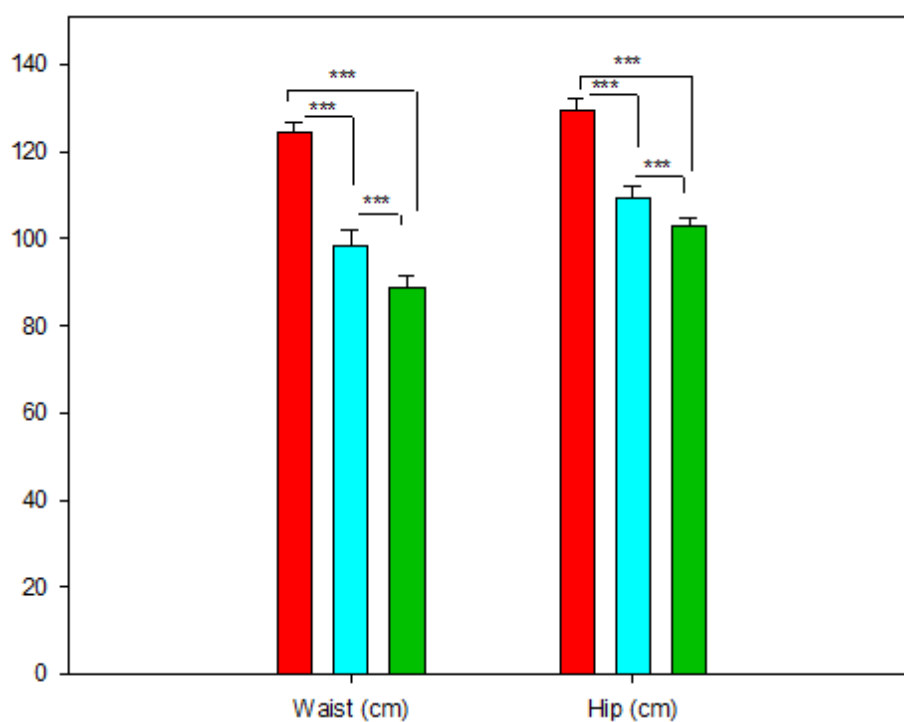
Figure 3-2: Waist and hip circumference in obese participants before and 6 months after bariatric surgery and in non-obese Controls

3.2 Effects of adiposity on expression of OXPHOS proteins in colonocytes

To quantify mitochondrial OXPHOS protein levels, an established quadruple immunofluorescence protocol was performed on 26 matched pre- and post-surgery participants and 16 non-obese Controls. Figure 3-3 shows crypts stained for complexes I and IV, mitochondrial mass, Dapi (a nuclear stain) and the merged image from a transverse section of the colorectal mucosa of an obese individual recruited to the BOCABS Study. Complex I deficient crypts are clearly visible (reduced brightness of crypts shown in red colour) and partially complex IV deficient crypts can also be seen (reduced brightness of partial crypts shown in purple colour). As expected, crypts have a normal mitochondrial mass and Dapi staining.
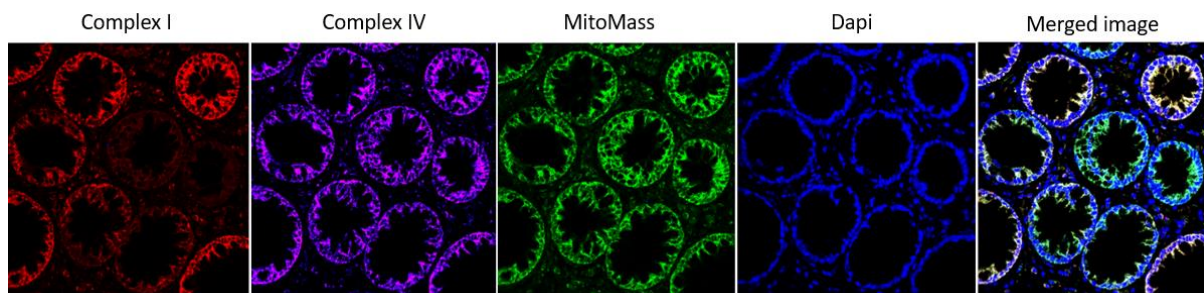
Figure 3-3: Expression of complexes I and IV, mitochondrial mass, nuclear marker (Dapi) and merged image in a transverse section of the colorectal mucosa from an obese individual recruited to the BOCABS Study

Protein abundance was estimated as described in the Methods Chapter (section 2.2.1.4) and categorised using z-scores. Based on the value of the z-score, each respiratory chain protein measured within a crypt was designated as overexpressed (z >2), normal (z <2), slightly deficient (z < -2), very deficient (z < -3) or depleted (z < -4) (Rocha et al., 2015) (see Appendix N). Figure 3-4 shows the mean percentage of complex I normal and deficient crypts in obese and non-obese participants. No statistically significant difference was detected. However, when analysing the level of deficiency, i.e. whether crypts are slightly or very deficient or depleted for complex I, obese individuals had a significantly higher prevalence of complex I depleted crypts (9.2%) when compared to Controls (0%) (p=0.046) (see Figure 3-5).
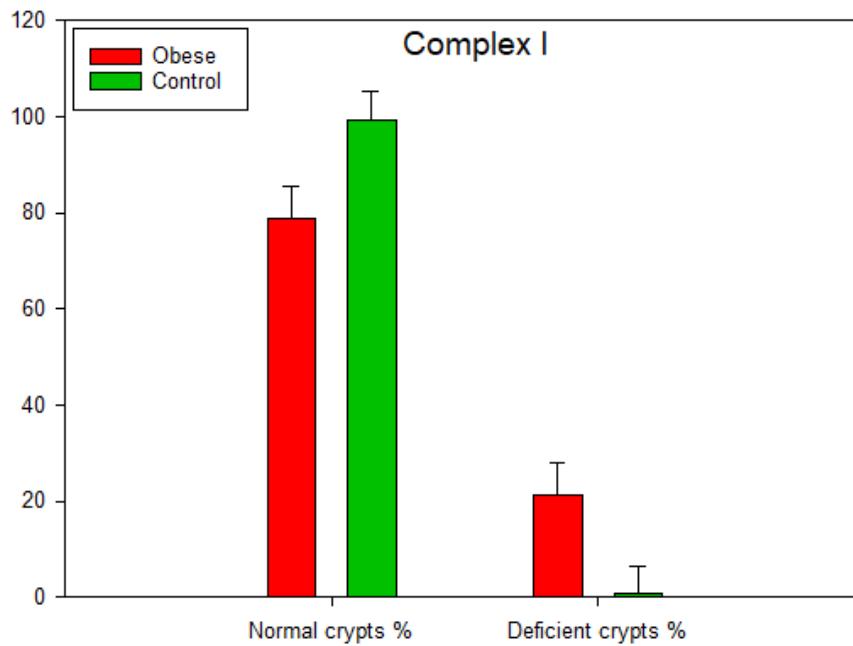
Figure 3-4: Percentage of normal and deficient complex I crypts in the colorectal mucosa of obese and non-obese (Control) individuals
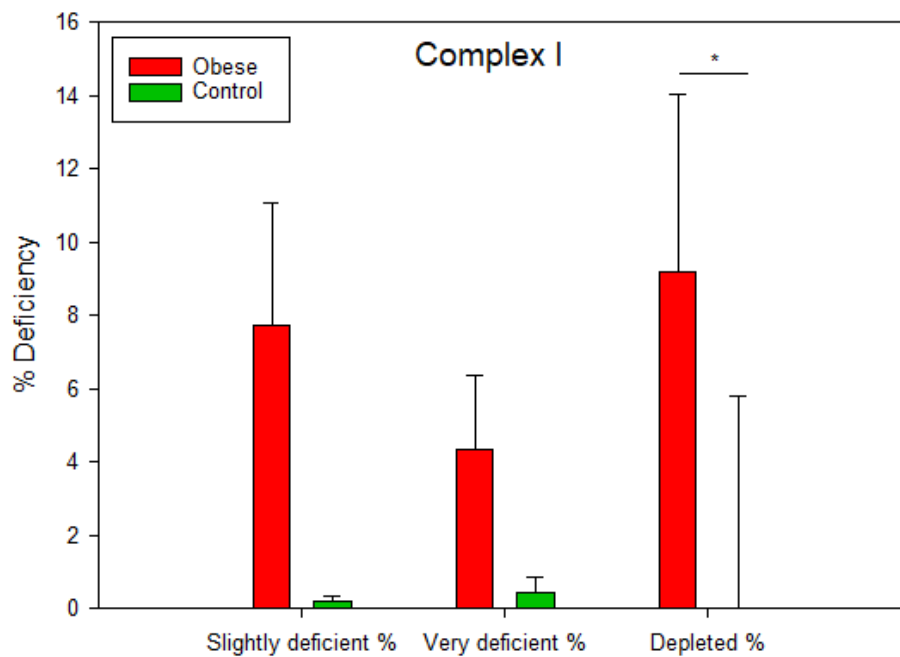
Figure 3-5: Percentage of level of deficiency (slightly, very or depleted) for complex I crypts in the colorectal mucosa of obese and non-obese (Control) individuals

Figure 3-6 shows the mean percentage of complex IV normal and deficient crypts in obese and non-obese (Control) participants. Obese individuals had significantly fewer crypts with normal complex IV (96.9%) compared with Controls (100%) and significantly more crypts with complex IV deficiency (3.1%) compared with Controls (0%) (p=0.03). Furthermore, when

analysing the level of deficiency, i.e. whether crypts are slightly or very deficient or depleted for complex IV, obese individuals had a significantly higher prevalence of complex IV slightly deficient crypts (2%) when compared with Controls (0%) (p=0.03) (see Figure 3-7).
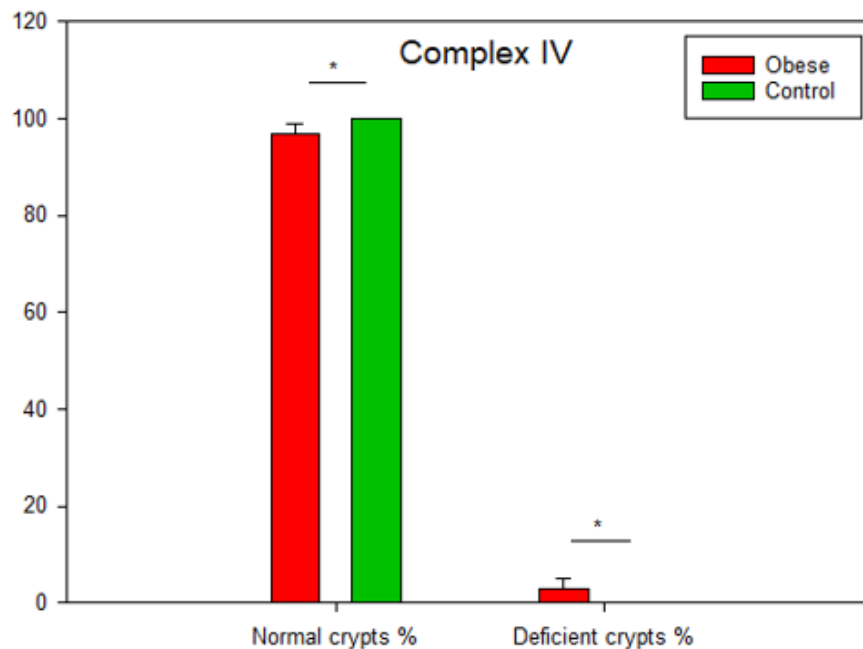
Figure 3-6: Percentage of normal and deficient complex IV crypts in the colorectal mucosa of obese and non-obese (Control) individuals
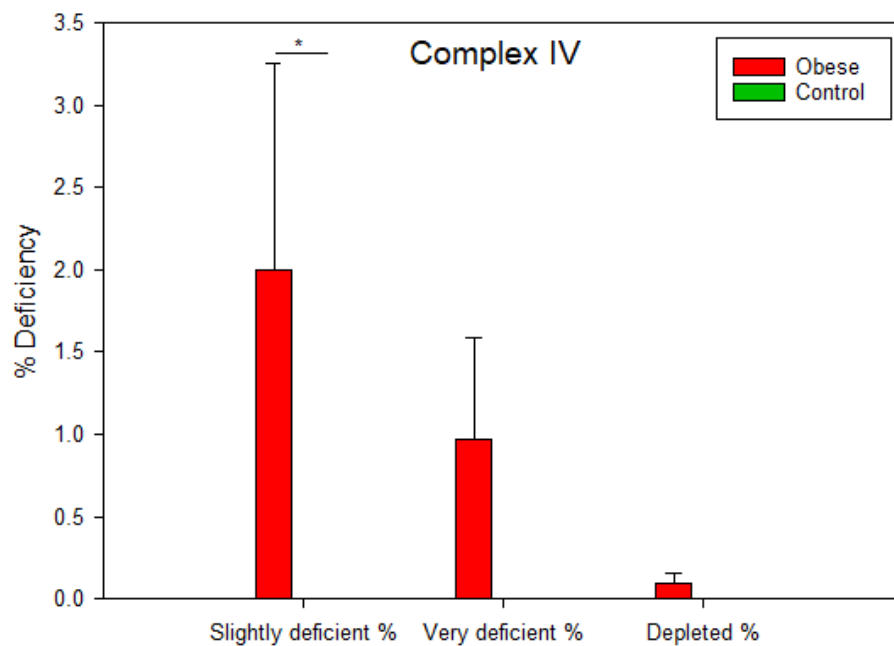
Figure 3-7: Percentage of deficiency (slightly, very or depleted) for complex IV in crypts from the colorectal mucosa of obese and non-obese (Control) individuals

Mitochondrial mass was quantified using the antibody TOMM20, which has been previously used and validated for the normalisation and quantification of MTCO1 and NDUFB8 in patients with mitochondrial disease (Latil et al., 2012, Tang et al., 2013). Figure 3-8 shows the mean percentage of crypts which had normal mitochondrial mass levels, or evidence of mitochondrial mass depletion in crypt cells from obese and non-obese (Control) participants. Obese individuals had significantly fewer crypts with normal mitochondrial mass (93.8%) compared with Controls (99.96%) and significantly more crypts with mitochondrial mass deficiency (6.2%) compared with Controls (0.04%) (p=0.03). Furthermore, when analysing the level of deficiency, i.e. whether crypts are slightly or very deficient or depleted for mitochondrial mass, obese individuals had a significantly higher prevalence of mitochondrial mass slightly deficient crypts (4.7%) when compared with Controls (0.04%) (p=0.03) (see Figure 3-9).
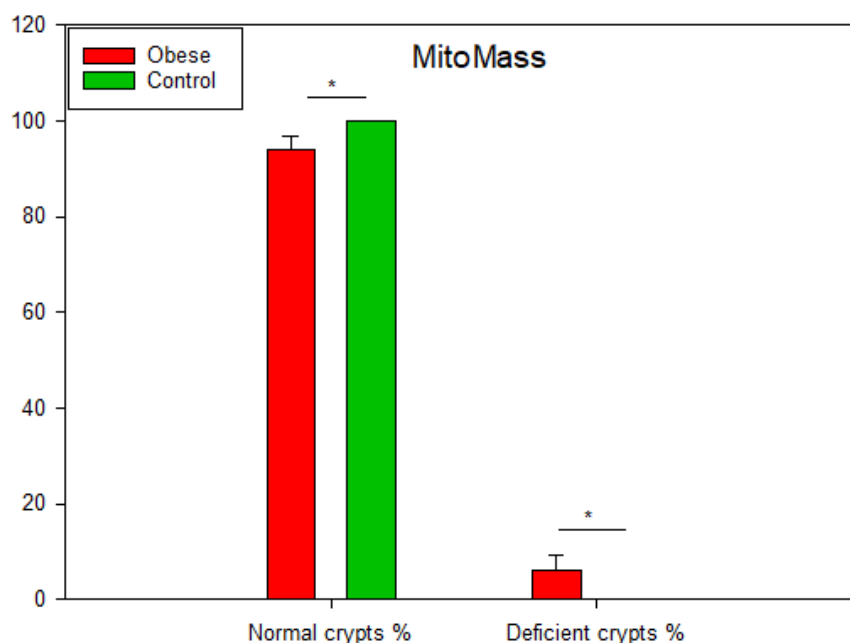
Figure 3-8: Percentage of crypts with normal and deficient mitochondrial mass crypts in the colorectal mucosa in obese and non-obese (Control) individuals
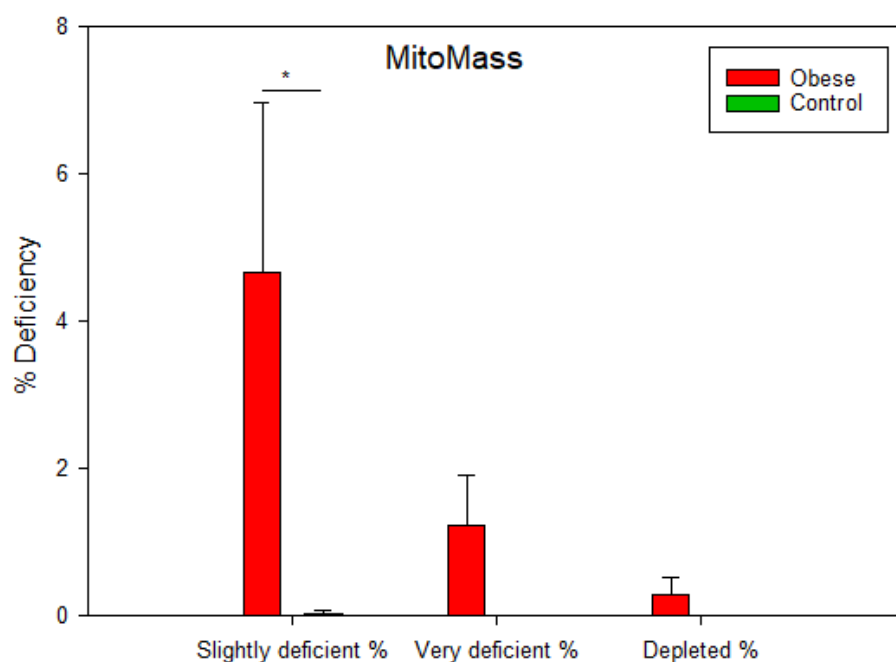
Figure 3-9: Percentage of crypts showing deficiency (slightly, very or depleted) for mitochondrial mass in the colorectal mucosa from obese and non-obese (Control) individuals

Figure 3-10, Figure 3-11 and Figure 3-12 show the mean percentage of complex I and IV and mitochondrial mass crypts in pre- and post-bariatric surgery patients, respectively. However, weight loss (mean 27kg) did not significantly change the levels of OXPHOS proteins in crypts at 6 months follow-up.
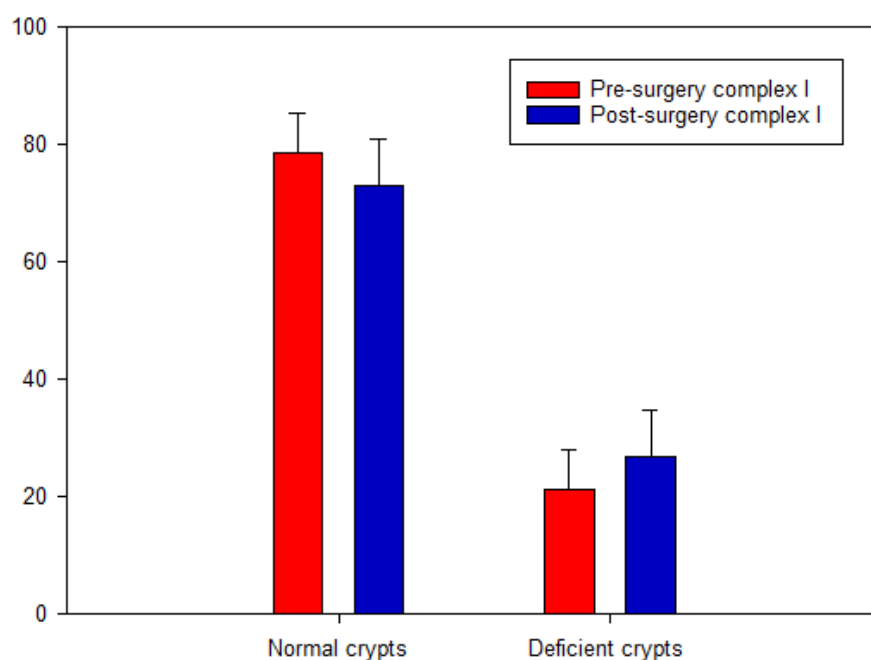
Figure 3-10: Percentage of crypts that were normal and deficient for complex I in the colorectal mucosa of obese participants pre- and post-bariatric surgery
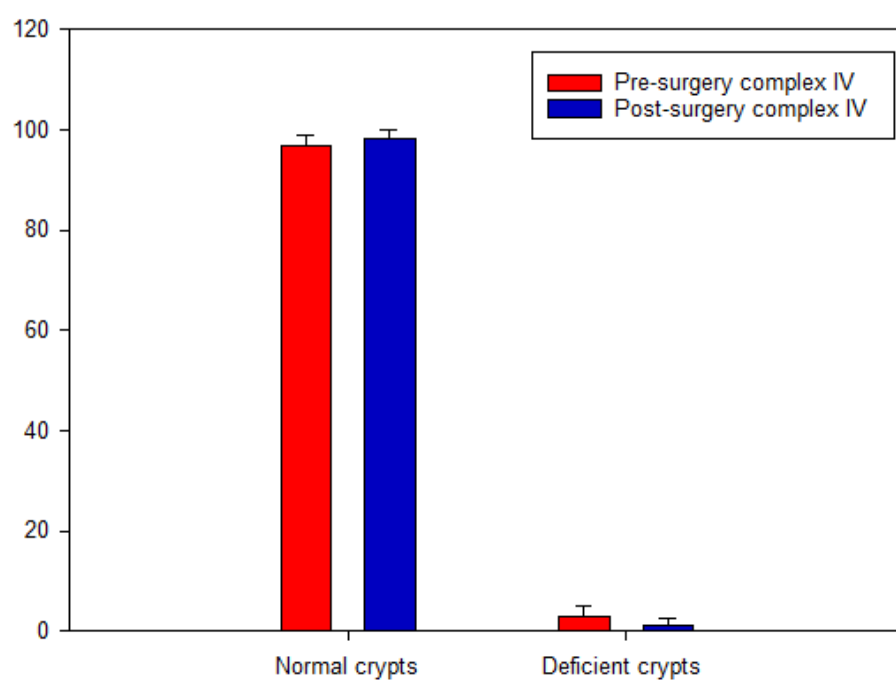
Figure 3-11: Percentage of normal and deficient complex IV crypts in pre- and post-bariatric surgery patients
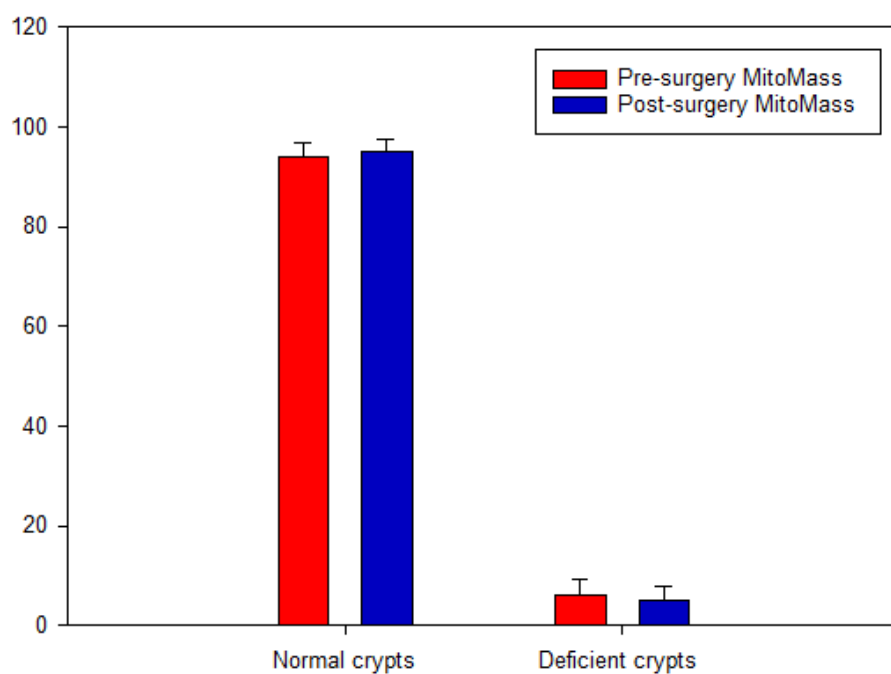
Figure 3-12: Percentage of normal and deficient mitochondrial mass crypts in pre- and post-bariatric surgery patients

3.3 Effects of ageing on expression of OXPHOS proteins in colonocytes

Data from obese and non-obese individuals were dichotomised at the median age (48 years) and divided into a younger (n=24, range 21 to 48 years) and older group (n=24, range 48 to 65 years) to investigate the effects of age on complex I and IV and mitochondrial mass levels. There was no significant association between age and complex I abundance. Figure 3-13 shows the percentage of normal and deficient complex I and IV and mitochondrial mass crypts in younger and older individuals. The prevalence of complex IV (1.3%) and mitochondrial mass (1.7%) deficiency was significantly greater in older (>48 years) compared with younger (≤48 years) individuals (p=0.03 and p=0.01, respectively).
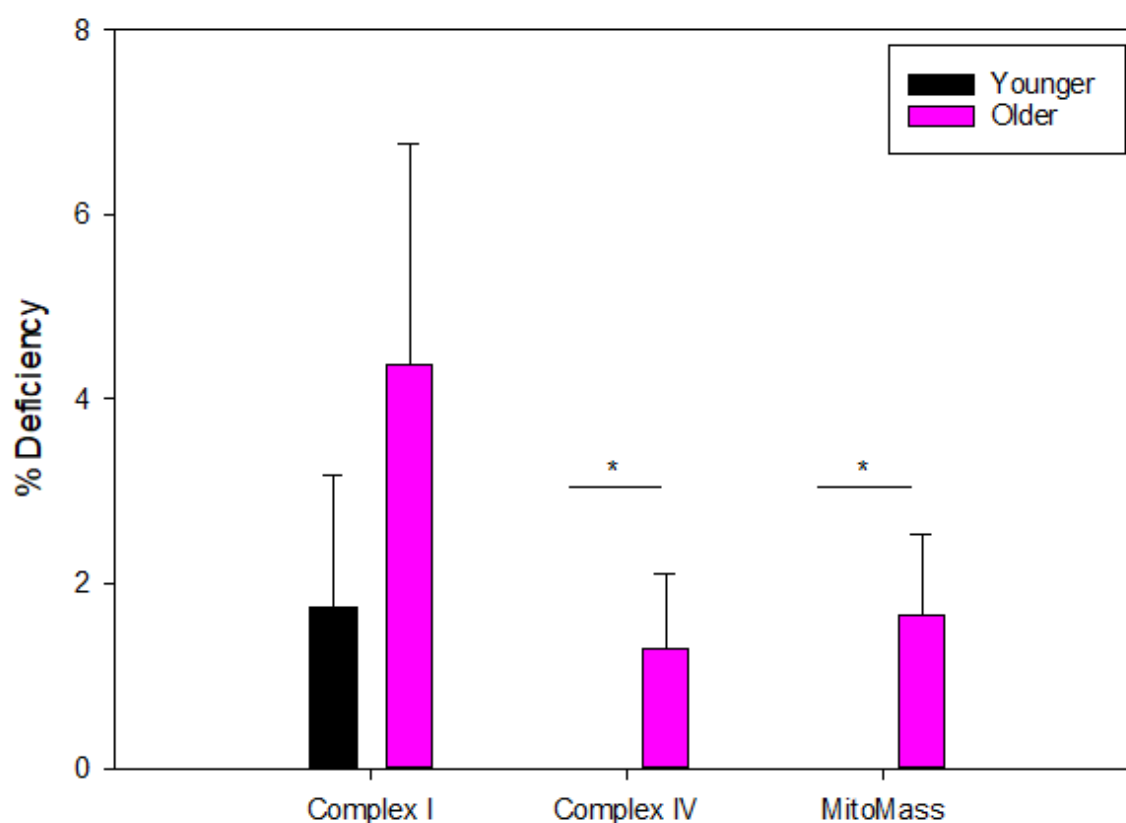
Figure 3-13: Percentage of crypts with normal and deficient complexes I and IV and mitochondrial mass in the colorectal mucosa from younger and older individuals

3.4 Effects of adiposity and weight loss on the mitochondrial genome

3.4.1 Mutations in the mitochondrial spectra

Next Generation Sequencing (NGS) of the mitochondrial genome was performed using colorectal mucosal biopsies from obese participants pre- and post-surgery and from non-

obese Controls. MtDNA was amplified in two overlapping 9 KB fragments, named Fragment A and Fragment B. Unfortunately, for the majority of the participants, amplification and quantification of fragment B was not successful (Appendix O). Due to time constraints it was not possible to repeat the amplification of fragment B, therefore the following results include data from NGS of Fragment A only i.e. approximately 60% of the mitochondrial genome.

A total of 9931bp of the mitochondrial genome were sequenced in the colorectal mucosa (Fragment A m.6222-m.16153) and a total of 987 mutations were detected. Out of all mtDNA mutations detected (n=987), 47.9% were somatic heteroplasmic mtDNA mutations. The remaining 52.1% were homoplasmic/ germline 'mutations' which define the individual participant-specific mitochondrial haplogroup. Table 3-3 shows the count and percentage of the distribution of heteroplasmic mutations in the colorectal mucosa in the obese individuals pre- and post-bariatric surgery and the non-obese Controls. Different haplogroups have different numbers of defining germline mutations and the proportions will change depending on which haplogroups are present in each individual.

	Mean number of somatic heteroplasmic mtDNA mutations	Total somatic heteroplasmic mtDNA mutations (%)
All BOCABS Study participants (n=49)	473	47.9 (range 1- 98.51)
Obese participants pre-surgery (n=20)	228	48.2 (range 1- 94.19)
Obese participants post-surgery (n=18)	122	25.8 (range 1- 98.51)
Non-obese Controls (n=11)	123	26.0 (range 1.01- 98.26)

Table 3-3: Heteroplasmic mtDNA mutations in the colorectal mucosa of obese individuals pre- and post-bariatric surgery and of non-obese Controls

Figure 3-14 shows the number of somatic mtDNA mutations identified for each participant (represented by a dot) in the obese pre- and post-surgery and the non-obese Controls. Obese individuals of the pre-surgery group tended to have greater frequency of somatic mtDNA

mutations compared with the post-bariatric surgery and the non-obese Controls, but the differences were not significant (p=0.500). One obese participant of the pre-surgery group carried nearly 100 somatic mtDNA mutations, a 10-fold, 16-fold and 12-fold higher frequency than the mean mutation frequency in the pre- and post-surgery group and non-obese Controls, respectively. No follow-up data are available, due to unsuccessful sequencing for this interesting participant who carried nearly 100 somatic mtDNA mutations at baseline so I do not know whether weight loss affected the frequency of mtDNA mutations. The differences in mean number of somatic mtDNA mutations between the groups is rather large, and surprisingly not significant, but this is likely due to the large inter-individual variation (see Figure 3-15).
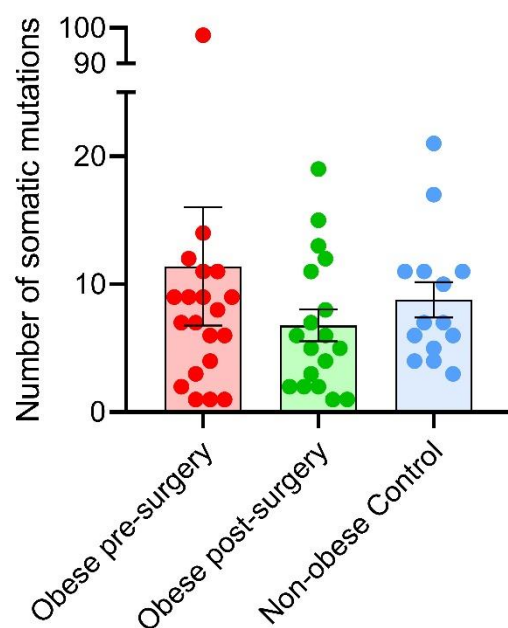
Figure 3-14: Number of somatic heteroplasmic mtDNA mutations detected for each participant (dot) in obese pre- and post-bariatric surgery and in non-obese Controls (p=0.500 Kruskal-Wallis H test). As a further sensitivity analysis differences between i) obese pre-surgery and non-obese Controls (p=0.610) and ii) unmatched pre- and post-surgery adults (p=528) were tested with a Mann Whitney U test
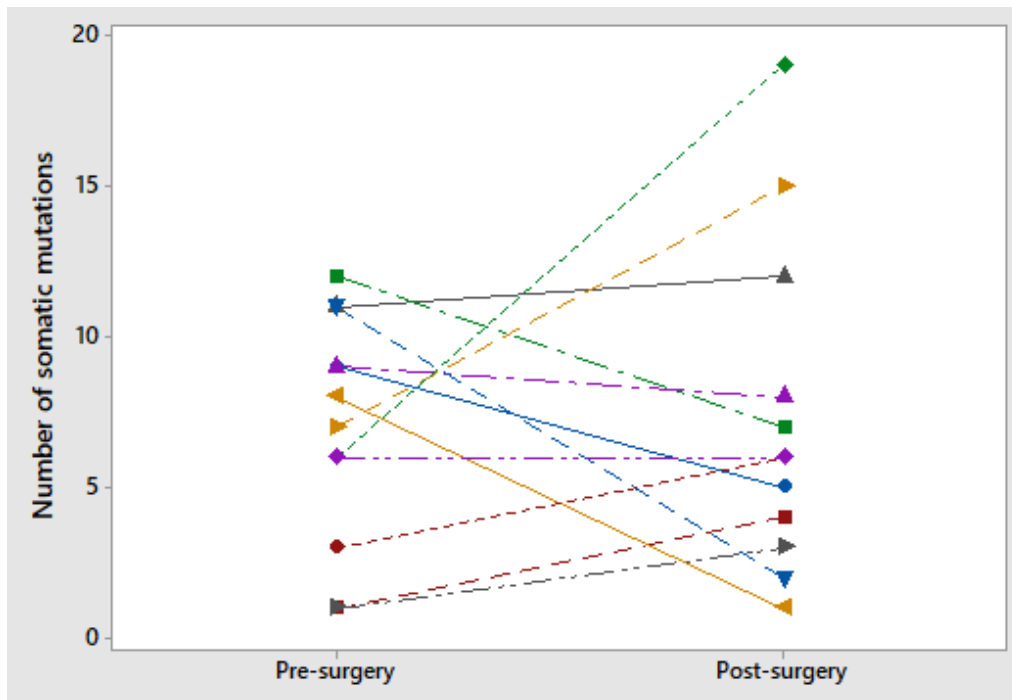
Figure 3-15: Number of somatic heteroplasmic mtDNA mutations detected in the colorectal mucosa for each initially obese individual before and after bariatric surgery.

The effects of higher levels of adiposity on the mitochondrial genome were investigated. MtDNA mutation frequency was calculated by dividing the percentage of somatic heteroplasmic mutations detected for each participant, by the total bases sequenced for that individual. Figure 3-16 shows the mtDNA mutation frequency quantified by NGS in the colorectal mucosa of obese pre-surgery participants and non-obese Controls on a Log(10) scale (see Appendix P for untransformed data). Obese pre-surgery participants appeared to have a higher mtDNA mutation frequency compared with non-obese Controls, but this difference was not statistically significant (P=0.544).
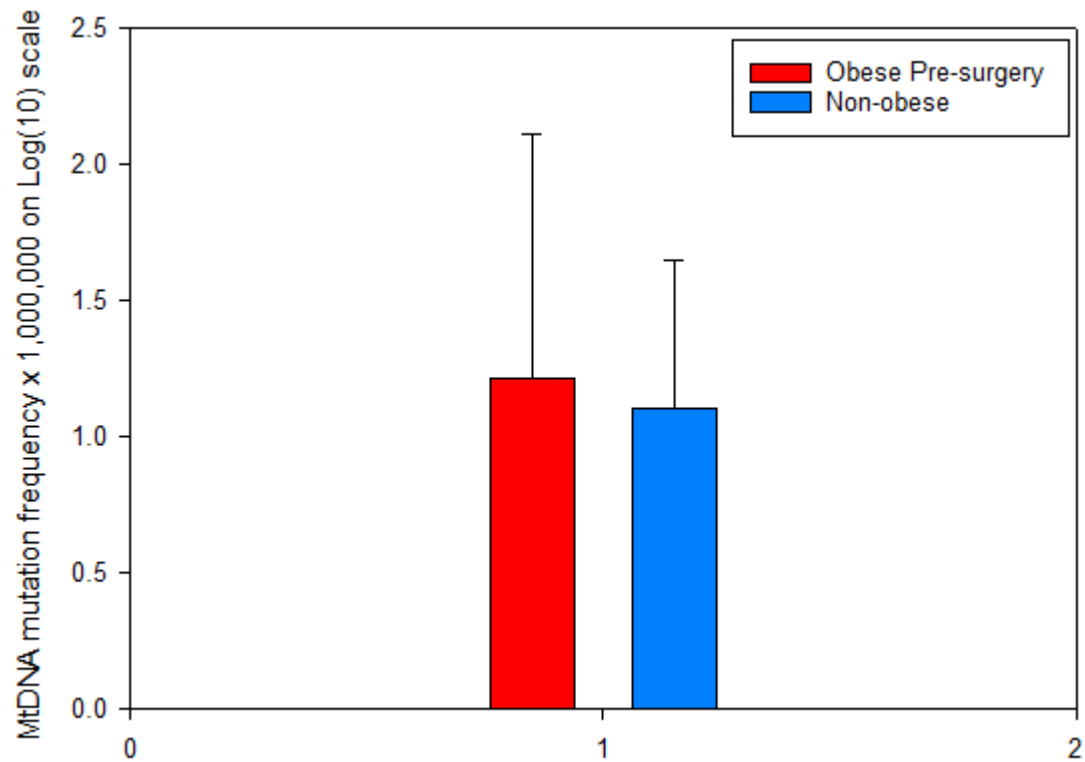
Figure 3-16: Frequency of mtDNA mutations detected by NGS in the colorectal mucosa of obese pre-surgery participants and non-obese Controls. Data in this Figure are presented on a Log(10) scale. Since zero values cannot be displayed in this way, data for n=3 and n=1 for the obese pre-surgery group and non-obese Controls, respectively are included in this figure with a zero value (p=0.544 Mann Whitney U test).

Figure 3-17 shows the mtDNA mutation frequency detected by NGS in the colorectal mucosa in the initially obese group before and after bariatric surgery on a Log(10) scale (see Appendix Q for untransformed data). MtDNA mutation frequency fell slightly, but not significantly (P=0.790), following weight loss by bariatric surgery.
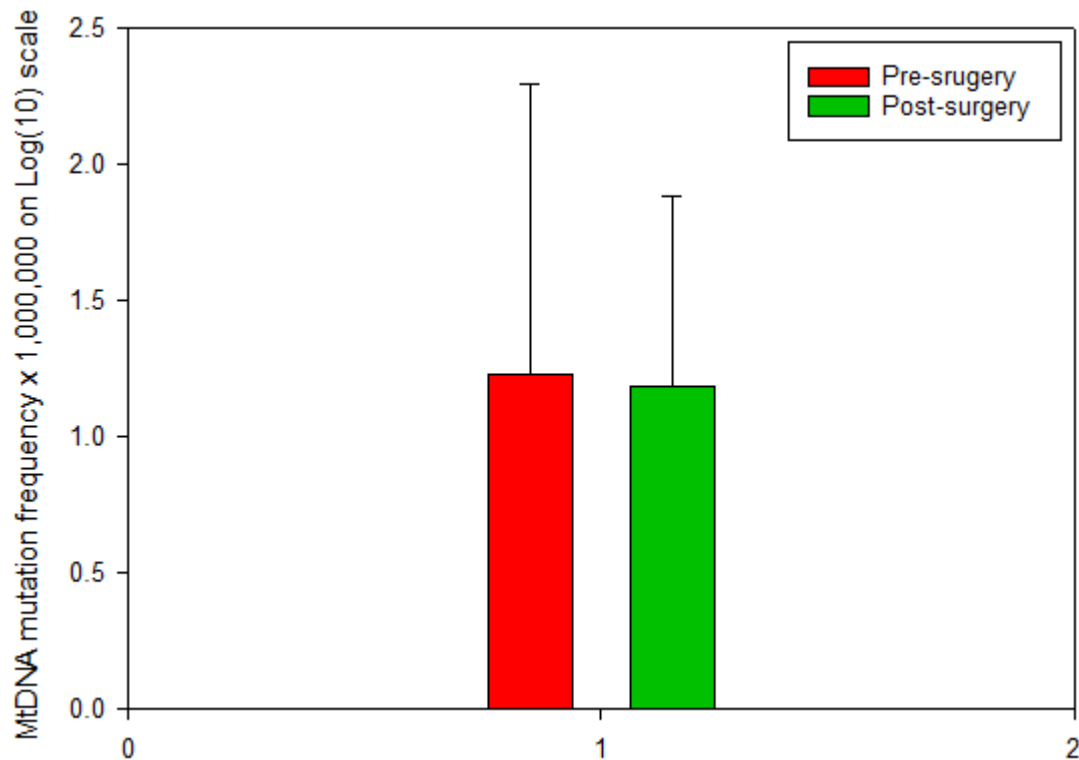
Figure 3-17: Frequency of mtDNA mutations detected by NGS in the colorectal mucosa of obese pre- and post-surgery participants. Data in this figure are presented on a Log(10) scale. Since zero values cannot be displayed in this way, data for n=3 and n=2 for both the obese pre- and post-surgery group are included in this figure with a zero value (p=0.790 Wilcoxon signed rank test)

Figure 3-18 illustrates the relationship between BMI and the frequency of mtDNA mutations detected by NGS in the colorectal mucosa for individuals in the study (obese pre- and post-surgery and non-obese Controls). Data are scattered and there was no significant correlation between adiposity and mtDNA mutation frequency. See Appendix R for untransformed data.

Although the mean ages of the study groups were matched, mitochondrial function has previously been shown to differ even over a 10 year period i.e. between 20- and 30-years old adults (Greaves et al., 2014). Figure 3-19 illustrates mtDNA mutation frequency quantified by NGS in the colorectal mucosa across the age span for each participant of the obese pre- and post-surgery group and non-obese Controls. With the exception of one pre-surgery participant, who at the age of 48 exhibits the lowest mtDNA mutation frequency of all individuals examined, a trend for a higher mtDNA mutation frequency can be seen in older individuals. However, there was no significant correlation between age and mtDNA mutation frequency.
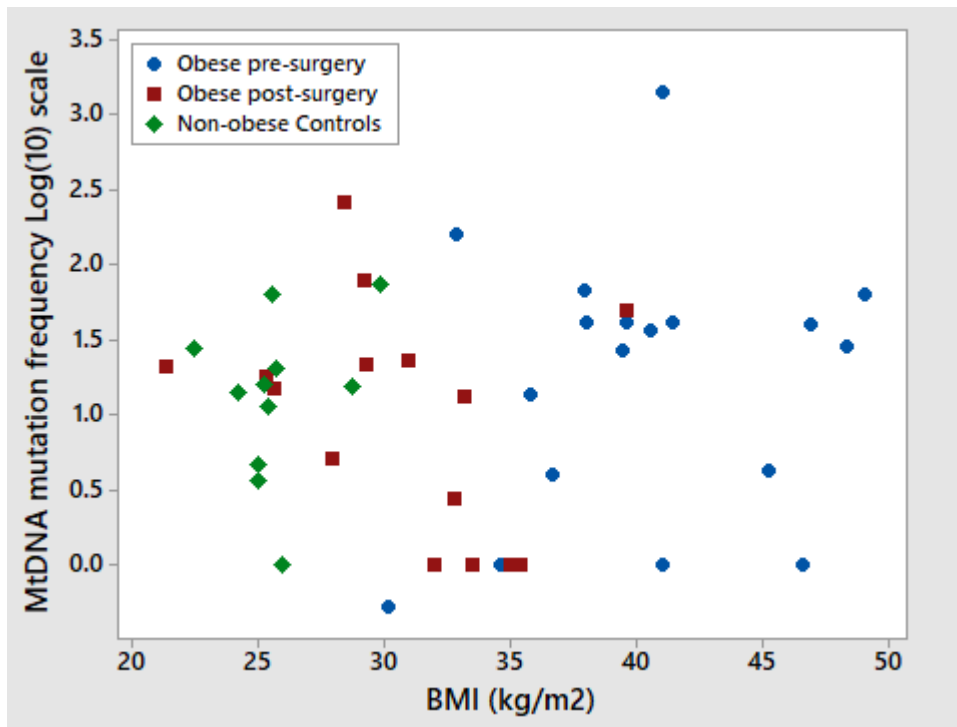
Figure 3-18: MtDNA mutations frequency detected by NGS in the colorectal mucosa across the BMI range for each initially obese pre- and post-surgery and non-obese Control individual. Since zero values cannot be displayed in this way, data for n=3, n=2 and n=1 for the pre- and post-surgery participants and non-obese Controls, respectively, are included in this figure with a zero value.
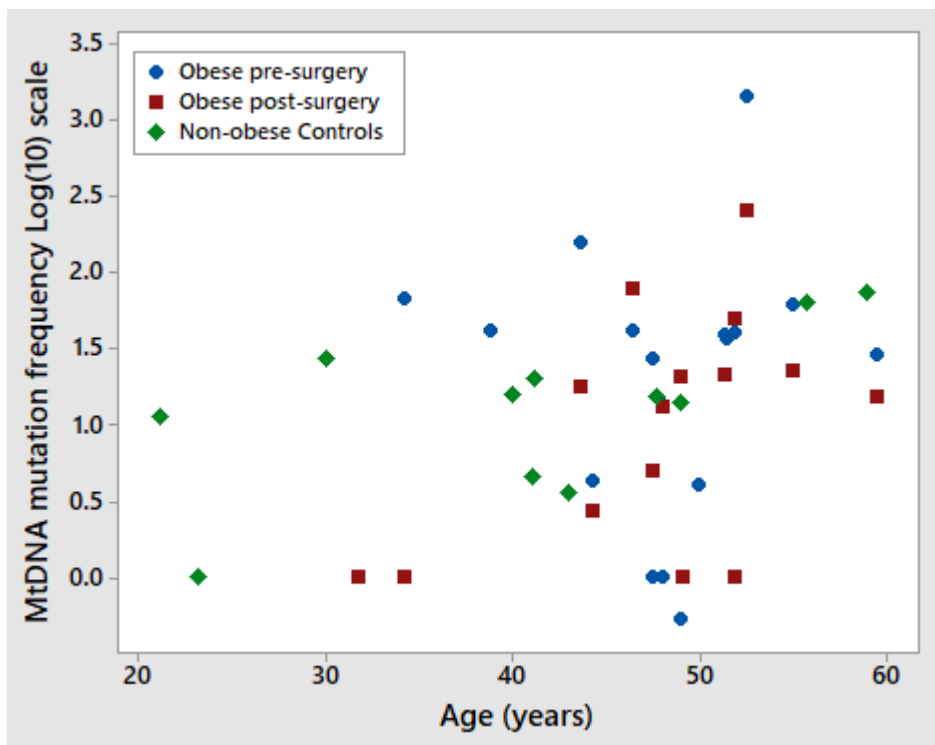
Figure 3-19: MtDNA mutations frequency detected by NGS in the colorectal mucosa across age for each initially obese pre- and post-surgery and non-obese Control individual. Since zero values cannot be displayed in this way, data for n=3, n=2 and

100

Previous studies have shown that, in the colonic mucosa, mtDNA mutations are randomly distributed throughout the genome with little evidence for mutation hotspots (Taylor et al., 2003, Greaves et al., 2010, Greaves et al., 2014). Therefore, I compared the mutational distribution for all BOCABS Study participants combined and for each of the 3 experimental groups separately, with what would be expected if mutations were distributed at random across the mitochondrial genome. Figure 3-20 shows the comparison between the expected and the observed rates of mtDNA mutations for each gene type (non-coding, Complex I, III, IV, V, tRNA and rRNA) for fragment A for all BOCABS Study participants combined and, separately, for each of the 3 study groups (i.e. initially obese pre- and post-surgery and non-obese Controls). Expected values were calculated based on the proportion of fragment A (9931bp) of the mitochondrial genome contributed by each gene category. No significant differences in the percentage of mtDNA mutations could be identified between the expected and observed values for each gene category. For all BOCABS Study participants combined and for the obese participants pre-surgery and non-obese Controls separately, the frequency of observed mutations was higher in complex III and IV and tRNA than the expected frequency if mitochondrial mutations occurred randomly across the mitochondrial genome, suggesting that these gene types might be mutation hotspots, although these differences did not reach significance, p=0.157 (see Figure 3-20 A, B and D). Similarly, in the obese participants post-surgery, there were apparently higher rates of mutation in complex III and V and tRNAs than would have been expected by chance, but these differences were not significant, p=0.157 (Figure 3-20 C).
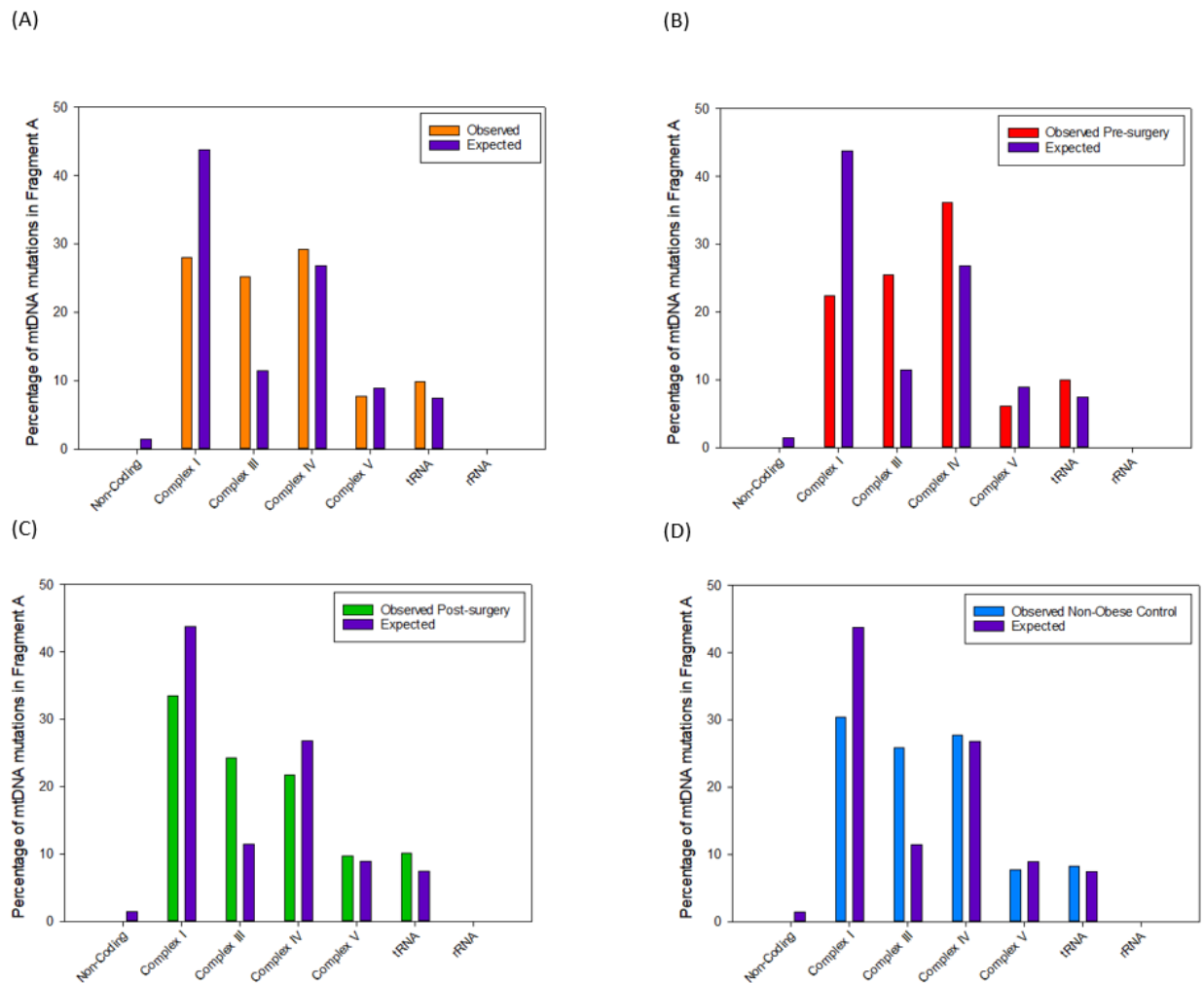
Figure 3-20: Observed and expected percentages of mtDNA mutations by gene type (non-coding, Complex I, III, IV and V, tRNA and rRNA) for Fragment A of the mitochondrial genome. A) For all BOCABS Study participants combined (i.e. obese pre- and post-surgery and non-obese Controls); B) For the obese participants pre-surgery; C) For the obese participants post-surgery and D) For the non-obese Controls. C*ross-tabulation was carried out using the Chi square test* (p=0.157).

It has been previously suggested that increased levels of ROS, as a result of inflammation, commonly lead to transversions and that replication errors result in transitions (Zheng et al., 2006, Kennedy et al., 2013). Since obesity is associated with low-level systemic inflammation, I investigated whether obesity could be a driver of inflammation-related mutations by examining the proportions of transitions and transversions in the spectrum of mutations in the BOCABS Study. Figure 3-21 illustrates the class of mtDNA mutations detected, transitions and mutations, in the colorectal mucosa of obese pre- and post-surgery participants and non-obese Controls. In all three groups, the prevalence of transitions was approximately 3-fold higher (77.5%, 78.7% and 73.4%, for the obese participants pre- and post-surgery and non-obese Controls, respectively) than that for transversions (22.5%, 21.3% and 26.6%, for the obese participants pre- and post-surgery and non-obese Controls, respectively). However,

these between-group differences were not significant (p=0.315). Next, I examined the prevalence (number and percentage) of each type of transition (i.e. A>G, C>T, G>A and T>C) and transversion (A>T, C>A, G>C and G>T) (see Figure 3-22). A>G and G>A transitions and C>A transversions were the most common in obese participants pre-surgery, 22.9%, 20.3% and 23.4%, respectively (see Figure 3-22 A). Whereas in the non-obese Controls A>G and G>A transitions were most frequently observed, with means of 29.6% and 24.8%, respectively (see Figure 3-22 A). None of the differences in number or % of types of transitions and transversions were statistically significant between obese (pre-surgery) and non-obese control groups. Significant weight loss at 6 months after bariatric surgery was associated with increased A>G and G>A transitions, (28.5% and 25.3%, respectively) and an apparent fall in C>A transversions (12%) (see Figure 3-22), but these changes were not statistically significant.
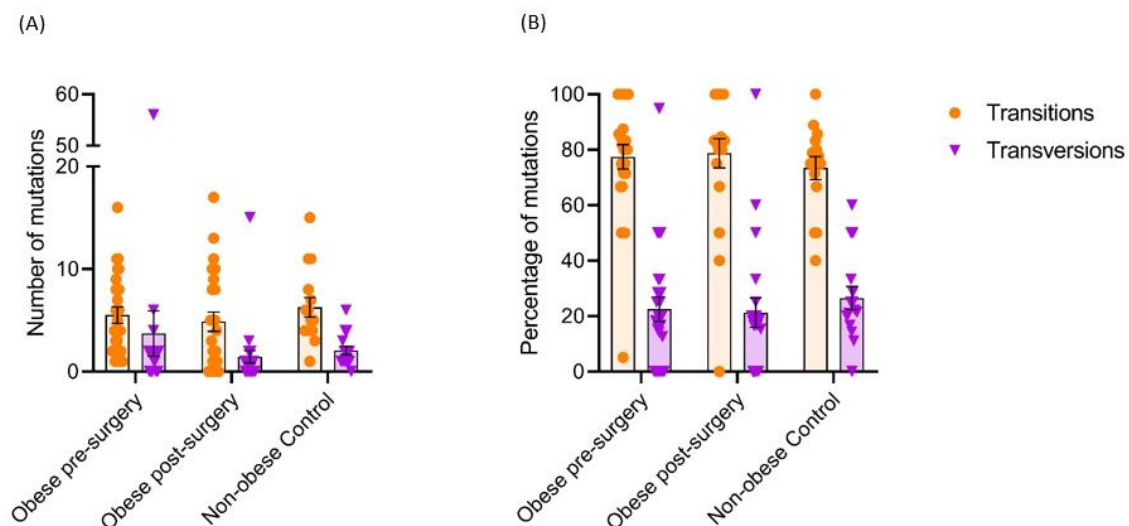
Figure 3-21: MtDNA mutations detected in the colorectal mucosa of obese pre- and post-surgery participant and non-obese Controls. A) Number of transitions and transversions for each participant (Differences in transitions (p=0.325) and transversions (p=0.058) between the 3 study groups were tested with a Kruskal-Wallis H test; As a further sensitivity analysis differences in transitions (p=0.391) and transversions (p=0.530) between obese pre-surgery and non-obese Controls were tested with a Mann Whitney U test; differences in transitions (p=0.304) and transversion (p=0.070) between the pre- and post-surgery adults were tested with a Wilcoxon signed rank test; B) Percentage of transitions and transversions for each participant (Differences in transitions (p=0.315) and transversions (p=0.315) between the 3 study groups were tested with a Kruskal-Wallis H test; As a further sensitivity analysis differences in transitions (p=0.339) and transversions (p=0.339) between obese pre-surgery and non-obese Controls were tested with a Mann Whitney U test; differences in transitions (p=0.463) and transversion (p=0.463) between the pre- and post-surgery adults were tested with a Wilcoxon signed rank test.
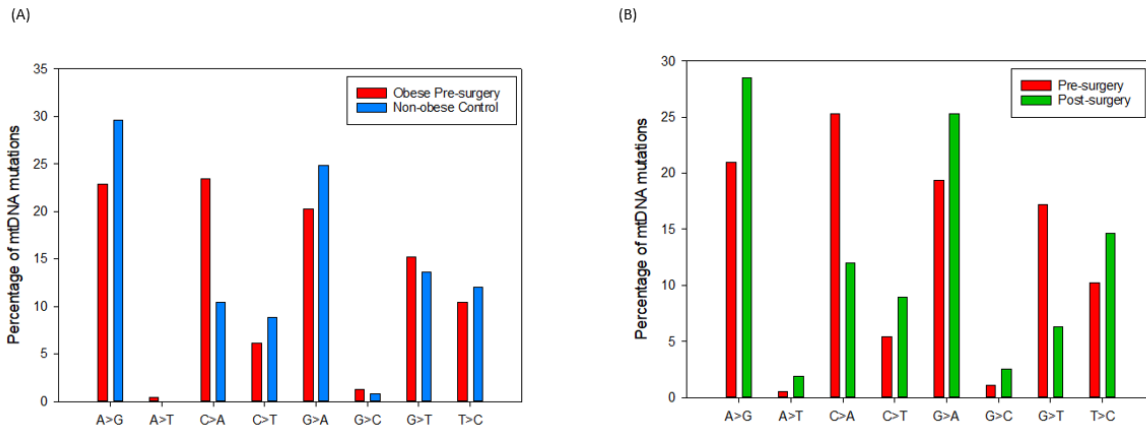
Figure 3-22: Types of transitions and transversions detected in the codon region. A) In obese pre-surgery compared to non-obese Controls and B) in pre- compared to post-surgery participants.

3.4.2   Mutations with functional consequences

To investigate possible differences in the pathogenicity of mtDNA mutations in the protein encoding regions in those with greater levels of adiposity, the frequency of silent and non-silent mutations in codon regions and their locations was investigated. Figure 3-23 illustrates the frequency of mtDNA mutations in protein encoding genes detected in the colorectal mucosa of obese participants pre-surgery and in non-obese Controls. The prevalence of silent (41.7% and 40.5%, respectively) and non-silent changes (58.3% and 59.5%) in the codon were similar for both obese (pre-surgery) and non-obese Controls. MtDNA mutations were observed more frequently in positions 1 and 2 of each codon in both study groups; mutations in these codon positions are more likely to be pathogenic (Stewart et al., 2008). Obese participants pre-surgery had 59.3% and 39% of mutations in positions 1 and 2 of the codons, respectively. For non-obese Controls, the corresponding values were 52% and 47% respectively. No significant differences between obese and non-obese participants were detected.
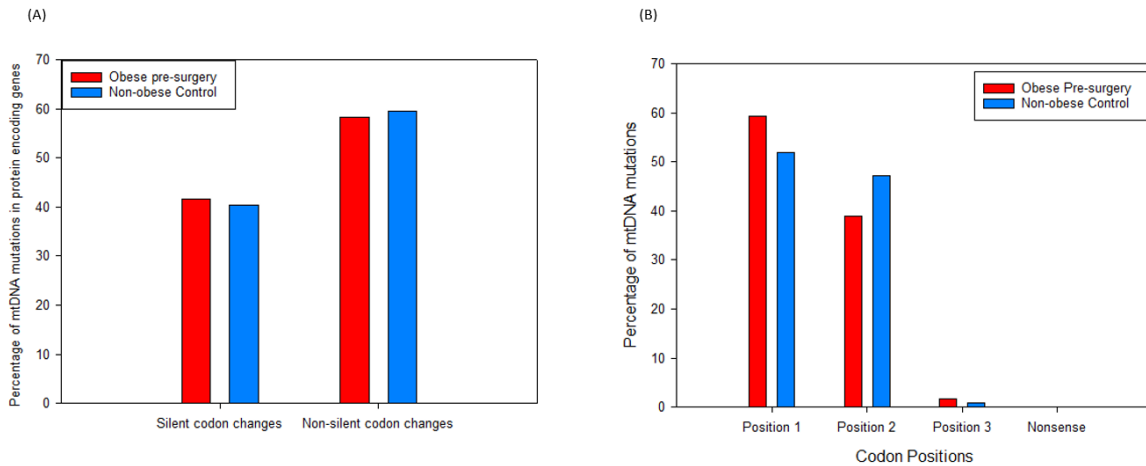
Figure 3-23: MtDNA mutations in protein encoding genes detected in the colorectal mucosa of obese participants pre-surgery and non-obese Controls: A) Frequency of silent and non-silent codon changes. B) Proportions (%) of mtDNA mutations at each of the three codon positions.

Figure 3-24 shows the prevalence of mtDNA mutations in protein encoding genes detected in the colorectal mucosa of pre- and post-surgery participants. Following significant weight loss, at 6 months follow-up, a rise in silent codon changes was seen from 40.5% to 46.6% and a fall in non-silent codon changes from 59.5% to 53.4%. However, these changes were not significant. At both time points (pre- and post-surgery), mtDNA mutations were more frequently observed in positions 1 and 2 of each codon and were similar (56.5% and 58.9% in position 1 of the pre- and post-surgery group, respectively and, 41.4% and 40.5% in position 1 of the pre- and post-surgery group). Only one stop-codon/ nonsense mutation was detected in the post-surgery group.
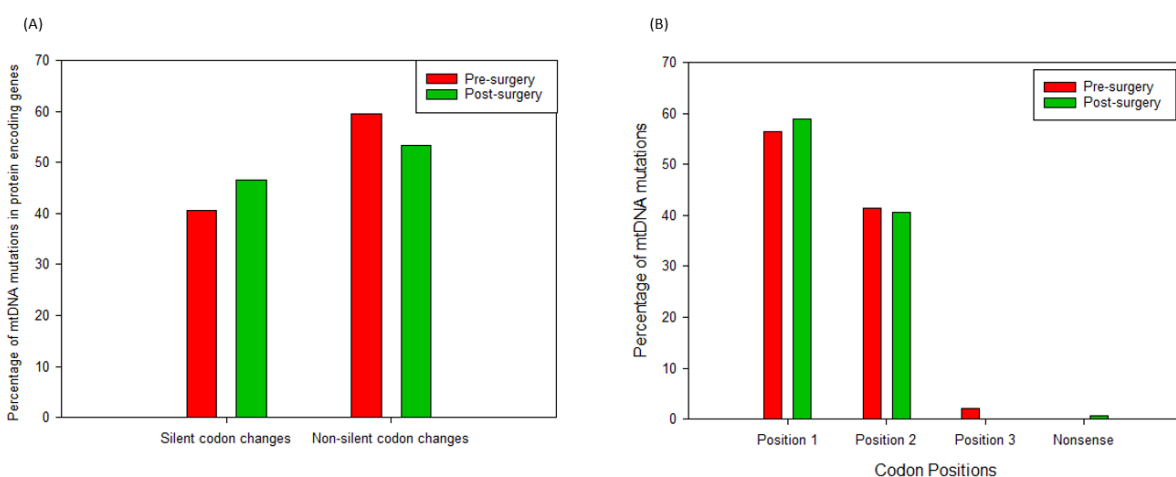
Figure 3-24: MtDNA mutations in protein encoding genes detected in the colorectal mucosa of pre- and post-surgery participants: A) Frequency of silent and non-silent codon changes. B) Proportions (%) of mtDNA mutations at each of the three codon positions.

I investigated whether obesity had an effect on the mechanism of the mtDNA mutation occurrence, i.e. if it changes the mutational spectra due to increased levels of ROS as a result of inflammation, as suggested previously (Zheng et al., 2006, Kennedy et al., 2013), which would result in different mutation types. Figure 3-25 shows the percentage of mtDNA mutations and their predicted functional consequences (synonymous, missense and pre-mature stop codon) of the detected protein encoding mtDNA mutations in obese pre-surgery participants and non-obese Controls. Synonymous is a silent AA change and missense is a single base change which produces a codon that codes for a different AA. The percentage of synonymous and missense was roughly equally distributed in obese pre-surgery participants (48.8% and 51.2%, respectively) and in non-obese Controls (46.6% and 53.4%, respectively). No significant differences between the two groups were detected. The NGS is unable to detect single or small insertions or deletions which would result in non-sense deletions, which change the rest of the AA sequence from the mutation point onwards.
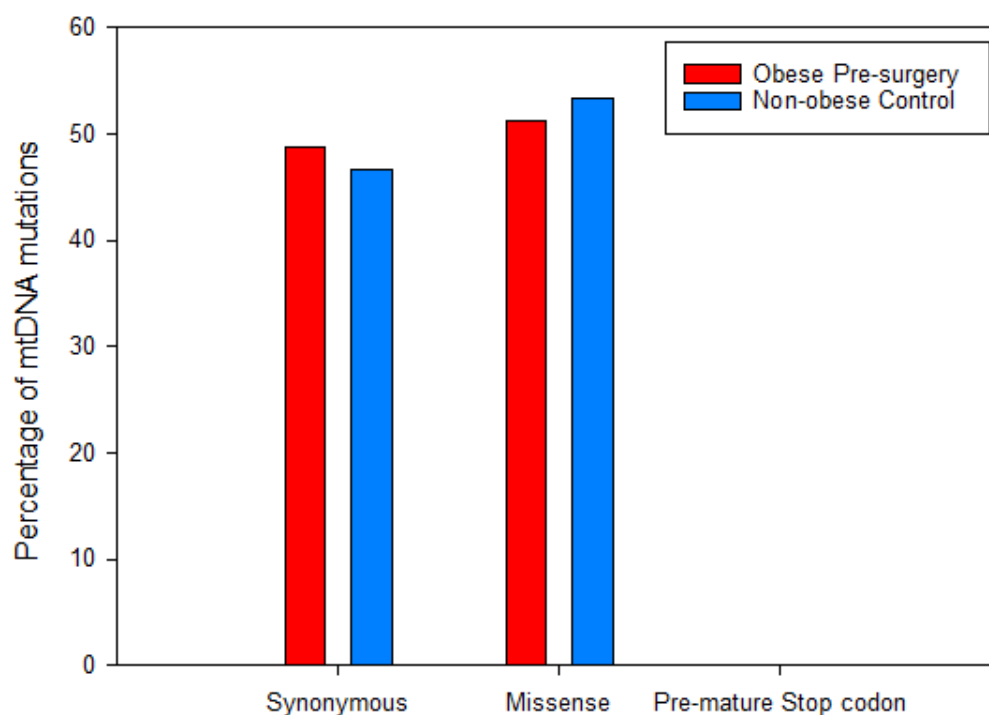
Figure 3-25: Percentage of the mtDNA mutations in the colorectal mucosa and their predicted functional consequences of the detected protein encoding mtDNA mutations in obese pre-surgery participants and non-obese Controls. Synonymous is a silent change and missense is an AA change.

Figure 3-26 shows the percentage of mtDNA mutations and their predicted functional consequences (synonymous, missense and pre-mature stop codon) of the detected protein encoding mtDNA mutations in pre- and post-surgery participants. The percentage of synonymous and missense was roughly equally distributed in pre- (50.4% and 49.6%, respectively) and post-surgery participants (53.4% and 46.6%, respectively). No significant differences following significant weight loss at 6 months follow-up were detected.
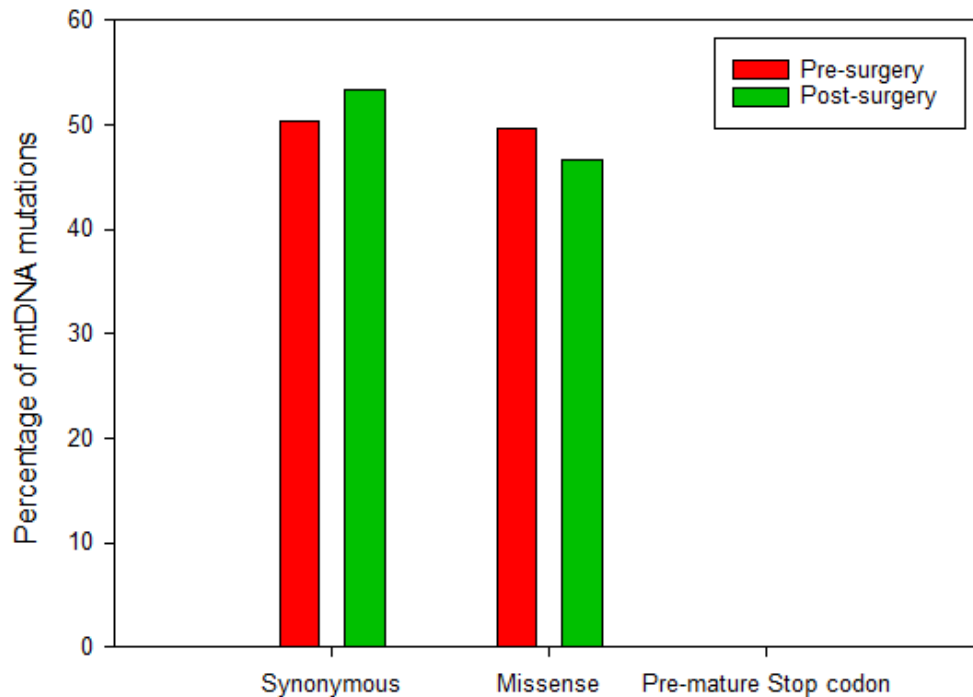
Figure 3-26: Percentage of the mtDNA mutations in the colorectal mucosa and their predicted functional consequences of the detected protein encoding mtDNA mutations in pre- and post-surgery participants. Synonymous is a silent change and missense is an AA change.

I investigated whether obesity had an effect on the mechanism of the mtDNA mutation occurrence, i.e. if it changes the mutational spectra due to increased levels of ROS as a result of inflammation, as suggested previously (Zheng et al., 2006, Kennedy et al., 2013), which would result in different amino acid (AA) changes. Figure 3-27 illustrates the types of AA changes detected in the mitochondrial genome by NGS in the colorectal mucosa of obese pre-surgery participants and non-obese Controls. A total of 57 types of AA substitutions were identified and the most common change was threonine to alanine (T>A), 19% and 24% in obese pre-surgery participants and in non-obese Controls, respectively. For the obese pre-

surgery participants, the next 4 most common AA changes identified were (in this order) alanine to threonine (A>T, 9.5%), glycine to valine (G>V, 7.6%), proline to histidine (P>H, 6.6%) and leucine to isoleucine (L>I, 5.2%). Whereas, for the non-obese Controls the next 4 most common AA changes detected were (in this order) glycine to valine (G>V, 9.6%), alanine to threonine (A>T, 6.4%), threonine to isoleucine (T>I, 5.6%) and leucine to isoleucine (L>I, 4.8%). The AA changes that occurred in the two study groups did not differ significantly.
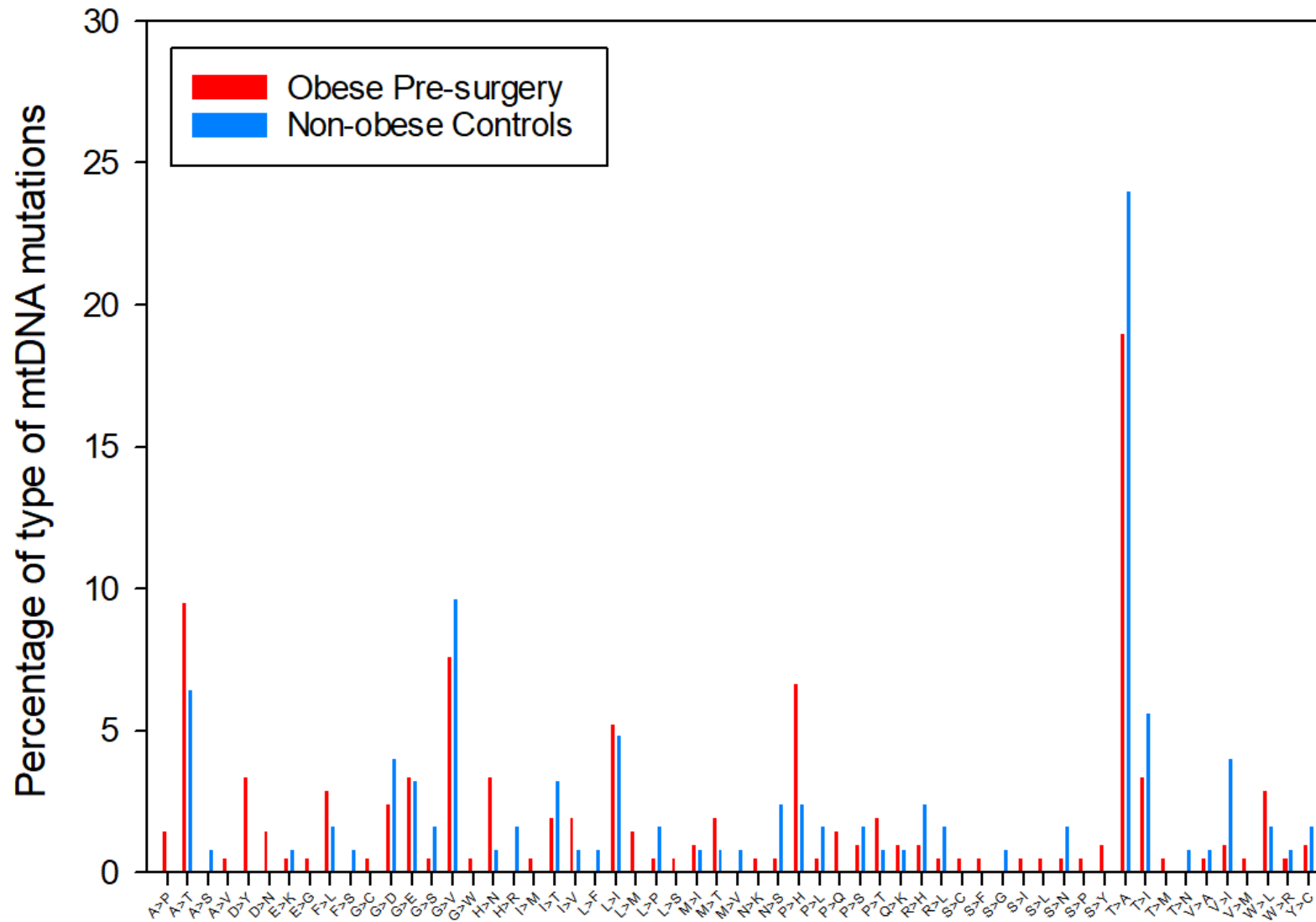
Figure 3-27: Predicted amino acid changes based on mutations in the mitochondrial genome detected by NGS in the colorectal mucosa of obese participants pre-surgery and in non-obese Controls

Figure 3-28 illustrates the predicted amino acid (AA) changes resulting from mutations in the mitochondrial genome detected by NGS in the colorectal mucosa of obese participants pre- and post-surgery. A total of 53 types of AA substitutions were predicted, of which the most common change was threonine to alanine (T>A), accounting for 15.8% and 26.6% in the obese participants pre- and post-surgery, respectively. For the pre-surgery participants, the next 4 most common AA changes identified were (in this order) proline to histidine (P>H, 9%), alanine to threonine (A>T, 7.5%), glycine to valine (G>V, 6.8%) and leucine to isoleucine (L>I,6%). Whereas, for the post-surgery participants the next 4 most common AA changes identified were (in this order) alanine to threonine (A>T, 8.2%), threonine to isoleucine (T>I, 7%), glycine to valine (G>V, 6.3%) and proline to histidine (P>H, 5.7%). Out of all the AA changes detected, about half increased (49%) and the remaining half decreased (51%) following weight loss by bariatric surgery. Weight loss resulted in an increase of threonine to alanine (T>A), alanine to threonine (A>T), phenylalanine to leucine (F>L), threonine to isoleucine (T>I), glycine to glutamic acid (G>E), isoleucine to threonine (I>T), aspartic acid to asparagine (D>N), alanine to valine (A>V), cysteine to arginine (C>R), aspartic acid to glycine (D>G), glutamic acid to lysine (E>K), phenylalanine to serine (F>S), glycine to alanine (G>A), glycine to serine (G>S), histidine to arginine (H>R), leucine to proline (L>P), asparagine to serine (N>S), asparagine to tyrosine (N>Y), proline to leucine (P>L), arginine to glutamine (R>Q), threonine to methionine (T>M), valine to alanine (V>A), valine to isoleucine (V>I), valine to leucine (V>L), valine to methionine (V>M) and tryptophan to arginine (W>R). Weight loss resulted in a decrease of proline to histidine (P>H), glycine to valine (G>V), leucine to isoleucine (L>I), aspartic acid to tyrosine (D>Y), histidine to asparagine (H>N), tryptophan to leucine (W>L), glycine to aspartic acid (G>D), proline to threonine (P>T), methionine to threonine (M>T), proline to glutamine (P>Q), alanine to proline (A>P), isoleucine to valine (I>V), leucine to methionine (L>M), methionine to isoleucine (M>I), glutamine to lysine (Q>K), arginine to histidine (R>H), serine to tyrosine (S>Y), tyrosine to cysteine (Y>C), glycine to tryptophan (G>W), isoleucine to methionine (I>M), asparagine to lysine (N>K), proline to serine (P>S), arginine to leucine (R>L), serine to cysteine (S>C), serine to phenylalanine (S>F), serine to isoleucine (S>I) and serine to asparagine (S>N). Although weight loss following bariatric surgery was substantial (mean 27kg), there were no significant differences in the predicted AA changes detected in the mitochondrial genome at 6 months follow-up.
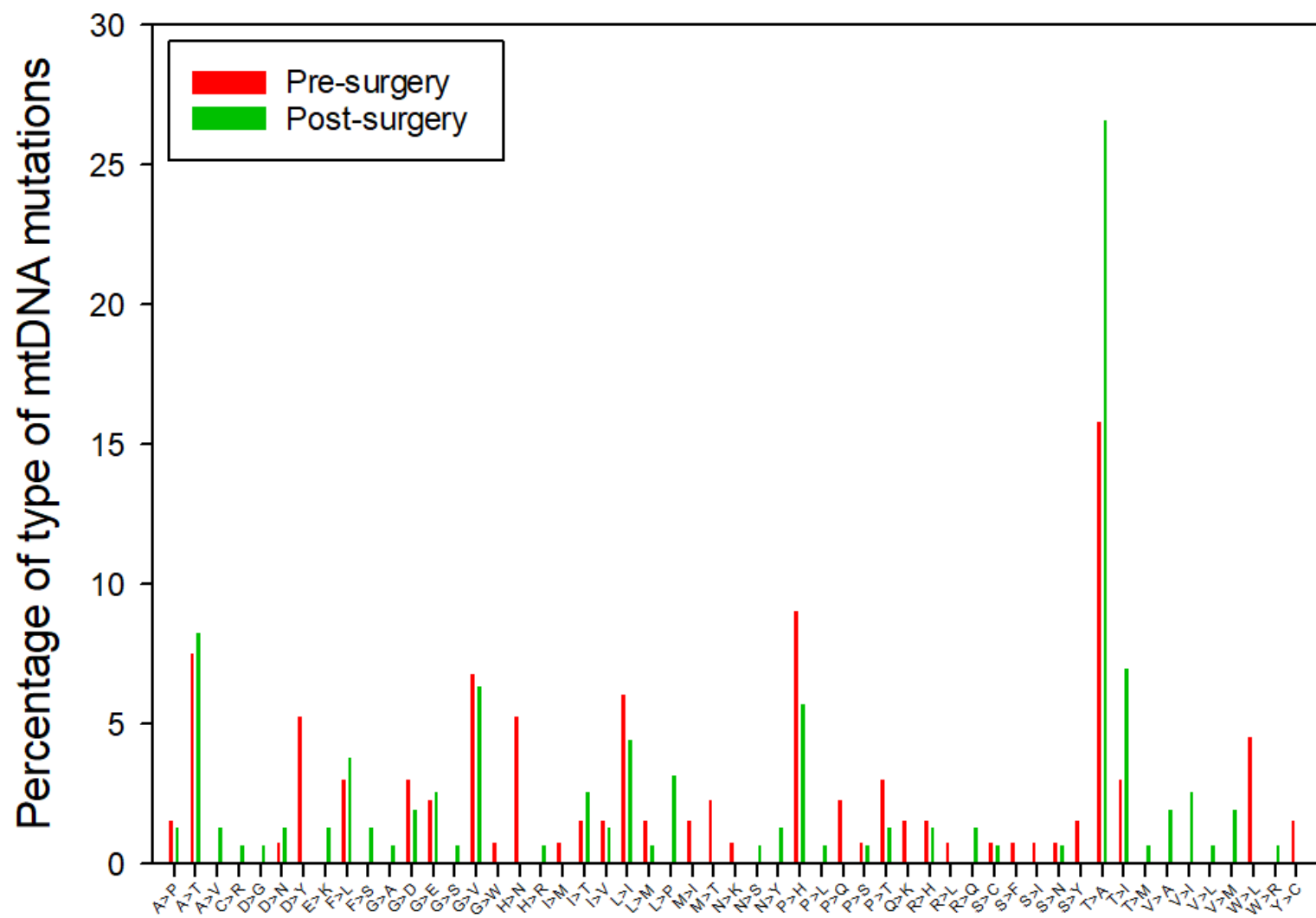
Figure 3-28: Predicted amino acid changes based on mutations in the mitochondrial genome detected by NGS in the colorectal mucosa of pre- and post-surgery participants

3.5 Discussion

To my knowledge, no previous publications have investigated the effects of weight loss (following bariatric surgery) on mitochondria in the human colorectal mucosa. I have investigated two aspects of mitochondrial structure/ function: i) mitochondrial protein expression using immunofluorescence and ii) the spectrum of mtDNA mutations assessed using NGS of approximately 60% of the mitochondrial genome.

3.5.1 Main findings

I found that there was a significantly higher proportion of crypts with complex I and IV deficiencies in the colorectal mucosa of obese participants pre-surgery when compared with non-obese Controls. Furthermore, older people had significantly more complex I and IV deficiencies in the colorectal mucosa for both obese and non-obese groups. Bariatric surgery resulted in significant weight loss, mean 27kg, but, at least when investigated at 6 months following surgery, there was no significant effect on the expression of OXPHOS proteins. Obese participants pre-surgery and, again, at 6 months following bariatric surgery tended to have higher mtDNA mutation frequency compared with non-obese, but these differences were not statistically significant. The types of mtDNA mutations were examined, i.e. global mutations identified in the mitochondrial spectra and mutations with functional consequences. I also observed for the majority of the different types of mutations (i.e. transversions) a trend for higher prevalence in individuals with greater adiposity compared with non-obese Controls, but the differences were not significant. Weight loss following bariatric surgery in initially obese individuals tended to reduce the different types of mutations, for example transversions and non-silent codon changes, and increased silent codon changes, but these changes were not statistically significant.

3.5.1.1 Interpretation of main findings

In the introductory chapter (see section 1.4.2), I have reviewed evidence that over-feeding and obesity in humans result in mitochondrial dysfunction (Breininger et al., 2019). In addition, there is evidence from human studies that weight loss, as a result of bariatric surgery, may improve the structure and function of mitochondria (Breininger et al., 2019). However, most of this evidence has been obtained from measurements made in skeletal muscle (Bach et al., 2005, Civitarese et al., 2007, Toledo et al., 2008, Coen et al., 2015, Fernstrom et al., 2016, Camastra et al., 2017), two studies have reported the effects in adipose tissue (Jahansouz et

al., 2015, Moreno-Castellanos et al., 2016) and there have been no comparable data from measurements made in the colorectal epithelium.

Here, I used an immunofluorescent labelling method, a robust method for assessment of patterns of OXPHOS protein abundance (complex I and IV and mitochondrial mass), to reveal higher prevalence of crypts of the colorectal mucosa that were deficient in complex I and IV in obese individuals compared with non-obese Controls, as hypothesised (see Table 3-4) (Rocha et al., 2015). Surprisingly, major weight loss (mean 27 kg) following bariatric surgery in these initially obese adults did not improve the expression of OXPHOS proteins (see Table 3-4). The prevalence of complex IV and mitochondrial mass deficiency was higher with advancing age, as hypothesised. Then, I extended the investigation to characterise and to quantify mtDNA mutations in crypt cells in the same colorectal mucosal biopsies. To ensure that the resulting data could be attributed unambiguously to crypt cells and to avoid potential confounding by other cell types within the biopsies, crypts were laser-microdissected from frozen sections of biopsy. I then used a NGS method, which provides a broad, unbiased, assessment of the mutations present in the mitochondrial genome. Surprisingly, I did not find any significant differences in the prevalence, or types, of mutations between initially obese individuals at baseline or following weight loss at 6 months post-surgery and non-obese Controls (see Table 3-4). There was a trend for a higher mutation frequency in the obese compared with non-obese Controls and, for this to fall following weight loss by bariatric surgery, but these differences were not statistically significant.

Mitochondrial marker	Association with obesity	Effects of weight loss following bariatric surgery
Complex I	↓	No significant change
Complex IV	↓	No significant change
Mitochondrial mass	↓	No significant change
Mutation frequency	No significant change	No significant change
Location of mtDNA mutation by gene type	No significant change	No significant change
AA changes (protein encoding genes only)	No significant change	No significant change

Transitions in codon region	No significant change	No significant change
Transversion in codon region	No significant change	No significant change
Position changes in codon region	No significant change	No significant change

Table 3-4: Summary of effects of obesity and of weight loss (following bariatric surgery) on mitochondrial markers in the human colorectal mucosa

3.5.2 The effect of obesity on expression of OXPHOS proteins

Given the link between adiposity and mitochondrial dysfunction, my finding of higher abundance of crypts showing deficient complex I and IV and mitochondrial mass expression in the obese when compared with the non-obese Controls is consistent with the hypothesis that role of obesity, perhaps via obesity-induced inflammation, results in mitochondrial damage. Heinonen (Heinonen et al., 2015) found reduced expression of subunits of complex IV in subcutaneous adipose tissue of obese monozygotic twins. Sparks (Sparks et al., 2005) also reported reduced complex IV expression in male vastus lateralis and gastrocnemius muscle following consumption of a high fat diet for 3 days, but in this short-term study it seems more likely that the observed effects on biomarkers of mitochondrial function result from the altered macronutrient intake rather than from any change in adiposity which would be very small after 3 days.

A few studies using animal models have investigated the effects of overfeeding and/ or obesity on mitochondrial OXPHOS protein abundance. After feeding a high-fat diet for 21 days, there was a decline in cytochrome *c* protein concentration and reduced expression of genes encoding OXPHOS proteins I-IV in skeletal muscle from mice (Sparks et al., 2005). In rats, diet-induced obesity led to a fall in mitochondrial mass in liver cells (Putti et al., 2015). COX IV and cytochrome I were reduced in white adipose tissue of mice fed a high-fat diet, obese mice and in obese Zucker rats (Valerio et al., 2006). Similarly, there were reduced levels of complex IV and cytochrome *c* in adipose tissue of male rats fed a high fat diet (Sutherland et al., 2008). A study comparing liver, muscle and adipocytes in different types of mice including normal, diabetic mice and, both obese and diabetic mice reported complex II and III deficiency in adipocytes (Choo et al., 2006). Mitochondrial capacity, assessed as mitochondrial fusion-fission rates, respiratory function and ATP content, was reduced in skeletal muscle from obese

mice (Liu et al., 2014). These data show that a high-fat diet fed to rodents, and increased levels of adiposity, lead to reduced abundance of OXPHOS proteins and defective mitochondria in multiple organs and tissues.

To date, changes in OXPHOS protein abundance in colon tissue of mouse models has been observed in pathogenicity, including CRC (Baines et al., 2014, Pate et al., 2014), but there have been no published studies investigating effects of obesity in this tissue.

3.5.3 The effect of weight loss on expression of OXPHOS proteins

Given the adverse effects of excess energy intake and body weight gain on the structure and function of mitochondria, I hypothesised that bariatric surgery (BS) -induced weight loss would reverse these effects, so my finding of no effect on OXPHOS protein expression following significant and sustained weight loss in initially obese individuals was unexpected. Potential explanations for this observation may be:

- On average, participants remained obese (mean BMI of 31.7 kg/m^2) at 6 months after BS and a return to normal body weight may be necessary to abrogate the adverse effects of obesity on mitochondria. Furthermore, it is possible that 6 months is too short a time to reverse the effects of obesity. Coen (2015) showed that respiration of mitochondria in vastus lateralis muscle was improved in 101 patients at 6 months after RYGB plus an exercise intervention when they had achieved mean 23.6kg weight loss. However, given the design of the study, it is impossible to separate any effects of increased physical activity from the putative effects of BS-induced weight loss in this study. In addition, coupled respiration in vastus lateralis muscle (assessed using a Clark-type electrode and measured oxidative phosphorylation of ADP to ATP) was increased in 11 obese females at 6 months after RYGB when they had lost mean 25.5kg body weight (Fernstrom et al., 2016). In contrast, there were no effects on uncoupled respiration (oxygen consumption without ADP phosphorylation) or on respiratory control index (a quality measure of isolated mitochondria) even though participants accomplished a significant weight loss they stayed overweight after surgery (mean BMI 29.6 kg/m^2) (Fernstrom et al., 2016).
- Alternatively, it is possible that the adverse effects of obesity on mitochondrial OXPHOS protein abundance may be permanent and are not reversible by weight loss

alone, despite the associated reduction in inflammatory markers and potential mitochondrial damage.

3.5.4 The effect of ageing on expression of OXPHOS proteins

Mitochondrial dysfunction is one of the 9 hallmarks of ageing (López-Otín et al., 2013), so my finding of higher prevalence of complex I and IV deficient crypts in the colorectal mucosa from older people was as expected. Previous studies from Newcastle, and elsewhere, have shown that individual crypts in the human colorectal mucosa accumulate somatic mtDNA mutations with age, and that these expand clonally resulting, eventually, in OXPHOS dysfunction that can be observed as loss of cytochrome c oxidase activity or reduction in OXPHOS protein subunit expression (Greaves et al., 2010, Greaves et al., 2012, Greaves et al., 2014).

3.5.5 The effect of obesity on the mitochondrial genome

Given the link between adiposity and mtDNA mutations, my finding of no significant difference in mtDNA mutations between obese pre-surgery participants and non-obese Controls was unexpected. A wide range of different types of mitochondrial mutations were examined, i.e. mutations in the mitochondrial spectra (predicted AA changes as a consequence of mutations detected in the mitochondrial genome, transitions and transversions in codon regions) and mutations with functional consequences (synonymous/ silent or missense protein encoding mtDNA mutations, silent or non-silent protein encoding mtDNA mutations in codon regions and, location of the position of mutation in codon region). For the majority of those mtDNA mutations, obese individuals pre-surgery tended to have greater frequency compared with the non-obese Controls, but the differences were not significant. Potential explanations for this observation may be:

- The sample size for the study on the effects of adiposity on mtDNA mutations was slightly smaller, n=20 for obese pre-surgery and n=11 for non-obese controls, compared with the sample size for the study on the effects of adiposity on OXPHOS protein abundance (n=26 and n=16, respectively, see section 3.1.4 of this Chapter). Although the sample size was smaller for the study on mtDNA mutations, there were no significant differences in anthropometric measurements and participant characteristics (p>0.05) between those participants whose tissues were used for NGS and those used for assessing OXPHOS protein abundance. Nevertheless, the age range

was rather large between the groups, even though the mean ages of the study groups were matched. Age is an important factor, as mitochondrial function has previously been shown to differ between 20- and 30-years old adults (Greaves et al., 2014). Here, age was not included as a covariate on the study of adiposity on the measured mitochondrial outcomes and it is difficult to determine if age confounded the results. Therefore, it is possible that no significant differences on mtDNA mutations could be detected between obese pre-surgery participants and non-obese Controls due to the smaller sample size. However, other studies that investigated the effects of obesity on mitochondrial markers, which are consistent with my data on OXPHOS protein levels, had smaller samples sizes, including n=6 (Ejarque et al., 2018), n=10 (Sparks et al., 2005), n=17 (Kras et al., 2018) or the same sample size n=20 (Yin et al., 2014) and were still able to detect significant differences in OXPHOS protein levels when compared with non-obese. However, these studies investigated markers related to mitochondrial function (see section 1.4.2) and not mtDNA mutations, which has not been examined before, and it is possible that for the investigation of the mutation spectrum a larger sample size is needed.

- The mitochondrial genome is comprised of 16569bp (Case and Wallace, 1981). In the current study it was possible to sequence 60% of the mitochondrial genome in the colorectal mucosa (Fragment A m.6222-m.16153 comprising a total of 9931bp). It is possible that differences in mtDNA mutations between obese and non-obese individuals were present in the remaining 40% of the genome which was not sequenced.

- Defects in OXPHOS protein function are attributed to different mechanisms, i.e. approximately 70% is estimated to be due to underlying mutations and the remaining 30% to other mechanism including damage to the proteins themselves as a result of elevated levels of ROS and inflammation (Taylor et al., 2003). Therefore, it is possible that the significantly higher abundance of OXPHOS protein defects detected in the obese participants could have been caused by mechanisms other than mtDNA mutations. It is possible that the observed deficiency in OXPHOS function was due to inflammatory damage at the protein level rather than the DNA level.

3.5.6   The effect of weight loss on the mitochondrial genome

Given the link between the effects of significant and sustained weight loss following bariatric surgery on function and structure of mitochondria, it was surprising that the frequency of mtDNA mutations did not change significantly in the post-bariatric surgery group at 6 months follow-up in this study. A wide range of different types of mitochondrial mutations were examined, i.e. mutations in the mitochondrial spectra (AA changes detected in the mitochondrial genome, transitions and transversions in codon regions) and mutations with functional consequences (synonymous/ silent or missense protein encoding mtDNA mutations, silent or non-silent protein encoding mtDNA mutations in codon regions and, location of the position of mutation in codon region). For some of those mtDNA mutations, a trend for a reduction (mtDNA mutation frequency, AA changes in the mitochondrial genome, transversions and non-silent codon changes in protein encoding genes), an increase (transitions, synonymous mtDNA mutations in protein encoding genes, silent codon changes in protein encoding genes, changes in codon position 1) or no change (changes in codon position 2) was observed following significant weight loss at 6 months follow-up, although the differences did not reach significance. Potential explanations for this observation may be:

- The matched sample size of pre- and post-surgery participants for the study on the effects of adiposity on mtDNA mutations was 54% lower (n=12), compared with the sample size for the study on the effects of adiposity on OXPHOS protein abundance (see section 3.1.4). Even though the sample size was smaller for the study on mtDNA mutations, there were no significant differences in anthropometric measurements and participant characteristics (p>0.05) from the sample size on the study on OXPHOS protein abundance. It is possible that significant differences could have been detected if the sample size was larger. One previous study by Fernstrom (2016) comprised a similar sample size to the current study, i.e. n=11, and was able to detect improvements in mitochondrial function following weight loss by bariatric surgery, however this was in the muscle tissue. In contrast, other studies that found improvements in mitochondrial markers by investigating the effects of bariatric surgery comprised larger sample sizes including n= 15 (Bach et al., 2005), n=16 (Jahansouz et al., 2015), n=18 (Moreno-Castellanos et al., 2016), n=28 (Camastra et al., 2017) and n=101 (Coen et al., 2015). However, these studies investigated other

mitochondrial markers of function (see section 1.4.4) and not mtDNA mutations and it is possible that for the study of mutations a larger sample size is required. Furthermore, as mentioned earlier (see section 3.5.5), age modulates mitochondrial function significantly and, as previously reported, mitochondrial function can differ even between 20- and 30-years old adults (Greaves et al., 2014). Here, age was not included as a covariate on the study of weight loss on the measured mitochondrial outcomes and it is difficult to determine if age confounded the results.

- The mitochondrial genome is comprised of 16569bp (Case and Wallace, 1981). In the current study it was possible to sequence 60% of the mitochondrial genome in the colorectal mucosa (Fragment A m.6222-m.16153 comprising a total of 9931bp). It is possible that a reduction in mtDNA mutations occurred in the remaining 40% of the genome which was not sequenced.

- Obesity and its increased inflammatory state coupled with oxidative stress lead to permanent mtDNA mutations which become fixed and cannot be altered even by significant and sustained weight loss.

- The level of mtDNA mutation frequency detected here was relatively low (~1.5 x 1,000,000 on a Log(10) scale). It is likely that the sequencing here only picked up high levels of clonal expansion at the homogenate level. Even if mtDNA mutation rate (new mutations occurring) decreased following weight loss by bariatric surgery, it is possible that the level of sensitivity of the NGS would be unable to detect such a change in low levels of mtDNA mutations and, that only high levels of clonal expansion would be detected. Therefore, single crypt or cell (i.e. epithelial cells) sequencing pose an interesting area for future research to increase the level of sensitivity by NGS.

3.6   Conclusion

Here, for the first time, an immunofluorescent labelling and a NGS approach were used to investigate OXPHOS protein abundance and to screen for genome-wide changes in mtDNA mutations, respectively, in the colorectal mucosa of i) obese individuals compared with non-obese Controls and ii) following the effects of massive weight loss in initially obese individuals after bariatric surgery. This revealed that individuals with greater adiposity and older age comprise significantly more complex I and IV deficient crypts in the human colorectal mucosa. Contrarily, neither great levels of adiposity nor significant and sustained weight loss resulted

in significant differences in mtDNA mutations between the study groups. In summary, my findings provide evidence that adults with greater adiposity and older age have reduced OXPHOS protein abundance in the human colorectal mucosa. Deliberate weight loss following bariatric surgery does not affect the expression of OXPHOS protein abundance at least at 6 months follow-up. It remains to be discovered whether increased OXPHOS protein deficiencies in the human colorectal mucosa contribute to age related CRC risk or whether it is a non-causal age-associated phenomenon.

4 Effects of adiposity and weight loss on microRNA expression in the colorectal mucosa (The BOCABS Study)

4.1 General introduction

A detailed description about miRNAs can be found in the Introduction Chapter (see section 1.3).

In brief, every nucleated cell contains miRNAs which are small (approximately 22 nucleotides long), single stranded, non-coding RNA molecules, that regulate gene expression at the post-transcriptional levels (Heneghan et al., 2010). MiRNAs bind to the complementary region in the 3' –untranslated mRNA regions which in turn regulates translation of mRNA to protein (Lai, 2002) including a wide range of key cellular molecules such as transcription factors, signalling proteins and RNA binding proteins (Ding et al., 2018).

MiRNAs play crucial roles in many biological processes including cell proliferation, differentiation and apoptosis. Dysregulated patterns of miRNA expression contribute to pathological mechanisms and are implicated in tumorigenesis, including the development of CRC (Heneghan et al., 2010, Van Roosbroeck and Calin, 2017). Several studies, summarised in a recent review, have revealed the roles of miRNAs as tumour suppressor genes (TSG) and oncogenes (Ding et al., 2018). Aberrant patterns of miRNA expression can activate pathways associated with CRC, for example the WNT signalling pathway (Ding et al., 2018). Obesity is a major risk factor for CRC and aberrant patterns of miRNA have been observed in those with obesity (Esau et al., 2004, Lin et al., 2009, Xie et al., 2009) (see section 1.4.6). An inverse pattern of miRNA expression in differentiating adipocytes and obese tissue has been observed, for example miRNAs induced during adipogenesis with their primary role being increased and accelerated development of fat cells, were reported to be downregulated in obesity (Xie et al., 2009). This shows that obesity can result in a loss of miRNAs that describe fully metabolically active and differentiated adipocytes (Heneghan et al., 2010). It is believed that these modifications occur due to chronic inflammation present in obese adipose tissue (Heneghan et al., 2010). Moreover, weight loss, including weight loss following bariatric surgery, is associated with changes in miRNA expression (see section 1.4.7) and it appears that significant and sustained weight loss may reverse aberrant patterns of miRNA expression that accompany excess adiposity.

Obesity is a major risk factor for CRC risk and deliberate weight loss in initially obese individuals appears to lower CRC risk (Afshar et al., 2018, Schauer et al., 2019). If dysregulation of miRNA expression in obesity is causal for CRC risk, then one would anticipate that weight loss would "normalise" miRNA expression in this tissue. However, with the exception of the study reported by Afshar (2016a), there is no evidence of the effects of weight loss following bariatric surgery on the expression of miRNAs in the colorectal mucosa of humans.

4.2   Hypotheses

The hypotheses for this study were:

- MiRNA expression in the colorectal mucosa is dysregulated in obese compared with non-obese adults.
- Weight loss following Roux-en-Y gastric bypass (RYGB) in initially obese adults "normalises" miRNA expression in the colorectal mucosa.

4.3   Aims

The aims of this study were:

- To test the above hypotheses by quantifying patterns of miRNA expression in the colorectal mucosa of i) matched groups of obese and non-obese adults, ii) obese adults before and after bariatric surgery and iii) non-obese adults and adults post-bariatric surgery.

4.4   Objectives

The objectives of this study were:

- To use biological samples (mucosal biopsies) and data from the BOCABS Study (Afshar et al., 2018) to investigate effects of obesity, and of deliberate weight loss, on patterns of miRNA expression in the human colorectal mucosa.
- To use Next Generation Sequencing (NGS) to provide global, unbiased, quantification of patterns of miRNA expression in colorectal mucosal biopsies.

- To quantify miRNA expression in the colorectal mucosa of obese individuals before, and at 6 months after, RYGB and in a matched group of non-obese individuals.

- To select a panel of miRNAs showing the most significant changes in miRNA expression from pre- to post-RYGB (excluding miRNAs examined by Dr Sorena Afshar in analysis of the same samples (Afshar, 2016a)).

- To validate the findings from NGS by using quantitative Polymerase Chain Reaction (qPCR) to quantify expression of the selected panel of miRNAs in pre- and post-RYGB patients and in non-obese adults.

4.5   Overview of methods

A detailed description of the experimental procedures and methods for quantifying miRNA expression can be found in the Methods Chapter (see section 2.2.3).

In the BOCABS Study, initially obese participants (n=29) underwent RYBG, sleeve gastrectomy or gastric balloon surgery. For the purposes of this study, I selected those participants who underwent RYGB (currently the most widely used form of bariatric surgery) and for whom there were matched before and after samples of mucosal tissue (n=22). This reduced the overall cost of the study and minimised potential confounding due to different surgery types. In addition, the BOCABS Study recruited matched non-obese (Control) individuals.

In brief, RNA was extracted from colorectal mucosal biopsies (see section 2.2.3.1) and a library of small RNA was constructed (see section 2.2.3.3 to 2.2.3.5). Next generation sequencing (NGS) of miRNAs was carried out (see section 2.2.3.6) and data were analysed using standard bioinformatics approaches (see section 2.2.3.7) to identify the most abundantly expressed miRNAs (n=1654) in the three groups of participants (i.e. initially obese patients pre- and post RYGB and Control (non-obese) participants.

The following criteria were used to select a panel of differentially expressed miRNAs for validation and quantification by qPCR:

- The top 4 up- and top 4 down-regulated miRNAs with the greatest, and significant, fold change in expression between pre- and post-RYBG for which validated miScript primer assays were available from Qiagen.

- MiRNAs that had not been identified by the miRNome array conducted previously by Dr Sorena Afshar using these samples (Afshar, 2016a).

123

Then RNA was reverse transcribed into cDNA (see section 2.2.3.8) and miRNA expression was quantified by qPCR (see section 2.2.3.9).

Statistical analyses were performed using IBM® SPSS® Statistics Version 21. The Shapiro-Wilk test showed that data were not normally distributed. Consequently, the Mann-Whitney U test was used to compare miRNA expression between the obese and non-obese groups and the Wilcoxon signed rank test was used to examine miRNA expression in initially obese individuals pre- and post-RYBG. Finally, linear regression analyses were used to examine the associations of weight loss on changes in patterns of miRNA expression.

4.6 Effects of adiposity and weight loss on miRNA expression in the colorectal mucosa identified by Next Generation Sequencing

4.6.1 Participant characteristics and anthropometry

Table 4-1 summarises characteristics and anthropometric measurements for those participants included in the analysis of miRNA expression in colorectal mucosal biopsies pre- and post-RYGB, and of non-obese Control participants from the BOCABS Study. For this analysis, data and samples were used from 22 participants for whom paired pre- and post-samples were available. Those participants had a mean age of 47 years (range 30.9 to 65.2 years) and this study group was comprised of more females (n=18; 82%) than males (n=4; 18%). They had a mean BMI of 42.4 kg/m^2 and body fat of 47.6% which dropped to 31.3 kg/m^2 and 36.1%, respectively, at six months follow-up. Their waist: hip ratio was 1.07 and 0.89 for males and females which declined to 0.99 and 0.84, respectively, at six months follow-up. Non-smoking was a stringent selection and inclusion criterion by the NHS clinical team for bariatric surgery candidates, hence no one from the pre-surgery group was known to be a current smoker. However, at six months follow-up one participant (5%) had started smoking daily and 11 (52%) occasionally.

The non-obese Control group consisted of 20 participants who had a mean age of 46 (range 21- 61) years. The group had more females (60%; n=12) than males (40%; n=8) with mean BMI of 25.4 kg/m^2 (range 20- 30 kg/m^2), mean body fat 30.3% (range 21.2- 36.2%) and mean waist: hip ratio of 0.93 and 0.82 (range 0.74- 0.95) for males and females, respectively. The

majority of participants (60%; n=12) had never smoked, a third (n=6) reported being current

smokers (smoked daily/ occasionally) and only 10% (n=2) were ex-smokers.

	Non-obese Controls (n=20)	Obese pre-surgery (n=22)	Obese post-surgery (n=22)	Control vs pre-surgery p-value*	Pre- vs post-surgery p-value**
Age (years)	46.0 (2.6)	47.0 (1.2)	-	0.72	-
Gender N (%)					
Male	8 (40)	4 (18)	-	0.175†	-
Female	12 (60)	18 (82)	-		-
Smoking N (%)					
Daily	5 (25)	0	1 (5)	0.002†	< 0.001‡
Occasional	1 (5)	0	11 (52)		
Ex-smoker	2 (10)	11 (50)	9 (43)		
Never smoked	12 (60)	10 (45)	0		
Missing data	0	1 (4)	0		
Weight (kg)	71.8 (2.8)	114.8 (3.7)	86.3 (3.5)	< 0.001	< 0.001
BMI (kg/m^2)	25.4 (0.5)	42.4 (1.4)	31.3 (1.2)	< 0.001	< 0.001
Body fat (%)	30.3 (1.3)	47.6 (1.0)	36.1 (1.5)	< 0.001	< 0.001
Waist (W; cm)					
Male	95.9 (2.9)	137.3 (2.0)	112.5 (4.5)	< 0.001	0.007
Female	83.4 (2.2)	117.5 (2.2)	91.9 (3.5)	< 0.001	< 0.001

W:H ratio					
Male	0.93 (0.01)	1.07 (0.03)	0.99 (0.03)	0.001	0.067
Female	0.82 (0.02)	0.89 (0.01)	0.84 (0.02)	0.01	0.007

Table 4-1: Characteristics of initially obese participants pre- and post-Roux-en-Y bypass (RYGB) and of non-obese Controls for whom analysis of miRNA expression in the colorectal mucosa was conducted

Data presented as mean (SEM) unless otherwise stated.

*Unpaired t-test

**Paired t-test

† Fisher's exact test

‡ Wilcoxon sign test

4.6.2   Total RNA quality and quantity

RNA was isolated from frozen colorectal mucosal biopsies using the Qiagen miRNeasy Mini Kit and its purity and concentration were measured using spectrophotometry as described in the Methods (see section 2.2.3.1). The mean extracted RNA concentration was 92.2ng/μL, 65.8ng/μL and 57ng/μL for the pre- and post-surgery and non-obese Controls, respectively (see Figure 4-1 A). However, due to considerable variability in the sizes of biopsies available, this concentration ranged from 13.5ng/μL to 167.5ng/μL. The RNA purity was evaluated by quantifying absorbance at 260/280 ratio. This showed the same mean value of 2.06 for the pre-surgery group and non-obese Controls and a value of 2.05 for the post-surgery group, indicating good purity of the RNA (see Figure 4-1 B).
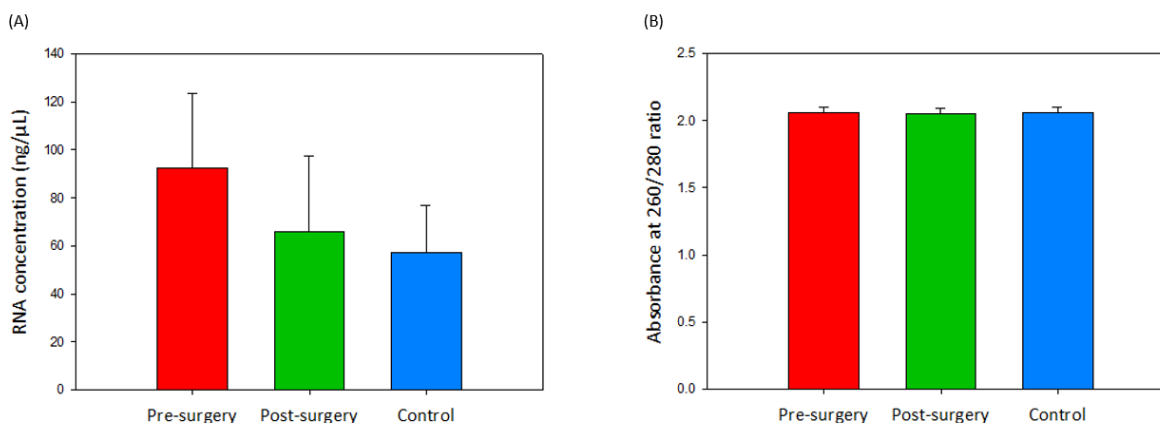
Figure 4-1: (A) RNA concentrations and (B) absorbance at 260/280 ratios for the pre- and post- surgery group and non-obese Controls

4.6.3   Genome-wide miRNA expression using Next Generation Sequencing

Bioinformatics analyses were performed as described in the Methods section 2.2.3.7. A file containing all the counts for all miRNAs identified in the samples was obtained and those participants with extremely low counts of miRNAs, as indicated in Figure 4-2, were removed. Figure 4-3 (A) shows the pre-normalised miRNA counts following the removal of the extremely low miRNA counts and Figure 4-3 (B) shows the normalised counts following the application of the DESeq2 package in R Studio software. Additionally, the normalised miRNA counts were plotted to verify the dispersion (i.e. biological variation from the mean) for each miRNA under consideration and a figure can be seen in Appendix S.
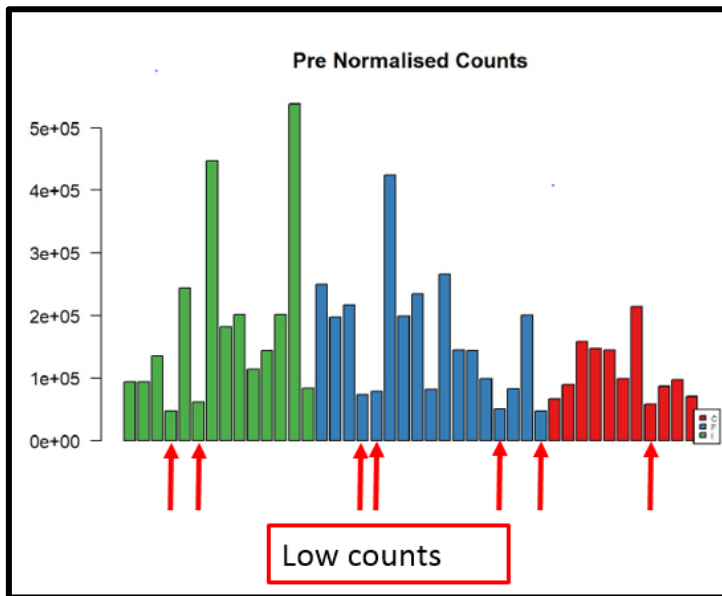
Figure 4-2: Pre-normalised miRNA counts for all participants. Participants with extremely low miRNA counts are indicated with red arrows and these participants were removed from subsequent analyses (green bars: pre-surgery; blue bars: post-surgery and red bars: non-obese Controls).
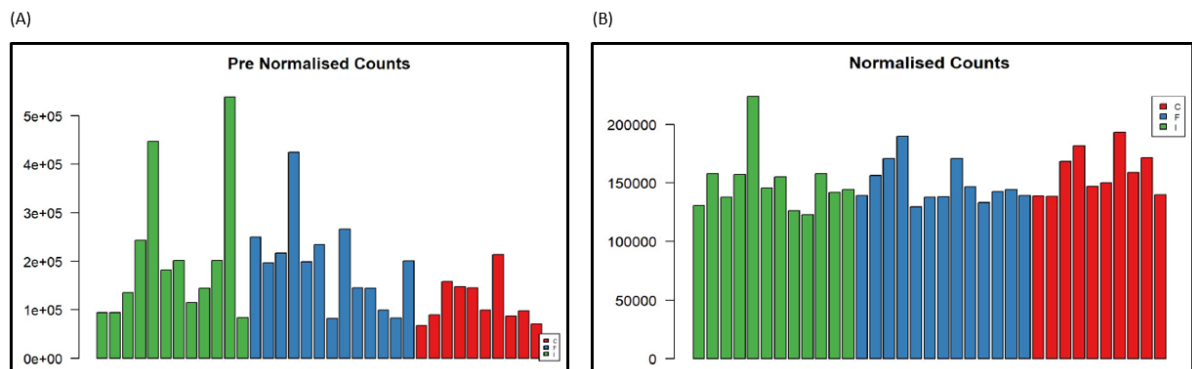
Figure 4-3: (A) Pre-normalised miRNA counts after removing the low miRNA counts; (B) Normalised miRNA counts (green bars: pre-surgery; blue bars: post-surgery and red bars: non-obese Controls).

A total of 1654 individual miRNAs were identified (see Appendix T). Then the following computation and transformation were applied to the miRNA counts and heatmaps were produced which are shown in the Appendix:

- A heatmap of sample to sample correlation of clustered (aggregation of individual participants according to participant group, i.e. pre- and post-surgery and non-obese Controls) and non-clustered raw miRNA counts is shown in Appendix U.

- A heatmap of sample to sample correlation of clustered and non-clustered miRNA counts after applying a variance of stabilising transformation (VST) to the count of the miRNAs is show in Appendix V. This transformation yields a distribution with

homoscedastic values, which means that values have a constant variance along the range of mean values, and was used to check for outliers, clustering and linear analysis.

- A heatmap of sample to sample correlation of clustered and non-clustered miRNA counts after computing the binary logarithms to the miRNA counts is shown in Appendix W.

- A heatmap of sample to sample correlation of clustered and non-clustered miRNA counts after computing the binary logarithms to the miRNA counts is shown in Appendix X.

Then a sample to sample principle component analysis (PCA) was performed on the VST-adjusted miRNA counts (see Figure 4-4). The PCA demonstrates clear patterns and clustering of miRNA counts of the individuals within each of the three groups. Patterns of miRNA expression differed between participant groups with most of the pre-RYGB group being clustered separately from the same individuals post-RYGB. In addition, there was significant overlap between the non-obese Controls and the initially obese individuals post-RYGB. There are three apparent outliers (green dots) from the pre-RYGB group who were clustered with the post-RYGB group and with the non-obese Controls. None of the participants characteristics examined including measures of adiposity (initial weight, BMI, body fat percentage, waist: hip ratio), diet, physical activity or medication use, explained this differential pattern of miRNA expression.
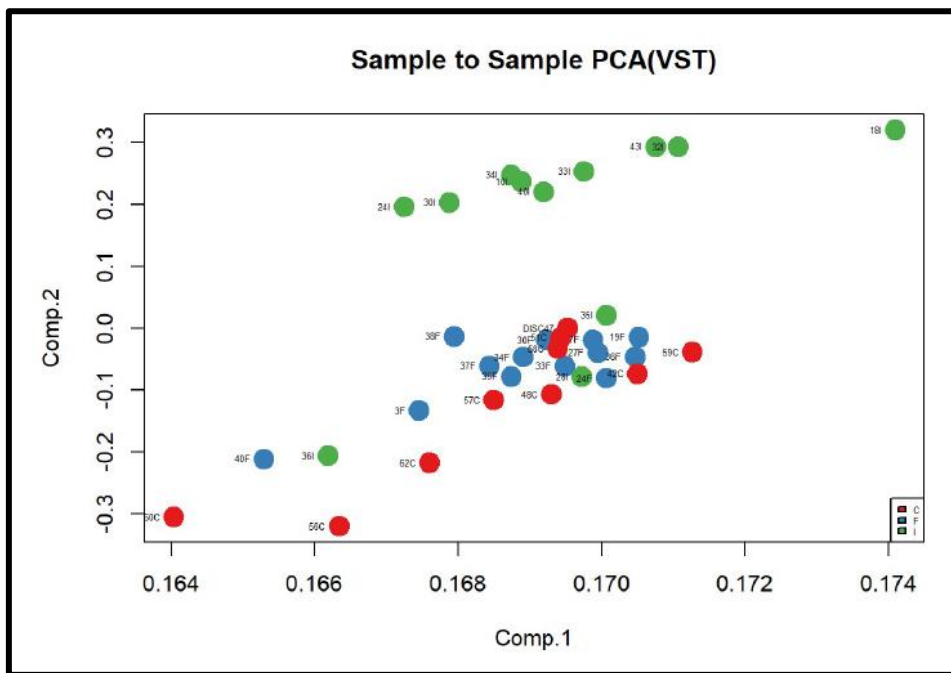
Figure 4-4: Outcomes of PCA on VST adjusted miRNA counts for all 3 groups of participants (green dots: obese participants pre-surgery; blue dots: initially obese participants post-surgery and red dots: non-obese Controls).

Following PCA analysis, further computation and transformation was applied to the miRNA counts, i.e. to determine how frequently each copy of miRNA was present across all samples, and heatmaps of the top 80 miRNA counts are shown in the Appendices Y and Z:

- A heatmap of the top 80 clustered and non-clustered miRNA counts is shown in Appendix Y. Clustering refers to the aggregation of individual participants according to participant group, i.e. pre- and post-surgery and non-obese Controls.
- A heatmap of the top 80 scaled (based on a scaled row z-score ranging from -3 to 3) for clustered and non-clustered miRNA counts is shown in Appendix Z.

Appendix AA shows a bar plot of the top 80 miRNA counts for all 3 participant groups from which the top five miRNAs were let-7g-5p, let-71-5p, miR-192-5p, miR-200b-3p and miR-26a-5p.

Finally, using data for all 1654 miRNAs identified by the NGS, the fold changes in miRNA expression between participant groups were investigated.

Comparison of genome-wide miRNA expression in obese individuals before RYGB with that in the non-obese Controls: A total of 112 significant miRNAs were detected (see Appendix BB) which are depicted in a volcano plot in Figure 4-5 (and in Appendix CC with their name annotations). The top five miRNAs with the most significant fold change, i.e. with the lowest p-value (p< 0.0001), included miR-200b-5p which was downregulated (fold change = 1.5) and

miR-30a-5p, miR-31-5p, miR-215-5p and miR-215-3p which were upregulated (fold changes 2.7, 6.0, 3.2, and 3.6, respectively). Figure 4-6 provides a heatmap of the miRNAs, for which expression differed significantly between the obese individuals pre-RYGB and the non-obese Controls, across all participants (see Appendix DD for the clustered heatmap). Within this heatmap, each row represents a significant miRNA and each column a sample from a participant (green bars: obese participants pre-surgery; blue bars: initially obese participants post-surgery and red bars: non-obese Controls). The colour, and intensity of that colour, of each of the boxes represent the extent of change in expression for each individual miRNA between the obese participants pre- and post-RYGB and the non-obese Controls. In this heatmap, blue boxes represent up-regulated miRNAs and green down-regulated miRNAs. The top 9 miRNAs which were significantly upregulated in the obese compared with Controls were (in this order): miR-31-5p, miR-31-3p, miR-215-3p, miR-338-3p, miR-215-5p, miR-450a-5p, miR-30a-5p, miR-126-5p and miR887-3p (fold-changes 6.0, 4, 3.6, 3.5, 3.2, 3.0, 2.7, 2.6 and 2.4, respectively). These miRNAs were consistently upregulated in most of the obese individuals in this study. Contrarily, the top 9 miRNAs which were significantly downregulated in the obese compared with the Controls were (in this order): miR-1247-3p, miR-486-3p, miR-3150b-3p, miR-642b-5p, miR-3196, miR-552-5p, miR-552-3p, miR-196a-5p and miR-1247-5p (fold-changes 3.8, 3.5, 2.8, 2.8, 2.7, 2.7, 2.5, 2.5 and 2.5, respectively). These miRNAs were consistently downregulated in most obese individuals in this study.
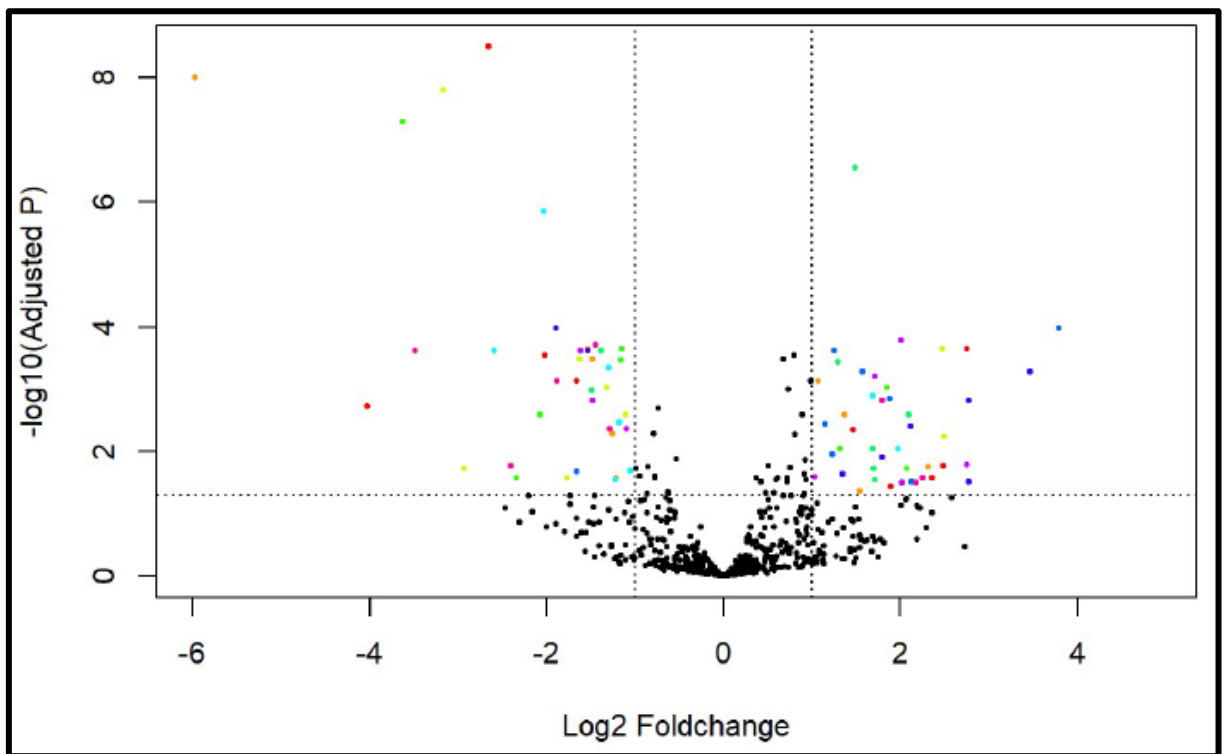
Figure 4-5: Volcano plot illustrating significant fold change for the miRNAs (each coloured dot represents an individual miRNA) which differed in abundance between obese individuals pre-RYGB and the non-obese Controls.
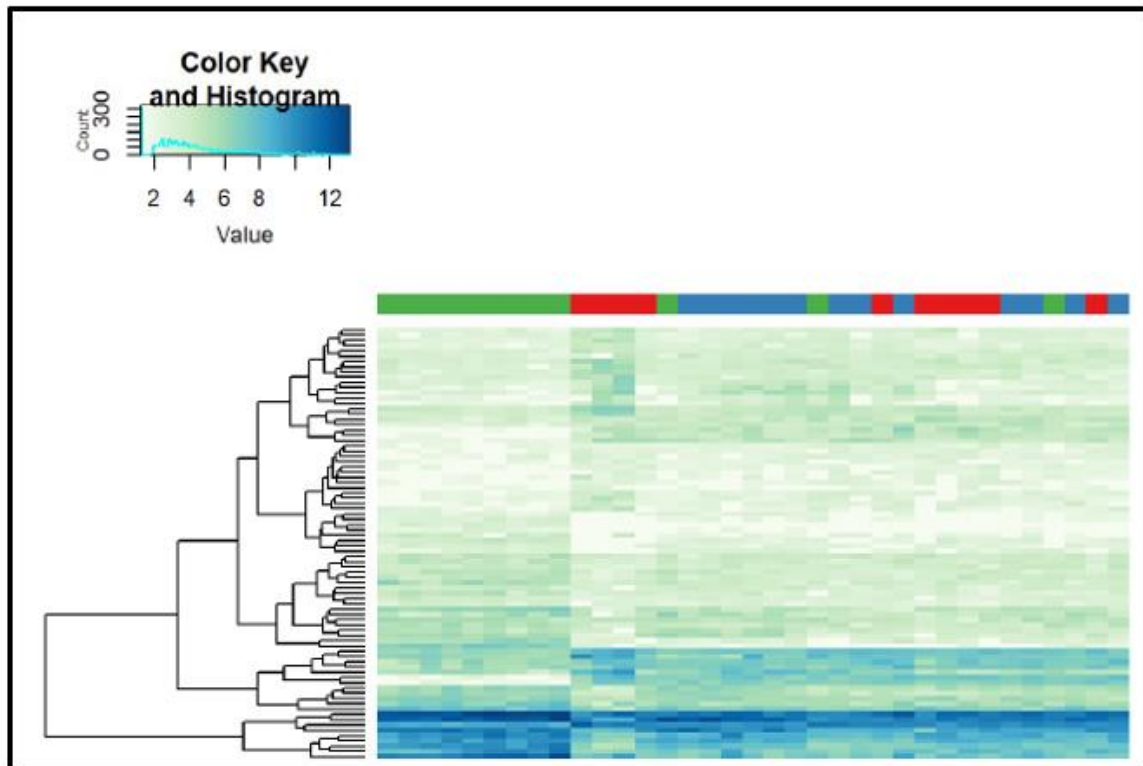
Figure 4-6: Heatmap of the miRNAs, for which expression differed significantly between the obese participants pre-RYGB and the non-obese Controls, for all participants (green bars: pre-RYGB; blue bars: post-RYGB and red bars: Control group).

133

Comparison of genome-wide miRNA expression in obese individuals before and after RYGB: A total of 60 significant miRNAs were detected (see Appendix EE) which are depicted in a volcano plot in Figure 4-7 (and in Appendix FF with their name annotations). The top five miRNAs with the most significant fold change, i.e. with the lowest p-value (p< 0.0001), included miR-31-5p, miR-204-5p, miR-215-5p, miR-215-3p and miR-30a-5p which were downregulated (fold changes 6.3, 2.2, 3.0, 3.1 and 2.1, respectively). Figure 4-8 provides a heatmap of the 45 miRNAs for which expression differed significantly between the obese individuals pre- and post-RYGB, across all participants (see Appendix GG for the clustered heatmap- clustering is referred to the aggregation of individual participants according to participant group, i.e. obese pre- and post-RYGB and non-obese Controls). Similarly, to the previously explained heatmap, each row represents a significant miRNA and each column a sample from a participant (green bars: obese participants pre-RYGB; blue bars: initially obese participants post-surgery and red bars: non-obese Controls). The colour, and intensity of that colour, of each of the boxes represent the extent of change in expression for each individual miRNA between the obese participants pre- and post-RYGB and the non-obese Controls. In this heatmap, blue boxes represent up-regulated miRNAs and green down-regulated miRNAs. The top 5 miRNAs which were significantly upregulated in the obese individuals post-RYGB compared with pre-RYGB were (in this order), miR-211-5p, miR-4516, miR-1247-3p, miR-552-5p and miR-552-3p (fold changes 2.8, 2.7, 2.7, 2.6 and 2.5, respectively). These miRNAs were consistently upregulated in most of the initially-obese individuals post-RYGB in this study. Contrarily, the top 5 miRNAs which were significantly downregulated in the obese individuals post-RYGB compared with the pre-RYGB were (in this order): miR-31-5p, miR-31-3p, miR-424-5p, miR-215-3p and miR-892c-3p (fold changes 6.3, 4.8, 3.4, 3.1 and 3.0, respectively). These miRNAs were consistently downregulated in most initially-obese individuals post-RYGB in this study.
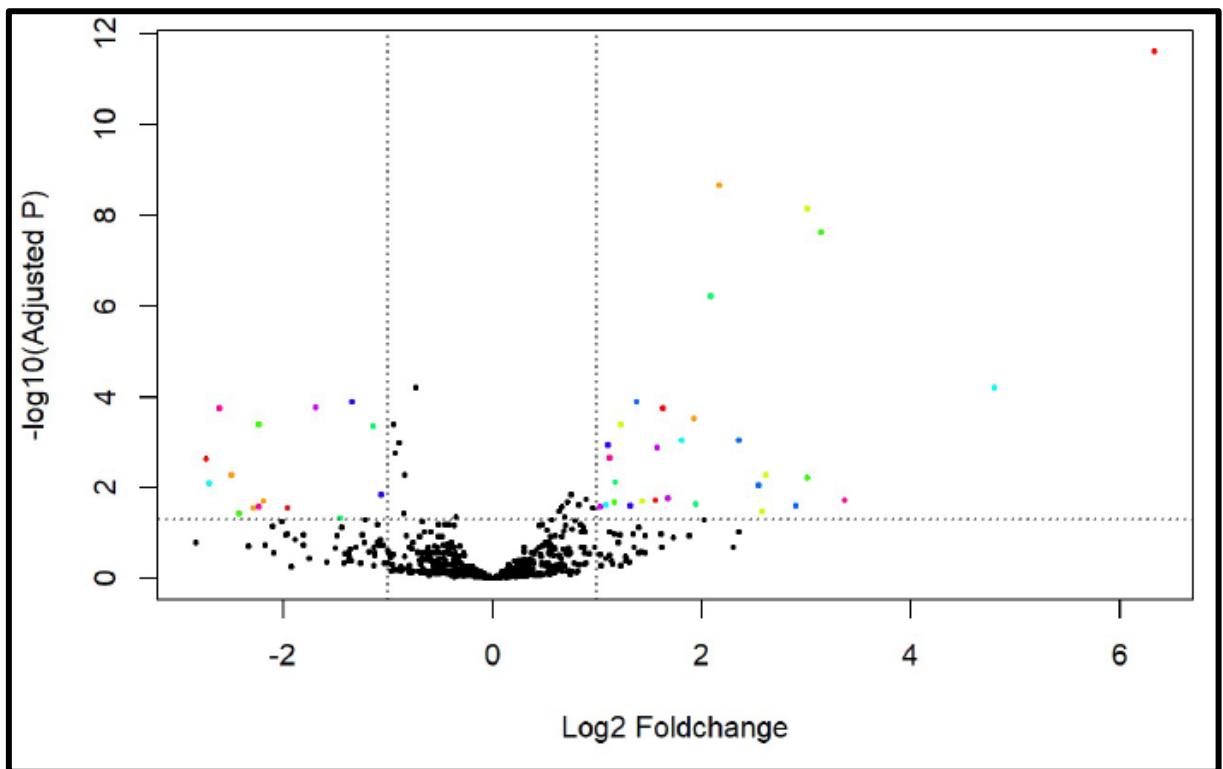
Figure 4-7: Volcano plot illustrating significant fold change for the miRNAs (each coloured dot represents an individual miRNA) which differed in abundance between the obese individuals pre- and post-RYGB.
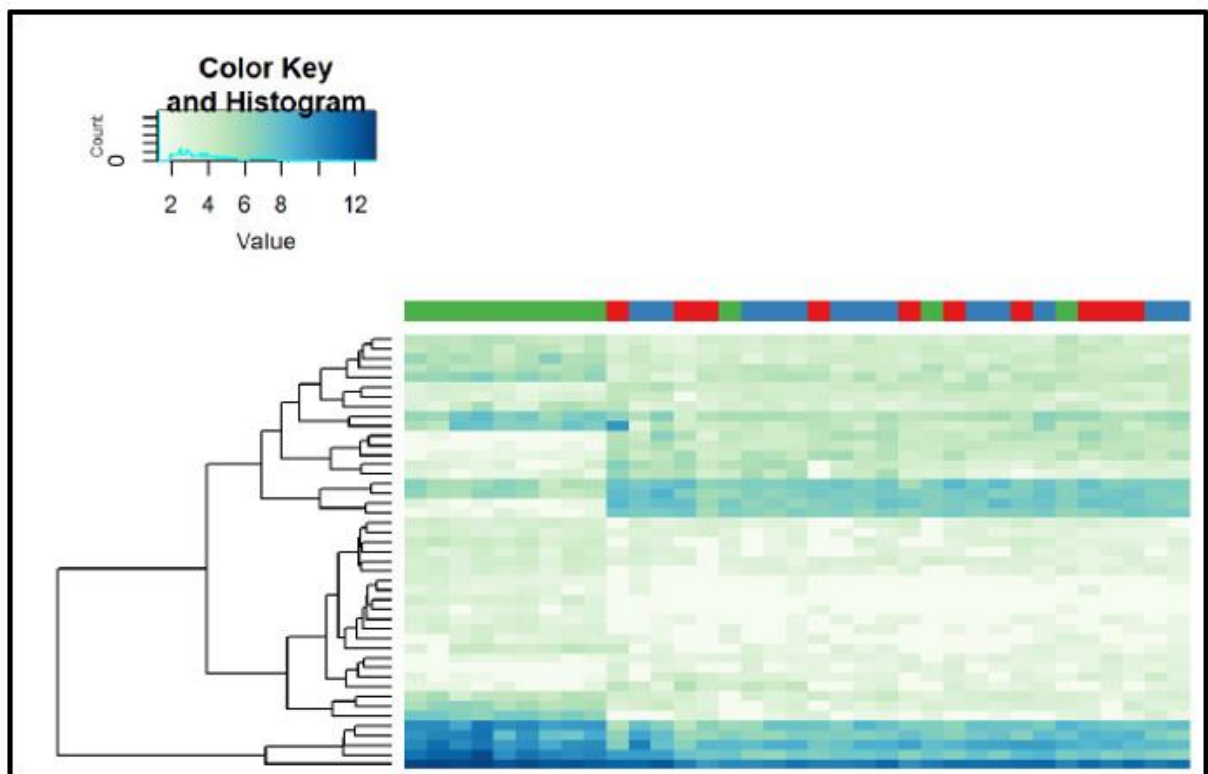
Figure 4-8: Heatmap of the miRNAs, for which expression differed significantly between the obese participants pre- and post-RYGB, for all participants (green bars: pre-RYGB; blue bars: post-RYGB and red bars: Control group).

<u>*Comparison of genome-wide miRNA expression in obese individuals after RYGB with that in the non-obese Controls:*</u> No significant miRNAs were detected (see Figure 4-9).
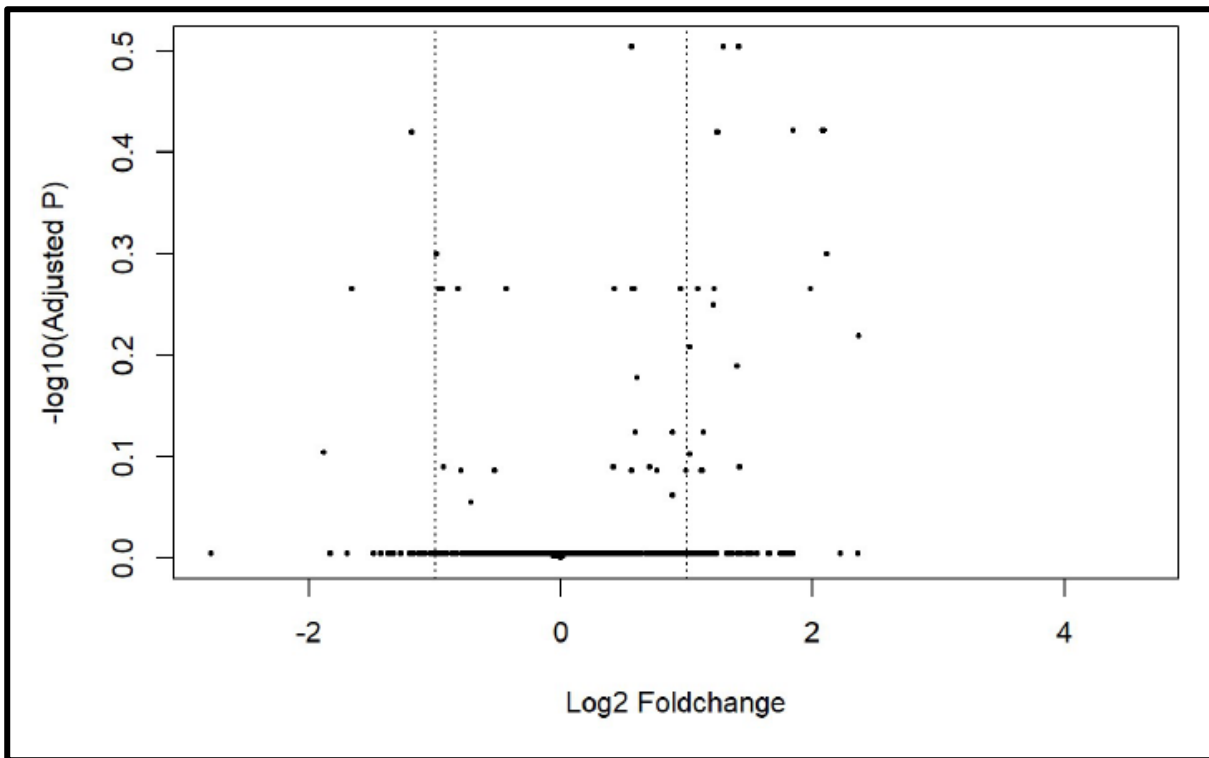
Figure 4-9: Volcano plot illustrating no significant fold change for the miRNAs identified which did not differ in abundance between the obese individual post-RYGB and non-obese Controls.

A total of 36 identical miRNAs differed significantly in both the comparisons of i) the obese participants pre-RYGB with the non-obese Controls and ii) the initially obese individuals pre- and post-RYGB (see Appendix HH). These differentially expressed miRNAs are predicted to be implicated in pathways linked with inflammation, obesity and cancer (see Appendix HH) (Vlachos, 2015). Of these 36 miRNAs, the following 13 including miR-552-5p, miR-3150, miR-455-3p, miR-3656, miR-3196, miR-671-5p, miR-4516, miR-450a-5p, miR-655-5p, miR-4284, miR-1247-3p, miR-203a-3p and miR-215-3p were not detected by the probes on the miRNome array which was conducted previously by Dr Sorena Afshar in analysis of the same samples (Afshar, 2016a).

Both the miRNome array and the NGS (by MiSeq) identified a total of 44 identical and significant miRNAs when comparing the initially obese individuals pre- and post-RYGB (see Figure 4-10). The majority of miRNAs had a differential fold regulation in the opposite direction of change, i.e. a downregulation with NGS and up-regulation using the miRNome array, with the exception of 15 miRNAs which showed significant up-regulation in the both the NGS and miRNome array. These included: mir-552-3p, miR-196a-5p, miR-196b-5p, miR-1247-5p, miR-3150b-3p, miR-147b, miR-1262, miR-203a, miR-210-3p, miR-185-5p, miR-200b-5p, miR-125b-5p, miR-200b-3p, miR-191-5p and miR-28-3p (see Figure 4-10). Since it may be

more difficult to detect accurately the fold change in expression between two participant groups for miRNAs with very low levels of expression, I checked the Ct-value for these 29 miRNAs obtained using the miRNome array. The mean Ct value was 26.2 for the obese participants pre-surgery and 26.6 for the same individuals post-surgery. 6 miRNAs i.e. miR-31-5, miR-30c-2-3, miR-129-5, miR-181a-3, miR-450a and miR-582-5 had CT values above 30, which is indicative of low expression and might have explained the differential direction of fold regulation between the two techniques (see Appendix II) (Afshar, 2016a).
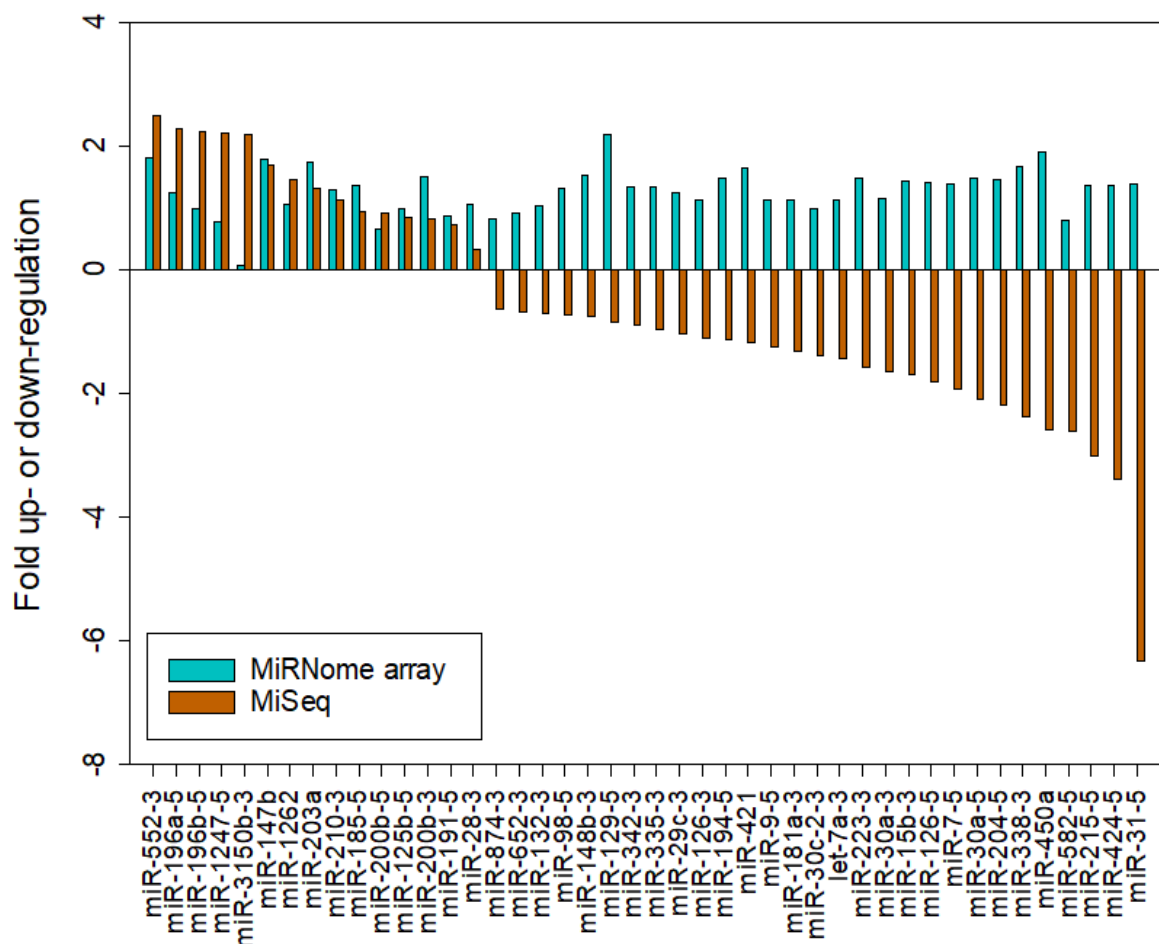
Figure 4-10: Fold change in expression determined by two techniques, miRNome array and NGS, for 44 miRNA that were differentially expressed in initially obese individuals before and after RYGB.

Furthermore, when comparing miRNA expression in the initially obese group pre- and post-surgery, NGS picked up 16 significant miRNAs that were not detected by the probes on the miRNome array which was conducted previously by Dr Sorena Afshar in analysis of the same samples (Afshar, 2016a) (see Figure 4-12). These miRNAs are predicted to be involved in KEGG (Kyoto Encyclopedia of Genes and Genomes) pathways implicated in obesity inflammation and cancer, including CRC. The cancer-related pathways include TGF-β, MAPK, Wnt and Hedgehog signalling pathways (see Figure 4-11) (Vlachos, 2015). From these 16 miRNAs, a

panel of 8 miRNAs was selected by choosing the top 4 up- (miR-4516, miR-3196, miR-1247-3p and miR-671-5p) and the top 4 down-regulated miRNAs (miR-31-3p, miR-204-3p, miR-215-3p and miR-892c-3p) for which validated primers were available from Qiagen. This panel was used to validate the NGS screening data by quantifying miRNA expression using qPCR (see Figure 4-13).

#	KEGG pathway	p-value	#genes		#miRNAs
1.	Prion diseases (hsa05020)	1.43723477415e-13	6	see genes	6
2.	Glycosphingolipid biosynthesis - ganglio series (hsa00604)	1.06836275947e-08	7	see genes	3
3.	Morphine addiction (hsa05032)	6.79322844992e-07	28	see genes	10
4.	ErbB signaling pathway (hsa04012)	0.000675973149061	26	see genes	12
5.	GABAergic synapse (hsa04727)	0.000736148137597	24	see genes	11
6.	Glutamatergic synapse (hsa04724)	0.000956761164534	28	see genes	11
7.	Thyroid hormone synthesis (hsa04918)	0.00108185785381	20	see genes	11
8.	Lysine degradation (hsa00310)	0.0033757596288	14	see genes	8
9.	N-Glycan biosynthesis (hsa00510)	0.00348143330401	13	see genes	7
10.	Signaling pathways regulating pluripotency of stem cells (hsa04550)	0.00442631913943	36	see genes	12
11.	Chronic myeloid leukemia (hsa05220)	0.00510466707544	24	see genes	12
12.	TGF-beta signaling pathway (hsa04350)	0.00563995273526	17	see genes	8
13.	Glycosaminoglycan biosynthesis - chondroitin sulfate / dermatan sulfate (hsa00532)	0.00595167449717	6	see genes	5
14.	Proteoglycans in cancer (hsa05205)	0.00853008464369	51	see genes	12
15.	Melanogenesis (hsa04916)	0.0089218536987	31	see genes	10
16.	Hippo signaling pathway (hsa04390)	0.0108882742899	35	see genes	12
17.	Retrograde endocannabinoid signaling (hsa04723)	0.011239565355	27	see genes	10
18.	Pathways in cancer (hsa05200)	0.0152891145421	92	see genes	15
19.	Other types of O-glycan biosynthesis (hsa00514)	0.0172020526703	10	see genes	9
20.	MAPK signaling pathway (hsa04010)	0.0172020526703	61	see genes	12
21.	Wnt signaling pathway (hsa04310)	0.019402152321	35	see genes	12
22.	Hedgehog signaling pathway (hsa04340)	0.0209712322614	17	see genes	7
23.	Basal cell carcinoma (hsa05217)	0.0209712322614	18	see genes	8
24.	Cell adhesion molecules (CAMs) (hsa04514)	0.0214342029143	30	see genes	10
25.	Adrenergic signaling in cardiomyocytes (hsa04261)	0.0481860125075	38	see genes	12
26.	Estrogen signaling pathway (hsa04915)	0.0499868462319	26	see genes	9

Figure 4-11: Predicted KEGG pathways in which the 16 differentially expressed* miRNAs are involved. These pathways were identified using DIANA Tools (Vlachos, 2015). *Differentially and significantly expressed in initially obese individuals before and after RYGB as measured by NGS.
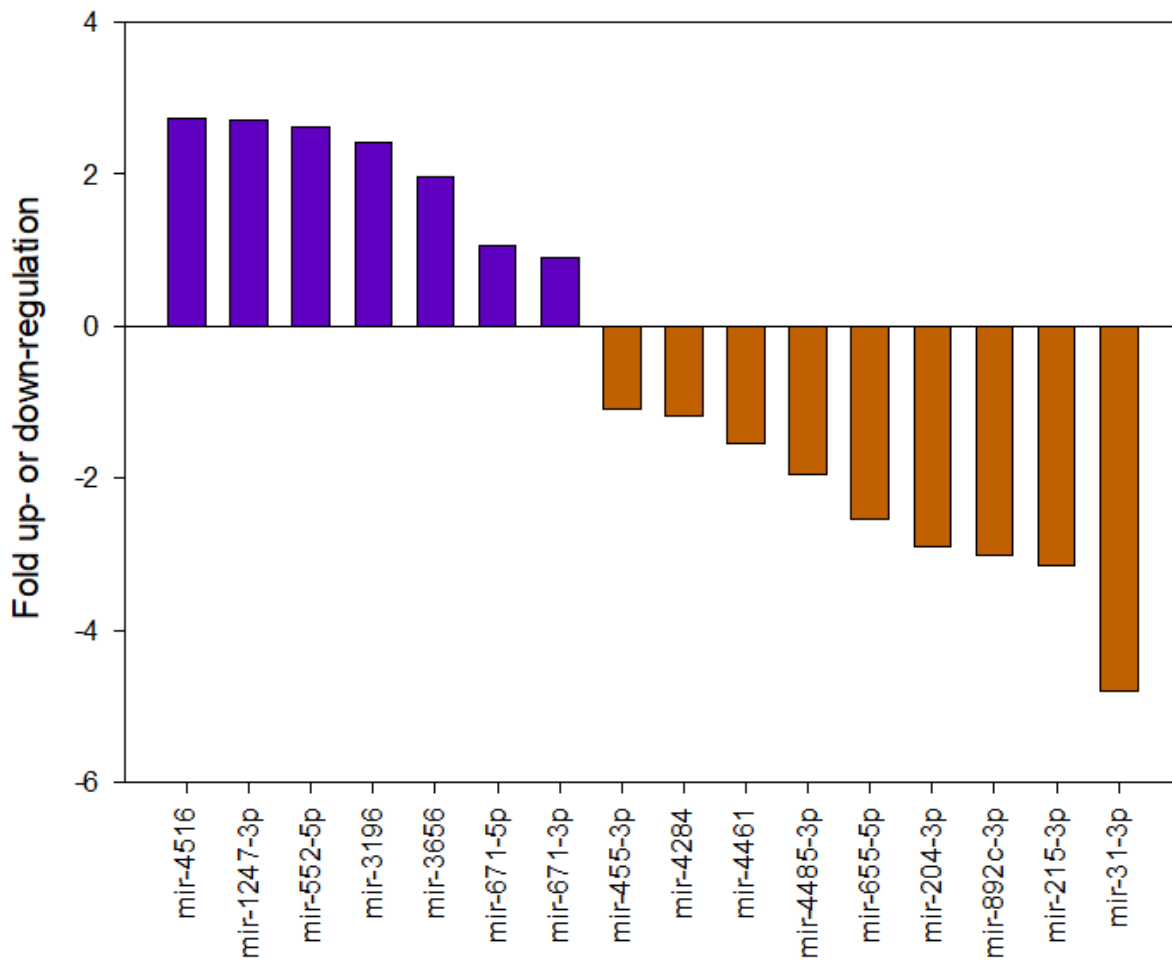
Figure 4-12: Change in expression (fold up- or down-regulation) of 16 significant miRNAs for which expression differed in initially obese individuals before and after RYGB. These differentially expressed miRNA were identified by NGS, but not by the miRNome array
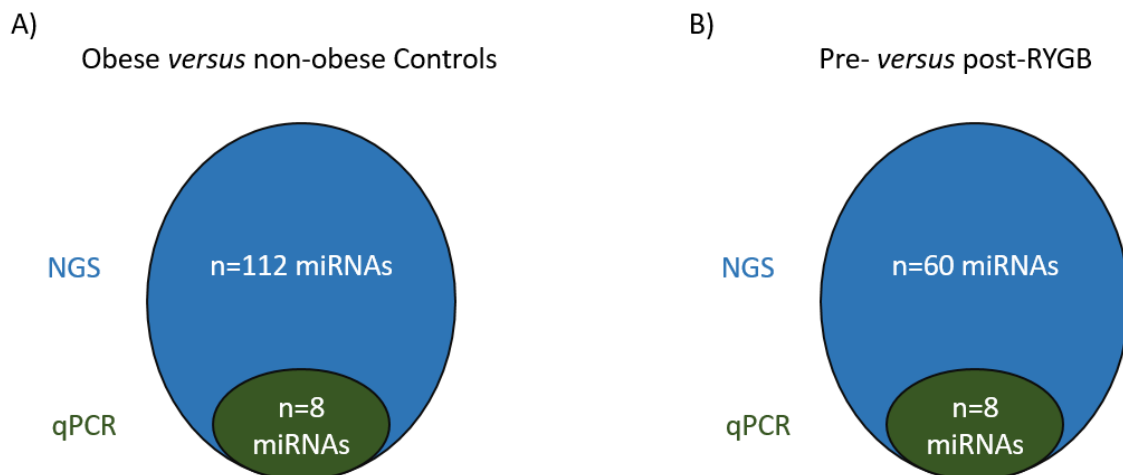
Figure 4-13: A) In the comparison of Obese versus non-Obese Controls a total of n=112 miRNAs were identified by NGS (see Appendix BB for individual miRNA names) out of which n=8 were selected for validation by qPCR; B) In the comparison of

An *in-silico* target prediction analysis tool by Vlachos (Vlachos, 2015) was utilised to detect potential Kyoto Encyclopedia of Genes and Genomes (KEGG) pathways enriched for predicted mRNA gene targets of these 16 miRNAs (see Figure 4-14). The microT-CDS algorithm was used to undertake the enrichment analysis where a p-value for each one of the 4 miRNAs was calculated and a merged p-value for each pathway was obtained using a Fisher's meta-analysis. The p-value shown illustrates the 1 minus the probability that the shown pathway (see Figure 4-14) is enriched with gene targets for at least one of the 4 selected miRNAs (the orange colour illustrates a higher probability). Many KEGG pathways implicated in metabolism were enriched for predicted mRNA gene targets identified by NGS but not the miRNome array, including pathways in morphine addiction, lysine degradation, glycosphingolipid biosynthesis, ECM-receptor interaction, drug metabolism and prion disease which play important roles in the morphogenesis and maintenance of cell and tissue structure and function.
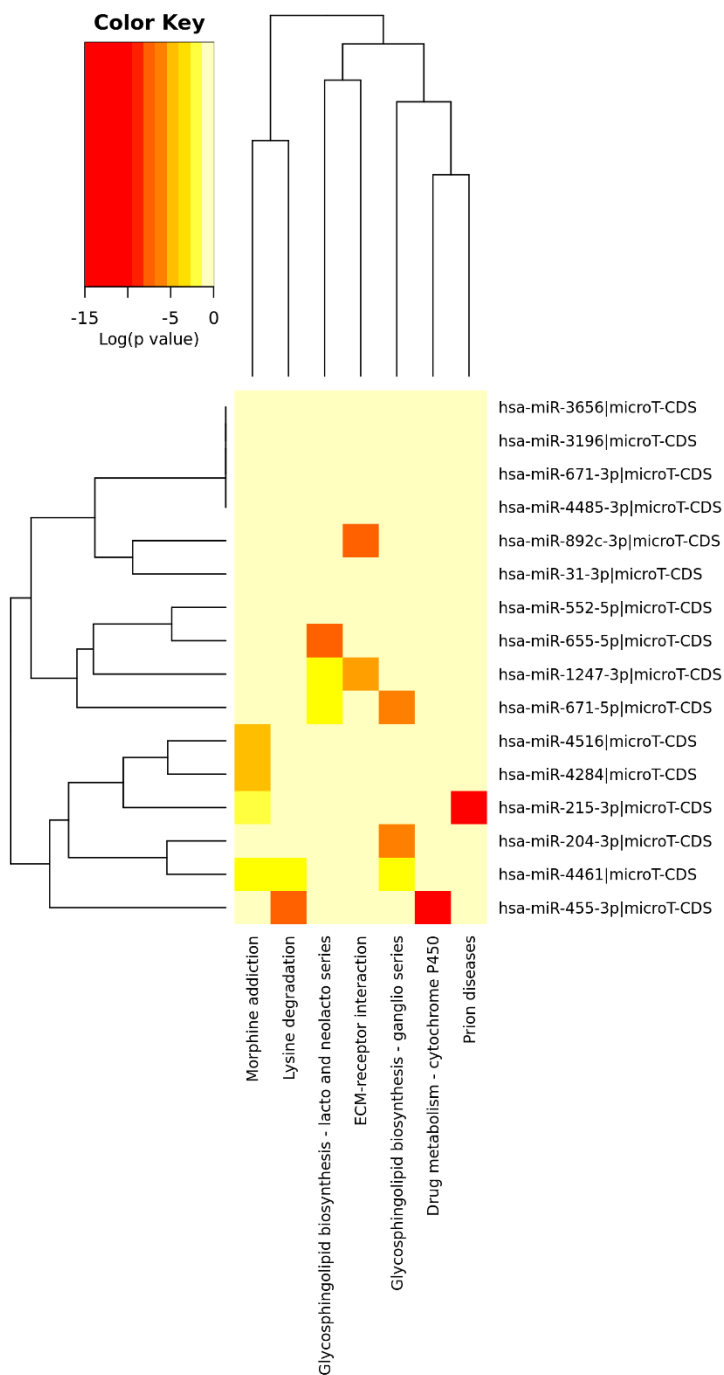
Figure 4-14: Heatmap illustrating KEGG pathway unions for predicted mRNA gene targets of the 16 *significant miRNAs for which expression differed in initially obese individuals before and after RYGB. These differentially expressed miRNA were identified by NGS, but not by the miRNome array* (log(p-value), orange colour illustrates higher probability) (Vlachos, 2015).

4.7 Effects of adiposity and weight loss on expression of selected panel of miRNAs in the colorectal mucosa measured using qPCR

Figure 4-15 shows expression of the selected panel of miRNAs quantified in the colorectal mucosa of obese individuals (pre-RYGB) and of the non-obese Controls. MiR-4516 and miR-

892c-3 were the most abundantly expressed miRNAs in the panel in both the obese and non-obese individuals. Of the 8 miRNAs, four showed significantly higher expression in the obese compared with non-obese Controls i.e. miR-31-3, miR-215-3, miR-3196 and miR-4516 which were upregulated 143-fold, 15-fold, 2.6-fold and 2.6-fold, respectively. For the other 4 miRNAs i.e. miR-204-3, miR-671-5, miR-892c-3 and miR-1247-3, expression tended to be higher in the obese but the differences were not significant.

When quantified by NGS, miR-3196 was downregulated in the obese compared with the non-obese Controls. However when quantified using qPCR miR-3196 was upregulated in the obese compared to the non-obese Controls and hence, did not validate due to the different direction of expression. For this reason miR-3196 will be excluded from any subsequent analysis in this comparison group.
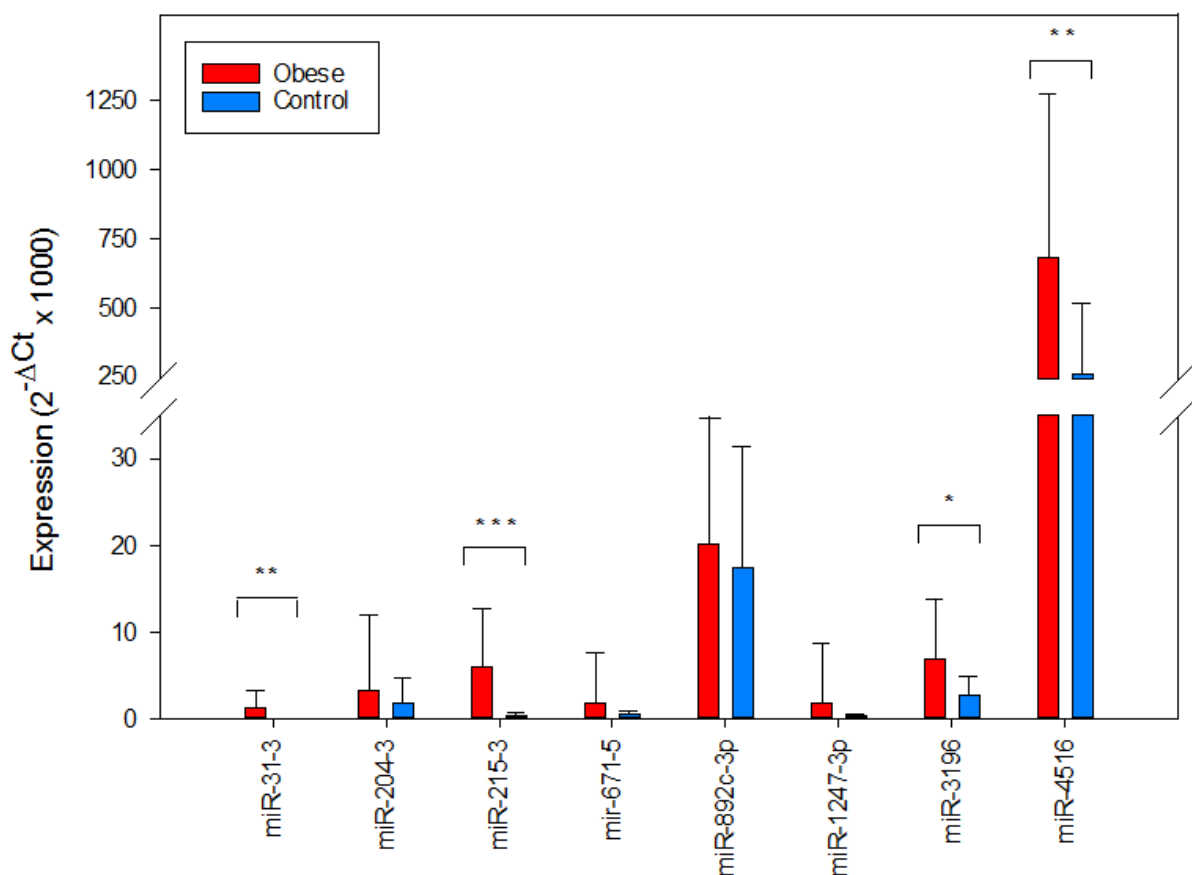
Figure 4-15: MiRNA expression determined by qPCR in the colorectal mucosa of obese individuals pre-RYGB and non-obese Controls.

Figure 4-16 shows expression of the selected panel of miRNAs quantified in the colorectal mucosa in the initially obese group before and after RYGB. As for the previous comparison,

miR-4516 and miR-892c-3 were the most abundantly expressed miRNAs in these participants. At 6 months after surgery, expression of miR-31-3, miR-215-3 and miR-3196 was 15.9, 7.3 and 1.2% lower than pre-surgery, and levels of expression of these miRNAs following RYGB were similar to those of the non-obese Controls. In contrast, there were no significant changes in expression of miR-204-3, miR-671-5, miR-892c-3, miR-1247-3 and miR-4516 following RYGB surgery.
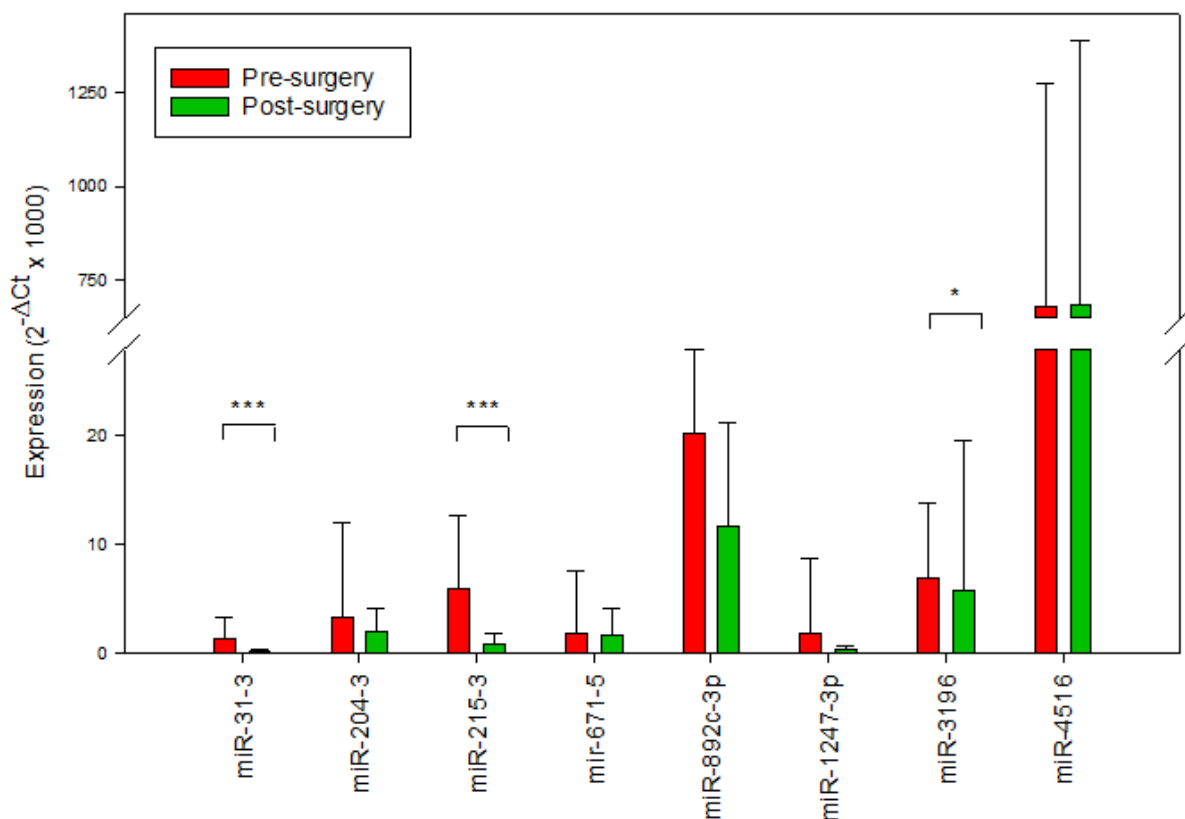
Figure 4-16: MiRNA expression determined by qPCR in the colorectal mucosa of the initially obese individuals pre- and post-RYGB.

Figure 4-17 shows miR-31-3, miR-215 and miR-3196 expression for each initially obese individual before and after RYGB, which were significant. For the large majority of individuals, the fall in miR-31-3, miR-2115 and miR-3196 expression after bariatric surgery was clear and substantial but one, two and one, respectively, individual(s) showed a contrary change. Although the trend for the majority of the participants, for all 3 miRNAs, shows a downregulation in the miRNAs quantified, the inter-individual variation in miRNA change for the remaining participants is rather great.
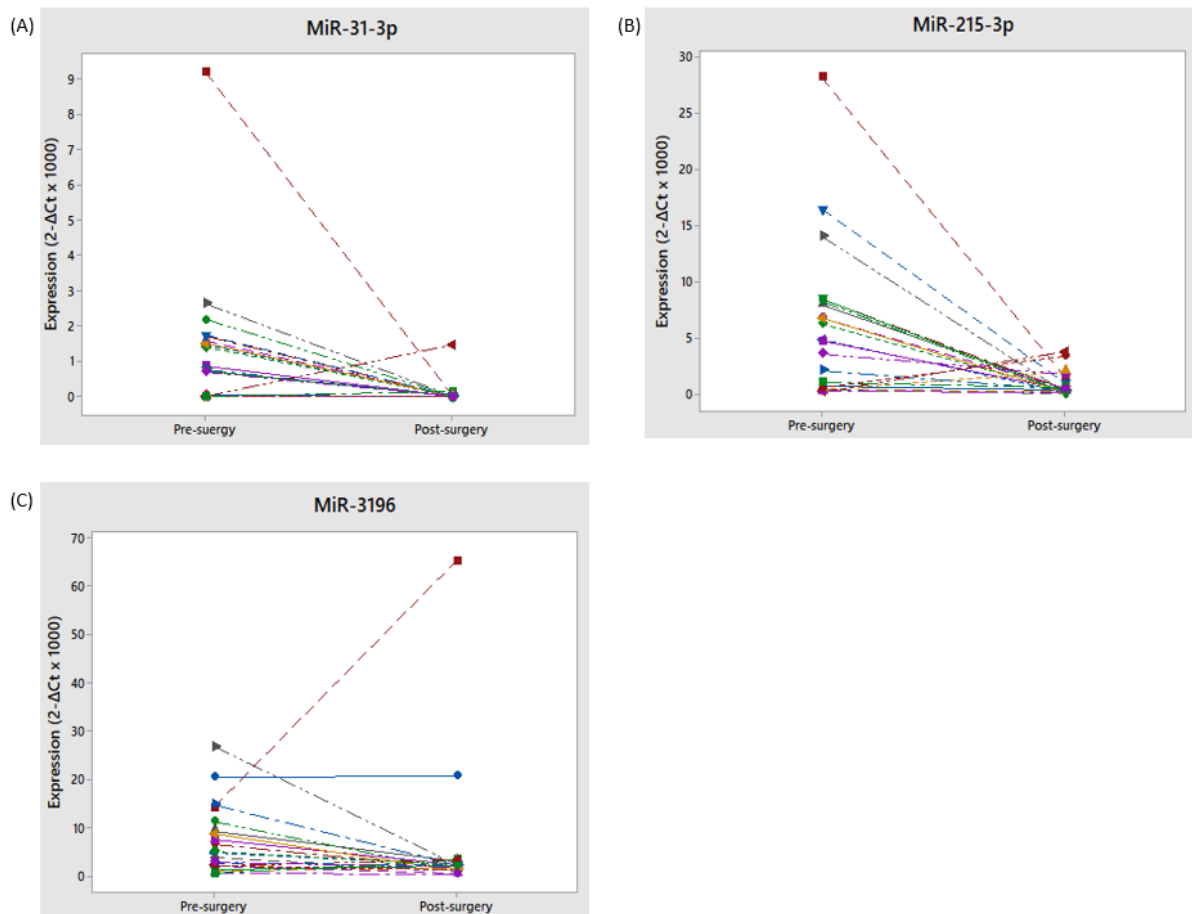
Figure 4-17: MiRNA expression in the colorectal mucosa for each initially obese individual before and after RYGB. A) MiR-31-3p expression B) MiR-215-3p expression C) MiR-3196 expression.

When quantified by NGS, miR-3196 was upregulated in the post-RYGB group compared with the pre-RYGB group. However when quantified using qPCR miR-3196 was downregulated in the post-RYGB group compared to the pre-RYGB group and hence, did not validate due to the different direction of expression change. For this reason miR-3196 will be excluded from any subsequent analysis in this comparison group.

4.7.1 Associations between weight loss following RYGB and miRNA expression in the colorectal mucosa

The relationship between the degree of weight loss following RYGB (post-surgery weight minus baseline weight), and changes in miRNA expression (follow-up miRNA expression minus baseline miRNA expression) in the colorectal mucosa was examined using linear regression. There were no statistically significant correlations between changes in body weight, i.e. the degree of weight loss, and expression of any of the 3 miRNAs examined ($p > 0.05$) (see Table 4-2). The R values show a low degree of correlation for all 3 miRNAs ($R < 0.224$) and the R^2 indicates that less than 5% of the total variation in miRNA expression can be explained by weight loss following RYGB (see Table 4-2).

	Mean change in miRNA expression between pre- and post-RYGB	R value	R^2 value	p-value
miR-31	-1.19 (2.0)	0.212	0.045	0.343
miR-215	-5.14 (6.9)	0.224	0.050	0.316
miR-4516	2.55 (601.6)	0.051	0.003	0.823

Table 4-2: Relationship between weight loss following RYGB and miRNA expression (mean (SD)) in the colorectal mucosa at pre- and post-surgery.

Then a second analysis was performed using the Mann-Whitney-U test, as data were not normally distributed, where the median weight loss (28kg) was used as a cut-off to investigate if the changes in miRNA expression differed between the participants who lost up to 28kg weight (range 10- 27.3kg) or lost more than 28kg weight (range 29- 59kg) at 6 months follow-up. No significant differences could be detected (p>0.05) (see Table 4-3). Only miR-215 was close to significance (p=0.053) and it is likely that if the sample size was bigger, significance would have been detected. Even though data were not normally distributed, the analysis was repeated using the one-way ANCOVA which is a robust statistical test, to directly compare changes in miRNA expression over the period (pre- to post-surgery) in each of the groups (lost <28kg *versus* lost >28kg) where gender, baseline/ pre-surgery BMI and age were included as covariates. Once more, no significant differences could be detected (p>0.05) (see Table 4-3).

miRNA	Lost weight <28 kg (n=11)	Lost weight >28kg (n=11)	P-value*	P-value†
miR-31	-0.005 (-2.6 – 1.5)	-1.477 (-9.2 – 0.0)	0.061	0.213
miR-215	-0.429 (-13.8 – 3.6)	-6.606 (-26.7 – 1.6)	0.053	0.086
miR-4516	274.1 (-698.5 - 801)	-198.8 (-1499 – 1040)	0.200	0.254

Table 4-3: Mean change in expression of selected miRNA in the colorectal mucosa of those who lost <28kg and >28kg following RYGB at 6 months follow-up. Data are presented as Median (range).
*Mann-Whitney-U test
†Adjusted ANCOVA test

These results show that changes in miRNA expression are not associated and cannot be predicted based on the degree of weight loss following RYGB. Furthermore, changes in miRNA expression do not differ between participants who lost more or less than 28kg body weight over the study period, even when adjusted for potential confounding factors including gender, baseline BMI and age.

4.7.2   Predicted biological roles of the 8 selected miRNAs

An *in-silico* target prediction analysis tool by Vlachos (Vlachos, 2015) was utilised to detect potential Kyoto Encyclopedia of Genes and Genomes (KEGG) pathways enriched for predicted mRNA gene targets of the 8 selected miRNAs analysed (see Figure 4-18). The microT-CDS algorithm was used to undertake the enrichment analysis where a p-value for each one of the 8 miRNAs was calculated and a merged p-value for each pathway was obtained using a Fisher's meta-analysis. The p-value shown illustrates the 1 minus the probability that the shown pathway (see Figure 4-18) is enriched with gene targets for at least one of the 8 selected miRNAs (the orange colour illustrates a higher probability). Many KEGG pathways implicated in metabolism were enriched for predicted mRNA gene targets of my selected miRNAs, including pathways in biotin metabolism, protein processing in endoplasmic reticulum and ECM-receptor interaction all of which play important roles in the morphogenesis and maintenance of cell and tissue structure and function.
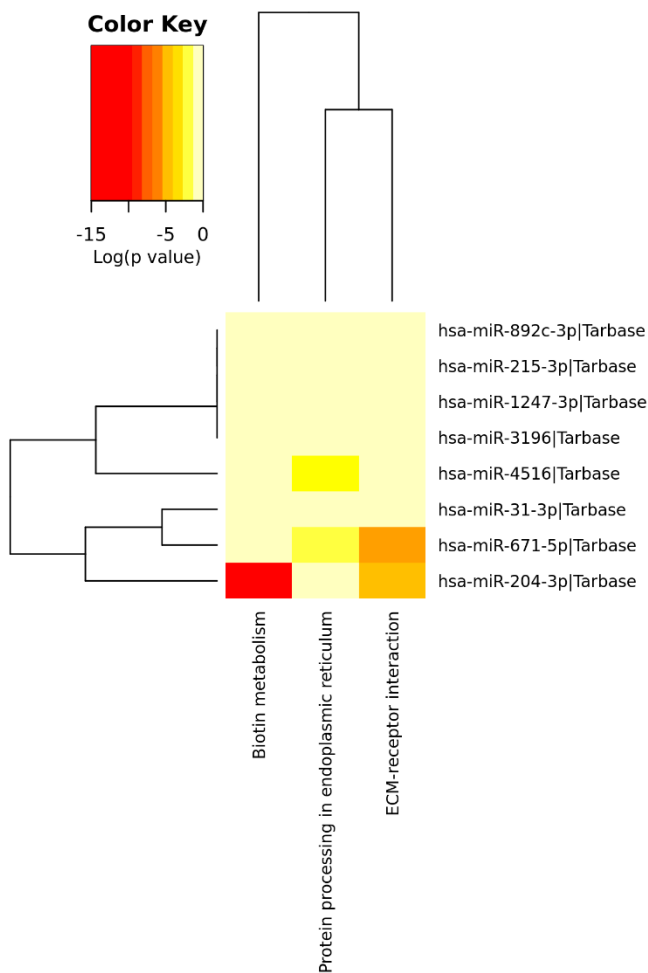
Figure 4-18: Heatmap illustrating KEGG pathway unions for predicted mRNA gene targets of the 8 selected miRNAs (log(p-value), orange colour illustrates higher probability) (Vlachos, 2015).

4.8 Discussion

To my knowledge, apart from Afshar (2016a), no previous publications have investigated the effects of weight loss (following bariatric surgery) on the expression of miRNAs in the human colorectal mucosa. I have extended Afshar's analysis by using NGS which provides a wider, unbiased assessment of genome-wide miRNA expression than is possible by the miRNome array approach used by Afshar (2016a).

4.8.1 The effect of obesity on miR-31, miR-215 and miR-4516 in the colorectal mucosa

Given the link between adiposity and CRC risk, my finding of increased miR-31 expression in human colorectal mucosal biopsies in the obese when compared with the non-obese Controls is consistent with the role of miR-31 as an oncogene. Similarly, a study by Kurylowicz (2017) using NGS also found that miR-31 was significantly upregulated in obese participants, however in a different tissue, when comparing 44 samples of visceral and subcutaneous adipose from

normal weight (7 individuals), obese (10 individuals) and obese post-bariatric surgery (10 individuals). Another study investigated the baseline miRNA signature in visceral fat (VF) and subcutaneous fat (SF) of the adipose tissue in 20 bariatric-surgery patients (mean BMI 42.4 kg/m^2) and 8 non-obese (mean BMI 24.6 kg/m^2) and showed differential miRNA profiles in obese SF and VF; 12 miRNAs were upregulated, miR-31 was amongst them, and 6 were down regulated in the VF of obese (Liao et al., 2018). However, it is important to note that both of these studies were conducted in adipose tissue.

Given the link between adiposity and CRC risk and the role of miR-215 as a tumour suppressor gene, my finding of increased miR-215 expression in human colorectal mucosal biopsies in the obese when compared with the non-obese Controls is unexpected. However this finding is line with findings from by Kurylowicz (2017) who also observed increased expression of miR-215 in the obese group when compared with normal weight adults. Potential explanations for this observation may be:

- With the role of miR-215 being a TSG, a reduction and not an increase of this miRNA was expected in the obese, (downregulated miR-215) which would be suggestive of an increased CRC risk. However, miR-215 was the only miRNA of the panel examined which has been previously described to play a tumour suppressive role in CRC and, therefore the assumption of a reduced CRC risk in the obese based on one single miRNA (miR-215 upregulation) cannot be made. More miRNAs with the role of a TSG should be examined to draw coherent and strong conclusions on CRC risk. The observed changes in miR-215 expression with greater adiposity in this study and the study by Kurylowicz (2017), although the latter was in the adipose tissue, may be unrelated to pathology. It is known that one single miRNA can target multiple pathways, hence miR-215 may be involved in more and other pathways than CRC, for example obesity and therefore be unrelated to CRC in this context. Additionally, it is important to keep in mind that the tissue examined in this study was 'healthy' and not derived from tumour tissue, hence the observed changes in miR-215 expression might be within the 'normal range' and so not indicative of altered CRC risk.

- Recruitment of the non-obese Controls occurred following referral for flexible sigmoidoscopy or colonoscopy for GI symptoms. Even though patients were only recruited if their endoscopy was normal and no pathology was found, this method for recruitment might have selected unhealthy participants with undiagnosed GI pathology. A systematic review and other studies have observed neoplasia, adenoma

and polyp miss rates ranging between 6-27% following lower GI endoscopy (Hixson et al., 1991, Bensen et al., 1999, van Rijn et al., 2006, Kaltenbach et al., 2008) which suggests that the diagnosis of pathology in some Control participants could have been missed. However, as adenomas do not commonly cause symptoms, it is not expected to find a higher adenoma miss rate in the non-obese Controls who were symptomatic patients with a normal endoscopy, compared with the obese patients. Finally, the normal weight Controls (n=7) from the study by Kurylowicz (2017) which detected similar changes in miRNA expression patterns to my study, underwent elective cholecystectomy or were operated for inguinal hernia. Since the observed effects in miRNA expression were similar in both studies (by Kurylowicz (2017) and mine), it suggests that recruitment strategy for the Controls in the BOCABS Study was satisfactory to enable detection of changes in miRNA expression when compared with adults with severe adiposity, i.e. BMI above >40 kg/m^2.

- The differential miRNA expression pattern depending on the cellular composition of tissue has been noted for multiple miRNAs, especially for TSGs including the miR-143/145 cluster (Kent et al., 2014). The miR-134/145 cluster is more expressed in mesenchymal cells (i.e. fibroblasts and smooth muscle cells) than in colonic epithelial cells and failure to consider this issue could lead to misinterpretation of differential miRNA expression patterns (in CRC) (Kent et al., 2014). Furthermore, a reduction or even loss in miRNA expression acting as TSG from normal epithelial cells has been reported when they differentiate and acquire malignant features, due to the shift in cellular composition in CRC when compared with normal colon (Kent et al., 2014). In previous work on the colorectal mucosal biopsy samples examined here, cellular biopsy composition was investigated by measuring smooth muscle actin (*SMA*) and Cytokeratin 20 (*CK20*) as markers of mesenchymal and epithelial cells, respectively (Afshar, 2016a). The *SMA: CK20* ratio did not differ between the non-obese Controls and the individuals pre- and post- RYGB, therefore it is not anticipated that differences in the cellular composition of biopsies from the different study groups would be a confounding factor for miRNA expression in the present study. In addition, for miR-215, the cellular make-up of biopsies is unlikely to be a confounder because Kent (2014) reported no miR-215 expression in lymphocytes, endothelial, smooth muscle, fibroblasts and red blood cells, whereas miR-215 was highly expressed in epithelial

cells. Therefore, a shift in cellular composition in obesity is not expected to affect miR-215 expression.

To date, there is no literature published about the role of miR-4516 as a TSG or an oncogene in the colorectal mucosa, therefore it is difficult to discuss whether the increased expression of this miRNA observed in the obese individuals here is considered abnormal.

4.8.2   Main findings

I found that obesity resulted in significant overexpression of miR-31, miR-215 and miR-4516 in the human colorectal mucosa when compared to that in the colorectal mucosa of non-obese individuals. I also observed that a mean 28.5kg weight loss by RYGB led to a significant fall in expression of miR-31 and miR-215 in initially obese individuals at 6 months follow-up, and these expression levels at 6 months follow-up were similar to those observed in the non-obese Controls.

4.8.2.1   4.8.2 Interpretation of main findings

In the introductory chapter (see section 1.4.6), I have reviewed evidence that obesity in humans is associated with abnormal patterns of miRNA expression. In addition, there is evidence that patterns of miRNA expression are "normalised" to some extent following significant and sustained weight loss as a result of bariatric surgery. However, most of this evidence has been obtained from measurements made in blood, only two studies have reported miRNA expression in adipose tissue (Kristensen et al., 2017, Liao et al., 2018) and there are no comparable data, apart from those by (2016a), from measurements made in the colorectal epithelium.

Here I used a NGS method, which is a broader, unbiased assessment of genome-wide miRNA expression than is possible by the miRNome array approach used by Afshar in the same samples (2016a), and this made the detection of more miRNA targets feasible. The miRNome array approach screened for the 1008 most abundantly expressed and best characterised miRNAs in the human genome, but use of NGS here detected expression of 1654 miRNA, 39% more targets, with the potential to provide more novel insights. Then, I extended and validated the investigation by using a robust method, qPCR, for quantification of a selected miRNA panel on an individual participant level. I found that, 4 (miR-31, miR-215, miR-3196 and miR-4516) of the 8 miRNAs quantified by qPCR, following assessment by NGS, were significantly overexpressed in obese individuals compared with non-obese Controls in the

human colorectal mucosa, as hypothesised (see Table 4-4), although miR-3196 showed a different direction of expression change by qPCR compared to NGS and was hence excluded from further analyses. Furthermore, 28.5kg weight loss following RYGB in initially obese adults, significantly reduced and normalised miR-31, miR-215 and miR-3196 expression at 6 months follow-up in the human colorectal mucosa to levels which were similar to those of the non-obese Controls, as hypothesised (see Table 4-4) but once more, miR-3196 showed a different direction of expression change by qPCR compared to NGS and was hence excluded from further analyses. The expression of the remaining miRNAs (miR-204, miR-671, miR-892, miR-1247 and miR-4516) examined also fell, although it did not reach significance.

miRNA	Chromosomal location	Association with obesity	Effects of weight loss following RYGB
miR-31	9p21.3	↑	↓
miR-215	1q41	↑	↓
miR-4516	16p13.3	↑	No significant change

Table 4-4: Summary of effects of obesity and of weight loss (following RYGB) on miRNA expression in the human colorectal mucosa.

4.8.3 The effect of weight loss on miR-31 and miR-215 in the colorectal mucosa

Given the link between adiposity and CRC risk, my finding of reduced miR-31 expression in human colorectal mucosal biopsies in the post-RYGB group following weight loss is consistent with the role of miR-31 as an oncogene and is indicative of a reduction in CRC risk following weight loss. My finding of reduced miR-215 expression in human colorectal mucosal biopsies in the post-RYGB group following weight loss is entirely consistent given the earlier observation of upregulated miR-215 in the initially obese group (found in the study here and in the study by Kurylowicz (2017) (see 4.8.1)). Hence, a reduction in miR-215 expression following weight loss, follows the expected expression pattern of miR-215. Although Kurylowicz (2017) observed increased miR-215 expression in obese adults, no results were reported for the effect of weight loss on this miRNA.

4.8.4 MiR-4516 is differentially expressed in obese individuals when compared with non-obese, but is not modulated following RYGB

Expression of miR-4516 in the colorectal mucosa was significantly higher (2.6-fold) in the obese than in the non-obese group as hypothesised, but, unexpectedly, miR-4516 expression was not altered by weight loss following RYGB. Potential explanation for this observation may be:

- It is possible that miR-4516 is not responsive to weight loss or, that the weight loss achieved by participants, although significant, was not sufficient to result in altered expression patterns of miR-4516, as they remained in the obese range even post-RYGB. Therefore, more research is needed to understand and describe the role of the differential expression pattern of the novel miRNA, miR-4516, observed with different levels of adiposity.

MiR-4516 is a novel miRNA which is expressed in several human tissues including the colorectal mucosa but whose functions remain to be clarified.

4.8.5 Tissues specific action as either a TSG or oncogene for miR-31 and miR-215

Since miRNA expression is tissue specific (Lim et al., 2005), the same miRNA can act as an oncogene in one cell type and as a TSG in another cell type because of its different targets and mechanism of action (Svoronos et al., 2016). This ambivalent tissue dependent action in tumourigenicity has been established for both miR-31 and miR-215 (Yu et al., 2018, Vychytilova-Faltejskova and Slaby, 2019) whereas to date less is known about the novel miRNAs including miR-3196 and miR-4516.

4.8.6 MiR-31 as an oncogene in CRC

Many functional studies have yielded findings, which confirmed the role of miR-31 as an oncogene in CRC. A study in intestinal mice stem cells revealed that miR-31 overexpression induced proliferation and repressed apoptosis via the TGFβ, BMP and Wnt pathways (Tian et al., 2017). MiR-31 targets *SMAD3, SMAD4* and *BMPR1A* which are involved in the TGF-β/BMP pathway and, *AXIN1, DKK1* and *GSK3β* which are involved in the WNT signalling pathway, leading to proliferation and repression of apoptosis (Clevers et al., 2014, Reynolds et al., 2014). Interestingly, it has been reported that *KRAS* upregulates miR-31 expression in CRC cells via the MARK pathway (as opposed to the PI3K/AKT pathway), allowing it to target TSGs, i.e.

RASA1, of the RAS/MAPK pathway leading to increased cell proliferation (Kent et al., 2016, Yu et al., 2018). Chen (2014b) showed that miR-31 repressed HIF-1α, a tumour suppressor, in CRC samples and cell lines. E2F2, a protein that correlates with regulation of metastasis and invasion in CRC, was shown to be regulated by miR-31 in human colon cancer cell lines which resulted in increased proliferation (Li et al., 2015). Furthermore, EZH2 knockdown led to miR-31 overexpression and *vice versa* miR-31 knockdown resulted in increased EZH2 levels in colon cancer cell lines, and this inverse relationship was also observed in a database of 301 CRC patients (Kurihara et al., 2016). Another study also found miR-31 overexpression in 30 CRC patients and further investigated in human HT29 CRC cells its target and function; it revealed that miR-31 knockdown supressed proliferation, migration, invasion and, induced cell cycle arrest and apoptosis, whereas its overexpression resulted in reduced *NUMB,* which plays a role in inhibiting cell proliferation, migration, invasion and induces apoptosis and cell cycle arrest in CRC (Peng et al., 2019). Interestingly, it was reported that miR-31 represses E-selectin expression and thereby modulates trans-endothelial migration of colon cancer cells, indicating an anti-metastatic role of miR-31 against CRC (Zhong et al., 2017).

Research from human studies has shown that miR-31 is upregulated in CRC tissue of patients when compared with normal mucosa and positively correlated with the TNM (tumour node metastasis) stage (Bandrés et al., 2006, Slaby et al., 2007, Motoyama et al., 2009, Wang et al., 2009, Earle et al., 2010) as well as in serum of CRC patients where a correlation with cancer progression was also observed (Wang et al., 2014b). A recent review by Yu (2018) found miR-31 levels to be elevated (in colonic tumours) and modulated by the RAS/MAPK/ERK1/2 pathway and reported its role as an oncogene in CRC. MiR-31 was overexpressed in CRC cells derived from metastatic foci and in human primary CRC tissues with lymph node metastases and further investigation showed that miR-31 lead to increased proliferation, invasion and metastasis via repression of the tumour suppressor *SATB2* (Yang et al., 2014). Furthermore, miR-31 represses *RASA1* translation which initiates the RAS signalling pathway and thereby promotes tumour cell proliferation in human CRC (Sun et al., 2013). MiR-31 was overexpressed in 40 submucosal invasive CRC patient samples when compared with the non-tumour samples and 29% of the tumour samples comprised a *KRAS* mutation (Tateishi et al., 2015). Interestingly, in the same study, miR-31 expression showed no correlation with *KRAS* mutation, tumour cell budding, lymph node metastasis, lymphatic/venous infiltration, tumour differentiation, tumour location, depth of invasion or patients' sex (Tateishi et al., 2015). A microarray analysis revealed that miR-31 was the most upregulated miRNA out of 760 miRNAs

in 29 human CRC with mutated *BRAF* compared to wild-type *BRAF* and further analyses showed that its increased expression was associated with mutations in *BRAF* and *KRAS* and proximal location (Nosho et al., 2014) which was later also observed by Lundberg (2018). They also found that miR-31 inhibitor resulted in reduced cell invasion and proliferation (Nosho et al., 2014). Similarly, Ito (2014) also observed an association between miR-31 expression and *BRAF* mutations in CRC patients, especially in serrated lesions.

Ample studies have identified upregulated levels of miR-31 in human CRC cell lines, as well as in samples of CRC patients and, its role in CRC initiation, development and progression.

4.8.7   MiR-215 as a tumour suppressor gene in CRC

MiRNA-215 is highly conserved across 28 different species suggesting that it has vital functions which have been preserved during evolution (Khella et al., 2013). A recent review by Vychytilova-Faltejskova (2019) reported miR-215 dysregulation in many pathological conditions and summarised the extensively studied role of miR-215 in human cancer, including CRC.

Functional studies have yielded data which indicate the role of miR-215 as TSG in CRC. Chen (2016) reported that miR-215 directly targets the transcription factor YY1 in CRC, which modulates the metabolism of tumour cells via G6PD activation (a rate-limiting enzyme in the pentose phosphate pathway), which in turn leads to enhanced DNA synthesis and nucleotide production and reduced intracellular ROS. An association between expression levels of miR-215 and SRPX2 (a down-stream gene of the PI3K/ AKT signalling pathway) was seen in CRC and miR-215 upregulation resulted in reduced glucose uptake, lactate production and proliferation (Zhao et al., 2018). MiRNA profiling of patient derived cancer stem cells identified miR-215 as the primary hypoxia-induced miRNA in different primary colon tumour cultures, and showed its action as a tumour suppressor via a negative feedback regulation of hypoxia induced cancer stem cell activity (Ullmann et al., 2019). Reduced miR-215 expression has also been reported in APC and colitis-associated colonic tumours of chronically inflamed or genetic APC(Min/+) mouse models (Necela et al., 2011). In a mouse model that was xenotransplanted with human colon cancer cells, miR-215 was downregulated in tumour organoids of the intestine, when compared with organoids of normal epithelium and miR-215 induction suppressed LGR5 and EREG, both of which are stem cell markers commonly overexpressed in cancers leading to the activation of cell proliferation signalling pathways (Kobayashi et al.,

2012). An upregulation of miR-215 was seen during differentiation in a colon cancer stem cell line model using a microarray which was then validated by qPCR (Yu et al., 2011). Similarly, Song (2010) also observed miR-215 overexpression in CD133+HI/CD44+HI colon cancer stem cell line, which was coupled with a reduced rate of cell proliferation and triggered cell cycle arrest at the G2 phase. These studies suggests a potential role of miR-215 in metabolic reprogramming of CRC cells (Vychytilova-Faltejskova and Slaby, 2019). Recent studies found that lncRNA UICLM (upregulated in CRC liver metastasis) and FTX (five prime to Xist) act as competing endogenous RNAs (ceRNAs) for miR-215, which results in i) upregulated ZEB2 levels in CRC cells and ii) inhibition of vimentin phosphorylation, and hence leads to the initiation and progression of CRC respectively (Chen et al., 2017, Yang et al., 2018). Additionally, sequencing of isolated colonic epithelial cells and colonic enteroids demonstrated high abundance of miR-215 levels, which could not be identified in endothelial cells and fibroblasts, indicating the potential role of miR-215 as an epithelial marker (Rosenberg et al., 2018).

In 2008 a microarray, for the first time, revealed the association of aberrant miR-215 expression and CRC and its role in cellular adhesion and induced cell detachment; miR-215 was less expressed in stage II colon cancers of 49 patients when compared with normal mucosa (Braun et al., 2008). Since then, more human studies frequently observed miR-215 downregulation in colon tumour samples when compared with normal tissue (Earle et al., 2010). MiR-215 downregulation was seen in 34 samples of CRC tumour tissue when compared with 34 samples of the adjacent non-tumour mucosa, and it was hypothesised that this downregulation results in increased proliferation (Karaayvaz et al., 2011). Furthermore, miR-215 downregulation has been observed in early stage tumours of inflammatory as well as genetic origin, indicating its participation in the early stages of CRC development (Necela et al., 2011). A later study observed a similar miR-215 expression pattern in CRC and found that that it correlated with clinical stage, grade and positivity of lymph nodes (Faltejskova et al., 2012) which was confirmed later in a Czech and Spanish cohort of CRC patients using data from 448 tumour tissues when compared with samples from 325 adjacent healthy tissue (Vychytilova-Faltejskova et al., 2017).

Taking the above data together, there seems to be strong evidence that this miR-215 is a tumour suppressor in CRC.

4.8.8   Studies on the novel miRNA, miR-4516

Chowdhari (Chowdhari and Saini, 2014) demonstrated in a HaCaT cell line that miR-4516 targets *STAT3* transcripts which subsequently leads to reduced STAT3, pSTAT3 and BclxL expression and hence reduced apoptosis. Later, it was discovered that inhibiting miR-4516, with LSINCT5 which is a competing endogenous RNA for miR-4516, resulted in upregulated BclxL and STAT3 expression which initiated apoptosis in hepatocellular carcinoma (Li et al., 2018). Recently, miR-4516 expression was correlated with poor prognosis in samples from 268 glioblastoma patients and lead to proliferation and invasion of glioblastoma cells via the PTPN14/ Hippo pathway (Cui et al., 2019). These limited studies suggest a potential role as an oncogene for miR-4516. Vlachos (2015) predict that miR-4516 targets 23 genes (*PANK4, TCF4, CCND2, PPP3R1, UBE2J1, IGLL5, ASH1L, OXA1L, HECTD2, RAB11FIP2, RIF1, PTPN6, MED7, PCBP1, HIC1, IDH1, SHOC2, C12orf55, RACGAP1, UBE2G1, CTTNBP2NL, ATF7, NCOA1*) and 5 pathways (Pantothenate and CoA biosynthesis, 2-Oxocarboxylic acid metabolism, Protein processing in endoplasmic reticulum, Lysine degradation and TCA cycle). To date, few studies have investigated the role of the novel miRNA, miR-4516, and its role in cancer, including CRC, and the investigation of miR-4516 (predicted) targets (genes and pathways) associated with CRC is an interesting area for future research.

4.9   Conclusion

Here, for the first time, a NGS approach was used to screen for genome-wide changes in miRNA expression in the colorectal mucosa of i) obese individuals compared with non-obese Controls and ii) following the effects of massive weight loss in initially obese individuals after RYGB. This revealed that a total of a 1654 miRNAs were expressed in the human colorectal mucosa. A total of 112 miRNAs were differentially expressed in obese individuals compared with the non-obese Controls. Additionally, a total of 60 miRNAs changed expression in initially obese individuals after RYGB. Of the 1654, a panel of 8 miRNAs was selected for further validation and to quantify the expression of these miRNAs using qPCR in the colorectal mucosa of i) obese individuals compared with non-obese Controls and ii) initially obese individuals before and after RYGB. Four of the miRNAs i.e. miR-31, miR-215, miR-3196 and miR-4516, were differentially expressed in obese *versus* non-obese Controls and 3 miRNAs i.e. miR-31, miR-215 and miR-3196, changed expression in the initially obese individuals after RYGB. However, miR-3196 showed a different direction of expression change by qPCR compared to

NGS for both comparison groups, showing that this miRNA did not validate and was hence excluded from further analyses. The obesity-associated changes in expression of miR-31 i.e. increased expression with greater adiposity, may contribute to the increased CRC risk in the obese and to the reduction in CRC risk following weight loss. In contrast, the observed changes in miR-215 expression did not fit with the expected role of this miRNA as a TSG. However, the differences in expression within my study were consistent (higher expression in those with greater adiposity) and matched the differences observed by Kurylowicz (2017) in obese and non-obese individuals. Therefore, my findings on changes in miR-215 expression appear to be robust and, functional consequences of these changes remain to be elucidated. For the more recently discovered miRNA that was differentially expressed in this study i.e. miR-4516 much less is known about its role in obesity and whether changes in its expression in the colorectal mucosa has implications for CRC risk. In summary, my findings provide further evidence that miRNA expression in the colorectal mucosa is altered in obesity and by deliberate weight loss (Mathers et al., 2010, Malcomson and Mathers, 2017). However, to grasp the impact of the observed differential changes in expression of these miRNAs, downstream analyses including gene expression and proteomic studies need to be conducted.

5 Effect of adiposity and of ageing on microRNA expression in the colorectal mucosa (The BORICC Study and the BFU Study)

5.1 General introduction

A detailed description about miRNAs can be found in the Introduction chapter (see section 1.3).

In brief, miRNAs were discovered for the first time in 1993 in *C. elegans* (Lee et al., 1993). They are endogenous, small, non-coding RNA molecules that bind covalently to the complementary 3' untranslated region of one or more mRNA species to regulate translation of mRNAs to proteins (Lai, 2002). MiRNAs regulate expression of a wide range of key molecules including transcription factors, RNA binding proteins and signalling proteins (Ding et al., 2018). Bioinformatics analyses predict that miRNAs regulate more that 60% of protein encoding genes (Friedman et al., 2009).

During miRNA biogenesis, when the short double stranded RNA duplex (pre-miRNA) is loaded onto the AGO protein, one strand/ arm (either miRNA-3p or -5p) becomes degraded and the other becomes the mature miRNA (see Figure 5-1) (Chen et al., 2018). Selection of the -3p or -5p arm does not occur randomly, but is based on the duplex end stability governed by Dicer cleavage with a specific strand selection capability based on thermodynamics, structure and 5' nucleotide identity. The arm whose 5' end comprises less structure and lower internal stability, which has a thermodynamic measure of Δ0.5 kcal/mol (an amount of energy/ number of molecules), is selected to become the mature miRNA (Khvorova et al., 2003, Noland and Doudna, 2013). Furthermore, AGO proteins have preference for different nucleotides; for example, AGO1 selects predominantly the strand with the U at the 5' end, whereas AGO2 selects the strand with the pA or pU 5' end (Chen et al., 2018). Dependent on the developmental stage, tissue type and species, different arms are selected to become the mature miRNA, which is known as 'arm switching' (Chen et al., 2018). For the majority of miRNAs, including miR-31 and miR-215, it seems that both the -3p and -5p arms exhibit similar functional effects downstream (Chen et al., 2018). Furthermore, it has been shown that miRNAs -3p and -5p are commonly co-expressed and regulated. For example, miR-31 is co-upregulated in 4 colon cancer cell lines (relative to two normal colon tissues) and no significant differences have been shown in arm switching patterns in CRC (Choo et al., 2014, Chen et al., 2018).
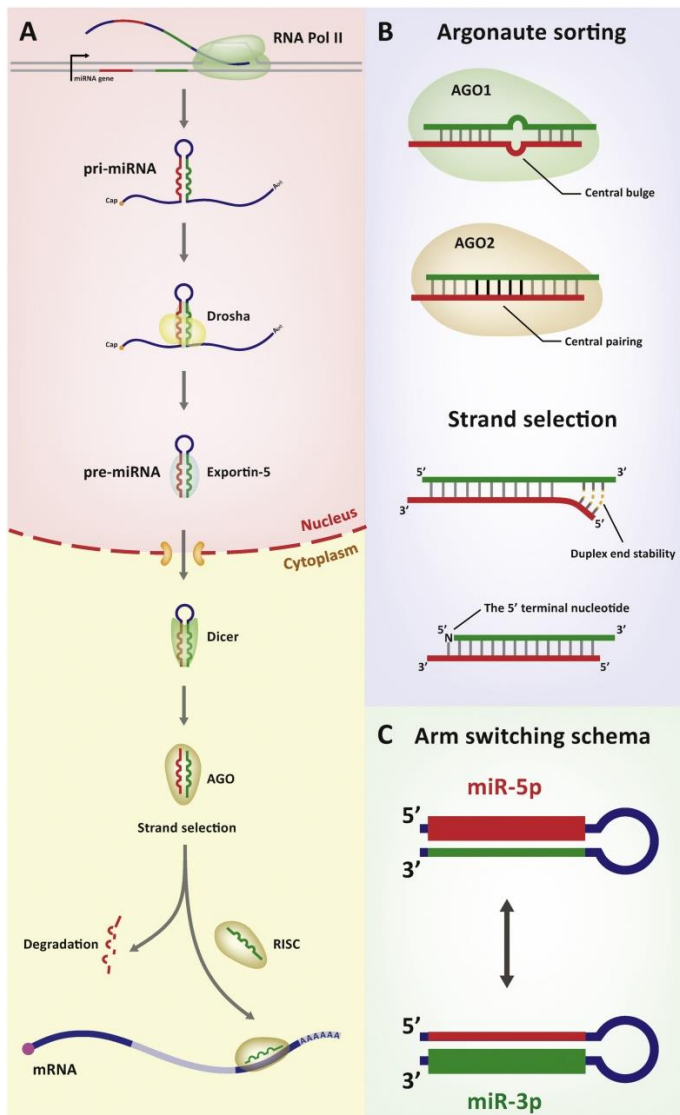
Figure 5-1: Overview of miRNA biogenesis (Chen et al., 2018) (Copyright: figure is open-access).

MiRNAs play a vital role in numerous biological pathways and processes and dysregulated patterns of miRNA expression have been observed in multiple pathologies, including CRC (Heneghan et al., 2010, Van Roosbroeck and Calin, 2017). Several studies, summarised in a recent review (Ding et al., 2018), have revealed the roles of miRNAs as tumour suppressor genes (TSG) and oncogenes. Aberrant patterns of miRNA expression can activate pathways associated with CRC, for example the WNT signalling pathway (Ding et al., 2018). Obesity is a major risk factor for CRC and aberrant patterns of miRNA expression have been observed in those with obesity which may be due to chronic inflammation present in obese adipose tissue (Esau et al., 2004, Lin et al., 2009, Xie et al., 2009, Heneghan et al., 2010) as described in detail in the Introduction Chapter (see section 1.4.6) and the Chapter 4 (see section 4.1.).

Obesity and ageing are major risk factors for CRC risk. If dysregulation of miRNA expression in obesity and ageing are causal for CRC risk, then one would anticipate that younger and normal weight individuals would have "normal" miRNA expression in this tissue. However, to date, there have been no published investigations of the effects of adiposity and ageing on the expression of miRNAs in the colorectal mucosa of humans.

5.2 Hypotheses

The hypotheses for this study were:

- The pattern of miRNA expression in the colorectal mucosa is altered during ageing.
- MiRNA expression in the colorectal mucosa differs in obese and overweight individuals compared with normal weight adults.
- The pattern of miRNA expression in the colorectal mucosa is i) altered by effects of weight change (gain or loss) and ii) not affected in individuals whose weight was 'stable' over a 12+ year time period.

5.3 Aims

The aims of this study were:

- To test the above hypotheses by quantifying i) the effects of ageing on patterns of miRNA expression in the colorectal mucosa of adults participating in the BORICC Study (baseline) and, again, 12+ years later in the BFU Study, ii) associations between adiposity and patterns of miRNA expression cross-sectionally within the BORICC and BFU Studies and iii) changes in miRNA expression associated with changes in adiposity over 12+ years for individuals in the BORICC Study who also participated in the BFU Study.

5.4 Objectives

The objectives of this study were:

- To use biological samples (mucosal biopsies) and data from the BORICC (baseline) (Mathers, 2009) and BFU (12+ years follow-up) (Malcomson and Mathers, 2017)

Studies to investigate effects of adiposity and ageing on patterns of miRNA expression in the human colorectal mucosa cross-sectionally in both studies and, also, longitudinally.

- To select the miRNAs that were significantly differently expressed and validated (i.e. showing the same direction in expression change by NGS and qPCR) between obese and non-obese participants from the BOCABS Study (see section 4.7).

- Using qPCR, to quantify expression of this panel of miRNAs in the colorectal mucosa of adults recruited to the BORICC Study (at baseline) and at 12+ years follow-up (in the BFU Study).

- To investigate differences in the expression of these miRNAs in i) older and younger adults by dichotomising the data at the median age and ii) in obese, overweight and normal weight adults cross-sectionally in the BORICC and BFU Studies.

- To investigate the effects of weight change on changes in patterns of miRNA expression in the human colorectal mucosa longitudinally using regression analyses.

5.5   Overview of methods

A detailed description of the experimental procedures and methods for quantifying miRNA expression can be found in the Methods Chapter (see section 2.2.3.9).

In brief, RNA was extracted from colorectal mucosal biopsies frozen in RNAlater (see section 2.2.3.1). After RNA was extracted, a RNA quality control check was performed on 11 random samples from the BORICC Study (n=8) and BFU Study (n=3) to check for the integrity and quality of the RNA, as the BORICC samples had been stored at -80 °C for up to 14 years (see section 2.2.3.2). RNA was reverse transcribed into cDNA (see section 2.2.3.8), then qPCR was carried out on a panel of miRNAs (see section 2.2.3.9) and data were processed to quantify the expression of miRNAs relative to *SNORD68* and *RNU6* reference genes (see section 2.2.3.10). Participants with paired colorectal mucosal biopsies (n=33) from the BORICC Study and the BFU Study were included in the present analysis.

The miRNA panel used in the present study consisted of the 4 miRNAs that were significantly differentially expressed in obese compared with non-obese participants of the BOCABS Study (see section 4.7).

Statistical analyses were performed using IBM® SPSS® Statistics Version 21. The Shapiro-Wilk test showed that data were not normally distributed. Consequently, the Wilcoxon signed rank test was used to examine miRNA expression in the BORICC (baseline) and BFU (12+ years follow-up) Studies. Then participants' data from the BORICC and BFU Studies were dichotomised at median age (56 years) and a Mann-Whitney-U test was used to examine differences in miRNA expression between the younger and older adults cross-sectionally in both studies. A one-way ANOVA test was conducted to investigate whether miRNA expression differed between i) normal weight, overweight and obese and ii) non-obese and obese, in participants at baseline and 12+ years follow-up, i.e. in the BORICC and BFU Studies, respectively. Finally, linear regression analyses were used to examine the effects of weight change on changes in patterns of miRNA expression.

5.6 Effects of adiposity and ageing on selected panel of miRNAs in colorectal mucosal biopsies

5.6.1 Participant characteristics and anthropometry

Table 5-1 summarises the characteristics and anthropometric measurements of those participants from the BORICC Study and the BFU Study who were included in this analysis of miRNA expression in colorectal mucosal biopsies. For this analysis, I used samples and data from 33 individuals for whom paired baseline (BORICC Study) and 12+ year follow-up (BFU Study) samples were available. All BORICC Study participants were Caucasian, had a mean age of 55 years (range 37 to 69 years) and comprised almost equal numbers of females (n=17; 52%) and males (n=16; 48%). They had a mean BMI of 28 kg/m^2 and waist to hip ratio of 0.9. Approximately half of the participants had never smoked and only 4 (12%) were current smokers. When the same participants were reassessed 12+ years later, there were no significant changes in measures of adiposity and a further 3 participants (9%) had stopped smoking.

	BORICC Study (n=33)	BFU Study (n=33)	p-value
Age (years)	55.5 (8.6)	67.5 (8.6)	-

Gender N (%)			
Male	16 (48)	-	-
Female	17 (52)	-	-
Smoking N (%)			
Never-smoker	17 (51.5)	16 (48.5)	0.038 ‡
Smoker	4 (12.1)	1 (3.0)	
Ex-smoker	11 (33.3)	16 (48.5)	
Missing data	1 (3.0)	0	
Weight (kg)	82.3 (18)	82.6 (18.1)	0.78†
BMI (kg/m^2)	28.0 (4.4)	28.4 (4.7)	0.40†
Body fat (%)	-	35.4 (7.2)	-
Waist (W; cm)	94.6 (14.2)*	97.4 (14.5)	0.08†
Hip (H; cm)	104.5 (10.3)*	105.6 (9.3)	0.46†
W:H ratio	0.90 (0.08)*	0.92 (0.08)	0.21†

Table 5-1: Characteristics of selected participants at baseline (BORICC Study) and 12+ year later at follow-up (BFU Study).
Data presented as mean (SD) unless otherwise stated
*for these measurements n=32
†Paired t-test
‡ Wilcoxon sign test

5.6.2   Total RNA quality and quantity

RNA was isolated from colorectal mucosal biopsies that had been stored in RNAlater and frozen at -80°C, using the Qiagen miRNeasy Mini Kit as described in the Methods Chapter section 2.2.3.1. A RNA quality control check using the Agilent RNA 6000 Pico Kit was run on 11 random samples (see section 2.2.3.1) and the purity and concentration of all RNA samples were measured using spectrophotometry (see section 2.2.3.1). The mean extracted RNA concentration was 76.5ng/µL and 50.5ng/µL for the BORICC and BFU samples, respectively (see Figure 5-2). However, this concentration ranged from 3.4ng/µL to 127.1ng/µL because of the large inter-participant variability in biopsy size and quality. The purity of the RNA was evaluated by assessing absorbance at the 260/280 ratio with a mean value of 2.08 and 2.1 for the BORICC and BFU samples, respectively, indicating good purity of the extracted RNA (see Figure 5-2).
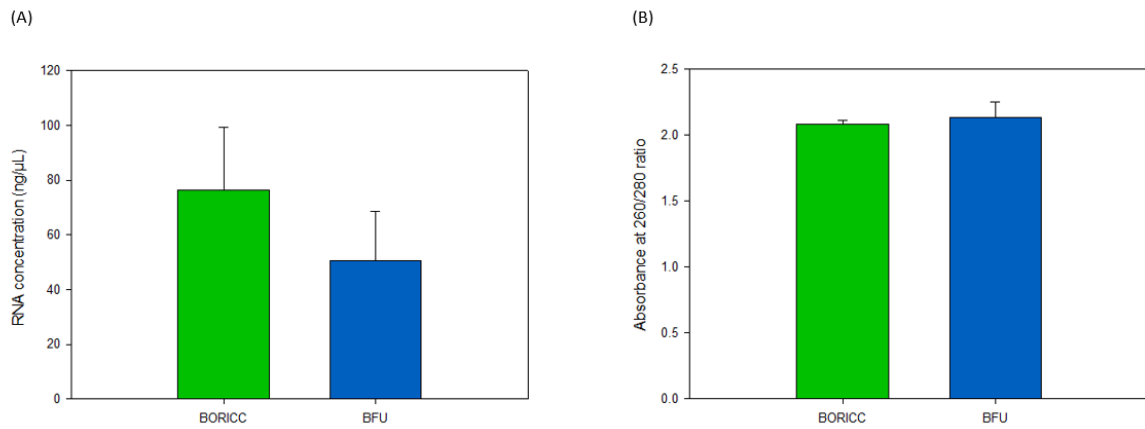
Figure 5-2: (A) RNA concentrations and (B) absorbance at 260/280 ratios for participants (n=33) at baseline (BORICC Study) and at follow-up 12+years later (BFU Study).

5.6.3 Effects of ageing on selected panel of miRNAs in the colorectal mucosa

Figure 5-3 shows expression of the selected panel of miRNAs quantified in the colorectal mucosa at baseline (BORICC Study) and at follow-up 12+ years later (BFU Study). MiR-215-3 expression was nearly 4-fold greater (p<0.001) at follow-up than at baseline. However, for the other 2 miRNAs i.e. miR-31-3 and miR-4516, there was no statistically significant difference in expression between baseline and at 12+ years follow-up. MiR-4516 was the most abundantly expressed miRNA at both baseline and 12+ years later at follow-up.
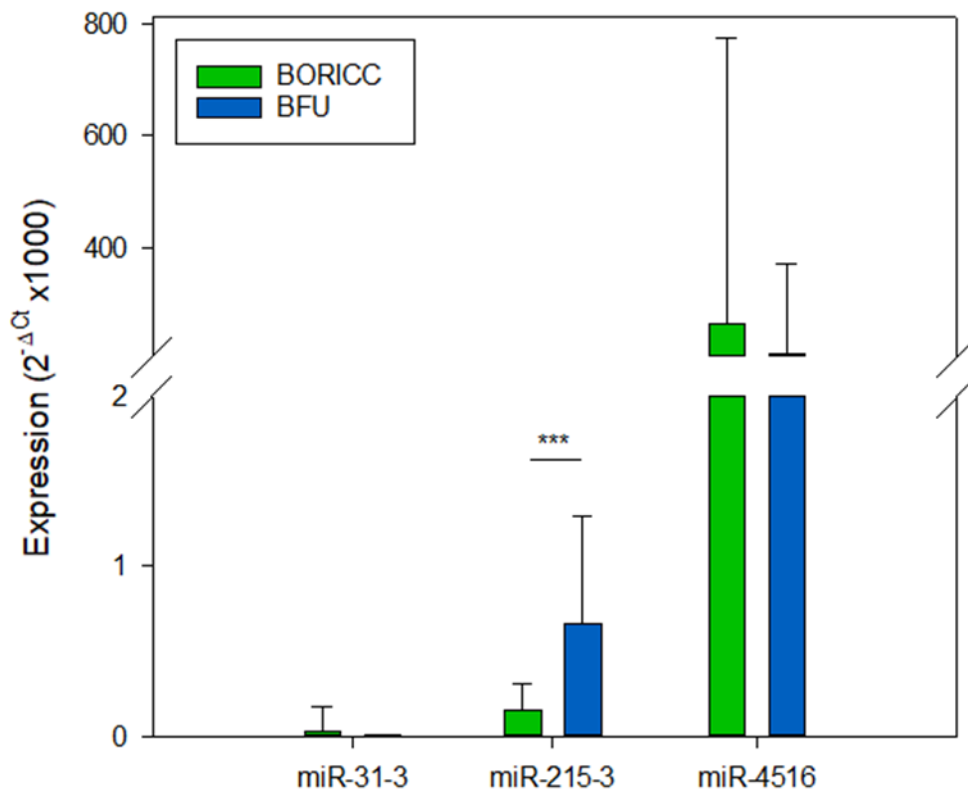
Figure 5-3: MiRNA expression determined by qPCR in the colorectal mucosa in BORICC and BFU participants; for miR-31-3 n=29.

Figure 5-4 illustrates the inter-individual change in miR-215-3 expression and shows that, for the majority of participants, miR-215-3 expression increased (in some cases very substantially) at 12+ years follow-up. One participant (depicted with a red line and triangles) shows an enormous increase in miR-215 expression at 12+ years follow-up. The relevant data were checked and no errors were identified. In addition, I explored characteristics of this individual and did not identify and factors such as medical history or adiposity (BMI 22.5 kg/m^2 and 23.9 kg/m^2 for BORICC and BFU, respectively), which might have explained this dramatic rise in miR-215 expression. Nevertheless, it may be significant that this was one of the older participants (73 years old at follow-up in the BFU Study) who had had an adenomatous polyp when initially recruited to BORICC Study and hence was at increased CRC risk.
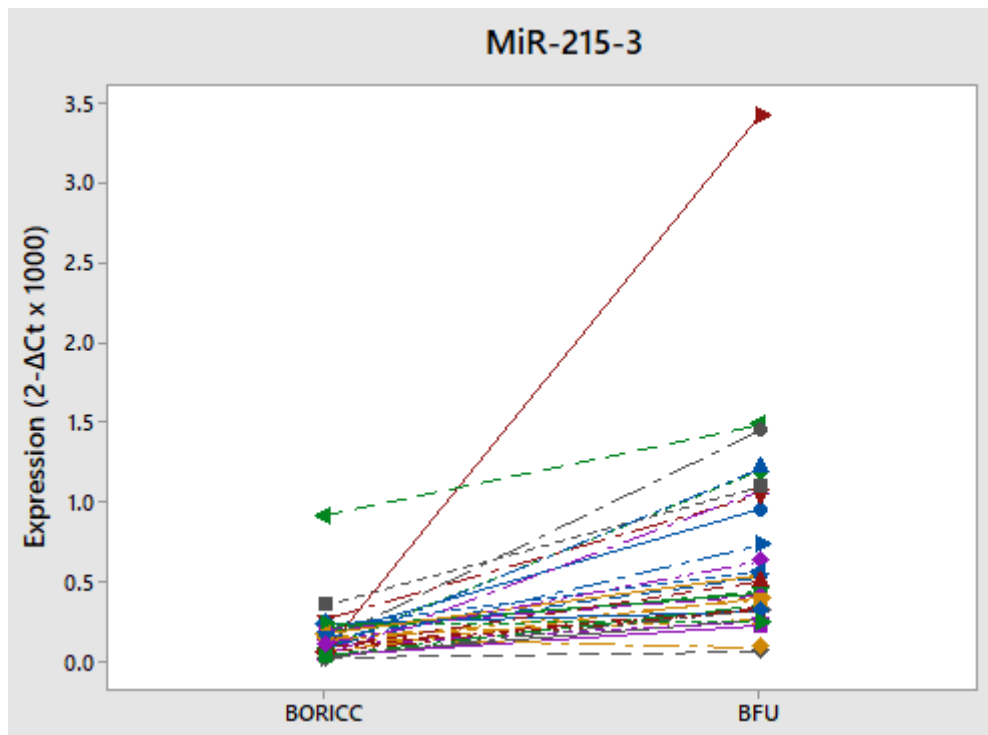
Figure 5-4: Inter-individual change in miR-215-3 expression in the colorectal mucosa of participants at baseline (BORICC Study) and at follow-up 12+ years later (BFU Study).

To examine the effect of age cross-sectionally, the participants were dichotomised at the median age (56 years in the BORICC Study). Figure 5-5 shows the miRNA expression for the younger and older groups at both baseline (BORICC Study) and 12+ years later at follow-up (BFU Study). There was an apparent trend for higher expression of all miRNAs in the older group at both time-points. The age-related difference was significant for miR-31-3 in the BORICC Study and for miR-215-3 in the BFU Study. At baseline (BORICC Study) miR-31-3 was 15-fold more highly expressed in the older group but these values returned to levels similar to those in the younger participants at 12+ years follow-up. In the BFU Study, miR-215-3 was two-fold up-regulated in the older group.
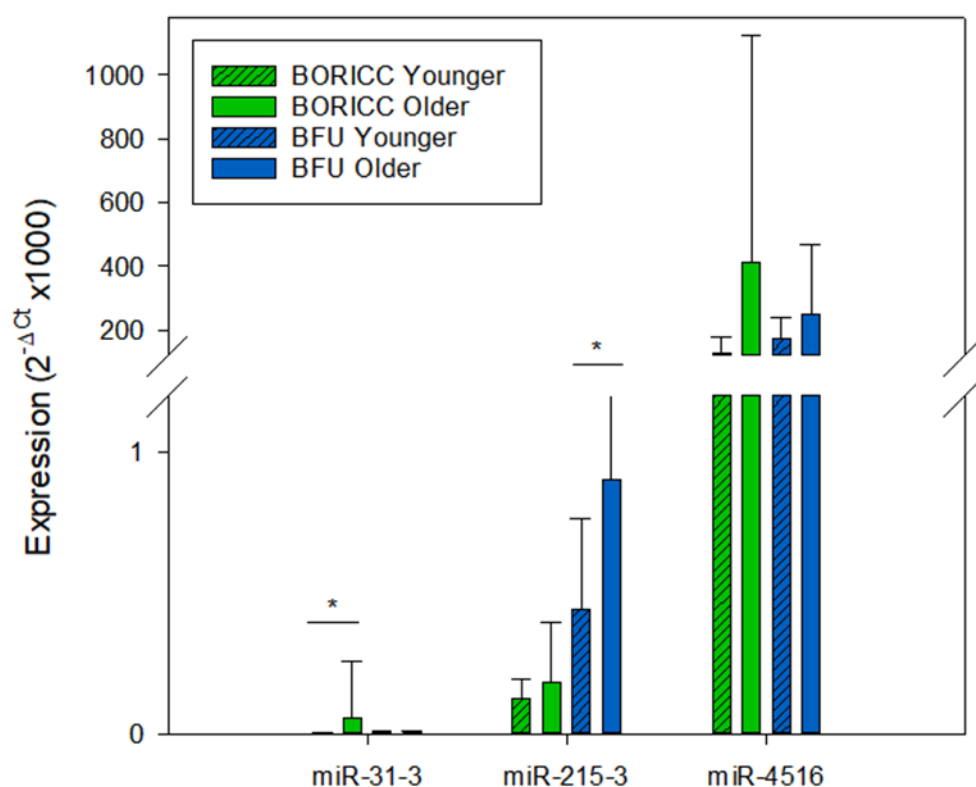
Figure 5-5: MiRNA expression determined by qPCR in the colorectal mucosa of younger and older (data dichotomised at median age 56 years) BORICC and BFU participants; for miR-31-3 n=29.

5.6.4 Effects of adiposity on expression of selected miRNAs in the colorectal mucosa

Although there was no overall difference in mean body weight between baseline (BORICC Study) and follow-up 12+ years later (BFU Study) (p=0.78), Figure 5-6 shows that there were considerable inter-individual differences in body weight change with some individuals gaining weight (up to 25kg) and others losing weight (up to 20kg) over the period of observation.
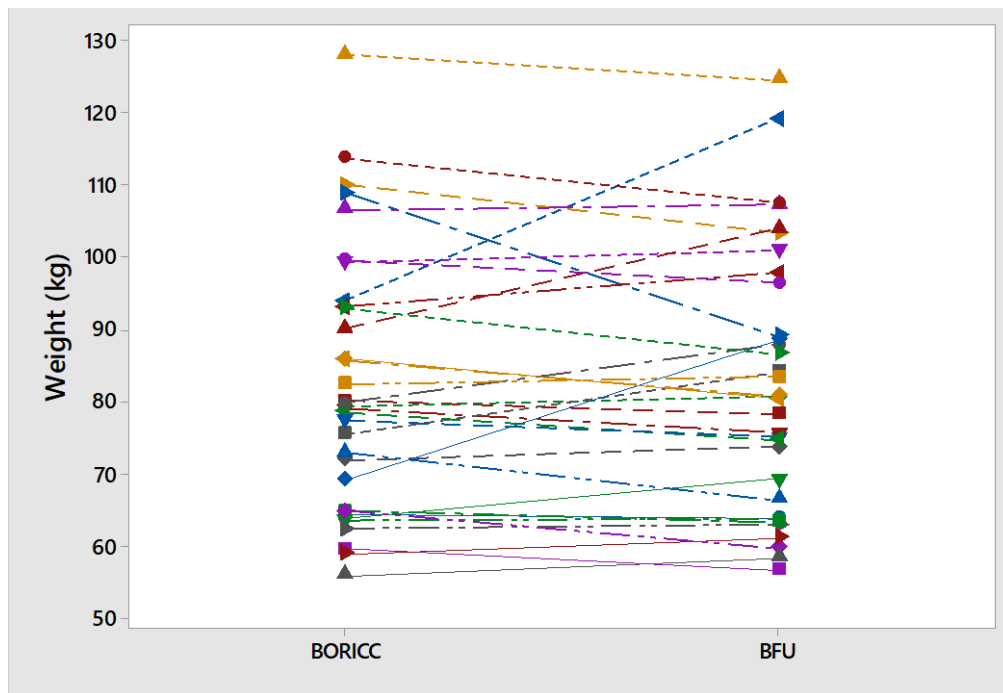
Figure 5-6: Intra-individual change in body weight (kg) over 12+ years for participants in the BORICC and BFU Studies.

To examine cross-sectional relationships between adiposity and miRNA expression, the available data were examined in two ways: i) comparing miRNA expression for the 3 major adiposity categories (normal weight, overweight and obese – using WHO criteria) and ii) comparing miRNA expression in those who were obese and those who were not obese (as was done in the BOCABS Study – see Chapter 4). Table 5-2 shows the expression of the 3 miRNAs for normal weight, overweight and obese participants at baseline and 12+ years follow-up. Surprisingly, there was no significant association between markers of adiposity and expression of any of these miRNAs.

	Normal BMI (n=9)	Overweight BMI (n=14)	Obese BMI (n=10)	p-value†
BORICC Study				
miR-31-3*	0.007 (0.004)	0.005 (0.003)	0.086 (0.250)	0.366
miR-215-3	0.098 (0.075)	0.201 (0.223)	0.137 (0.066)	0.295
miR-4516	166.5 (108.7)	431.3 (758.5)	119.0 (77.7)	0.274
BFU Study				
miR-31-3*	0.008 (0.005)	0.007 (0.005)	0.007 (0.005)	0.896
miR-215-3	0.751 (1.021)	0.675 (0.440)	0.569 (0.416)	0.824
miR-4516	179.3 (69.8)	259.5 (233.9)	163.3 (45.5)	0.299

Table 5-3 shows the expression of the 3 miRNAs in non-obese (BMI <30) and in obese (BMI ≥30) participants at baseline (BORICC Study) and after 12+ years follow-up (BFU Study). There were no significant associations between markers of adiposity and expression of these miRNAs at either time-point.

	Non-obese (n=23)	Obese (n=10)	p-value†
BORICC Study			
miR-31-3*	0.006 (0.003)	0.086 (0.250)	0.152
miR-215-3	0.161 (0.185)	0.137 (0.066)	0.699
miR-4516	327.7 (601.4)	119.0 (77.7)	0.287
BFU Study			
miR-31-3*	0.007 (0.005)	0.007 (0.005)	0.798
miR-215-3	0.705 (0.703)	0.569 (0.416)	0.574
miR-4516	228.1 (188.9)	163.3 (45.5)	0.296

Table 5-3: MiRNA expression in non-obese and obese participants in the BORICC Study (at baseline) and in the BFU Study (12+ years follow-up).
Data presented as mean (SD) unless otherwise stated
*for these measurements n=29
†ANOVA test

5.6.5 Associations between body weight change over 12+ years and miRNA expression in the colorectal mucosa

The relationship between changes in body weight (follow-up weight minus baseline weight), i.e. weight gain or loss, and changes in miRNA expression (follow-up miRNA expression minus baseline miRNA expression) in the colorectal mucosa from baseline (BORICC Study) to follow-up 12+ years later (BFU Study) was examined using linear regression. There were no statistically significant correlations between changes in body weight and expression of any of the 3 miRNAs examined (p>0.05) (see Table 5-4). The R values show a low degree of correlation for all 4 miRNAs (R<0.135) and the R^2 indicates that less than 1.8% of the total variation in miRNA expression can be explained by changes in body weight (see Table 5-4).

	Mean change in miRNA expression between BORICC and BFU participants	R value	R² value	p-value
miR-31*	-0.02 (0.1)	0.135	0.018	0.485
miR-215	0.51 (0.6)	0.016	0.000	0.931
miR-4516	-55.9 (378.2)	0.034	0.001	0.853

Table 5-4: Relationship between changes in body weight and miRNA expression (mean (SD)) in the colorectal mucosa at 12+ year follow-up for all participants.
*n=29 participants

Then a second analysis was performed using the Mann-Whitney-U test, as data were not normally distributed, to investigate if the changes in miRNA expression differed between the participants who gained (range 0.1- 25kg) or lost (range 0.4- 20kg) body mass after 12+ years. No significant differences could be detected (p>0.05) (see Table 5-5). Even though data were not normally distributed, the analysis was repeated using the one-way ANCOVA which is a robust statistical test, to directly compare changes in miRNA expression over the period of study in each of the groups (gained *versus* lost weight) where gender, baseline BMI and age were included as covariates. Once more, no significant differences could be detected (p>0.05) (see Table 5-5).

miRNA	Lost weight (n=17)	Gained weight (n=16)	P-value†	P-value‡
miR-31*	0.0008 (-0.8 - 0.01)	0.002 (-0.003 - 0.01)	0.535	0.630
miR-215	0.3 (-0.06 – 1.1)	0.3 (0.05 – 3.4)	0.746	0.318
miR-4516	47.5 (-1071.2 – 127.7)	42.6 (-1829.6 – 117.8)	0.943	0.569

Table 5-5: Mean change in expression of selected miRNA in the colorectal mucosa of those who gained, compared with those who lost, body weight over 12+ years between participation in the BORICC (baseline) and BFU (follow-up) studies.
Data are presented as Median (range).
*for these measurements n=17 for lost and n=12 for gained weight respectively
†Mann-Whitney-U test
‡Adjusted ANCOVA test

These results show that changes in miRNA expression are not associated and cannot be predicted based on changes in body weight over a 12+ year period. Furthermore, changes in miRNA expression do not differ in participants who lost or gained weight over the study period, even when adjusted for potential confounding factors including gender, baseline BMI and age.

5.6.6 Predicted biological roles of selected miRNAs

An *in-silico* target prediction analysis tool by Vlachos (Vlachos, 2015) was utilised to detect potential Kyoto Encyclopedia of Genes and Genomes (KEGG) pathways enriched for predicted mRNA gene targets of the 4 selected miRNAs analysed and for two of those 4 selected miRNAs a pathway union could be identified (see Figure 5-7). The microT-CDS algorithm was used to undertake the enrichment analysis where a separate p-value for each of the 2 miRNAs was calculated and a merged p-value for 2 of the miRNAs i.e. miR-31 and miR-4516 was estimated using a Fisher's meta-analysis. The brighter yellow colour illustrates a higher probability that the shown pathway (see Figure 5-7) is enriched with gene targets for at least one of the 2 miRNAs. Many KEGG pathways implicated in metabolism were enriched for predicted mRNA gene targets for 2 of my selected miRNAs, including pathways in glycosaminoglycan biosynthesis, protein processing in endoplasmic reticulum, pantothenate and CoA biosynthesis and 2-oxocarboxylic acid metabolism which play important roles in the morphogenesis and maintenance of cell and tissue structure and function.
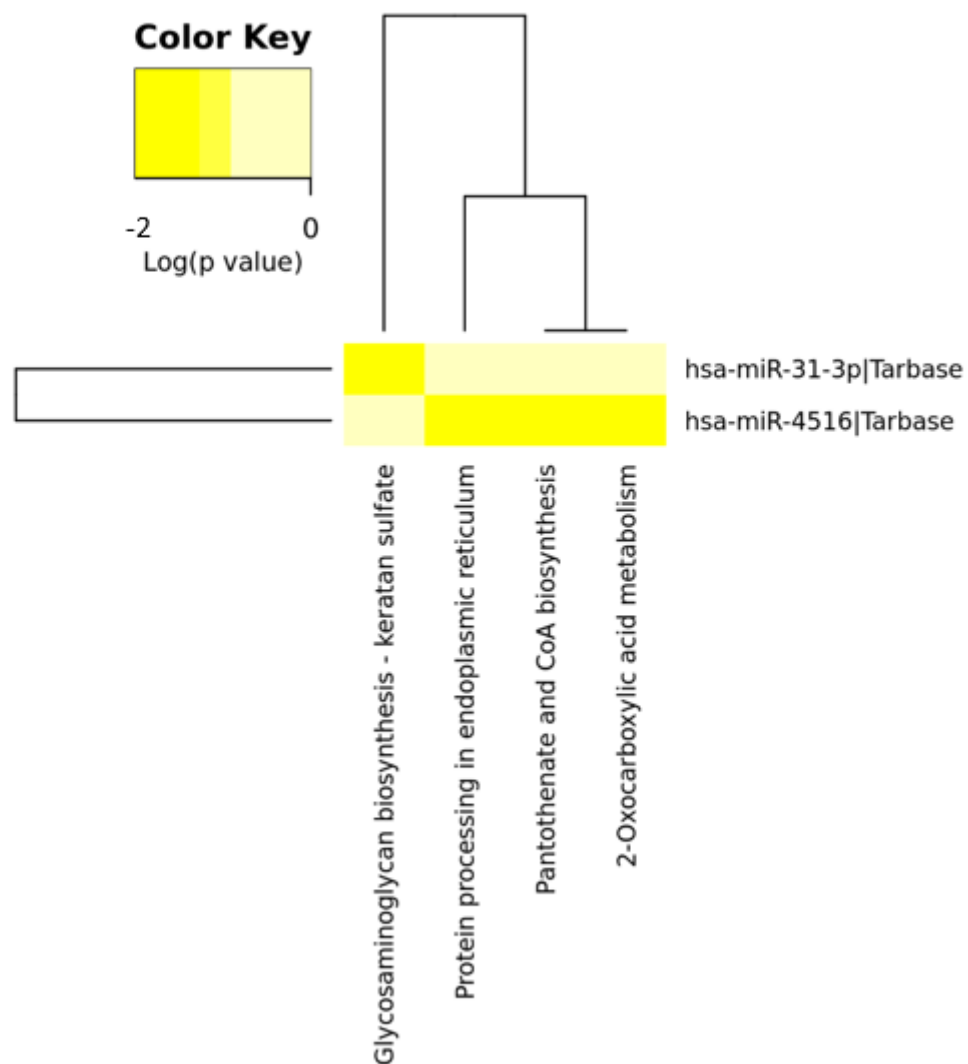
Figure 5-7: Heatmap illustrating KEGG pathway unions for predicted mRNA gene targets of miRNAs quantified (log(p-value), orange colour illustrates higher probability) (Vlachos, 2015).

5.7   Discussion

To my knowledge, this is the first study to investigate differences in miRNA expression in the human colorectal mucosa longitudinally over 12+ years follow-up.

5.7.1   Main findings

MiR-215 was significantly overexpressed in the human colorectal mucosa at 12+ years follow-up (BFU Study) when compared with expression at baseline (BORICC Study). In cross-sectional analyses of associations with age, there was an apparent trend for higher expression of all miRNAs in the older group at both time-points, which was significant for miR-31-3 in the BORICC Study and for miR-215-3 in the BFU Study. In contrast, cross-sectional analyses in both

173

studies, revealed no significant associations between markers of adiposity (BMI) and expression of these miRNAs at either time-point. Investigation of the relationship between weight change and miRNA expression over the 12+ year follow-up did also not yield significant results, even following adjustment for gender, baseline BMI and age.

5.7.2 Interpretation of main findings

In the introductory chapter (see section 1.3.1), I have discussed the evidence that epigenetic mechanisms, including miRNAs, are plastic throughout the life course and respond appropriately to the changing environment. However, most of this evidence has been obtained from measurements made in easily accessible tissue such as the blood and there are no comparable data on miRNA expression from measurements made in the colorectal epithelium. Furthermore, I also reviewed in the Introduction chapter (see section 1.4.6) evidence that obesity in humans is associated with abnormal patterns of miRNA expression. In addition, there is evidence that patterns of miRNA expression are "normalised" to some extent following weight loss by lifestyle interventions including diet and exercise (see Introduction Chapter section 1.4.7 and Chapter 4). However, most of this evidence has been obtained from measurement made in blood and adipose tissue and there are no comparable data, apart from those by Afshar (2016a) (who investigated the effects of bariatric surgery) and the extended analyses that I have reported in Chapter 4, from measurements made in the colorectal epithelium.

Here, I examined expression of a panel of 4 miRNAs (miR-31, miR-215, miR-3196 and miR-4516) which were significantly overexpressed in obese individuals compared with non-obese Controls in the human colorectal mucosa of the BOCABS Study (see Chapter 4). In the present study, I used qPCR to quantify expression of these 4 miRNAs at an individual participant level and to investigate associations with ageing and with adiposity longitudinally (over a 12+ years follow-up) in the colorectal epithelium of participants with a wide age range (37 to 69 years at baseline, BORICC Study).

MiR-215 was significantly overexpressed in the human colorectal mucosa at 12+ years follow-up (BFU Study) when compared with baseline levels (BORICC Study) (see Table 5-6), as hypothesised. As also hypothesised, cross-sectional analysis showed significant overexpression of miR-31-3 in the BORICC Study and for miR-215-3 in the BFU Study in older participants (see Table 5-6). However, since the panel of 4 miRNAs used in this study had been

selected based on their associations with adiposity in the BOCABS Study (Chapter 4) it was surprising that there were no significant associations between markers of adiposity and expression of these 4 miRNAs in the BORICC and BFU Studies. In addition, given that expression of 3 out of these 4 miRNAs (miR-31-3, miR-215 and miR-3196) responded to weight loss following bariatric surgery in the BOCABS Study (Chapter 4), it was surprising that there were no associations with weight gain or with weight loss over the 12+ year follow-up in the present study.

miRNA	Chromosomal location	Association with ageing longitudinally (BORICC *v.* BFU Study)	Association with ageing cross-sectionally in the BORICC Study	Association with ageing cross-sectionally in the BFU Study
miR-31	9p21.3	No significant change	↑	No significant change
miR-215	1q41	↑	No significant change	↑

Table 5-6: Summary of associations of age with miRNA expression in the human colorectal mucosa in the BORICC and BFU Studies.

5.7.3 The effect of age and ageing on expression of miR-31 and miR-215 in the colorectal mucosa

Since increased age is a well-established risk factor for CRC (Siegel et al., 2017), my finding of increased miR-31 expression cross-sectionally in human colorectal mucosal biopsies in older participants of the BORICC Study is consistent with the role of miR-31 as an oncogene. Given the link between ageing and CRC risk and the role of miR-31 as an oncogene and miR-215 as a TSG, my finding of no significant change in miR-31 expression and increased miR-215 expression in human colorectal mucosal biopsies longitudinally is unexpected. Furthermore, my findings of no significant changes in miR-215 and miR-31 expression in human colorectal mucosal biopsies cross-sectionally in the older participants of the BORICC and BFU Studies, respectively, and of increased miR-215 expression cross-sectionally in the older participants of the BFU Study are also unexpected with the role of miR-31 as an oncogene and miR-215 as a TSG. Potential explanations for this observation may be:

- With the role of miR-31 being an oncogene, an increased expression and not an insignificant change of this miRNA was expected in i) the BFU Study when compared with the BORICC Study (longitudinal investigation) and ii) the older group of the BFU Study cross-sectionally. However, miR-31 was the only miRNA of the panel examined which has been previously described to play an oncogenic role in CRC and, therefore the assumption of no CRC risk in ageing based on one single miRNA (no significant change in miR-31 expression) cannot be made. More oncogenic miRNAs should be examined to draw coherent and strong conclusions on CRC risk.

- With the role of miR-215 being a TSG, a reduction and not an increase of this miRNA was expected in i) the BFU Study when compared to the BORICC Study (longitudinal investigation) and ii) the older group of the BFU Study cross-sectionally, (downregulated miR-215) which would be suggestive of an increased CRC risk. However, miR-215 was the only miRNA of the panel examined which has been previously described to play a tumour suppressive role in CRC and, therefore the assumption of a reduced CRC risk with ageing based on one single miRNA (miR-215 upregulation) cannot be made. More miRNAs with the role of a TSG should be examined to draw coherent and strong conclusions on CRC risk.

- As also discussed in Chapter 4 (see section 4.8.2), the differential miRNA expression pattern dependent on the cellular composition of tissue especially, for miR-215 is not expected to pose an issue, as Kent (2014) found no miR-215 expression in lymphocytes, endothelial, smooth muscle, fibroblasts and red blood cells, whereas miR-215 was highly expressed in epithelial cells. Therefore, a shift in cellular composition in ageing is not expected to affect miR-215 expression.

- The panel of miRNAs examined here, was chosen based on the miRNA's significant differential expression with i) increased levels of adiposity and ii) response to massive weight loss following RYGB (as described in section 4.7). These might not be appropriate criteria to select miRNAs when examining the effects of age and ageing. Therefore, the lack of effect on these miRNAs observed here may be entirely consistent with age and ageing. Previous evidence from cell and animal models, as well as human studies, shows a correlation with a wide range of miRNAs and ageing. Most of this evidence has been obtained from serum, liver, brain, skeletal muscle, cardiovascular tissue and vascular tissue (Smith-Vikos and Slack, 2012, Noren Hooten et al., 2013, de Lucia et al., 2017, Huan et al., 2018) and I am unaware of studies in

human colon. Menghini (2009) reported a significant upregulation of miR-31 in human endothelial cells (in a human umbilical vein endothelial cell model) during ageing, which is consistent with the findings of this study. Contrarily, Noren Hooten (2010) observed miR-31 downregulation in peripheral blood mononuclear cells when comparing old individuals (64 years) with young individuals (30 years). This differential expression pattern might be tissue specific. No data could be identified for miR-215 and miR-4516 in ageing research. However, a recent review by Williams (2017) has identified a vast range of miRNAs involved in cellular pathways of ageing and senescence, including lin-4, miR-7a, miR-14, miR-24-3p, miR-29a, miR-29c, miR-148b-3p, miR-185, miR-195, miR-301a/b, miR-405a, miR-497 and miR-539. These might have been better targets for use in this study.

5.7.4 Associations of miRNA expression in the colorectal mucosa with adiposity and with change in adiposity over time

Given the link between weight change (especially increased adiposity), ageing and CRC risk, my finding of no association between differential patterns of miRNA expression and i) weight change in body mass as a continuous variable (see Table 5-4) and ii) those who lost or gained weight (see Table 5-5) was unexpected. This was particularly surprising as the miRNA panel examined here was selected based on differential expression with i) increased levels of adiposity and ii) response to massive weight loss following RYGB (as described in section 4.7). Potentially the samples size was 'too' small to detect significant changes, just 36% (n=12) of participants had a BMI over 30kg/m^2 at follow-up (BFU Study). Furthermore, evidence from the BOCABS Study (see section 4.7.1) shows that the degree of weight loss following RYGB was not associated with the extent of change in expression of any of these 3 miRNAs. These results show that miRNA expression may not be associated and cannot be predicted based on changes in body weight over a 12+ year period in a small sample size where the effects of weight change were relatively small.

5.7.5 Tissues specific action as either a TSG or oncogene for miR-31 and miR-215

Other studies have investigated miRNA expression and their functional role (TSG *versus* oncogene) and downstream targets cross-sectionally in the colorectal cell lines, mouse models or human colon tissue. The expression of miRNAs is tissue specific and hence defines the

physiological nature of cells (Lim et al., 2005). The same miRNA can act as an oncogene in one cell type and as a TSG in another cell type because of its different targets and mechanism of action (Svoronos et al., 2016). This ambivalent tissue dependent action in tumourigenicity has been established for both miR-31 and miR-215 (Yu et al., 2018, Vychytilova-Faltejskova and Slaby, 2019).

5.7.6 MiR-31 as an oncogene in CRC

As described in detail in chapter 4 (see section 4.8.6), many functional studies have yielded findings, which confirmed the role of miR-31 as an oncogene in CRC. In brief, miR-31 overexpression targets *SMAD3, SMAD4*, *BMPR1A, AXIN1, DKK1, RASA1* and *GSK3β* via TGFβ, BMP, RAS/MAPK and Wnt pathways, which subsequently increases proliferation and represses apoptosis (Clevers et al., 2014, Reynolds et al., 2014, Kent et al., 2016, Tian et al., 2017, Yu et al., 2018).

Also human studies indicate that miR-31 acts as an oncogene in CRC. Mir-31 was overexpressed in CRC tissue when compared with normal tissue of patients, as well as in serum samples, and its expression correlates with CRC progression (Wang et al., 2009, Nosho et al., 2014, Wang et al., 2014b, Yang et al., 2014, Tateishi et al., 2015).

Ample studies have identified upregulated levels of miR-31 in human CRC cell lines, as well as in samples of CRC patients and, described its role initiation, development and progression of CRC.

5.7.7 MiR-215 as a tumour suppressor gene in CRC

As described in detail in chapter 4 (see section 4.8.7), data obtained from functional studies suggest that miR-215 acts as a TSG in CRC. In brief, miR-215 targets YY1, SRPX2 via PI3K/ AKT signalling pathway, which enhances DNA synthesis, nucleotide production and reduced intracellular ROS, glucose uptake, lactate production and proliferation (Chen et al., 2016, Zhao et al., 2018, Vychytilova-Faltejskova and Slaby, 2019).

Also, human studies suggest that miR-215 acts as a TSG in CRC. Mir-215 was downregulated in CRC tissue when compared with normal colorectal mucosa and that correlated with clinical stage, grade and positivity of lymph nodes (Braun et al., 2008, Karaayvaz et al., 2011, Necela et al., 2011, Faltejskova et al., 2012, Vychytilova-Faltejskova et al., 2017).

These data show strong evidence that this miR-215 is a tumour suppressor in CRC.

5.8   Conclusion

I examined expression of a panel of 3 miRNAs (miR-31, miR-215 and miR-4516) in the colorectal mucosa of 33 participants in the BORICC Study who also participated in the BFU Study 12+ years later. This study design allowed me to investigate, for the first time, associations between miRNA expression and i) ageing and adiposity longitudinally (over a 12+ year follow-up) and ii) age and adiposity cross-sectionally in both the BORICC and BFU Studies. There was evidence that ageing is associated with significantly increased miR-215 expression over 12+ years follow-up and, within the BFU Study, that miR-215 expression was higher in older participants. Cross-sectional analysis also suggested that expression of the other 3 miRNAs may be higher in older individuals but this association was significant only for miR-31 in the BORICC Study.

Given the rationale for selection of the 3 miRNAs investigated in this chapter, the absence of significant associations with adiposity and with change in body weight longitudinally was unexpected. It is possible that the lack of evidence for associations is due to the relatively small size of the study (33 individuals examined at two time points) and larger studies will be needed to test the hypothesis more thoroughly. In addition, it is possible that the inter-individual range in BMI within the BORICC and BFU Studies was insufficiently great to allow detection of an adiposity effect. Obese participants at baseline (pre-surgery) in the BOCABS study were considerably heavier (mean BMI = 42.4 kg/m2) than obese participants in either the BORICC Study (mean BMI = 33.4 kg/m2) or in the BFU Study (mean BMI = 33.2 kg/m2). Finally, it is possible that the degree of weight change within individuals that occurred over 12+ years of follow up was insufficient to reveal an effect of change in adiposity. Individual body weight change during the period of follow-up was substantial and ranged from +25 kg to -20 kg but the amount of weight change needed to trigger a change in miRNA expression is unknown. These data are consistent with evidence obtained from the BOCABS Study (see section 4.7.1) which demonstrates that the degree of weight loss following RYGB was not associated with the extent of change in expression of any of these 3 miRNAs.

6   General Discussion

6.1   Summary of main findings

The aim of this PhD project was to examine i) the effects of obesity and weight loss following bariatric surgery (using data from the BOCABS Study) and ii) the effects of age and ageing (using data from the BORICC and BFU Studies) on biomarkers of CRC risk, including mitochondrial mutations and changes in expression of miRNAs. The investigations were designed to test the hypotheses that i) biomarkers of CRC risk are elevated in obese compared with non-obese individuals, ii) weight loss following bariatric surgery ameliorates molecular pathways which are mechanistically associated with CRC risk and iii) that these obesity-related biomarkers of CRC risk are exacerbated by ageing. The main findings are summarised below.

6.1.1   Effects of adiposity and of ageing on mitochondrial dysfunction and mtDNA mutations in the colorectal mucosa

I tested the hypothesis that obese individuals exhibit greater mitochondrial dysfunction and increased mtDNA mutation frequency (i.e. global mutations identified in the mitochondrial spectra and mutations with functional consequences) and that weight loss following bariatric surgery reduces the rate of clonal expansion of mutated mtDNA, when compared with non-obese adults. This is the first study to examine mitochondrial OXPHOS protein abundance and to sequence the mtDNA in human colorectal mucosal biopsies in obese individuals pre- and post-bariatric surgery and in non-obese Controls. Furthermore, I examined the effect of age on both OXPHOS protein abundance and mtDNA mutation frequency.

I detected significantly more crypts with complex I and IV deficiencies in the colorectal mucosa of obese pre-surgery participants when compared with non-obese Controls. This finding is consistent with previous human studies, although those measurements were made in other tissues including skeletal muscle and adipose tissue (Sparks et al., 2005, Rocha et al., 2015, Heinonen et al., 2015). I also observed that advancing age is associated with significantly greater complex I and IV deficiencies in the colorectal mucosa in both obese and non-obese people, which is in line with earlier research findings (Greaves et al., 2010, Greaves et al., 2012, Greaves et al., 2014). The latter studies did not investigate effects of adiposity. Whilst bariatric surgery resulted in very substantial weight loss, mean 27kg after 6 months, it did not lead to altered abundance of OXPHOS protein levels, which was surprising. This finding is inconsistent

180

with other studies which reported improvement in mitochondrial respiration at 6 months after bariatric surgery-induced weight loss (Coen et al., 2015, Fernstrom et al., 2016). It is likely, that the lack of improvements in OXPHOS protein abundance in my study was due to the fact that, despite significant weight loss, the participants remained obese at 6-month follow-up (mean BMI 31.7 kg/m^2). Alternatively, the adverse effects of excess adiposity may damage expression of mitochondrial OXPHOS proteins permanently. The underlying mechanisms for the associations between age-related CRC risk, greater adiposity and increased OXPHOS protein deficiencies in the human colorectal mucosa warrant further research.

Using NGS to sequence approximately 60% of the mitochondrial genome, I observed no associations between adiposity and/ or age and frequency or pattern of mtDNA mutations when comparing i) matched groups of obese pre-surgery participants and non-obese Controls and ii) obese adults before and after bariatric surgery. There were no significant differences in the types of mtDNA mutations detected, including global mutations identified in the mitochondrial spectra and mutations with functional consequences. There was a trend for transversions to occur more frequently in adults with higher levels of adiposity when compared with non-obese Controls, but this observation was not significant. In addition, there was a tendency towards lower frequency of transversions and non-silent codon changes in those who had undergone bariatric surgery, but these changes were not statistically significant. Inter-individual variation in mitochondrial mutation frequency was large, which may have precluded detection of significant effects.

In summary, my data provide evidence that greater levels of adiposity result in deficient complex I and IV and mitochondrial mass expression in human colorectal mucosal biopsies, which does not seem to be caused by mutations in the corresponding mitochondrially-encoded genes. Taylor (2003) demonstrated that defective OXPHOS proteins are caused by about 70% underlying mutations and 30% other mechanisms, including damage due to elevated levels of ROS and inflammation. It is plausible to propose that the observed OXPHOS defects in this study are driven by inflammatory and oxidative stress damage at the protein level rather than the DNA level. If the latter is true, then one would expect that weight loss, coupled with its associated reductions in inflammatory markers and oxidative stress, would decrease damage at the protein level. In addition, although the reduced inflammation and oxidative stress may lower the frequency of new mtDNA mutations, once a mutation has

occurred, clonally expanded and reached the threshold level, it is irreversible and formerly individuals may carry those mutations with them even if they return to normal weight.

6.1.2 Effects of adiposity, age and ageing on miRNA expression in the colorectal mucosa

I tested the hypothesis that weight loss following RYGB in initially obese participants modulates miRNA expression in the colorectal mucosa. This was the first study which used NGS to screen for changes in mature miRNA in the human colorectal mucosa and to investigate the effects of obesity and of weight loss following RYGB. I further examined and validated differential expression of a panel of miRNAs between i) obese and non-obese individuals and ii) in initially obese people pre- and post-RYGB. Furthermore, I investigated the effects of adiposity, age and of ageing on expression of the same panel of miRNAs in the human colorectal mucosa in a 12+ years follow-up study.

Expression of miR-31, a recognised oncogene in CRC, was significantly upregulated in obese adults when compared with non-obese, and declined significantly following weight loss by RYGB. This finding is consistent with the role of this miRNA as an oncogene and its increased expression with CRC risk and during CRC pathology (Bandrés et al., 2006, Slaby et al., 2007, Motoyama et al., 2009, Wang et al., 2009, Earle et al., 2010, Ito et al., 2014, Nosho et al., 2014, Yang et al., 2014, Tateishi et al., 2015, Lundberg et al., 2018). This finding is also consistent with the observation of reduced CRC risk following significant and sustained surgery-induced weight loss (Afshar et al., 2018). Furthermore, I observed that miR-31 expression was increased in older participants (>56 years) recruited to the BORICC Study. Perhaps surprisingly, miR-31 expression fell significantly in the same individuals when investigated 12+ years later to levels comparable to those of the younger group of BORICC Study participants. It is well-established that miRNA expression and other epigenetic marks and molecules are plastic and that they respond to a wide range of environmental exposures (Mathers et al., 2010, Malcomson and Mathers, 2017). It is likely that ageing, unchanged measures in adiposity or nutritional factors (the latter needs to be explored within these studies; BORICC and BFU), interacted with the epigenome. And this interaction may have determined the phenotype of these adults, and resulted in a reduced CRC risk which was consistent with the lack of CRC cases at the time of the recruitment at 12+ years follow-up (the BFU Study). However, the underlying mechanisms responsible for this relationship and outcome are currently incompletely understood.

Expression of miR-215, a TSG involved in the aetiology of CRC, was significantly upregulated in obese adults, when compared with non-obese, and declined significantly following weight loss by RYGB. This finding is unexpected and inconsistent with the role of this miRNA as a TSG and its downregulation with CRC risk or during CRC pathology (Braun et al., 2008, Karaayvaz et al., 2011, Necela et al., 2011, Faltejskova et al., 2012, Vychytilova-Faltejskova et al., 2017). The reasons for this observation are unclear. Moreover, I observed that miR-215 expression increased during 12+ years of ageing (BFU Study), when compared with baseline levels (BORICC Study). Since CRC risk increases with age (Siegel et al., 2017), the greater expression of miR-215 in older people was unexpected and more research is warranted to reveal the underlying mechanisms and to determine whether this has implications for CRC development.

I also observed increased expression of two novel miRNAs, miR-3196 and miR-4516, in obese adults, when compared with non-obese Controls, and expression of miR-3196 only fell significantly following weight loss by RYGB. However, miR-3196 showed a different direction of expression change by qPCR compared to NGS for both comparison groups, showing that this miRNA did not validate and was hence excluded from further analyses. To date, few studies have investigated the role of these novel miRNAs, and their potential roles in obesity and in cancer, including CRC, remain to be discovered. No significant changes in miR-4516 expression during ageing was detected.

In summary, my data demonstrate that expression of three miRNAs (miR-31, miR-215 and miR-4516) is significantly higher in the colorectal mucosa of obese individuals and that expression of two out of those three miRNAs (miR-31 and miR-215) is reduced significantly following weight loss by RYGB when compared with initially obese adults. Two of these miRNAs (miR-31 and miR-215, an oncogene and TSG, respectively) are implicated in CRC and the observed changes in expression are associated with greater adiposity and with weight loss, suggesting that the associated machinery for regulating miRNA gene expression senses, and responds to, changes in measures of adiposity. Furthermore, expression of miR-215 increased significantly in the same individuals investigated at baseline and after 12+ years follow-up. This suggests that expression of this miRNA is associated with ageing (to date no previous studies have identified miR-215 in ageing research), but how such age-related expression is regulated remains to be discovered. Based on this evidence, I propose that adiposity, age and ageing, to some extent, modulate miRNA expression in the colorectal mucosa and so may influence CRC risk.

6.1.3 Comparison of miRNA expression in the human colorectal mucosa across multiple studies

For consistency, and to facilitate the pooling of data, the same house keeping genes (HKG) and methods for analysis were used for quantification of miRNA expression in all three studies i.e. the BOCABS, BORICC and BFU Studies included in this thesis. To investigate associations with age and adiposity, I pooled data for miRNA expression for all participants across all 3 studies (see Figure 6-1 for relationships with adiposity and Figure 6-2 for relationships with age). Figure 6-1 shows that, of the 3 miRNAs, miR-215 expression has the most evident association with BMI. Expression of miR-215 is relatively low for non-obese participants but increases steeply at higher levels of adiposity. The data in Figure 6-2 show an apparent peak in miRNA expression in mid-life, i.e. between age 45-55 years, for all 3 miRNAs examined. However, this is unlikely to be a simple age-dependent phenomenon since most of these higher values are contributed by the obese participants pre-surgery from the BOCABS Study (blue symbols in Figure 6-2) so that this apparent age effect is likely confounded by between study group differences in adiposity. CRC risk increases rapidly after the age of 50 years, which may explain the higher expression of the oncogene miR-31 as seen in Figure 6-2 (A).
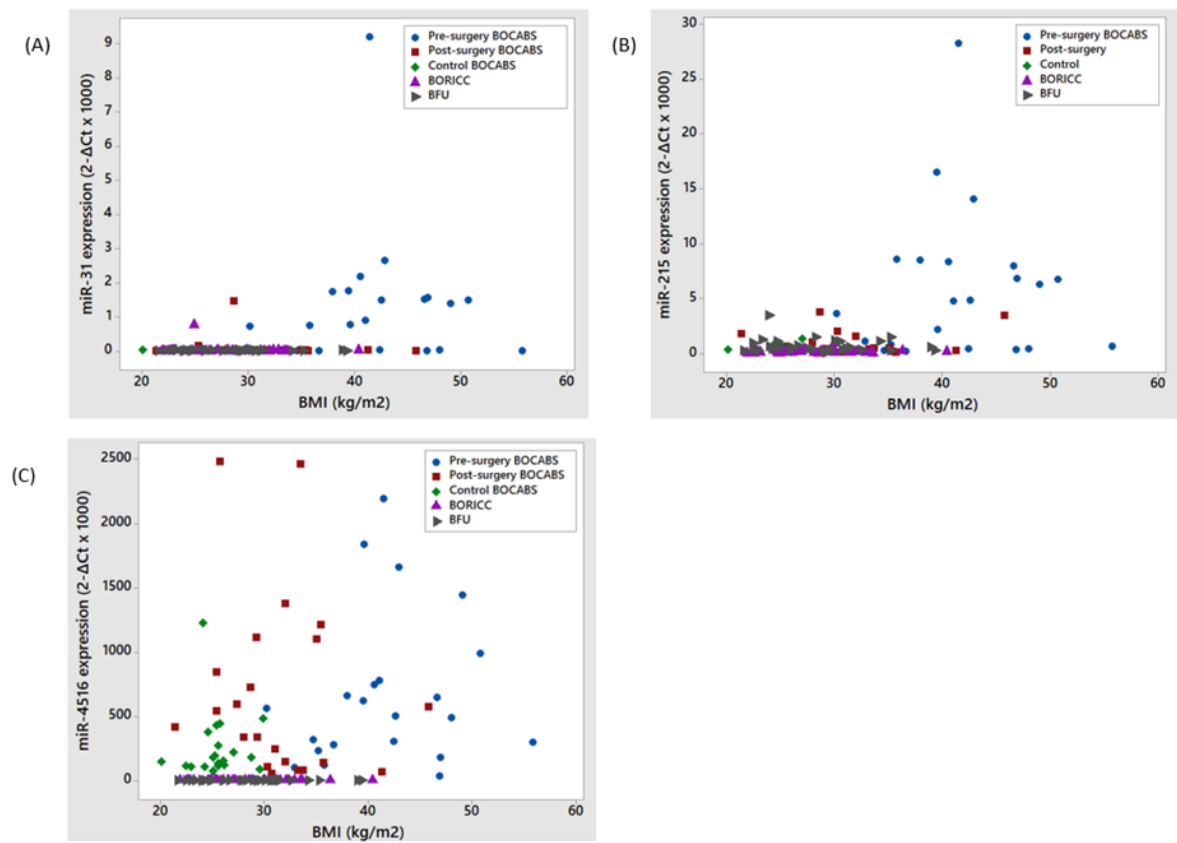
Figure 6-1: Expression of miRNAs (which were significant between obese and non-obese after qPCR quantification) across the BMI range in all study groups, BOCABS: pre- and post-surgery and non-obese controls, BORICC and BFU Studies. A) miR-31 expression. B) miR-215 expression C) miR-4516 expression.
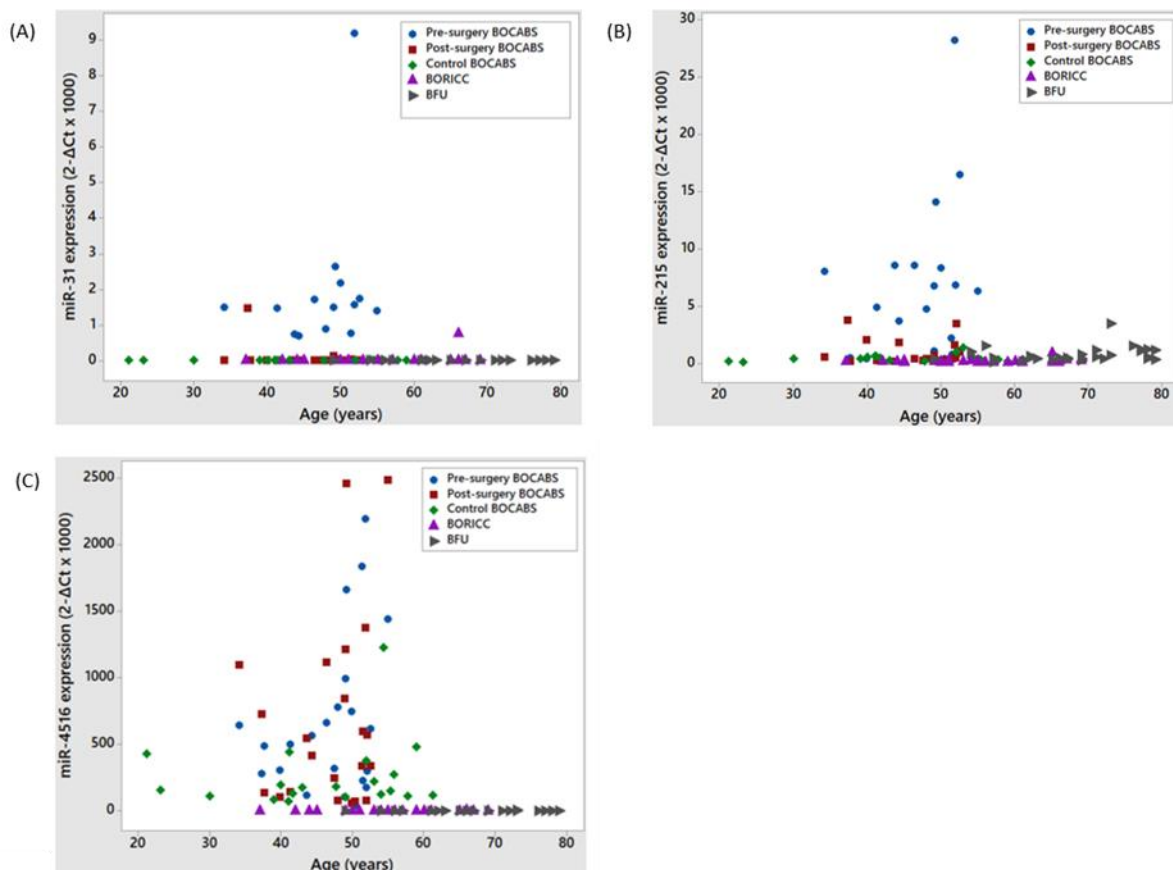
Figure 6-2: Expression of miRNAs (which were significant between obese and non-obese after qPCR quantification) across the age span in all study groups, BOCABS: pre- and post-surgery and non-obese controls, BORICC and BFU Studies. A) miR-31 expression. B) miR-215 expression C) miR-4516 expression.

In Figure 6-3, I have combined data on miRNA expression published by Afshar (2016a) and the new data from this thesis to provide a more comprehensive overview of the effects of obesity on miRNA expression. I found significant overexpression for three miRNAs (miR-31, miR-215 and miR-4516), whereas Afshar (2016a) observed significant overexpression of one miRNA (miR-143) and downregulation of three miRNAs (miR-1273a, miR-144 and miR-451a) in obese, when compared with non-obese, participants in the BOCABS Study. Table 6-1 shows the validated pathways that are known to be regulated by each of these 7 miRNAs. An overexpression of one oncogene, miR-31 which targets TGFβ, BMP and WNT pathways, and downregulation of 2 TSG (miR-144 and miR-451a) was seen, which activates PI3K /AKT and WNT pathways. Taken together, this differential expression of these miRNAs results in the induction of proliferation and repression of apoptosis. This is in line with the hypothesis that greater levels of adiposity modulate molecular pathways which are mechanistically linked to CRC risk. However, two TSG (miR-143 and miR-215) were upregulated in the obese, which is unexpected. As discussed earlier (see section 4.8), because each of these pathways is

regulated by multiple miRNAs, it is not appropriate to draw a conclusion about altered CRC risk in the obese based on two TSG (for one of which affected pathway(s) remain unknown).
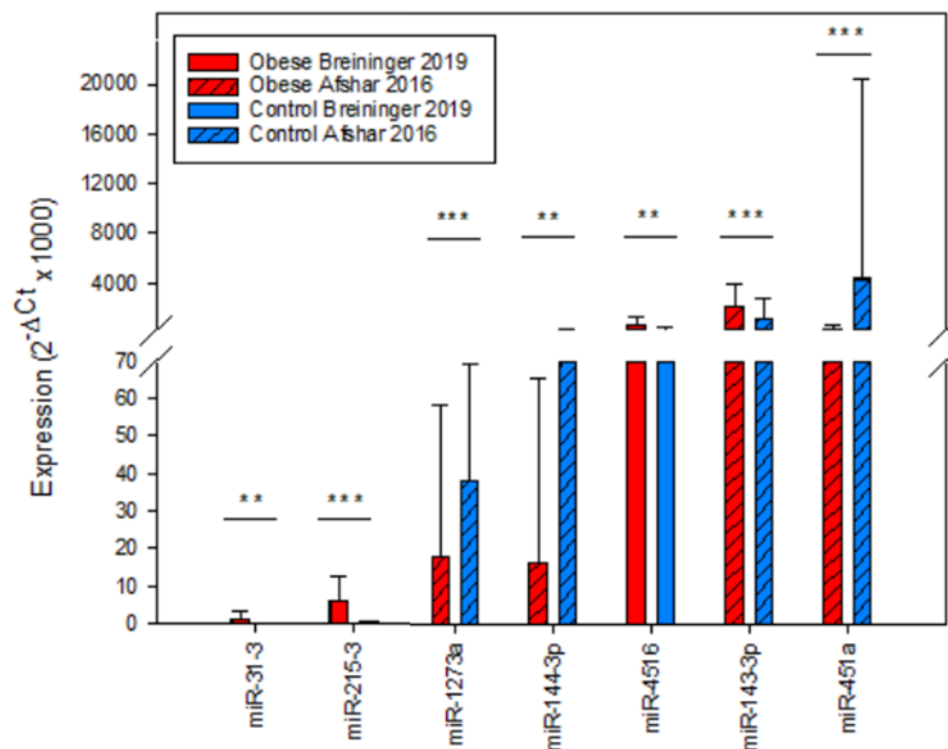
Figure 6-3: Combined data on expression of miRNAs which were significantly modulated by increased adiposity in the colorectal mucosa of participants to the BOCABS Study, identified by Afshar (2016a) and myself. Samples sizes studied by Afshar (2016a) were for miR-1273a n=36 obese and n=18 non-obese; for miR-144-3p n=36 obese and n=19 non-obese; for miR-143-3p n=37 obese and n=20 non-obese; for miR-451a n=36 obese and n=20 non-obese. In my study the sample sizes for all 3 miRNAs were n=22 obese and n=20 non-obese.

miRNA	Role	Association with obesity	Validated pathways affected
miR-31	Oncogene	↑	TGFβ, BMP and WNT
miR-215	TSG	↑	Unknown
miR-143	TSG	↑	RAS-MAPK
miR-144	TSG	↓	PI3K /AKT
miR-451a	TSG	↓	WNT
miR-1273a	Unknown	↓	Unknown
miR-4516	Unknown	↑	Unknown

Table 6-1: Significantly modulated miRNAs in the colorectal mucosa of obese compared with non-obese Controls in the BOCABS Study and their targeted pathways.

Finally, Figure 6-4 illustrates the effects of deliberate and sustained weight loss following bariatric surgery on miRNA expression in the colorectal mucosa within the BOCABS Study combining data from Afshar (2016a) and this thesis. I found significant downregulation of three miRNAs (miR-31 and miR-215) and Afshar (2016a) observed significant overexpression of one miRNA (miR-451a) and downregulation of one miRNA (miR-143) in the post-surgery participants at 6 months follow-up. The combined data expands our understanding of the pathways affected by significant and sustained weight loss following bariatric surgery. Table 6-2 shows the validated pathways which are regulated by these miRNAs.

The observed downregulation of the oncogene miR-31, which targets TGFβ, BMP and WNT pathways, and is involved in upregulation of the TSG miR-451a, may result in repressed cell proliferation and increased apoptosis. This is consistent with the hypothesis that weight loss reduces CRC risk by modulating molecular pathways which are causal in its aetiology. MiR-143, which affects the RAS-MAPK pathway, and miR-215 were downregulated in the post-surgery group which is surprising given their role as TSGs but, as discussed above, conclusion cannot be made based on two single miRNAs only.
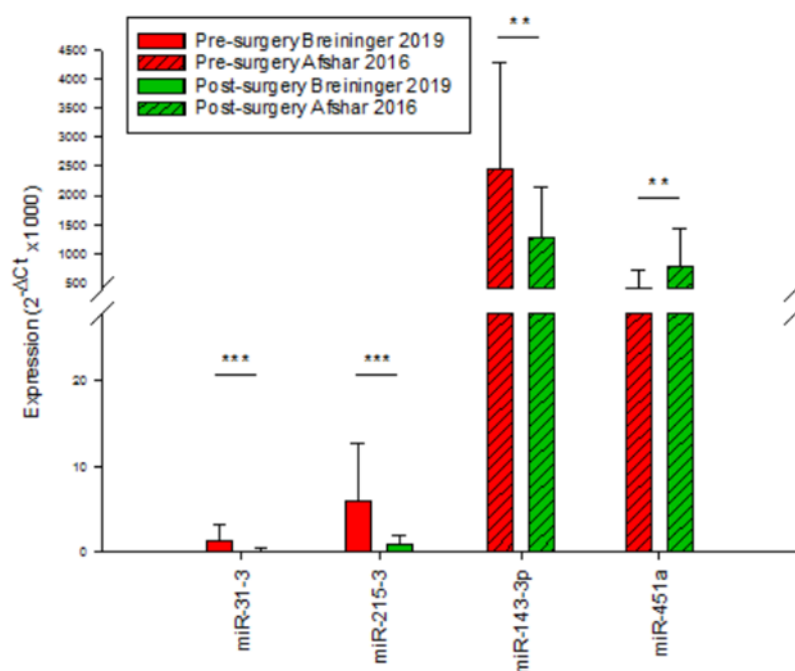
Figure 6-4: Combined data on expression of miRNAs, which were significantly modulated by sustained weight loss following bariatric surgery at 6 months follow-up in the colorectal mucosa of participants to the BOCABS Study, identified by Afshar (2016a) were for miR-143-3p n=29 for matched pre- and post-surgery and for miR451a n=28 for matched pre- and post-surgery. In my study sample sizes for all 2 miRNAs n=22 for matched pre- and post-surgery.

miRNA	Role	Effects of weight loss following RYGB	Validated pathways affected
miR-31	Oncogene	↓	TGFβ, BMP and WNT
miR-143	TSG	↓	RAS-MAPK
miR-451a	TSG	↑	WNT
miR-215	TSG	↓	Unknown

Table 6-2: Significantly modulated miRNAs in the colorectal mucosa following deliberate and sustained weight loss by bariatric surgery in participants of the BOCABS Study and their targeted pathways.

6.2   Strengths and Limitations of Studies

The main strengths of both the BOCABS and BFU Studies was the ability to measure the biomarkers in the tissue of interest, namely the colon. This is a particularly important strength since, to date, this is the first human study to examine the effects of adiposity and of weight loss and their association to CRC risk on these biomarkers in the colon tissue. Other studies have primarily investigated miRNA expression in surrogate and adipose tissue (see Table 6-3). Further strengths of both the BOCABS and BFU Studies are the use of paired colorectal mucosal biopsies from unprepared bowel, which limited the potential confounding effect on biomarkers of interest, from the same individuals before and after bariatric surgery and at baseline and 12+ years follow-up, respectively. In both studies, rigid sigmoidoscopies were used which is cheaper compared with standard flexible endoscopes. A further strength of both studies was the use of stringent inclusion and exclusion criteria for participants, limiting the effect of potential confounding factors. The collection of rectal mucosal biopsies from the same anatomical site within the large bowel in all participants and by the same researchers allows data to be directly comparable and not subject to confounding by differences due to sample site. Both studies collected extensive phenotypic data of participants, including anthropometry, diet, lifestyle, physical activity and sedentary behaviour, and biological samples (blood, stool and urine), which facilitates the study of factors that play a role in modulating molecular and mechanistic pathways. Finally, for the BOCABS Study, a further strength was that the bariatric surgery was performed by two surgeons, restricting heterogeneity in the aspect of surgery procedure. And, for the BFU Study, a further strength was that buccal, bone density, upper and lower body strength measurements were collected.

The main limitations of both the BOCABS and BFU Studies are that the utilisation of colorectal mucosal biopsies at the mid-rectum, 10cm distanced from the anal verge, to evaluate CRC risk and, it is likely not to be representative of the whole colorectum. Nevertheless, initial changes, including cell proliferation, which result in the development from normal mucosa to adenoma and subsequently CRC occur in the entire colorectum (Terpstra et al., 1987).

Another limitation is the relatively small samples size of paired samples, n=22-26 and n=33 for the BOCABS and BFU Studies, respectively, which did restrict the performance of sub-group analyses. For example, effects of type of bariatric surgery or low vs high CRC risk participants in the BOCABS and BFU participants, respectively, on measured outcomes in the present study. Table 6-3 compares participant characteristics and methods of investigation in the tissue of interest from the BOCABS, BORICC and BFU studies (highlighted in green) to other studies in this field. Two studies which examined the effect of weight loss by bariatric surgery on CRC risk had similar sample sizes, i.e. n=26 (Sainsbury et al., 2008) and n=19 (Kant et al., 2011). Additionally, studies investigating the effect of weight loss by bariatric surgery on circulating miRNA expression had also comparable samples sizes to the present study, i.e. n=21 (Hulsmans et al., 2012), n=22 (Ortega et al., 2013), n=22 (Nunez Lopez et al., 2017); or even smaller sample sizes, i.e. n=13 (Lirun et al., 2015), n=9 (Alkandari et al., 2018), n=6 (Hubal et al., 2017) and, only one study comprised a greater sample size, i.e. n=58 (Hohensinner et al., 2018). One study examining the effect of weight loss by bariatric surgery on miRNA expression in the adipose tissue also comprised a comparable sample size to the present study, i.e. n=16 (Ortega et al., 2015a), or once again smaller sample sizes, i.e. n=9 (Ortega et al., 2015b) and n=3 (Nardelli et al., 2017).

Additionally, for the recruitment of the BFU Study a power calculation was conducted (based on the effect of age on faecal calprotectin in the BORICC Study) which estimated the requirement of a recruitment target n=53 but a total of n=47 were actually recruited which might be a potential limitation (Malcomson et al. 2019). However, it is important to note that this power calculation was based on a longitudinal age difference of 10+ years as opposed to 12+ years and on cross-sectional data, but here comparisons over time were analysed which are likely to exhibit greater statistical power to detect effects of ageing on the measured outcomes.

Table 6-3 shows the participant characteristics, tissue of interest and miRNA quantification method of the BOCABS, BORRIC and BFU studies compared with previously published research

which also investigated the effect of weight loss on miRNA expression. When comparing the extremes of adiposity, which is the case for the majority of the studies ((Hulsmans et al., 2012, Ortega et al., 2013, Ortega et al., 2015a, Ortega et al., 2015b, Nardelli et al., 2017, Hubal et al., 2017, Alkandari et al., 2018, Hohensinner et al., 2018) and the BOCABS Study) it becomes clear that, where participants comprise a higher baseline BMI above >40 kg/m^2, they remain in the obese range after surgery at follow-up. This might be a natural limitation when studying adults with extreme levels of adiposity as they may struggle to achieve a weight within the normal range. All studies comprise a greater proportion of women and, when investigating miRNAs in relation to obesity related CRC risk, this might pose a confounder, as CRC is more common in men. The risk for CRC increases significantly with age, especially after mid-life (Siegel et al., 2017). CRC results from unrepaired genomic damage to stem cells and their progeny located in the crypts of the colorectal mucosa which takes many years to accumulate and develop into pathology. In the studies to date, the mean age range is 39-68 years (with the exception of one study where the mean age is 28 years (Lirun et al., 2015)) and it would be interesting to investigate the changing patterns of miRNAs from early adulthood until mid-life when CRC develops. A final limitation is the differential methods utilised across studies for the quantification of miRNA abundance, including TaqMan low-density array and RT-PCR, Affymetrix GeneChip miRNA Array, microarray, Exiqon miRCURY locked nucleic acid and PCR, real time PCR, qPCR and NGS. The use of different methods does not allow a uniform comparison of miRNA expression across the different studies.

A possible limitation of the BOCABS Study was the recruitment of the non-obese Controls occurred following referral for flexible sigmoidoscopy or colonoscopy for GI symptoms. Even though patients were only recruited if their endoscopy was normal and no pathology was found, this method for recruitment might have selected unhealthy participants with undiagnosed GI pathology. A systematic review and other studies have observed that neoplasia, adenoma and polyp miss rates range between 6-27%, which suggests that the diagnosis of pathology may be missed (Hixson et al., 1991, Bensen et al., 1999, van Rijn et al., 2006, Kaltenbach et al., 2008). Furthermore, as adenomas do not commonly cause symptoms, it is not expected to find a higher adenoma diagnosis rate in the non-obese Controls who were symptomatic patients with a normal endoscopy, compared with the obese patients. Hence, the non-obese Controls of this study might carry undiagnosed pathology of the colon. But, at least for the study of miRNA expression, this point does not pose an issue as the study by

Kurylowicz (2017) identified similar effects and the normal weight Controls were undergoing elective cholecystectomy or were operated for inguinal hernia. This shows that the recruitment strategy for the Controls in the BOCABS Study was satisfactory to enable detection of changes in miRNA expression when compared with adults with severe adiposity, i.e. BMI above >40 kg/m^2.

6.2.1 Strengths of the mitochondrial and epigenetic biomarkers

The laboratory methods used, including qPCR and immunofluorescent labelling, provide robust quantification for investigating epigenetic and mitochondrial biomarkers. NGS provides global and unbiased, quantification of patterns mutational load of mtDNA mutations and miRNA abundance in crypts of colorectal mucosal biopsies.

Another strength is that Afshar (Afshar, 2016a) has previously tested the correlation between miRNA expression and the *SMA:CK20* ratio in colorectal mucosal biopsies of participants to the BOCABS Study. He found that the ratio was uniform across the biopsies from the different groups (pre- and post-surgery and controls) and therefore cellular composition is uniform in these biopsies and not a confounding factor for the results on miRNA expression. Due to this validation, it is not anticipated that the cellular composition of biopsies differs in BORICC and BFU Study participants and acts as a confounder for miRNA expression.

6.2.2 Limitations of the mitochondrial biomarkers

A significant limitation was the smaller sample size when examining the effects of adiposity and weight loss on mtDNA mutations. Additionally, it was possible to sequence 60% of the mitochondrial genome in the colorectal mucosa, which limited the opportunity to identify possible mtDNA mutations present in the remaining 40% of the genome which was not sequenced.

Study	Sample size (n)	Gender M, F (%)	Age (years)	BMI (kg/m^2) before weight loss	BMI (kg/m^2) after weight loss	Tissue	Investigation	miRNA quantitation method
BOCABS Study	22	18, 82	47	42.4	31.3	Colon	Obesity, bariatric surgery, CRC risk	NGS, qPCR
BORICC Study	33	48, 52	56	28	N/A	Colon	Age and ageing	qPCR
BFU Study	33	48, 52	68	28.4	N/A	Colon	Age and ageing	qPCR
(Hulsmans et al., 2012)	21	33, 67	39	44	36	Monocytes	Bariatric surgery	Microarray
(Ortega et al., 2013)	22	23, 77	44	42.9	28.9	Surrogate	Bariatric surgery	TaqMan low-density array and qRT-PCR

(Nunez Lopez et al., 2017)	22	18, 82	43	39.5	30.2	Surrogate	RYGBP plus exercise program	Real time PCR
(Lirun et al., 2015) low BMI group (≤30 kg/m²)	7	29, 71	41	26.8	22.4	Surrogate	RYGB	Affymetrix GeneChip miRNA Array
(Lirun et al., 2015) high BMI group (≥30 kg/m²)	8	25, 75	28	35.4	28.9	Surrogate	RYGB	Affymetrix GeneChip miRNA Array
(Alkandari et al., 2018)	9	44, 56	46	49	30.7	Surrogate	Bariatric surgery	Exiqon miRCURY locked nucleic acid and PCR
(Hubal et al., 2017)	6	0, 100	39	51.2	32.6	Surrogate	Bariatric surgery	Affymetrix GeneChip miRNA Array

(Hohensinner et al., 2018)	58	29, 71	42	44.0	28.0	Surrogate	Bariatric surgery	RT-qPCR
(Ortega et al., 2015a)	16	0, 100	48	43.1	29.2	Adipose tissue	Laparoscopic sleeve gastrectomy	Affymetrix GeneChip miRNA Array and RT-PCR
(Ortega et al., 2015b)	9	0, 100	48	43.4	Available in supplementary file	Adipose tissue	Bariatric surgery	TaqMan low-density array and RT-PCR
(Nardelli et al., 2017)	3	0, 100	48	42.9	32	Adipose tissue	Bariatric surgery	TaqMan low-density array and RT-PCR

Table 6-3: Comparison of participant characteristics and miRNA quantification methods in tissue of interest in the BOCABS, BORICC and BFU Studies with previously published studies investigating the effects of deliberate and sustained weight loss by bariatric surgery on miRNA abundance.

6.3   General proposals for future work

The differences between the study designs of the BOCABS and BFU Studies has been discussed in detail earlier. These differences provide an evidence gap that should be an important focus for future research. It would be interesting to expand the investigation on the association between the outcomes of interest with additional markers of adiposity (apart from BMI) and include, for example, body fat percentage, waist and hip circumference and waist: hip ratio. When examining the relationships with waist circumference, care is needed to adjust for gender because of the well-established gender dimorphism in body shapes between males and females (Singh, 1994). Another interesting area for future work is the investigation of the links between socioeconomic status and lifestyle factors involved in the aetiology of obesity, i.e. diet, physical activity and smoking, on mitochondrial and epigenetic (miRNA expression) biomarkers measured in the colorectal mucosa of participants in the BOCABS and BFU Studies. Investigating this link may provide a more holistic picture of how lifestyle factors interplay with molecular mechanisms.

As discussed in the introductory chapter (see section 1.5), there is a big research gap on whether obesity modulates CRC risk via effects on the mitochondria. It would be interesting to establish whether an interaction between miRNAs and mitochondria during obesity plays a role in the development of CRC. More specifically, to examine whether i) epigenetic regulation via miRNAs can affect the expression of mitochondrial genes and the generation of mitochondrial proteins (i.e. OXPHOS proteins) and ii) if such an epigenetic regulation will affect the morphology, respiration and function of mitochondria.

6.3.1   Proposals for future work on the investigation of miRNAs

Epigenetic changes modulating gene expression, and by doing so regulating cell proliferation and apoptosis, play an important role in the link between obesity, weight loss and CRC risk. I investigated changes in miRNA expression following RYGB, age and ageing, which is one of the known epigenetic mechanisms. It would be interesting to further investigate in the future the effect of obesity, weight loss, age and ageing on other epigenetic mechanisms, including DNA methylation, post-translational histone and epi-transcriptome modifications. This will enhance our knowledge about the functions and molecular mechanisms of how adiposity modulates CRC risk. It is likely to also result in the detection of prognostic biomarkers as well as targets for prevention and treatment.

MiRNAs have been increasingly proposed for diagnostic biomarkers and therapeutic targets in CRC (Ren et al., 2015, Lin et al., 2017, Hibner et al., 2018) . However, research on miRNAs provides information on one aspect of epigenetic mechanisms and modifications. Conducting further research of downstream analyses will provide a deeper understanding of molecular mechanisms involved in the link between obesity, weight loss and CRC risk. It would be interesting to carry out gene expression and protein quantification analyses of the downstream targets of the miRNAs identified in this study and then validate predicted pathways which may be targeted by these miRNAs.

Given the unexpected and opposite direction of expression of the TSG miR-215 with obesity and weight loss, it would be interesting to examine a broader panel of miRNAs which have been previously identified as TSG and oncogenes in CRC. Furthermore, to quantify the expression of the miRNAs identified in pathology, i.e. in tissue derived from CRC, and compare expression levels with the data derived from this study. This will enhance our understanding of the link between CRC and obesity and their 'expected' expression levels. In such a case, it is important to avoid confounding factors and take into account the altered cellular composition of pathological tissue by examining single cell miRNA expression patterns of the colon.

Another proposal for future research is the examination of the same miRNA panel in surrogate tissue, including blood, and then compare expression levels found in blood to that found in the colon. If miRNA expression proves to be similar, blood could serve as a less invasive biomarker for CRC risk.

It has not been previously evaluated how bowel preparation and enema affect and potentially modulate miRNA expression in the colon. Investigating this research gap will shed light on a potential confounding factor and help provide robust results on miRNA expression levels obtained from colorectal mucosal biopsies collected following bowel preparation and enema.

6.3.2   Proposals for future work on the investigation on mitochondria

As previous research has revealed that older individuals have higher rates of somatic mtDNA mutations, which clonally expand to high levels resulting in OXPHOS dysfunction (Greaves et al., 2010, Greaves et al., 2012, Greaves et al., 2014), it is fundamental to add age of participants as a covariate when investigating mitochondrial outcomes.

Considering the observed lack of effect of adiposity and weight loss on mtDNA mutations in the colorectal mucosal biopsies, it would be interesting to investigate the following:

- Potentially NGS used in the samples here can only pick up high levels of clonal expansion at the homogenate level, due to low sensitivity. Therefore, I propose for future research to carry out single crypt or cell sequencing (i.e. epithelial cells) to increase the sensitivity and facilitate the detection of changes in low levels of mtDNA mutations from obese patients and age-matched non-obese Controls.

- Taylor (2003) showed that defects in OXPHOS protein function are attributed to differential mechanisms, i.e. in approximately 70% of OXPHOS deficient crypts there is an underlying mtDNA mutation, however in the remaining 30% of crypts no mtDNA mutation is detected. This suggests that there are other potential causes of OXPHOS defects in these crypts, including elevated levels of ROS and inflammation. As the mitochondrial genome did not seem to be the underlying cause of the enhanced levels of OXPHOS deficient crypts in the obese subjects here, it is plausible to assume that they are caused by inflammatory damage and ROS at the protein level rather than the DNA level. Examination of inflammatory markers including TNF-α, IL-6, -8, -12, C-reactive protein, NF-κB, cyclooxygenase-1 and-2, proinflammatory macrophages and markers of oxidative stress (i.e. superoxide anion and nitric oxide) would clarify this. These markers have been shown to positively correlate with obesity and CRC risk (Erlinger et al., 2004, Wei et al., 2005, Gunter, et al., 2006, John et al., 2006, Otani, et al., 2006, Tuo et al., 2016).

Previous data showed that colorectal mucosal crypts with mtDNA mutations show small but significant changes in cell proliferation and apoptosis (Nooteboom et al., 2010). Hence, another area for future research is the investigation of apoptosis in the colorectal mucosal biopsies from the BOCABS Study, to improve our knowledge on the effects of adiposity and weight loss on the state of this tissue. Validated markers utilising immunohistochemistry include cleaved cytokeratin-18 and activated caspase-3 (Duan et al., 2003, Nooteboom et al., 2010).

Finally, it would be interesting to conduct sequencing of the mtDNA in the colorectal mucosal biopsies of participants to the BFU Study and compare the results to the baseline data of the

BORICC Study (Greaves et al., 2010, Nooteboom et al., 2010, Greaves et al., 2012, Greaves et al., 2014). This would be the first investigation on the longitudinal effects of ageing on mitochondrial biomarkers in the colorectal mucosa in a 12+ year follow-up study.

6.4   Conclusions

Results obtained from one outcome measure on miRNA expression and OXPHOS protein abundance support my main hypothesis that biomarkers of CRC risk are elevated in obese compared with normal weight participants. Given the link between obesity and CRC risk, these findings provide further evidence that obesity increases CRC risk on a molecular level and adversely affects underlying mechanisms. Genome-wide sequencing did not reveal any evidence of an increase in mtDNA mutations in the colorectal mucosa of individuals with increased adiposity. The lack of this observation might be due to the fact that the observed OXPHOS defects in the obese are caused by inflammatory damage and ROS at the protein level rather than the DNA level.

The data derived from the other outcome measure on miRNA expression support my second hypothesis that weight loss in the obese has beneficial effects on these biomarkers of CRC risk. To date, it remains to be discovered if intentional weight loss in obese adults modulates CRC risk. My data of epigenetic mechanisms suggests that there is some evidence that weight loss following bariatric surgery reduces CRC risk, but this cannot be supported with the data obtained on mitochondrial markers, as weight loss showed no effects. There is a possibility that the lack of effect by weight loss was due to the insensitivity of the technique to detect low level changes in mtDNA mutations. This warrants more research.

Finally, I also hypothesised that these obesity-related biomarkers of CRC risk are exacerbated by age and ageing, which can be supported by the data obtained here.

This research enables the broadening of our knowledge on the mechanistic pathways of obesity related CRC risk and provides novel evidence on the effects of intentional weight loss by bariatric surgery on these biomarkers in the colon. These findings highlight the further need to investigate the effects and implications of weight loss on CRC risk in adults with increased adiposity.

7 References

AFSHAR, S. 2016a. *Obesity, weight loss surgery and biomarkers of colorectal cancer risk.* Doctor of Philosophy, Newcastle University.

AFSHAR, S. 2016b. *Obesity, weight loss surgery and biomarkers of colorectal cancer risk.* Newcastle University.

AFSHAR, S., KELLY, S. B., SEYMOUR, K., LARA, J., WOODCOCK, S. & MATHERS, J. C. 2014. The effects of bariatric surgery on colorectal cancer risk: systematic review and meta-analysis. *Obes Surg,* 24**,** 1793-9.

AFSHAR, S., KELLY, S. B., SEYMOUR, K., WOODCOCK, S., WERNER, A. D. & MATHERS, J. C. 2016. The Effects of Bariatric Procedures on Bowel Habit. *Obes Surg,* 26**,** 2348-54.

AFSHAR, S., MALCOMSON, F., KELLY, S. B., SEYMOUR, K., WOODCOCK, S. & MATHERS, J. C. 2018. Biomarkers of Colorectal Cancer Risk Decrease 6 months After Roux-en-Y Gastric Bypass Surgery. *Obes Surg,* 28**,** 945-954.

AFSHAR, S., SEYMOUR, K., KELLY, S. B., WOODCOCK, S., VAN HEES, V. T. & MATHERS, J. C. 2017. Changes in physical activity after bariatric surgery: using objective and self-reported measures. *Surg Obes Relat Dis,* 13**,** 474-483.

ALKANDARI, A., ASHRAFIAN, H., SATHYAPALAN, T., SEDMAN, P., DARZI, A., HOLMES, E., ATHANASIOU, T., ATKIN, S. L. & GOODERHAM, N. J. 2018. Improved physiology and metabolic flux after Roux-en-Y gastric bypass is associated with temporal changes in the circulating microRNAome: a longitudinal study in humans. *BMC Obes,* 5**,** 20.

ALLEN, J. A. & COOMBS, M. M. 1980. Covalent binding of polycyclic aromatic compounds to mitochondrial and nuclear DNA. *Nature,* 287**,** 244-5.

AMERES, S. L. & ZAMORE, P. D. 2013. Diversifying microRNA sequence and function. *Nat Rev Mol Cell Biol,* 14**,** 475-88.

ANDERSON, S., BANKIER, A. T., BARRELL, B. G., DE BRUIJN, M. H. L., COULSON, A. R., DROUIN, J., EPERON, I. C., NIERLICH, D. P., ROE, B. A., SANGER, F., SCHREIER, P. H., SMITH, A. J. H., STADEN, R. & YOUNG, I. G. 1981. Sequence and organization of the human mitochondrial genome. *Nature,* 290**,** 457.

ARAVANI, A., DOWNING, A., THOMAS, J. D., LAGERGREN, J., MORRIS, E. J. A. & HULL, M. A. 2018. Obesity surgery and risk of colorectal and other obesity-related cancers: An English population-based cohort study. *Cancer Epidemiol,* 53**,** 99-104.

ARMAGHANY, T., WILSON, J. D., CHU, Q. & MILLS, G. 2012. Genetic alterations in colorectal cancer. *Gastrointest Cancer Res,* 5**,** 19-27.

ARNOLD, M., PANDEYA, N., BYRNES, G., RENEHAN, A. G., STEVENS, G. A., EZZATI, M., FERLAY, J., MIRANDA, J. J., ROMIEU, I., DIKSHIT, R., FORMAN, D. & SOERJOMATARAM, I. 2015. Global burden of cancer attributable to high body-mass index in 2012: a population-based study. *Lancet Oncol,* 16**,** 36-46.

ARNOLD, M., SIERRA, M. S., LAVERSANNE, M., SOERJOMATARAM, I., JEMAL, A. & BRAY, F. 2016. Global patterns and trends in colorectal cancer incidence and mortality. *Gut.*

ASANGANI, I. A., RASHEED, S. A., NIKOLOVA, D. A., LEUPOLD, J. H., COLBURN, N. H., POST, S. & ALLGAYER, H. 2008. MicroRNA-21 (miR-21) post-transcriptionally downregulates tumor suppressor Pdcd4 and stimulates invasion, intravasation and metastasis in colorectal cancer. *Oncogene,* 27**,** 2128-36.

ASCIERTO, P. A., KIRKWOOD, J. M., GROB, J. J., SIMEONE, E., GRIMALDI, A. M., MAIO, M., PALMIERI, G., TESTORI, A., MARINCOLA, F. M. & MOZZILLO, N. 2012. The role of BRAF V600 mutation in melanoma. *J Transl Med,* 10**,** 85.

BACH, D., NAON, D., PICH, S., SORIANO, F. X., VEGA, N., RIEUSSET, J., LAVILLE, M., GUILLET, C., BOIRIE, Y., WALLBERG-HENRIKSSON, H., MANCO, M., CALVANI, M., CASTAGNETO, M., PALACIN, M., MINGRONE, G., ZIERATH, J. R., VIDAL, H. & ZORZANO, A. 2005. Expression of

Mfn2, the Charcot-Marie-Tooth neuropathy type 2A gene, in human skeletal muscle: effects of type 2 diabetes, obesity, weight loss, and the regulatory role of tumor necrosis factor alpha and interleukin-6. *Diabetes,* 54**,** 2685-93.

BAINES, H. L., STEWART, J. B., STAMP, C., ZUPANIC, A., KIRKWOOD, T. B., LARSSON, N. G., TURNBULL, D. M. & GREAVES, L. C. 2014. Similar patterns of clonally expanded somatic mtDNA mutations in the colon of heterozygous mtDNA mutator mice and ageing humans. *Mech Ageing Dev,* 139**,** 22-30.

BANDRÉS, E., CUBEDO, E., AGIRRE, X., MALUMBRES, R., ZÁRATE, R., RAMIREZ, N., ABAJO, A., NAVARRO, A., MORENO, I., MONZÓ, M. & GARCÍA-FONCILLAS, J. 2006. Identification by Real-time PCR of 13 mature microRNAs differentially expressed in colorectal cancer and non-tumoral tissues. *Molecular Cancer,* 5**,** 29.

BEEKEN, R. J., CROKER, H., HEINRICH, M., OBICHERE, A., FINER, N., MURPHY, N., GOLDIN, R., GUPPY, N. J., WILSON, R., FISHER, A., STEPTOE, A., GUNTER, M. J. & WARDLE, J. 2017. The Impact of Diet-Induced Weight Loss on Biomarkers for Colorectal Cancer: An Exploratory Study (INTERCEPT). *Obesity (Silver Spring),* 25 Suppl 2**,** S95-s101.

BENJAMINI, Y. & HOCHBERG, Y. 1995. Controlling the False Discovery Rate: A Practical and Powerful Approach to Multiple Testing. *Journal of the Royal Statistical Society. Series B (Methodological),* 57**,** 289-300.

BENSEN, S., MOTT, L. A., DAIN, B., ROTHSTEIN, R. & BARON, J. 1999. The colonoscopic miss rate and true one-year recurrence of colorectal neoplastic polyps. Polyp Prevention Study Group. *Am J Gastroenterol,* 94**,** 194-9.

BIRCH-MACHIN, M. A. & SWALWELL, H. 2010. How mitochondria record the effects of UV exposure and oxidative stress using human skin as a model tissue. *Mutagenesis,* 25**,** 101-7.

BLAND, J. M. & ALTMAN, D. G. 1996. Transforming data. *Bmj,* 312**,** 770.

BOEKE, C. E., STORFER-ISSER, A., REDLINE, S. & TAVERAS, E. M. 2014. Childhood sleep duration and quality in relation to leptin concentration in two cohort studies. *Sleep,* 37**,** 613-20.

BOLMESON, C., ESGUERRA, J. L., SALEHI, A., SPEIDEL, D., ELIASSON, L. & CILIO, C. M. 2011. Differences in islet-enriched miRNAs in healthy and glucose intolerant human subjects. *Biochem Biophys Res Commun,* 404**,** 16-22.

BOULET, L., KARPATI, G. & SHOUBRIDGE, E. A. 1992. Distribution and threshold expression of the tRNA(Lys) mutation in skeletal muscle of patients with myoclonic epilepsy and ragged-red fibers (MERRF). *Am J Hum Genet,* 51**,** 1187-200.

BOURNAT, J. C. & BROWN, C. W. 2010. Mitochondrial dysfunction in obesity. *Curr Opin Endocrinol Diabetes Obes,* 17**,** 446-52.

BRAUN, C. J., ZHANG, X., SAVELYEVA, I., WOLFF, S., MOLL, U. M., SCHEPELER, T., ORNTOFT, T. F., ANDERSEN, C. L. & DOBBELSTEIN, M. 2008. p53-Responsive micrornas 192 and 215 are capable of inducing cell cycle arrest. *Cancer Res,* 68**,** 10094-104.

BREININGER, S. P., MALCOMSON, F. C., AFSHAR, S., TURNBULL, D. M., GREAVES, L. & MATHERS, J. C. 2019. Effects of obesity and weight loss on mitochondrial structure and function and implications for colorectal cancer risk. *Proceedings of the Nutrition Society***,** 1-12.

CAKIR, Y., YANG, Z., KNIGHT, C. A., POMPILIUS, M., WESTBROOK, D., BAILEY, S. M., PINKERTON, K. E. & BALLINGER, S. W. 2007. Effect of alcohol and tobacco smoke on mtDNA damage and atherogenesis. *Free Radic Biol Med,* 43**,** 1279-88.

CAMASTRA, S., VITALI, A., ANSELMINO, M., GASTALDELLI, A., BELLINI, R., BERTA, R., SEVERI, I., BALDI, S., ASTIARRAGA, B., BARBATELLI, G., CINTI, S. & FERRANNINI, E. 2017. Muscle and adipose tissue morphology, insulin sensitivity and beta-cell function in diabetic and nondiabetic obese patients: effects of bariatric surgery. *Scientific Reports,* 7**,** 9007.

CAPPUZZO, F., SACCONI, A., LANDI, L., LUDOVINI, V., BIAGIONI, F., D'INCECCO, A., CAPODANNO, A., SALVINI, J., CORGNA, E., CUPINI, S., BARBARA, C., FONTANINI, G., CRINO, L. & BLANDINO, G. 2014. MicroRNA signature in metastatic colorectal cancer patients treated with anti-EGFR monoclonal antibodies. *Clin Colorectal Cancer,* 13**,** 37-45.e4.

CARLING, P. J., CREE, L. M. & CHINNERY, P. F. 2011. The implications of mitochondrial DNA copy number regulation during embryogenesis. *Mitochondrion,* 11**,** 686-92.

CASAGRANDE, D. S., ROSA, D. D., UMPIERRE, D., SARMENTO, R. A., RODRIGUES, C. G. & SCHAAN, B. D. 2014. Incidence of Cancer Following Bariatric Surgery: Systematic Review and Meta-analysis. *Obesity Surgery,* 24**,** 1499-1509.

CASE, J. T. & WALLACE, D. C. 1981. Maternal inheritance of mitochondrial DNA polymorphisms in cultured human fibroblasts. *Somatic Cell Genet,* 7**,** 103-8.

CHANG, H. Y., YE, S. P., PAN, S. L., KUO, T. T., LIU, B. C., CHEN, Y. L. & HUANG, T. C. 2017. Overexpression of miR-194 Reverses HMGA2-driven Signatures in Colorectal Cancer. *Theranostics,* 7**,** 3889-3900.

CHEN, D.-L., LU, Y.-X., ZHANG, J.-X., WEI, X.-L., WANG, F., ZENG, Z.-L., PAN, Z.-Z., YUAN, Y.-F., WANG, F.-H., PELICANO, H., CHIAO, P. J., HUANG, P., XIE, D., LI, Y.-H., JU, H.-Q. & XU, R.-H. 2017. Long non-coding RNA UICLM promotes colorectal cancer liver metastasis by acting as a ceRNA for microRNA-215 to regulate ZEB2 expression. *Theranostics,* 7**,** 4836-4849.

CHEN, L., CUI, J., HOU, J., LONG, J., LI, C. & LIU, L. 2014a. A novel negative regulator of adipogenesis: microRNA-363. *Stem Cells,* 32**,** 510-20.

CHEN, L., SUN, H., WANG, C., YANG, Y., ZHANG, M. & WONG, G. 2018. miRNA arm switching identifies novel tumour biomarkers. *EBioMedicine,* 38**,** 37-46.

CHEN, Q., VAZQUEZ, E. J., MOGHADDAS, S., HOPPEL, C. L. & LESNEFSKY, E. J. 2003. Production of reactive oxygen species by mitochondria: central role of complex III. *J Biol Chem,* 278**,** 36027-31.

CHEN, T., YAO, L. Q., SHI, Q., REN, Z., YE, L. C., XU, J. M., ZHOU, P. H. & ZHONG, Y. S. 2014b. MicroRNA-31 contributes to colorectal cancer development by targeting factor inhibiting HIF-1alpha (FIH-1). *Cancer Biol Ther,* 15**,** 516-23.

CHEN, Z., HAN, S., HUANG, W., WU, J., LIU, Y., CAI, S., HE, Y., WU, S. & SONG, W. 2016. MicroRNA-215 suppresses cell proliferation, migration and invasion of colon cancer by repressing Yin-Yang 1. *Biochem Biophys Res Commun,* 479**,** 482-488.

CHENG, Z. & ALMEIDA, F. A. 2014a. Mitochondrial alteration in type 2 diabetes and obesity: An epigenetic link. *Cell Cycle,* 13**,** 890-897.

CHENG, Z. & ALMEIDA, F. A. 2014b. Mitochondrial alteration in type 2 diabetes and obesity: an epigenetic link. *Cell Cycle,* 13**,** 890-7.

CHOO, H. J., KIM, J. H., KWON, O. B., LEE, C. S., MUN, J. Y., HAN, S. S., YOON, Y. S., YOON, G., CHOI, K. M. & KO, Y. G. 2006. Mitochondria are impaired in the adipocytes of type 2 diabetic mice. *Diabetologia,* 49**,** 784-791.

CHOO, K. B., SOON, Y. L., NGUYEN, P. N., HIEW, M. S. & HUANG, C. J. 2014. MicroRNA-5p and -3p co-expression and cross-targeting in colon cancer cells. *J Biomed Sci,* 21**,** 95.

CHOWDHARI, S. & SAINI, N. 2014. hsa-miR-4516 mediated downregulation of STAT3/CDK6/UBE2N plays a role in PUVA induced apoptosis in keratinocytes. *J Cell Physiol,* 229**,** 1630-8.

CIVITARESE, A. E., CARLING, S., HEILBRONN, L. K., HULVER, M. H., UKROPCOVA, B., DEUTSCH, W. A., SMITH, S. R. & RAVUSSIN, E. 2007. Calorie restriction increases muscle mitochondrial biogenesis in healthy humans. *PLoS Med,* 4**,** e76.

CLEVERS, H., LOH, K. M. & NUSSE, R. 2014. Stem cell signaling. An integral program for tissue renewal and regeneration: Wnt signaling and stem cell control. *Science,* 346**,** 1248012.

COEN, P. M., MENSHIKOVA, E. V., DISTEFANO, G., ZHENG, D., TANNER, C. J., STANDLEY, R. A., HELBLING, N. L., DUBIS, G. S., RITOV, V. B., XIE, H., DESIMONE, M. E., SMITH, S. R., STEFANOVIC-RACIC, M., TOLEDO, F. G., HOUMARD, J. A. & GOODPASTER, B. H. 2015. Exercise and Weight Loss Improve Muscle Mitochondrial Respiration, Lipid Partitioning, and Insulin Sensitivity After Gastric Bypass Surgery. *Diabetes,* 64**,** 3737-50.

CORDES, K. R., SHEEHY, N. T., WHITE, M. P., BERRY, E. C., MORTON, S. U., MUTH, A. N., LEE, T. H., MIANO, J. M., IVEY, K. N. & SRIVASTAVA, D. 2009. miR-145 and miR-143 regulate smooth muscle cell fate and plasticity. *Nature,* 460**,** 705-10.

CUI, T., BELL, E. H., MCELROY, J., BECKER, A. P., GULATI, P. M., GEURTS, M., MLADKOVA, N., GRAY, A., LIU, K., YANG, L., LIU, Z., FLEMING, J. L., HAQUE, S. J., BARNHOLTZ-SLOAN, J. S., LIGON, K. L., BEROUKHIM, R., ROBE, P. & CHAKRAVARTI, A. 2019. miR-4516 predicts poor prognosis and functions as a novel oncogene via targeting PTPN14 in human glioblastoma. *Oncogene,* 38**,** 2923-2936.

DE LUCIA, C., KOMICI, K., BORGHETTI, G., FEMMINELLA, G. D., BENCIVENGA, L., CANNAVO, A., CORBI, G., FERRARA, N., HOUSER, S. R., KOCH, W. J. & RENGO, G. 2017. microRNA in Cardiovascular Aging and Age-Related Cardiovascular Diseases. *Frontiers in medicine,* 4**,** 74-74.

DE MELLO, A. H., COSTA, A. B., ENGEL, J. D. G. & REZIN, G. T. 2018. Mitochondrial dysfunction in obesity. *Life Sciences,* 192**,** 26-32.

DIMAURO, S., SCHON, E. A., CARELLI, V. & HIRANO, M. 2013. The clinical maze of mitochondrial neurology. *Nat Rev Neurol,* 9**,** 429-44.

DING, L., LAN, Z., XIONG, X., AO, H., FENG, Y., GU, H., YU, M. & CUI, Q. 2018. The Dual Role of MicroRNAs in Colorectal Cancer Progression. *International journal of molecular sciences,* 19**,** 2791.

DONG, Y., ZHOU, J., ZHU, Y., LUO, L., HE, T., HU, H., LIU, H., ZHANG, Y., LUO, D., XU, S., XU, L., LIU, J., ZHANG, J. & TENG, Z. 2017. Abdominal obesity and colorectal cancer risk: systematic review and meta-analysis of prospective studies. *Bioscience reports,* 37**,** BSR20170945.

DORAK, M. T. 2006. *Real-time PCR*, Taylor and Francis.

DOUAIHER, J., RAVIPATI, A., GRAMS, B., CHOWDHURY, S., ALATISE, O. & ARE, C. 2017. Colorectal cancer-global burden, trends, and geographical variations. *J Surg Oncol,* 115**,** 619-630.

DUAN, W. R., GARNER, D. S., WILLIAMS, S. D., FUNCKES-SHIPPY, C. L., SPATH, I. S. & BLOMME, E. A. 2003. Comparison of immunohistochemistry for activated caspase-3 and cleaved cytokeratin 18 with the TUNEL method for quantification of apoptosis in histological sections of PC-3 subcutaneous xenografts. *The Journal of Pathology,* 199**,** 221-228.

DUPONT, C., ARMANT, D. R. & BRENNER, C. A. 2009. Epigenetics: definition, mechanisms and clinical perspective. *Seminars in reproductive medicine,* 27**,** 351-357.

EARLE, J. S. L., LUTHRA, R., ROMANS, A., ABRAHAM, R., ENSOR, J., YAO, H. & HAMILTON, S. R. 2010. Association of MicroRNA Expression with Microsatellite Instability Status in Colorectal Adenocarcinoma. *The Journal of Molecular Diagnostics,* 12**,** 433-440.

EJARQUE, M., CEPERUELO-MALLAFRÉ, V., SERENA, C., MAYMO-MASIP, E., DURAN, X., DÍAZ-RAMOS, A., MILLAN-SCHEIDING, M., NÚÑEZ-ÁLVAREZ, Y., NÚÑEZ-ROA, C., GAMA, P., GARCIA-ROVES, P. M., PEINADO, M. A., GIMBLE, J. M., ZORZANO, A., VENDRELL, J. & FERNÁNDEZ-VELEDO, S. 2018. Adipose tissue mitochondrial dysfunction in human obesity is linked to a specific DNA methylation signature in adipose-derived stem cells. *International Journal of Obesity*.

EMBLEY, T. M. & MARTIN, W. 2006. Eukaryotic evolution, changes and challenges. *Nature,* 440**,** 623-30.

ENRIGHT, A. J. & VITSIOS, D. M. 2015. Chimira: analysis of small RNA sequencing data and microRNA modifications. *Bioinformatics,* 31**,** 3365-3367.

EPPERT, K., SCHERER, S. W., OZCELIK, H., PIRONE, R., HOODLESS, P., KIM, H., TSUI, L. C., BAPAT, B., GALLINGER, S., ANDRULIS, I. L., THOMSEN, G. H., WRANA, J. L. & ATTISANO, L. 1996. MADR2 maps to 18q21 and encodes a TGFbeta-regulated MAD-related protein that is functionally mutated in colorectal carcinoma. *Cell,* 86**,** 543-52.

ERICSON, N. G., KULAWIEC, M., VERMULST, M., SHEAHAN, K., O'SULLIVAN, J., SALK, J. J. & BIELAS, J. H. 2012. Decreased mitochondrial DNA mutagenesis in human colorectal cancer. *PLoS Genet,* 8**,** e1002689.

ERLINGER, T. P., PLATZ, E. A., RIFAI, N. & HELZLSOUER, K. J. 2004. C-reactive protein and the risk of incident colorectal cancer. *Jama,* 291**,** 585-90.

ESAU, C., KANG, X., PERALTA, E., HANSON, E., MARCUSSON, E. G., RAVICHANDRAN, L. V., SUN, Y., KOO, S., PERERA, R. J., JAIN, R., DEAN, N. M., FREIER, S. M., BENNETT, C. F., LOLLO, B. &

GRIFFEY, R. 2004. MicroRNA-143 regulates adipocyte differentiation. *J Biol Chem,* 279**,** 52361-5.

ESLAMIZADEH, S., HEIDARI, M., AGAH, S., FAGHIHLOO, E., GHAZI, H., MIRZAEI, A. & AKBARI, A. 2018. The Role of MicroRNA Signature as Diagnostic Biomarkers in Different Clinical Stages of Colorectal Cancer. *Cell J,* 20**,** 220-230.

ESTELLER, M., SPARKS, A., TOYOTA, M., SANCHEZ-CESPEDES, M., CAPELLA, G., PEINADO, M. A., GONZALEZ, S., TARAFA, G., SIDRANSKY, D., MELTZER, S. J., BAYLIN, S. B. & HERMAN, J. G. 2000. Analysis of adenomatous polyposis coli promoter hypermethylation in human cancer. *Cancer Res,* 60**,** 4366-71.

FALTEJSKOVA, P., SVOBODA, M., SRUTOVA, K., MLCOCHOVA, J., BESSE, A., NEKVINDOVA, J., RADOVA, L., FABIAN, P., SLABA, K., KISS, I., VYZULA, R. & SLABY, O. 2012. Identification and functional screening of microRNAs highly deregulated in colorectal cancer. *J Cell Mol Med,* 16**,** 2655-66.

FANG, S. & FANG, X. 2016. Advances in glucose metabolism research in colorectal cancer. *Biomedical reports,* 5**,** 289-295.

FEARON, E. R. 2011. Molecular genetics of colorectal cancer. *Annu Rev Pathol,* 6**,** 479-507.

FERLAY, J., SOERJOMATARAM, I., DIKSHIT, R., ESER, S., MATHERS, C., REBELO, M., PARKIN, D. M., FORMAN, D. & BRAY, F. 2015. Cancer incidence and mortality worldwide: sources, methods and major patterns in GLOBOCAN 2012. *Int J Cancer,* 136**,** E359-86.

FERNANDEZ-SILVA, P., ENRIQUEZ, J. A. & MONTOYA, J. 2003. Replication and transcription of mammalian mitochondrial DNA. *Exp Physiol,* 88**,** 41-56.

FERNSTROM, M., BAKKMAN, L., LOOGNA, P., ROOYACKERS, O., SVENSSON, M., JAKOBSSON, T., BRANDT, L. & LAGERROS, Y. T. 2016. Improved Muscle Mitochondrial Capacity Following Gastric Bypass Surgery in Obese Subjects. *Obes Surg,* 26**,** 1391-7.

FLOOD, D. M., WEISS, N. S., COOK, L. S., EMERSON, J. C., SCHWARTZ, S. M. & POTTER, J. D. 2000. Colorectal cancer incidence in Asian migrants to the United States and their descendants. *Cancer Causes & Control,* 11**,** 403-411.

FREISLING, H., ARNOLD, M., SOERJOMATARAM, I., O'DOHERTY, M. G., ORDONEZ-MENA, J. M., BAMIA, C., KAMPMAN, E., LEITZMANN, M., ROMIEU, I., KEE, F., TSILIDIS, K., TJONNELAND, A., TRICHOPOULOU, A., BOFFETTA, P., BENETOU, V., BUENO-DE-MESQUITA, H. B. A., HUERTA, J. M., BRENNER, H., WILSGAARD, T. & JENAB, M. 2017. Comparison of general obesity and measures of body fat distribution in older adults in relation to cancer risk: meta-analysis of individual participant data of seven prospective cohorts in Europe. *Br J Cancer,* 116**,** 1486-1497.

FRIEDMAN, R. C., FARH, K. K., BURGE, C. B. & BARTEL, D. P. 2009. Most mammalian mRNAs are conserved targets of microRNAs. *Genome Res,* 19**,** 92-105.

GALLAGHER, I. J., SCHEELE, C., KELLER, P., NIELSEN, A. R., REMENYI, J., FISCHER, C. P., RODER, K., BABRAJ, J., WAHLESTEDT, C., HUTVAGNER, G., PEDERSEN, B. K. & TIMMONS, J. A. 2010. Integration of microRNA changes in vivo identifies novel molecular features of muscle insulin resistance in type 2 diabetes. *Genome Med,* 2**,** 9.

GAO, C. L., ZHU, C., ZHAO, Y. P., CHEN, X. H., JI, C. B., ZHANG, C. M., ZHU, J. G., XIA, Z. K., TONG, M. L. & GUO, X. R. 2010. Mitochondrial dysfunction is induced by high levels of glucose and free fatty acids in 3T3-L1 adipocytes. *Mol Cell Endocrinol,* 320**,** 25-33.

GAO, S., ZHOU, F., ZHAO, C., MA, Z., JIA, R., LIANG, S., ZHANG, M., ZHU, X., ZHANG, P., WANG, L., SU, F., ZHAO, J., LIU, G., PENG, B. & FENG, X. 2016. Gastric cardia adenocarcinoma microRNA profiling in Chinese patients. *Tumour Biol,* 37**,** 9411-22.

GEIERSBACH, K. B. & SAMOWITZ, W. S. 2011. Microsatellite instability and colorectal cancer. *Arch Pathol Lab Med,* 135**,** 1269-77.

GIARDINA, S., HERNANDEZ-ALONSO, P., DIAZ-LOPEZ, A., SALAS-HUETOS, A., SALAS-SALVADO, J. & BULLO, M. 2019. Changes in circulating miRNAs in healthy overweight and obese subjects: Effect of diet composition and weight loss. *Clin Nutr,* 38**,** 438-443.

GILKERSON, R., BRAVO, L., GARCIA, I., GAYTAN, N., HERRERA, A., MALDONADO, A. & QUINTANILLA, B. 2013. The mitochondrial nucleoid: integrating mitochondrial DNA into cellular homeostasis. *Cold Spring Harb Perspect Biol,* 5**,** a011080.

GOLDBERG, A. D., ALLIS, C. D. & BERNSTEIN, E. 2007. Epigenetics: a landscape takes shape. *Cell,* 128**,** 635-8.

GORMAN, G. S., CHINNERY, P. F., DIMAURO, S., HIRANO, M., KOGA, Y., MCFARLAND, R., SUOMALAINEN, A., THORBURN, D. R., ZEVIANI, M. & TURNBULL, D. M. 2016. Mitochondrial diseases. *Nat Rev Dis Primers,* 2**,** 16080.

GRADY, W. M., RAJPUT, A., MYEROFF, L., LIU, D. F., KWON, K., WILLIS, J. & MARKOWITZ, S. 1998. Mutation of the type II transforming growth factor-beta receptor is coincident with the transformation of human colon adenomas to malignant carcinomas. *Cancer Res,* 58**,** 3101-4.

GREAVES, L. C., BARRON, M. J., PLUSA, S., KIRKWOOD, T. B., MATHERS, J. C., TAYLOR, R. W. & TURNBULL, D. M. 2010. Defects in multiple complexes of the respiratory chain are present in ageing human colonic crypts. *Exp Gerontol,* 45**,** 573-9.

GREAVES, L. C., ELSON, J. L., NOOTEBOOM, M., GRADY, J. P., TAYLOR, G. A., TAYLOR, R. W., MATHERS, J. C., KIRKWOOD, T. B. L. & TURNBULL, D. M. 2012. Comparison of Mitochondrial Mutation Spectra in Ageing Human Colonic Epithelium and Disease: Absence of Evidence for Purifying Selection in Somatic Mitochondrial DNA Point Mutations. *PLOS Genetics,* 8**,** e1003082.

GREAVES, L. C., NOOTEBOOM, M., ELSON, J. L., TUPPEN, H. A., TAYLOR, G. A., COMMANE, D. M., ARASARADNAM, R. P., KHRAPKO, K., TAYLOR, R. W., KIRKWOOD, T. B., MATHERS, J. C. & TURNBULL, D. M. 2014. Clonal expansion of early to mid-life mitochondrial DNA point mutations drives mitochondrial dysfunction during human ageing. *PLoS Genet,* 10**,** e1004620.

GUNTER, M. J., STOLZENBERG-SOLOMON, R., CROSS, A. J., LEITZMANN, M. F., WEINSTEIN, S., WOOD, R. J., VIRTAMO, J., TAYLOR, P. R., ALBANES, D. & SINHA, R. 2006. A prospective study of serum C-reactive protein and colorectal cancer risk in men. *Cancer Res,* 66**,** 2483-7.

HANAHAN, D. & WEINBERG, R. A. 2011. Hallmarks of cancer: the next generation. *Cell,* 144**,** 646-74.

HANDSCHIN, C. & SPIEGELMAN, B. M. 2006. Peroxisome proliferator-activated receptor gamma coactivator 1 coactivators, energy homeostasis, and metabolism. *Endocr Rev,* 27**,** 728-35.

HARDY, T. M. & TOLLEFSBOL, T. O. 2011. Epigenetic diet: impact on the epigenome and cancer. *Epigenomics,* 3**,** 503-18.

HE, Y., WU, J., DRESSMAN, D. C., IACOBUZIO-DONAHUE, C., MARKOWITZ, S. D., VELCULESCU, V. E., DIAZ, L. A., JR., KINZLER, K. W., VOGELSTEIN, B. & PAPADOPOULOS, N. 2010. Heteroplasmic mitochondrial DNA mutations in normal and tumour cells. *Nature,* 464**,** 610-4.

HEINONEN, S., BUZKOVA, J., MUNIANDY, M., KAKSONEN, R., OLLIKAINEN, M., ISMAIL, K., HAKKARAINEN, A., LUNDBOM, J., LUNDBOM, N., VUOLTEENAHO, K., MOILANEN, E., KAPRIO, J., RISSANEN, A., SUOMALAINEN, A. & PIETILAINEN, K. H. 2015. Impaired Mitochondrial Biogenesis in Adipose Tissue in Acquired Obesity. *Diabetes,* 64**,** 3135-45.

HENEGHAN, H. M., MILLER, N. & KERIN, M. J. 2010. Role of microRNAs in obesity and the metabolic syndrome. *Obes Rev,* 11**,** 354-61.

HIBNER, G., KIMSA-FURDZIK, M. & FRANCUZ, T. 2018. Relevance of MicroRNAs as Potential Diagnostic and Prognostic Markers in Colorectal Cancer. *Int J Mol Sci,* 19.

HINOUE, T., WEISENBERGER, D. J., LANGE, C. P. E., SHEN, H., BYUN, H.-M., VAN DEN BERG, D., MALIK, S., PAN, F., NOUSHMEHR, H., VAN DIJK, C. M., TOLLENAAR, R. A. E. M. & LAIRD, P. W. 2012. Genome-scale analysis of aberrant DNA methylation in colorectal cancer. *Genome research,* 22**,** 271-282.

HIXSON, L. J., FENNERTY, M. B., SAMPLINER, R. E. & GAREWAL, H. S. 1991. Prospective blinded trial of the colonoscopic miss-rate of large colorectal polyps. *Gastrointest Endosc,* 37**,** 125-7.

HOHENSINNER, P. J., KAUN, C., EBENBAUER, B., HACKL, M., DEMYANETS, S., RICHTER, D., PRAGER, M., WOJTA, J. & REGA-KAUN, G. 2018. Reduction of Premature Aging Markers After Gastric Bypass Surgery in Morbidly Obese Patients. *Obes Surg,* 28**,** 2804-2810.

HUAN, T., CHEN, G., LIU, C., BHATTACHARYA, A., RONG, J., CHEN, B. H., SESHADRI, S., TANRIVERDI, K., FREEDMAN, J. E., LARSON, M. G., MURABITO, J. M. & LEVY, D. 2018. Age-associated microRNA expression in human peripheral blood is associated with all-cause mortality and age-related traits. *Aging cell,* 17**,** e12687.

HUANG, F., WEN, C., ZHUANSUN, Y., HUANG, L., CHEN, W., YANG, X. & LIU, H. 2018. A novel long noncoding RNA OECC promotes colorectal cancer development and is negatively regulated by miR-143-3p. *Biochem Biophys Res Commun,* 503**,** 2949-2955.

HUBAL, M. J., NADLER, E. P., FERRANTE, S. C., BARBERIO, M. D., SUH, J. H., WANG, J., DOHM, G. L., PORIES, W. J., MIETUS-SNYDER, M. & FREISHTAT, R. J. 2017. Circulating adipocyte-derived exosomal MicroRNAs associated with decreased insulin resistance after gastric bypass. *Obesity (Silver Spring),* 25**,** 102-110.

HULSMANS, M., SINNAEVE, P., VAN DER SCHUEREN, B., MATHIEU, C., JANSSENS, S. & HOLVOET, P. 2012. Decreased miR-181a expression in monocytes of obese patients is associated with the occurrence of metabolic syndrome and coronary artery disease. *J Clin Endocrinol Metab,* 97**,** E1213-8.

HUMPHRIES, A. & WRIGHT, N. A. 2008. Colonic crypt organization and tumorigenesis. *Nat Rev Cancer,* 8**,** 415-24.

HUNTZINGER, E. & IZAURRALDE, E. 2011. Gene silencing by microRNAs: contributions of translational repression and mRNA decay. *Nat Rev Genet,* 12**,** 99-110.

IACOMINO, G. & SIANI, A. 2017. Role of microRNAs in obesity and obesity-related diseases. *Genes & nutrition,* 12**,** 23-23.

ISHIKAWA, K., TAKENAGA, K., AKIMOTO, M., KOSHIKAWA, N., YAMAGUCHI, A., IMANISHI, H., NAKADA, K., HONMA, Y. & HAYASHI, J. 2008. ROS-generating mitochondrial DNA mutations can regulate tumor cell metastasis. *Science,* 320**,** 661-4.

ITO, M., MITSUHASHI, K., IGARASHI, H., NOSHO, K., NAITO, T., YOSHII, S., TAKAHASHI, H., FUJITA, M., SUKAWA, Y., YAMAMOTO, E., TAKAHASHI, T., ADACHI, Y., NOJIMA, M., SASAKI, Y., TOKINO, T., BABA, Y., MARUYAMA, R., SUZUKI, H., IMAI, K., YAMAMOTO, H. & SHINOMURA, Y. 2014. MicroRNA-31 expression in relation to BRAF mutation, CpG island methylation and colorectal continuum in serrated lesions. *Int J Cancer,* 135**,** 2507-15.

JAENISCH, R. & BIRD, A. 2003. Epigenetic regulation of gene expression: how the genome integrates intrinsic and environmental signals. *Nat Genet,* 33 Suppl**,** 245-54.

JAHANSOUZ, C., SERROT, F. J., FROHNERT, B. I., FONCEA, R. E., DORMAN, R. B., SLUSAREK, B., LESLIE, D. B., BERNLOHR, D. A. & IKRAMUDDIN, S. 2015. Roux-en-Y Gastric Bypass Acutely Decreases Protein Carbonylation and Increases Expression of Mitochondrial Biogenesis Genes in Subcutaneous Adipose Tissue. *Obes Surg,* 25**,** 2376-85.

JASS, J. R., YOUNG, J. & LEGGETT, B. A. 2002. Evolution of colorectal cancer: change of pace and change of direction. *J Gastroenterol Hepatol,* 17**,** 17-26.

JEMAL, A., SIEGEL, R., XU, J. & WARD, E. 2010. Cancer Statistics, 2010. *CA: A Cancer Journal for Clinicians,* 60**,** 277-300.

JING, H. Q., XU, H. W., WAN, J. M., YANG, Y., DING, H., CHEN, M. Y., LI, L. Z., LV, P., HU, J. W. & YANG, J. Y. 2014. Effect of Breastfeeding on Childhood BMI and Obesity The China Family Panel Studies. *Medicine,* 93**,** 7.

JOHN, B. J., IRUKULLA, S., ABULAFI, A. M., KUMAR, D. & MENDALL, M. A. 2006. Systematic review: adipose tissue, obesity and gastrointestinal diseases. *Aliment Pharmacol Ther,* 23**,** 1511-23.

JOHNS, D. R. 1995. Seminars in medicine of the Beth Israel Hospital, Boston. Mitochondrial DNA and disease. *N Engl J Med,* 333**,** 638-44.

JONAS, S. & IZAURRALDE, E. 2015. Towards a molecular understanding of microRNA-mediated gene silencing. *Nat Rev Genet,* 16**,** 421-33.

KAAR, J. L., CRUME, T., BRINTON, J. T., BISCHOFF, K. J., MCDUFFIE, R. & DABELEA, D. 2014. Maternal Obesity, Gestational Weight Gain, and Offspring Adiposity: The Exploring Perinatal Outcomes among Children Study. *Journal of Pediatrics,* 165**,** 509-515.

KALTENBACH, T., FRIEDLAND, S. & SOETIKNO, R. 2008. A randomised tandem colonoscopy trial of narrow band imaging versus white light examination to compare neoplasia miss rates. *Gut,* 57**,** 1406-12.

KANT, P., FAZAKERLEY, R. & HULL, M. A. 2013. Faecal calprotectin levels before and after weight loss in obese and overweight subjects. *Int J Obes (Lond),* 37**,** 317-9.

KANT, P., SAINSBURY, A., REED, K. R., POLLARD, S. G., SCOTT, N., CLARKE, A. R., COLETTA, P. L. & HULL, M. A. 2011. Rectal epithelial cell mitosis and expression of macrophage migration inhibitory factor are increased 3 years after Roux-en-Y gastric bypass (RYGB) for morbid obesity: implications for long-term neoplastic risk following RYGB. *Gut,* 60**,** 893-901.

KANTOR, E. D., UDUMYAN, R., SIGNORELLO, L. B., GIOVANNUCCI, E. L., MONTGOMERY, S. & FALL, K. 2016. Adolescent body mass index and erythrocyte sedimentation rate in relation to colorectal cancer risk. *Gut,* 65**,** 1289-95.

KARAAYVAZ, M., PAL, T., SONG, B., ZHANG, C., GEORGAKOPOULOS, P., MEHMOOD, S., BURKE, S., SHROYER, K. & JU, J. 2011. Prognostic significance of miR-215 in colon cancer. *Clin Colorectal Cancer,* 10**,** 340-7.

KARAHALIOS, A., ENGLISH, D. R. & SIMPSON, J. A. 2015. Weight change and risk of colorectal cancer: a systematic review and meta-analysis. *Am J Epidemiol,* 181**,** 832-45.

KARIN, M., CAO, Y., GRETEN, F. R. & LI, Z. W. 2002. NF-kappaB in cancer: from innocent bystander to major culprit. *Nat Rev Cancer,* 2**,** 301-10.

KENNEDY, S. R., SALK, J. J., SCHMITT, M. W. & LOEB, L. A. 2013. Ultra-sensitive sequencing reveals an age-related increase in somatic mitochondrial mutations that are inconsistent with oxidative damage. *PLoS Genet,* 9**,** e1003794.

KENT, O. A., MCCALL, M. N., CORNISH, T. C. & HALUSHKA, M. K. 2014. Lessons from miR-143/145: the importance of cell-type localization of miRNAs. *Nucleic Acids Research,* 42**,** 7528-7538.

KENT, O. A., MENDELL, J. T. & ROTTAPEL, R. 2016. Transcriptional Regulation of miR-31 by Oncogenic KRAS Mediates Metastatic Phenotypes by Repressing RASA1. *Molecular Cancer Research,* 14**,** 267.

KEUM, N., GREENWOOD, D. C., LEE, D. H., KIM, R., AUNE, D., JU, W., HU, F. B. & GIOVANNUCCI, E. L. 2015a. Adult weight gain and adiposity-related cancers: a dose-response meta-analysis of prospective observational studies. *J Natl Cancer Inst,* 107.

KEUM, N., LEE, D. H., KIM, R., GREENWOOD, D. C. & GIOVANNUCCI, E. L. 2015b. Visceral adiposity and colorectal adenomas: dose-response meta-analysis of observational studies. *Ann Oncol,* 26**,** 1101-9.

KHELLA, H. W., BAKHET, M., ALLO, G., JEWETT, M. A., GIRGIS, A. H., LATIF, A., GIRGIS, H., VON BOTH, I., BJARNASON, G. A. & YOUSEF, G. M. 2013. miR-192, miR-194 and miR-215: a convergent microRNA network suppressing tumor progression in renal cell carcinoma. *Carcinogenesis,* 34**,** 2231-9.

KHVOROVA, A., REYNOLDS, A. & JAYASENA, S. D. 2003. Functional siRNAs and miRNAs exhibit strand bias. *Cell,* 115**,** 209-16.

KING, M. P. & ATTARDI, G. 1989. Human cells lacking mtDNA: repopulation with exogenous mitochondria by complementation. *Science,* 246**,** 500-3.

KIRALY, O., GONG, G., OLIPITZ, W., MUTHUPALANI, S. & ENGELWARD, B. P. 2015. Inflammation-induced cell proliferation potentiates DNA damage-induced mutations in vivo. *PLoS Genet,* 11**,** e1004901.

KLOTING, N., BERTHOLD, S., KOVACS, P., SCHON, M. R., FASSHAUER, M., RUSCHKE, K., STUMVOLL, M. & BLUHER, M. 2009. MicroRNA expression in human omental and subcutaneous adipose tissue. *PLoS One,* 4**,** e4699.

KOBAYASHI, S., YAMADA-OKABE, H., SUZUKI, M., NATORI, O., KATO, A., MATSUBARA, K., JAU CHEN, Y., YAMAZAKI, M., FUNAHASHI, S., YOSHIDA, K., HASHIMOTO, E., WATANABE, Y., MUTOH, H., ASHIHARA, M., KATO, C., WATANABE, T., YOSHIKUBO, T., TAMAOKI, N., OCHIYA, T., KURODA, M., LEVINE, A. J. & YAMAZAKI, T. 2012. LGR5-positive colon cancer stem cells interconvert with drug-resistant LGR5-negative cells and are capable of tumor reconstitution. *Stem Cells,* 30**,** 2631-44.

KOBOLDT, D. C., CHEN, K., WYLIE, T., LARSON, D. E., MCLELLAN, M. D., MARDIS, E. R., WEINSTOCK, G. M., WILSON, R. K. & DING, L. 2009. VarScan: variant detection in massively parallel sequencing of individual and pooled samples. *Bioinformatics,* 25**,** 2283-5.

KOLONEL, L. N., HANKIN, J. H. & NOMURA, A. M. 1985. Multiethnic studies of diet, nutrition, and cancer in Hawaii. *Princess Takamatsu Symp,* 16**,** 29-40.

KRAS, K. A., LANGLAIS, P. R., HOFFMAN, N., ROUST, L. R., BENJAMIN, T. R., DE FILIPPIS, E. A., DINU, V. & KATSANOS, C. S. 2018. Obesity modifies the stoichiometry of mitochondrial proteins in a way that is distinct to the subcellular localization of the mitochondria in skeletal muscle. *Metabolism,* 89**,** 18-26.

KRISTENSEN, M. M., DAVIDSEN, P. K., VIGELSO, A., HANSEN, C. N., JENSEN, L. J., JESSEN, N., BRUUN, J. M., DELA, F. & HELGE, J. W. 2017. miRNAs in human subcutaneous adipose tissue: Effects of weight loss induced by hypocaloric diet and exercise. *Obesity (Silver Spring),* 25**,** 572-580.

KRITCHEVSKY, S. B., BEAVERS, K. M., MILLER, M. E., SHEA, M. K., HOUSTON, D. K., KITZMAN, D. W. & NICKLAS, B. J. 2015. Intentional Weight Loss and All-Cause Mortality: A Meta-Analysis of Randomized Clinical Trials. *PLOS ONE,* 10**,** e0121993.

KURIHARA, H., MARUYAMA, R., ISHIGURO, K., KANNO, S., YAMAMOTO, I., ISHIGAMI, K., MITSUHASHI, K., IGARASHI, H., ITO, M., TANUMA, T., SUKAWA, Y., OKITA, K., HASEGAWA, T., IMAI, K., YAMAMOTO, H., SHINOMURA, Y. & NOSHO, K. 2016. The relationship between EZH2 expression and microRNA-31 in colorectal cancer and the role in evolution of the serrated pathway. *Oncotarget,* 7**,** 12704-17.

KURYLOWICZ, A., WICIK, Z., OWCZARZ, M., JONAS, M. I., KOTLAREK, M., SWIERNIAK, M., LISIK, W., JONAS, M., NOSZCZYK, B. & PUZIANOWSKA-KUZNICKA, M. 2017. NGS Reveals Molecular Pathways Affected by Obesity and Weight Loss-Related Changes in miRNA Levels in Adipose Tissue. *Int J Mol Sci,* 19.

LAI, E. C. 2002. Micro RNAs are complementary to 3' UTR sequence motifs that mediate negative post-transcriptional regulation. *Nat Genet,* 30**,** 363-4.

LAKHDAR, N., DENGUEZLI, M., ZAOUALI, M., ZBIDI, A., TABKA, Z. & BOUASSIDA, A. 2013. Diet and diet combined with chronic aerobic exercise decreases body fat mass and alters plasma and adipose tissue inflammatory markers in obese women. *Inflammation,* 36**,** 1239-47.

LAO, V. V. & GRADY, W. M. 2011. Epigenetics and colorectal cancer. *Nat Rev Gastroenterol Hepatol,* 8**,** 686-700.

LARSSON, N. G. & CLAYTON, D. A. 1995. Molecular genetic aspects of human mitochondrial disorders. *Annu Rev Genet,* 29**,** 151-78.

LATIL, M., ROCHETEAU, P., CHATRE, L., SANULLI, S., MEMET, S., RICCHETTI, M., TAJBAKHSH, S. & CHRETIEN, F. 2012. Skeletal muscle stem cells adopt a dormant cell state post mortem and retain regenerative capacity. *Nat Commun,* 3**,** 903.

LEE, H. C., YIN, P. H., LIN, J. C., WU, C. C., CHEN, C. Y., WU, C. W., CHI, C. W., TAM, T. N. & WEI, Y. H. 2005. Mitochondrial genome instability and mtDNA depletion in human cancers. *Ann N Y Acad Sci,* 1042**,** 109-22.

LEE, R. C., FEINBAUM, R. L. & AMBROS, V. 1993. The C. elegans heterochronic gene lin-4 encodes small RNAs with antisense complementarity to lin-14. *Cell,* 75**,** 843-54.

LEGGETT, B. & WHITEHALL, V. 2010. Role of the serrated pathway in colorectal cancer pathogenesis. *Gastroenterology,* 138**,** 2088-100.

LI, H. & DURBIN, R. 2009. Fast and accurate short read alignment with Burrows-Wheeler transform. *Bioinformatics,* 25**,** 1754-60.

LI, O., LI, Z., TANG, Q., LI, Y., YUAN, S., SHEN, Y., ZHANG, Z., LI, N., CHU, K. & LEI, G. 2018. Long Stress Induced Non-Coding Transcripts 5 (LSINCT5) Promotes Hepatocellular Carcinoma Progression Through Interaction with High-Mobility Group AT-hook 2 and MiR-4516. *Med Sci Monit,* 24**,** 8510-8523.

LI, T., LUO, W., LIU, K., LV, X. & XI, T. 2015. miR-31 promotes proliferation of colon cancer cells by targeting E2F2. *Biotechnol Lett,* 37**,** 523-32.

LIAO, C. H., WANG, C. Y., LIU, K. H., LIU, Y. Y., WEN, M. S. & YEH, T. S. 2018. MiR-122 marks the differences between subcutaneous and visceral adipose tissues and associates with the outcome of bariatric surgery. *Obes Res Clin Pract,* 12**,** 570-577.

LIBERTI, M. V. & LOCASALE, J. W. 2016. The Warburg Effect: How Does it Benefit Cancer Cells? *Trends Biochem Sci,* 41**,** 211-218.

LIM, L. P., LAU, N. C., GARRETT-ENGELE, P., GRIMSON, A., SCHELTER, J. M., CASTLE, J., BARTEL, D. P., LINSLEY, P. S. & JOHNSON, J. M. 2005. Microarray analysis shows that some microRNAs downregulate large numbers of target mRNAs. *Nature,* 433**,** 769-73.

LIN, J., CHUANG, C.-C. & ZUO, L. 2017. Potential roles of microRNAs and ROS in colorectal cancer: diagnostic biomarkers and therapeutic targets. *Oncotarget,* 8**,** 17328-17346.

LIN, Q., GAO, Z., ALARCON, R. M., YE, J. & YUN, Z. 2009. A role of miR-27 in the regulation of adipogenesis. *Febs j,* 276**,** 2348-58.

LING, H. Y., WEN, G. B., FENG, S. D., TUO, Q. H., OU, H. S., YAO, C. H., ZHU, B. Y., GAO, Z. P., ZHANG, L. & LIAO, D. F. 2011. MicroRNA-375 promotes 3T3-L1 adipocyte differentiation through modulation of extracellular signal-regulated kinase signalling. *Clin Exp Pharmacol Physiol,* 38**,** 239-46.

LINK, A., BALAGUER, F. & GOEL, A. 2010. Cancer chemoprevention by dietary polyphenols: promising role for epigenetics. *Biochem Pharmacol,* 80**,** 1771-92.

LIRUN, K., SEWE, M. & YONG, W. 2015. A Pilot Study: The Effect of Roux-en-Y Gastric Bypass on the Serum MicroRNAs of the Type 2 Diabetes Patient. *Obes Surg,* 25**,** 2386-92.

LIU, R., JIN, P., LIQUNYU, WANG, Y., HAN, L., SHI, T. & LI, X. 2014. Impaired Mitochondrial Dynamics and Bioenergetics in Diabetic Skeletal Muscle. *PLOS ONE,* 9**,** e92810.

LÓPEZ-OTÍN, C., BLASCO, M. A., PARTRIDGE, L., SERRANO, M. & KROEMER, G. 2013. The hallmarks of aging. *Cell,* 153**,** 1194-1217.

LOVE, M. I., HUBER, W. & ANDERS, S. 2014. Moderated estimation of fold change and dispersion for RNA-seq data with DESeq2. *Genome Biol,* 15**,** 550.

LUNDBERG, I. V., WIKBERG, M. L., LJUSLINDER, I., LI, X., MYTE, R., ZINGMARK, C., LOFGREN-BURSTROM, A., EDIN, S. & PALMQVIST, R. 2018. MicroRNA Expression in KRAS- and BRAF-mutated Colorectal Cancers. *Anticancer Res,* 38**,** 677-683.

MA, C., AVENELL, A., BOLLAND, M., HUDSON, J., STEWART, F., ROBERTSON, C., SHARMA, P., FRASER, C. & MACLENNAN, G. 2017. Effects of weight loss interventions for adults who are obese on mortality, cardiovascular disease, and cancer: systematic review and meta-analysis. *Bmj,* 359**,** j4849.

MA, Y., YANG, Y., WANG, F., ZHANG, P., SHI, C., ZOU, Y. & QIN, H. 2013. Obesity and risk of colorectal cancer: a systematic review of prospective studies. *PLoS One,* 8**,** e53916.

MACHADO, A. M., FIGUEIREDO, C., SERUCA, R. & RASMUSSEN, L. J. 2010. Helicobacter pylori infection generates genetic instability in gastric cells. *Biochim Biophys Acta,* 1806**,** 58-65.

MALCOMSON, F. C., BREININGER, S. P., ELGENDY, K., JOEL, A., RANATHUNGA, R. M. T. K., HILL, T. R., BRADBURN, D. M., TURNBULL, D. M., GREAVES, L. C. & MATHERS, J. C. Design and baseline characteristics of the Biomarkers Of Risk In Colorectal Cancer (BORICC) Follow-Up study: A 12+ years follow-up. *Nutrition and Health,* 0**,** 0260106019866963.

MALCOMSON, F. C. & MATHERS, J. C. 2017. Nutrition, epigenetics and health through life. *Nutrition Bulletin,* 42**,** 254-265.

MANN, B., GELOS, M., SIEDOW, A., HANSKI, M. L., GRATCHEV, A., ILYAS, M., BODMER, W. F., MOYER, M. P., RIECKEN, E. O., BUHR, H. J. & HANSKI, C. 1999. Target genes of beta-catenin-T cell-

factor/lymphoid-enhancer-factor signaling in human colorectal carcinomas. *Proc Natl Acad Sci U S A,* 96**,** 1603-8.

MARGOLIS, L. M., RIVAS, D. A., PASIAKOS, S. M., MCCLUNG, J. P., CEGLIA, L. & FIELDING, R. A. 2017. Upregulation of circulating myomiR following short-term energy restriction is inversely associated with whole body protein synthesis. *Am J Physiol Regul Integr Comp Physiol,* 313**,** R298-r304.

MARQUES-ROCHA, J. L., MILAGRO, F. I., MANSEGO, M. L., ZULET, M. A., BRESSAN, J. & MARTÍNEZ, J. A. 2016. Expression of inflammation-related miRNAs in white blood cells from subjects with metabolic syndrome after 8 wk of following a Mediterranean diet–based weight loss program. *Nutrition,* 32**,** 48-55.

MARTIN, W. & KOWALLIK, K. V. 1999. Annotated English translation of Mereschkowsky's 1905 paper 'Über Natur und Ursprung der Chromatophoren im Pflanzenreiche'. *European Journal of Phycology,* 34**,** 287-295.

MARTINEZ DE LA ESCALERA, L., KYROU, I., VRBIKOVA, J., HAINER, V., SRAMKOVA, P., FRIED, M., PIYA, M. K., KUMAR, S., TRIPATHI, G. & MCTERNAN, P. G. 2017. Impact of gut hormone FGF-19 on type-2 diabetes and mitochondrial recovery in a prospective study of obese diabetic women undergoing bariatric surgery. *BMC Medicine,* 15**,** 34.

MASKARINEC, G. & NOH, J. J. 2004. The effect of migration on cancer incidence among Japanese in Hawaii. *Ethn Dis,* 14**,** 431-9.

MATHERS, J. C. 2018. Obesity and bowel cancer: from molecular mechanisms to interventions. *Nutr Res*.

MATHERS, J. C., STRATHDEE, G. & RELTON, C. L. 2010. Induction of epigenetic alterations by dietary and other environmental factors. *Adv Genet,* 71**,** 3-39.

MATHERS, J. C. J., I. T. TURNBULL, D. 2009. Validation of novel diet related biomarkers of colorectal cancer risk. *Technical Report.*

MATTHIESSEN, J., STOCKMARR, A., FAGT, S., KNUDSEN, V. K. & BILTOFT-JENSEN, A. 2014. Danish children born to parents with lower levels of education are more likely to become overweight. *Acta paediatrica (Oslo, Norway : 1992),* 103**,** 1083-8.

MCKAY, J. A. & MATHERS, J. C. 2011. Diet induced epigenetic changes and their implications for health. *Acta Physiol (Oxf),* 202**,** 103-18.

MEMEDI, R., TASIC, V., NIKOLIC, E., JANCEVSKA, A. & GUCEV, Z. 2013. Obesity in childhood and adolescence, genetic factors. *Prilozi/Makedonska akademija na naukite i umetnostite, Oddelenie za biološki i medicinski nauki= Contributions/Macedonian Academy of Sciences and Arts, Section of Biological and Medical Sciences,* 34**,** 85.

MENDELL, J. T. & OLSON, E. N. 2012. MicroRNAs in stress signaling and human disease. *Cell,* 148**,** 1172-87.

MENGHINI, R., CASAGRANDE, V., CARDELLINI, M., MARTELLI, E., TERRINONI, A., AMATI, F., VASA-NICOTERA, M., IPPOLITI, A., NOVELLI, G., MELINO, G., LAURO, R. & FEDERICI, M. 2009. MicroRNA 217 modulates endothelial cell senescence via silent information regulator 1. *Circulation,* 120**,** 1524-32.

MILAGRO, F. I., MIRANDA, J., PORTILLO, M. P., FERNANDEZ-QUINTELA, A., CAMPION, J. & MARTINEZ, J. A. 2013. High-throughput sequencing of microRNAs in peripheral blood mononuclear cells: identification of potential weight loss biomarkers. *PLoS One,* 8**,** e54319.

MORENO-CASTELLANOS, N., GUZMAN-RUIZ, R., CANO, D. A., MADRAZO-ATUTXA, A., PEINADO, J. R., PEREIRA-CUNILL, J. L., GARCIA-LUNA, P. P., MORALES-CONDE, S., SOCAS-MACIAS, M., VAZQUEZ-MARTINEZ, R., LEAL-CERRO, A. & MALAGON, M. M. 2016. The Effects of Bariatric Surgery-Induced Weight Loss on Adipose Tissue in Morbidly Obese Women Depends on the Initial Metabolic Status. *Obes Surg,* 26**,** 1757-67.

MOTOYAMA, K., INOUE, H., TAKATSUNO, Y., TANAKA, F., MIMORI, K., UETAKE, H., SUGIHARA, K. & MORI, M. 2009. Over-and under-expressed microRNAs in human colorectal cancer. *International journal of oncology,* 34**,** 1069-1075.

MUNDADE, R., IMPERIALE, T. F., PRABHU, L., LOEHRER, P. J. & LU, T. 2014. Genetic pathways, prevention, and treatment of sporadic colorectal cancer. *Oncoscience,* 1**,** 400-6.

NARDELLI, C., IAFFALDANO, L., PILONE, V., LABRUNA, G., FERRIGNO, M., CARLOMAGNO, N., DODARO, C. A., FORESTIERI, P., BUONO, P., SALVATORE, F. & SACCHETTI, L. 2017. Changes in the MicroRNA Profile Observed in the Subcutaneous Adipose Tissue of Obese Patients after Laparoscopic Adjustable Gastric Banding. *J Obes,* 2017**,** 6754734.

NECELA, B. M., CARR, J. M., ASMANN, Y. W. & THOMPSON, E. A. 2011. Differential expression of microRNAs in tumors from chronically inflamed or genetic (APC(Min/+)) models of colon cancer. *PLoS One,* 6**,** e18501.

NEWENGLAND BIOLABS. 2019. *NEBNext® Multiplex Small RNA Library Prep Set for Illumina®* [Online]. Available: https://international.neb.com/products/e7300-nebnext-multiplex-small-rna-library-prep-set-for-illumina-set-1#Product%20Information [Accessed 05.03.19].

NICKLAS, B. J., AMBROSIUS, W., MESSIER, S. P., MILLER, G. D., PENNINX, B. W., LOESER, R. F., PALLA, S., BLEECKER, E. & PAHOR, M. 2004. Diet-induced weight loss, exercise, and chronic inflammation in older, obese adults: a randomized controlled clinical trial. *Am J Clin Nutr,* 79**,** 544-51.

NING, Y., WANG, L. & GIOVANNUCCI, E. L. 2010. A quantitative analysis of body mass index and colorectal cancer: findings from 56 observational studies. *Obes Rev,* 11**,** 19-30.

NOLAND, C. L. & DOUDNA, J. A. 2013. Multiple sensors ensure guide strand selection in human RNAi pathways. *Rna,* 19**,** 639-48.

NOOTEBOOM, M., JOHNSON, R., TAYLOR, R. W., WRIGHT, N. A., LIGHTOWLERS, R. N., KIRKWOOD, T. B., MATHERS, J. C., TURNBULL, D. M. & GREAVES, L. C. 2010. Age-associated mitochondrial DNA mutations lead to small but significant changes in cell proliferation and apoptosis in human colonic crypts. *Aging Cell,* 9**,** 96-9.

NOREN HOOTEN, N., ABDELMOHSEN, K., GOROSPE, M., EJIOGU, N., ZONDERMAN, A. B. & EVANS, M. K. 2010. microRNA expression patterns reveal differential expression of target genes with age. *PloS one,* 5**,** e10724-e10724.

NOREN HOOTEN, N., FITZPATRICK, M., WOOD, W. H., 3RD, DE, S., EJIOGU, N., ZHANG, Y., MATTISON, J. A., BECKER, K. G., ZONDERMAN, A. B. & EVANS, M. K. 2013. Age-related changes in microRNA levels in serum. *Aging (Albany NY),* 5**,** 725-40.

NOSHO, K., IGARASHI, H., NOJIMA, M., ITO, M., MARUYAMA, R., YOSHII, S., NAITO, T., SUKAWA, Y., MIKAMI, M., SUMIOKA, W., YAMAMOTO, E., KUROKAWA, S., ADACHI, Y., TAKAHASHI, H., OKUDA, H., KUSUMI, T., HOSOKAWA, M., FUJITA, M., HASEGAWA, T., OKITA, K., HIRATA, K., SUZUKI, H., YAMAMOTO, H. & SHINOMURA, Y. 2014. Association of microRNA-31 with BRAF mutation, colorectal cancer survival and serrated pathway. *Carcinogenesis,* 35**,** 776-83.

NUNEZ LOPEZ, Y. O., COEN, P. M., GOODPASTER, B. H. & SEYHAN, A. A. 2017. Gastric bypass surgery with exercise alters plasma microRNAs that predict improvements in cardiometabolic risk. *Int J Obes (Lond),* 41**,** 1121-1130.

OMATA, F., DESHPANDE, G. A., OHDE, S., MINE, T. & FUKUI, T. 2013. The association between obesity and colorectal adenoma: systematic review and meta-analysis. *Scand J Gastroenterol,* 48**,** 136-46.

ORGANISATION, W. H. 2015. Obesity and Overweight. *Geneva: WHO Media Centre*.

ORTEGA, F. J., MERCADER, J. M., CATALAN, V., MORENO-NAVARRETE, J. M., PUEYO, N., SABATER, M., GOMEZ-AMBROSI, J., ANGLADA, R., FERNANDEZ-FORMOSO, J. A., RICART, W., FRUHBECK, G. & FERNANDEZ-REAL, J. M. 2013. Targeting the circulating microRNA signature of obesity. *Clin Chem,* 59**,** 781-92.

ORTEGA, F. J., MERCADER, J. M., MORENO-NAVARRETE, J. M., NONELL, L., PUIGDECANET, E., RODRIQUEZ-HERMOSA, J. I., ROVIRA, O., XIFRA, G., GUERRA, E., MORENO, M., MAYAS, D., MORENO-CASTELLANOS, N., FERNANDEZ-FORMOSO, J. A., RICART, W., TINAHONES, F. J., TORRENTS, D., MALAGON, M. M. & FERNANDEZ-REAL, J. M. 2015a. Surgery-Induced Weight

Loss Is Associated With the Downregulation of Genes Targeted by MicroRNAs in Adipose Tissue. *J Clin Endocrinol Metab,* 100**,** E1467-76.

ORTEGA, F. J., MORENO, M., MERCADER, J. M., MORENO-NAVARRETE, J. M., FUENTES-BATLLEVELL, N., SABATER, M., RICART, W. & FERNANDEZ-REAL, J. M. 2015b. Inflammation triggers specific microRNA profiles in human adipocytes and macrophages and in their supernatants. *Clin Epigenetics,* 7**,** 49.

OTANI, T., IWASAKI, M., SASAZUKI, S., INOUE, M. & TSUGANE, S. 2006. Plasma C-reactive protein and risk of colorectal cancer in a nested case-control study: Japan Public Health Center-based prospective study. *Cancer Epidemiol Biomarkers Prev,* 15**,** 690-5.

PARK, L. K., FRISO, S. & CHOI, S. W. 2012. Nutritional influences on epigenetics and age-related disease. *Proc Nutr Soc,* 71**,** 75-83.

PARR, E. B., CAMERA, D. M., BURKE, L. M., PHILLIPS, S. M., COFFEY, V. G. & HAWLEY, J. A. 2016. Circulating MicroRNA Responses between 'High' and 'Low' Responders to a 16-Wk Diet and Exercise Weight Loss Intervention. *PLoS One,* 11**,** e0152545.

PATE, K. T., STRINGARI, C., SPROWL-TANIO, S., WANG, K., TESLAA, T., HOVERTER, N. P., MCQUADE, M. M., GARNER, C., DIGMAN, M. A., TEITELL, M. A., EDWARDS, R. A., GRATTON, E. & WATERMAN, M. L. 2014. Wnt signaling directs a metabolic program of glycolysis and angiogenesis in colon cancer. *Embo j,* 33**,** 1454-73.

PENDYALA, S., NEFF, L. M., SUAREZ-FARINAS, M. & HOLT, P. R. 2011. Diet-induced weight loss reduces colorectal inflammation: implications for colorectal carcinogenesis. *Am J Clin Nutr,* 93**,** 234-42.

PENG, H., WANG, L., SU, Q., YI, K., DU, J. & WANG, Z. 2019. MiR-31-5p promotes the cell growth, migration and invasion of colorectal cancer cells by targeting NUMB. *Biomed Pharmacother,* 109**,** 208-216.

POLYAK, K., LI, Y., ZHU, H., LENGAUER, C., WILLSON, J. K., MARKOWITZ, S. D., TRUSH, M. A., KINZLER, K. W. & VOGELSTEIN, B. 1998. Somatic mutations of the mitochondrial genome in human colorectal tumours. *Nat Genet,* 20**,** 291-3.

POULLIS, A., FOSTER, R., SHETTY, A., FAGERHOL, M. K. & MENDALL, M. A. 2004. Bowel inflammation as measured by fecal calprotectin: a link between lifestyle factors and colorectal cancer risk. *Cancer Epidemiol Biomarkers Prev,* 13**,** 279-84.

POWELL, S. M., ZILZ, N., BEAZER-BARCLAY, Y., BRYAN, T. M., HAMILTON, S. R., THIBODEAU, S. N., VOGELSTEIN, B. & KINZLER, K. W. 1992. APC mutations occur early during colorectal tumorigenesis. *Nature,* 359**,** 235-7.

PRIOR, S. L., GRIFFITHS, A. P., BAXTER, J. M., BAXTER, P. W., HODDER, S. C., SILVESTER, K. C. & LEWIS, P. D. 2006. Mitochondrial DNA mutations in oral squamous cell carcinoma. *Carcinogenesis,* 27**,** 945-50.

PRUITT, K. & DER, C. J. 2001. Ras and Rho regulation of the cell cycle and oncogenesis. *Cancer Lett,* 171**,** 1-10.

PUTTI, R., SICA, R., MIGLIACCIO, V. & LIONETTI, L. 2015. Diet impact on mitochondrial bioenergetics and dynamics. *Front Physiol,* 6**,** 109.

QIAGEN. 2016. *PCR Protocols & Applications* [Online]. Available: https://www.qiagen.com/gb/resources/molecular-biology-methods/pcr/ [Accessed 04.07.2016].

REIK, W. 2007. Stability and flexibility of epigenetic gene regulation in mammalian development. *Nature,* 447**,** 425-32.

REN, A., DONG, Y., TSOI, H. & YU, J. 2015. Detection of miRNA as non-invasive biomarkers of colorectal cancer. *Int J Mol Sci,* 16**,** 2810-23.

REYNOLDS, A., WHARTON, N., PARRIS, A., MITCHELL, E., SOBOLEWSKI, A., KAM, C., BIGWOOD, L., EL HADI, A., MUNSTERBERG, A., LEWIS, M., SPEAKMAN, C., STEBBINGS, W., WHARTON, R., SARGEN, K., TIGHE, R., JAMIESON, C., HERNON, J., KAPUR, S., OUE, N., YASUI, W. &

WILLIAMS, M. R. 2014. Canonical Wnt signals combined with suppressed TGFbeta/BMP pathways promote renewal of the native human colonic epithelium. *Gut,* 63**,** 610-21.

ROCHA, M. C., GRADY, J. P., GRUNEWALD, A., VINCENT, A., DOBSON, P. F., TAYLOR, R. W., TURNBULL, D. M. & RYGIEL, K. A. 2015. A novel immunofluorescent assay to investigate oxidative phosphorylation deficiency in mitochondrial myopathy: understanding mechanisms and improving diagnosis. *Sci Rep,* 5**,** 15037.

ROGGE, M. M. 2009. The role of impaired mitochondrial lipid oxidation in obesity. *Biol Res Nurs,* 10**,** 356-73.

ROSENBERG, A. Z., WRIGHT, C., FOX-TALBOT, K., RAJPUROHIT, A., WILLIAMS, C., PORTER, C., KOVBASNJUK, O., MCCALL, M. N., SHIN, J. H. & HALUSHKA, M. K. 2018. xMD-miRNA-seq to generate near in vivo miRNA expression estimates in colon epithelial cells. *Sci Rep,* 8**,** 9783.

ROSS, J. M. 2011. Visualization of mitochondrial respiratory function using cytochrome c oxidase/succinate dehydrogenase (COX/SDH) double-labeling histochemistry. *Journal of visualized experiments : JoVE***,** e3266-e3266.

RUSSO, A., BARTOLINI, D., MENSA, E., TORQUATO, P., ALBERTINI, M. C., OLIVIERI, F., TESTA, R., ROSSI, S., PIRODDI, M., CRUCIANI, G., DE FEO, P. & GALLI, F. 2018. Physical Activity Modulates the Overexpression of the Inflammatory miR-146a-5p in Obese Patients. *IUBMB Life,* 70**,** 1012-1022.

RUSTGI, A. K. 2013. BRAF: a driver of the serrated pathway in colon cancer. *Cancer Cell,* 24, 1-2.

SAINSBURY, A., GOODLAD, R. A., PERRY, S. L., POLLARD, S. G., ROBINS, G. G. & HULL, M. A. 2008. Increased colorectal epithelial cell proliferation and crypt fission associated with obesity and roux-en-Y gastric bypass. *Cancer Epidemiol Biomarkers Prev,* 17**,** 1401-10.

SAND, M., SKRYGAN, M., SAND, D., GEORGAS, D., HAHN, S. A., GAMBICHLER, T., ALTMEYER, P. & BECHARA, F. G. 2012. Expression of microRNAs in basal cell carcinoma. *Br J Dermatol,* 167**,** 847-55.

SARIDAKI, Z., WEIDHAAS, J. B., LENZ, H. J., LAURENT-PUIG, P., JACOBS, B., DE SCHUTTER, J., DE ROOCK, W., SALZMAN, D. W., ZHANG, W., YANG, D., PILATI, C., BOUCHE, O., PIESSEVAUX, H. & TEJPAR, S. 2014. A let-7 microRNA-binding site polymorphism in KRAS predicts improved outcome in patients with metastatic colorectal cancer treated with salvage cetuximab/panitumumab monotherapy. *Clin Cancer Res,* 20**,** 4499-4510.

SAXENA, S., JONSSON, Z. O. & DUTTA, A. 2003. Small RNAs with imperfect match to endogenous mRNA repress translation. Implications for off-target activity of small inhibitory RNA in mammalian cells. *J Biol Chem,* 278**,** 44312-9.

SCHAUER, D. P., FEIGELSON, H. S., KOEBNICK, C., CAAN, B., WEINMANN, S., LEONARD, A. C., POWERS, J. D., YENUMULA, P. R. & ARTERBURN, D. E. 2017a. Association Between Weight Loss and the Risk of Cancer after Bariatric Surgery. *Obesity (Silver Spring),* 25 Suppl 2**,** S52-s57.

SCHAUER, D. P., FEIGELSON, H. S., KOEBNICK, C., CAAN, B., WEINMANN, S., LEONARD, A. C., POWERS, J. D., YENUMULA, P. R. & ARTERBURN, D. E. 2017b. Bariatric Surgery and the Risk of Cancer in a Large Multisite Cohort. *Ann Surg*.

SCHAUER, D. P., FEIGELSON, H. S., KOEBNICK, C., CAAN, B., WEINMANN, S., LEONARD, A. C., POWERS, J. D., YENUMULA, P. R. & ARTERBURN, D. E. 2019. Bariatric Surgery and the Risk of Cancer in a Large Multisite Cohort. *Ann Surg,* 269**,** 95-101.

SCHUBBERT, S., SHANNON, K. & BOLLAG, G. 2007. Hyperactive Ras in developmental disorders and cancer. *Nat Rev Cancer,* 7**,** 295-308.

SEMPLE, R. K., CROWLEY, V. C., SEWTER, C. P., LAUDES, M., CHRISTODOULIDES, C., CONSIDINE, R. V., VIDAL-PUIG, A. & O'RAHILLY, S. 2004. Expression of the thermogenic nuclear hormone receptor coactivator PGC-1alpha is reduced in the adipose tissue of morbidly obese subjects. *Int J Obes Relat Metab Disord,* 28**,** 176-9.

SHADEL, G. S. & CLAYTON, D. A. 1993. Mitochondrial transcription initiation. Variation and conservation. *Journal of Biological Chemistry,* 268**,** 16083-16086.

SHI, B., SEPP-LORENZINO, L., PRISCO, M., LINSLEY, P., DEANGELIS, T. & BASERGA, R. 2007. Micro RNA 145 targets the insulin receptor substrate-1 and inhibits the growth of colon cancer cells. *J Biol Chem,* 282**,** 32582-90.

SHIDARA, Y., YAMAGATA, K., KANAMORI, T., NAKANO, K., KWONG, J. Q., MANFREDI, G., ODA, H. & OHTA, S. 2005. Positive contribution of pathogenic mutations in the mitochondrial genome to the promotion of cancer by prevention from apoptosis. *Cancer Res,* 65**,** 1655-63.

SIEGEL, R. L., MILLER, K. D., FEDEWA, S. A., AHNEN, D. J., MEESTER, R. G. S., BARZI, A. & JEMAL, A. 2017. Colorectal cancer statistics, 2017. *CA Cancer J Clin,* 67**,** 177-193.

SINGH, D. 1994. Waist-to-hip ratio and judgment of attractiveness and healthiness of female figures by male and female physicians. *Int J Obes Relat Metab Disord,* 18**,** 731-7.

SJOBLOM, T., JONES, S., WOOD, L. D., PARSONS, D. W., LIN, J., BARBER, T. D., MANDELKER, D., LEARY, R. J., PTAK, J., SILLIMAN, N., SZABO, S., BUCKHAULTS, P., FARRELL, C., MEEH, P., MARKOWITZ, S. D., WILLIS, J., DAWSON, D., WILLSON, J. K., GAZDAR, A. F., HARTIGAN, J., WU, L., LIU, C., PARMIGIANI, G., PARK, B. H., BACHMAN, K. E., PAPADOPOULOS, N., VOGELSTEIN, B., KINZLER, K. W. & VELCULESCU, V. E. 2006. The consensus coding sequences of human breast and colorectal cancers. *Science,* 314**,** 268-74.

SLABY, O., SVOBODA, M., FABIAN, P., SMERDOVA, T., KNOFLICKOVA, D., BEDNARIKOVA, M., NENUTIL, R. & VYZULA, R. 2007. Altered Expression of miR-21, miR-31, miR-143 and miR-145 Is Related to Clinicopathologic Features of Colorectal Cancer. *Oncology,* 72**,** 397-402.

SLATTERY, M. L., MULLANY, L. E., SAKODA, L. C., WOLFF, R. K., SAMOWITZ, W. S. & HERRICK, J. S. 2018. The MAPK-Signaling Pathway in Colorectal Cancer: Dysregulated Genes and Their Association With MicroRNAs. *Cancer Inform,* 17**,** 1176935118766522.

SMITH-VIKOS, T. & SLACK, F. J. 2012. MicroRNAs and their roles in aging. *J Cell Sci,* 125**,** 7-17.

SONG, B., WANG, Y., TITMUS, M. A., BOTCHKINA, G., FORMENTINI, A., KORNMANN, M. & JU, J. 2010. Molecular mechanism of chemoresistance by miR-215 in osteosarcoma and colon cancer cells. *Mol Cancer,* 9**,** 96.

SOUSA, J. S., D'IMPRIMA, E. & VONCK, J. 2018. Mitochondrial Respiratory Chain Complexes. *Subcell Biochem,* 87**,** 167-227.

SPARKS, L. M., XIE, H., KOZA, R. A., MYNATT, R., HULVER, M. W., BRAY, G. A. & SMITH, S. R. 2005. A high-fat diet coordinately downregulates genes required for mitochondrial oxidative phosphorylation in skeletal muscle. *Diabetes,* 54**,** 1926-33.

STEWART, J. B. & CHINNERY, P. F. 2015. The dynamics of mitochondrial DNA heteroplasmy: implications for human health and disease. *Nat Rev Genet,* 16**,** 530-42.

STEWART, J. B., FREYER, C., ELSON, J. L. & LARSSON, N. G. 2008. Purifying selection of mtDNA and its implications for understanding evolution and mitochondrial disease. *Nat Rev Genet,* 9**,** 657-62.

SUN, D., YU, F., MA, Y., ZHAO, R., CHEN, X., ZHU, J., ZHANG, C.-Y., CHEN, J. & ZHANG, J. 2013. MicroRNA-31 Activates the RAS Pathway and Functions as an Oncogenic MicroRNA in Human Colorectal Cancer by Repressing RAS p21 GTPase Activating Protein 1 (RASA1). *Journal of Biological Chemistry,* 288**,** 9508-9518.

SUN, L. L., JIANG, B. G., LI, W. T., ZOU, J. J., SHI, Y. Q. & LIU, Z. M. 2011. MicroRNA-15a positively regulates insulin synthesis by inhibiting uncoupling protein-2 expression. *Diabetes Res Clin Pract,* 91**,** 94-100.

SUN, T., FU, M., BOOKOUT, A. L., KLIEWER, S. A. & MANGELSDORF, D. J. 2009. MicroRNA let-7 regulates 3T3-L1 adipogenesis. *Mol Endocrinol,* 23**,** 925-31.

SUTHERLAND, L. N., CAPOZZI, L. C., TURCHINSKY, N. J., BELL, R. C. & WRIGHT, D. C. 2008. Time course of high-fat diet-induced reductions in adipose tissue mitochondrial proteins: Potential mechanisms and the relationship to glucose intolerance. *American Journal of Physiology - Endocrinology and Metabolism,* 295**,** E1076-E1083.

SVORONOS, A. A., ENGELMAN, D. M. & SLACK, F. J. 2016. OncomiR or Tumor Suppressor? The Duplicity of MicroRNAs in Cancer. *Cancer Res,* 76**,** 3666-70.

TABET, F., CUESTA TORRES, L. F., ONG, K. L., SHRESTHA, S., CHOTEAU, S. A., BARTER, P. J., CLIFTON, P. & RYE, K. A. 2016. High-Density Lipoprotein-Associated miR-223 Is Altered after Diet-Induced Weight Loss in Overweight and Obese Males. *PLoS One,* 11**,** e0151061.

TAKAHASHI, M., SUNG, B., SHEN, Y., HUR, K., LINK, A., BOLAND, C. R., AGGARWAL, B. B. & GOEL, A. 2012. Boswellic acid exerts antitumor effects in colorectal cancer cells by modulating expression of the let-7 and miR-200 microRNA family. *Carcinogenesis,* 33**,** 2441-9.

TAKAKU, K., OSHIMA, M., MIYOSHI, H., MATSUI, M., SELDIN, M. F. & TAKETO, M. M. 1998. Intestinal tumorigenesis in compound mutant mice of both Dpc4 (Smad4) and Apc genes. *Cell,* 92**,** 645-56.

TAN, D., GOERLITZ, D. S., DUMITRESCU, R. G., HAN, D., SEILLIER-MOISEIWITSCH, F., SPERNAK, S. M., ORDEN, R. A., CHEN, J., GOLDMAN, R. & SHIELDS, P. G. 2008. Associations between cigarette smoking and mitochondrial DNA abnormalities in buccal cells. *Carcinogenesis,* 29**,** 1170-1177.

TANG, G., GUTIERREZ RIOS, P., KUO, S. H., AKMAN, H. O., ROSOKLIJA, G., TANJI, K., DWORK, A., SCHON, E. A., DIMAURO, S., GOLDMAN, J. & SULZER, D. 2013. Mitochondrial abnormalities in temporal lobe of autistic brain. *Neurobiol Dis,* 54**,** 349-61.

TATEISHI, Y., OKUDELA, K., MITSUI, H., UMEDA, S., SUZUKI, T., KOJIMA, Y., WATANABE, K., KAWANO, N., ENDO, I. & OHASHI, K. 2015. The potential role of microRNA-31 expression in early colorectal cancer. *Pathol Int,* 65**,** 513-8.

TAYLOR, R. W., BARRON, M. J., BORTHWICK, G. M., GOSPEL, A., CHINNERY, P. F., SAMUELS, D. C., TAYLOR, G. A., PLUSA, S. M., NEEDHAM, S. J., GREAVES, L. C., KIRKWOOD, T. B. & TURNBULL, D. M. 2003. Mitochondrial DNA mutations in human colonic crypt stem cells. *J Clin Invest,* 112**,** 1351-60.

TCHERNOF, A., NOLAN, A., SITES, C. K., ADES, P. A. & POEHLMAN, E. T. 2002. Weight loss reduces C-reactive protein levels in obese postmenopausal women. *Circulation,* 105**,** 564-9.

TERPSTRA, O. T., VAN BLANKENSTEIN, M., DEES, J. & EILERS, G. A. 1987. Abnormal pattern of cell proliferation in the entire colonic mucosa of patients with colon adenoma or cancer. *Gastroenterology,* 92**,** 704-708.

THOMAS, J., OHTSUKA, M., PICHLER, M. & LING, H. 2015. MicroRNAs: Clinical Relevance in Colorectal Cancer. *Int J Mol Sci,* 16**,** 28063-76.

THOMOU, T., MORI, M. A., DREYFUSS, J. M., KONISHI, M., SAKAGUCHI, M., WOLFRUM, C., RAO, T. N., WINNAY, J. N., GARCIA-MARTIN, R., GRINSPOON, S. K., GORDEN, P. & KAHN, C. R. 2017. Adipose-derived circulating miRNAs regulate gene expression in other tissues. *Nature,* 542**,** 450-455.

TIAN, Y., MA, X., LV, C., SHENG, X., LI, X., ZHAO, R., SONG, Y., ANDL, T., PLIKUS, M. V. & SUN, J. 2017. Stress responsive miR-31 is a major modulator of mouse intestinal stem cells during regeneration and tumorigenesis. *Elife,* 6**,** e29538.

TOLEDO, F. G. & GOODPASTER, B. H. 2013. The role of weight loss and exercise in correcting skeletal muscle mitochondrial abnormalities in obesity, diabetes and aging. *Mol Cell Endocrinol,* 379**,** 30-4.

TOLEDO, F. G., MENSHIKOVA, E. V., AZUMA, K., RADIKOVA, Z., KELLEY, C. A., RITOV, V. B. & KELLEY, D. E. 2008. Mitochondrial capacity in skeletal muscle is not stimulated by weight loss despite increases in insulin action and decreases in intramyocellular lipid content. *Diabetes,* 57**,** 987-94.

TUO, D., CHRISTOPHER, J. L., STEPHEN, B., MICHAEL, A. C. & WILLA, A. H. 2016. Obesity, Inflammation, and Cancer. *Annual Review of Pathology: Mechanisms of Disease,* 11**,** 421-449.

ULLMANN, P., NURMIK, M., SCHMITZ, M., RODRIGUEZ, F., WEILER, J., QURESHI-BAIG, K., FELTEN, P., NAZAROV, P. V., NICOT, N., ZUEGEL, N., HAAN, S. & LETELLIER, E. 2019. Tumor suppressor miR-215 counteracts hypoxia-induced colon cancer stem cell activity. *Cancer Lett,* 450**,** 32-41.

ULRICH, C. M., HIMBERT, C., HOLOWATYJ, A. N. & HURSTING, S. D. 2018. Energy balance and gastrointestinal cancer: risk, interventions, outcomes and mechanisms. *Nature reviews. Gastroenterology & hepatology,* 15**,** 683-698.

VALERI, N., GASPARINI, P., BRACONI, C., PAONE, A., LOVAT, F., FABBRI, M., SUMANI, K. M., ALDER, H., AMADORI, D., PATEL, T., NUOVO, G. J., FISHEL, R. & CROCE, C. M. 2010. MicroRNA-21 induces resistance to 5-fluorouracil by down-regulating human DNA MutS homolog 2 (hMSH2). *Proc Natl Acad Sci U S A,* 107**,** 21098-103.

VALERIO, A., CARDILE, A., COZZI, V., BRACALE, R., TEDESCO, L., PISCONTI, A., PALOMBA, L., CANTONI, O., CLEMENTI, E., MONCADA, S., CARRUBA, M. O. & NISOLI, E. 2006. TNF-alpha downregulates eNOS expression and mitochondrial biogenesis in fat and muscle of obese rodents. *J Clin Invest,* 116**,** 2791-8.

VAN RIJN, J. C., REITSMA, J. B., STOKER, J., BOSSUYT, P. M., VAN DEVENTER, S. J. & DEKKER, E. 2006. Polyp miss rate determined by tandem colonoscopy: a systematic review. *Am J Gastroenterol,* 101**,** 343-50.

VAN ROOSBROECK, K. & CALIN, G. A. 2017. Cancer Hallmarks and MicroRNAs: The Therapeutic Connection. *Adv Cancer Res,* 135**,** 119-149.

VAZQUEZ, A., BOND, E. E., LEVINE, A. J. & BOND, G. L. 2008. The genetics of the p53 pathway, apoptosis and cancer therapy. *Nat Rev Drug Discov,* 7**,** 979-87.

VLACHOS, I. S., KONSTANTINOS ZAGGANAS, MARIA D. PARASKEVOPOULOU, GEORGIOS GEORGAKILAS, DIMITRA KARAGKOUNI, THANASIS VERGOULIS, THEODORE DALAMAGAS, AND ARTEMIS G. HATZIGEORGIOU. 2015. *DIANA-miRPath v3. 0: deciphering microRNA function with experimental support." Nucleic acids research* [Online]. Available: http://snf-515788.vm.okeanos.grnet.gr/index.php?r=mirpath [Accessed].

VOGELSTEIN, B., FEARON, E. R., HAMILTON, S. R., KERN, S. E., PREISINGER, A. C., LEPPERT, M., NAKAMURA, Y., WHITE, R., SMITS, A. M. & BOS, J. L. 1988. Genetic alterations during colorectal-tumor development. *N Engl J Med,* 319**,** 525-32.

VYCHYTILOVA-FALTEJSKOVA, P., MERHAUTOVA, J., MACHACKOVA, T., GUTIERREZ-GARCIA, I., GARCIA-SOLANO, J., RADOVA, L., BRCHNELOVA, D., SLABA, K., SVOBODA, M., HALAMKOVA, J., DEMLOVA, R., KISS, I., VYZULA, R., CONESA-ZAMORA, P. & SLABY, O. 2017. MiR-215-5p is a tumor suppressor in colorectal cancer targeting EGFR ligand epiregulin and its transcriptional inducer HOXB9. *Oncogenesis,* 6**,** 399.

VYCHYTILOVA-FALTEJSKOVA, P. & SLABY, O. 2019. MicroRNA-215: From biology to theranostic applications. *Mol Aspects Med*.

WALTHER, A., JOHNSTONE, E., SWANTON, C., MIDGLEY, R., TOMLINSON, I. & KERR, D. 2009. Genetic prognostic and predictive markers in colorectal cancer. *Nat Rev Cancer,* 9**,** 489-99.

WANG, B., LI, J., SUN, M., SUN, L. & ZHANG, X. 2014a. miRNA expression in breast cancer varies with lymph node metastasis and other clinicopathologic features. *IUBMB Life,* 66**,** 371-7.

WANG, B., SHEN, Z. L., GAO, Z. D., ZHAO, G., WANG, C. Y., YANG, Y., ZHANG, J. Z., YAN, Y. C., SHEN, C., JIANG, K. W., YE, Y. J. & WANG, S. 2015. MiR-194, commonly repressed in colorectal cancer, suppresses tumor growth by regulating the MAP4K4/c-Jun/MDM2 signaling pathway. *Cell Cycle,* 14**,** 1046-58.

WANG, C. J., ZHOU, Z. G., WANG, L., YANG, L., ZHOU, B., GU, J., CHEN, H. Y. & SUN, X. F. 2009. Clinicopathological significance of microRNA-31, -143 and -145 expression in colorectal cancer. *Dis Markers,* 26**,** 27-34.

WANG, J., HUANG, S. K., ZHAO, M., YANG, M., ZHONG, J. L., GU, Y. Y., PENG, H., CHE, Y. Q. & HUANG, C. Z. 2014b. Identification of a circulating microRNA signature for colorectal cancer detection. *PLoS One,* 9**,** e87451.

WANG, K., LI, M. & HAKONARSON, H. 2010. ANNOVAR: functional annotation of genetic variants from high-throughput sequencing data. *Nucleic Acids Res,* 38**,** e164.

WANG, Y., LU, Z., WANG, N., FENG, J., ZHANG, J., LUAN, L., ZHAO, W. & ZENG, X. 2018. Long noncoding RNA DANCR promotes colorectal cancer proliferation and metastasis via miR-577 sponging. *Exp Mol Med,* 50**,** 57.

WARBURG, O. 1956. On respiratory impairment in cancer cells. *Science,* 124**,** 269-70.

WARNES. 2019. *Gplots: Various R Programming Tools for Plotting Data* [Online]. Available: https://cran.r-project.org/web/packages/gplots/index.html [Accessed 07.03.2019].

WEI, E. K., MA, J., POLLAK, M. N., RIFAI, N., FUCHS, C. S., HANKINSON, S. E. & GIOVANNUCCI, E. 2005. A prospective study of C-peptide, insulin-like growth factor-I, insulin-like growth factor binding protein-1, and the risk of colorectal cancer in women. *Cancer Epidemiol Biomarkers Prev,* 14**,** 850-5.

WILLIAM, M. G. & SANFORD, D. M. 2008. *28 TGF-β Signaling Pathway and Tumor Suppression*.

WILLIAMS, J., SMITH, F., KUMAR, S., VIJAYAN, M. & REDDY, P. H. 2017. Are microRNAs true sensors of ageing and cellular senescence? *Ageing Res Rev,* 35**,** 350-363.

WOOD, L. D., PARSONS, D. W., JONES, S., LIN, J., SJOBLOM, T., LEARY, R. J., SHEN, D., BOCA, S. M., BARBER, T., PTAK, J., SILLIMAN, N., SZABO, S., DEZSO, Z., USTYANKSKY, V., NIKOLSKAYA, T., NIKOLSKY, Y., KARCHIN, R., WILSON, P. A., KAMINKER, J. S., ZHANG, Z., CROSHAW, R., WILLIS, J., DAWSON, D., SHIPITSIN, M., WILLSON, J. K., SUKUMAR, S., POLYAK, K., PARK, B. H., PETHIYAGODA, C. L., PANT, P. V., BALLINGER, D. G., SPARKS, A. B., HARTIGAN, J., SMITH, D. R., SUH, E., PAPADOPOULOS, N., BUCKHAULTS, P., MARKOWITZ, S. D., PARMIGIANI, G., KINZLER, K. W., VELCULESCU, V. E. & VOGELSTEIN, B. 2007. The genomic landscapes of human breast and colorectal cancers. *Science,* 318**,** 1108-13.

WORLD CANCER RESEARCH FUND 2018. Diet, Nutrition, Physical Activity and Cancer: a Global Perspective.

WORLD HEALTH ORGANIZATION. 2015. Fact sheet: Obesity and overweight. Available: http://www.who.int/mediacentre/factsheets/fs311/en/ [Accessed October 2014].

WORLD OBESITY DAY. 2015. *World Obesity Day Press Release.*

XIE, H., LIM, B. & LODISH, H. F. 2009. MicroRNAs induced during adipogenesis that accelerate fat cell development are downregulated in obesity. *Diabetes,* 58**,** 1050-7.

XIONG, B., CHENG, Y., MA, L. & ZHANG, C. 2013. MiR-21 regulates biological behavior through the PTEN/PI-3 K/Akt signaling pathway in human colorectal cancer cells. *Int J Oncol,* 42**,** 219-28.

XU, C., ZHANG, L., DUAN, L. & LU, C. 2016. MicroRNA-3196 is inhibited by H2AX phosphorylation and attenuates lung cancer cell apoptosis by downregulating PUMA. *Oncotarget,* 7**,** 77764-77776.

YANG, D., OYAIZU, Y., OYAIZU, H., OLSEN, G. J. & WOESE, C. R. 1985. Mitochondrial origins. *Proceedings of the National Academy of Sciences of the United States of America,* 82**,** 4443-4447.

YANG, M.-H., YU, J., CHEN, N., WANG, X.-Y., LIU, X.-Y., WANG, S. & DING, Y.-Q. 2014. Elevated MicroRNA-31 Expression Regulates Colorectal Cancer Progression by Repressing Its Target Gene SATB2. *PLOS ONE,* 8**,** e85353.

YANG, Y., ZHANG, J., CHEN, X., XU, X., CAO, G., LI, H. & WU, T. 2018. LncRNA FTX sponges miR-215 and inhibits phosphorylation of vimentin for promoting colorectal cancer progression. *Gene Therapy,* 25**,** 321-330.

YIN, X., LANZA, I. R., SWAIN, J. M., SARR, M. G., NAIR, K. S. & JENSEN, M. D. 2014. Adipocyte Mitochondrial Function Is Reduced in Human Obesity Independent of Fat Cell Size. *The Journal of Clinical Endocrinology and Metabolism,* 99**,** E209-E216.

YONEYAMA, H., HARA, T., KATO, Y., YAMORI, T., MATSUURA, E. T. & KOIKE, K. 2005. Nucleotide sequence variation is frequent in the mitochondrial DNA displacement loop region of individual human tumor cells. *Mol Cancer Res,* 3**,** 14-20.

YU, T., MA, P., WU, D., SHU, Y. & GAO, W. 2018. Functions and mechanisms of microRNA-31 in human cancers. *Biomed Pharmacother,* 108**,** 1162-1169.

YU, X. F., ZOU, J., BAO, Z. J. & DONG, J. 2011. miR-93 suppresses proliferation and colony formation of human colon cancer stem cells. *World J Gastroenterol,* 17**,** 4711-7.

YUN, J., RAGO, C., CHEONG, I., PAGLIARINI, R., ANGENENDT, P., RAJAGOPALAN, H., SCHMIDT, K., WILLSON, J. K., MARKOWITZ, S., ZHOU, S., DIAZ, L. A., JR., VELCULESCU, V. E., LENGAUER, C., KINZLER, K. W., VOGELSTEIN, B. & PAPADOPOULOS, N. 2009. Glucose deprivation contributes to the development of KRAS pathway mutations in tumor cells. *Science,* 325**,** 1555-9.

ZHANG, Y., YANG, L., GAO, Y. F., FAN, Z. M., CAI, X. Y., LIU, M. Y., GUO, X. R., GAO, C. L. & XIA, Z. K. 2013. MicroRNA-106b induces mitochondrial dysfunction and insulin resistance in C2C12 myotubes by targeting mitofusin-2. *Mol Cell Endocrinol,* 381**,** 230-40.

ZHAO, H. J., REN, L. L., WANG, Z. H., SUN, T. T., YU, Y. N., WANG, Y. C., YAN, T. T., ZOU, W., HE, J., ZHANG, Y., HONG, J. & FANG, J. Y. 2014. MiR-194 deregulation contributes to colorectal carcinogenesis via targeting AKT2 pathway. *Theranostics,* 4**,** 1193-208.

ZHAO, J., XU, J. & ZHANG, R. 2018. SRPX2 regulates colon cancer cell metabolism by miR-192/215 via PI3K-Akt. *Am J Transl Res,* 10**,** 483-490.

ZHENG, W., KHRAPKO, K., COLLER, H. A., THILLY, W. G. & COPELAND, W. C. 2006. Origins of human mitochondrial point mutations as DNA polymerase gamma-mediated errors. *Mutat Res,* 599**,** 11-20.

ZHONG, L., SIMONEAU, B., HUOT, J. & SIMARD, M. J. 2017. p38 and JNK pathways control E-selectin-dependent extravasation of colon cancer cells by modulating miR-31 transcription. *Oncotarget,* 8**,** 1678-1687.

ZHU, H., SHYH-CHANG, N., SEGRE, A. V., SHINODA, G., SHAH, S. P., EINHORN, W. S., TAKEUCHI, A., ENGREITZ, J. M., HAGAN, J. P., KHARAS, M. G., URBACH, A., THORNTON, J. E., TRIBOULET, R., GREGORY, R. I., ALTSHULER, D. & DALEY, G. Q. 2011. The Lin28/let-7 axis regulates glucose metabolism. *Cell,* 147**,** 81-94.

ZINOVKINA, L. A. 2018. Mechanisms of Mitochondrial DNA Repair in Mammals. *Biochemistry (Mosc),* 83**,** 233-249.

8 Appendices

A. Biomarkers of Colorectal Cancer after Bariatric Surgery Exclusion Criteria

Pre-procedure	Post-procedure	Exclusion based on rigid sigmoidoscopy findings	Normal BMI control
Age <16 or >65	Pregnancy	CRC or active inflammation	Significant pathology on follow-up colonoscopy
Previous colorectal resection	Major post-operative complications	Macroscopically abnormal rectal mucosa	
Steroids, except topical, or other immunosuppressive medication		Unexpected microscopic abnormality on histological examination of rectal biopsies	
Active or previous history of Crohn's or Ulcerative Colitis		Difficulty in performing rigid sigmoidoscopy	
Other inflammatory bowel disease (IBD)		Other technical difficulty	
Familial polyposis syndrome			
Lynch syndrome (Amsterdam II criteria)			

Previous weight loss surgery			
Warfarin or other anticoagulation			
Pacemaker – NO BIOIMOPEDANCE			

Table 8-1: Exclusion criteria of participant's to the BOCABS Study for pre-procedure, post-procedure, based on rigid sigmoidoscopy findings and for normal BMI control.

NHS
Health Research Authority

West Midlands - Coventry & Warwickshire Research Ethics Committee

The Old Chapel

Royal Standard Place

Nottingham

NG1 6FS

Please note: This is an acknowledgement letter from the REC only and does not allow you to start your study at NHS sites in England until you receive HRA Approval

---

29 November 2016

Professor John C Mathers

Biomedical Research Building

Campus for Ageing and Vitality

Newcastle upon Tyne

NE4 5PL

Dear Professor Mathers,

Study title:	Mucosal biomarkers of bowel cancer risk: 10 year follow-up of BORICC Study
REC reference:	16/WM/0424
IRAS project ID:	207081

Thank you for your letter of 23rd November 2016. I can confirm the REC has received the documents listed below and that these comply with the approval conditions detailed in our letter dated 09 November 2016

Documents received

The documents received were as follows:

Document	Version	Date
Participant information sheet (PIS) [Invitation letter and information sheet]	2.1	22 November 2016

Approved documents

The final list of approved documentation for the study is therefore as follows:

Document	Version	Date
GP/consultant information sheets or letters [Letter to GP]	1	26 July 2016
IRAS Application Form [IRAS_Form_14092016]		14 September 2016
IRAS Checklist XML [Checklist_23112016]		23 November 2016
Letter from funder [TRF Funding Award Letter]	1	18 September 2015
Letter from sponsor	1	
Non-validated questionnaire [Sunlight exposure questionnaire]	1	26 July 2016
Other [Response to Ethics Committee Review]	1	01 November 2016
Other [PhD Student Information]		
Participant consent form [Consent form]	1	08 July 2016
Participant information sheet (PIS) [Invitation letter and information sheet]	2.1	22 November 2016
Referee's report or other scientific critique report [TRF reviewer's report 1]	1	01 August 2016
Referee's report or other scientific critique report [TRF reviewer's report 2]	1	01 August 2016

Research protocol or project proposal [Project Proposal]	1	02 August 2016
Summary CV for Chief Investigator (CI) [Chief Investigator CV]	1	01 August 2016
Summary CV for student [Abraham CV]	1	16 September 2016
Summary CV for student [Summary CV for PhD Student]	1	02 November 2016
Summary CV for supervisor (student research) [Bradburn CV]	1	12 September 2016
Summary CV for supervisor (student research) [Malcomson CV]	1	12 September 2016
Summary, synopsis or diagram (flowchart) of protocol in non technical language [Proposed schedule of interaction with participants for section A13]	1	02 August 2016
Validated questionnaire [FFQ]	1	01 August 2016
Validated questionnaire [Lifestyle questionnaire]	1	01 August 2016

You should ensure that the sponsor has a copy of the final documentation for the study. It is the sponsor's responsibility to ensure that the documentation is made available to R&D offices at all participating sites.

16/WM/0424	**Please quote this number on all correspondence**

Yours sincerely,

Rachel Nelson REC Manager

E-mail: NRESCommittee.WestMidlands-CoventryandWarwick@nhs.net

Copy to: Ms. Caroline Potts

West Midlands - Coventry & Warwickshire Research Ethics Committee

The Old Chapel

Royal Standard Place

Nottingham

NG1 6FS

Please note: This is the favourable opinion of the REC only and does not allow the amendment to be implemented at NHS sites in England until the outcome of the HRA assessment has been confirmed.

23 May 2017

Ms. Caroline Potts

Northumbria NHS Foundation Trust

Research Support Unit

North Tyneside General Hospital

Rake Lane, North Shields

NE29 8NH

Dear Ms. Potts

Study title:	Mucosal biomarkers of bowel cancer risk: 10 year follow-up of BORICC Study
REC reference:	16/WM/0424
Amendment number:	1
Amendment date:	11 April 2017
IRAS project ID:	207081

The above amendment was reviewed between 08 May and 23 May 2017 by the Sub-Committee in correspondence.

Ethical opinion

The members of the Committee taking part in the review gave a favourable ethical opinion of the amendment on the basis described in the notice of amendment form and supporting documentation.

The sub-committee asked the applicant to write the acronym BORICC in full in the invitation letter.

The sub-committee asked the applicant to confirm that patients in the original BORICC study (12 plus years ago) gave their consent to be approached in a follow up study.

The sub-committee queried with the applicant if checks will be made on participants have passed away before sending information out to them.

The above queries were made to the applicant by the REC office by means of email on 11th May 2017. *The applicant responded the same day in reply to the email with an updated invitation letter (version 3.1) which writes out the BORICC acronym.*

In the same response the applicants provided a cover letter confirming that although the original study did not get consent to approach participants for a new study, at an event held in April 2016 the idea of a followup study was received very positively by 90% of the attending participants who were very keen to participant in a follow-up. The applicant also assured that potential participants will be approached by their clinician.

In the same response the applicants confirmed in the cover letter that potential participants will be screened using the SIRUS and Single View platforms to identify participants who have passed away or who do not meet our inclusion criteria.

The sub-committee agreed that the amendment with the responses and updated invitation letter do not present any ethical issues.

Approved documents

The documents reviewed and approved at the meeting were:

Document	Version	Date
Letters of invitation to participant [BORICC Follow Up Study Invitation Letter v3.0.docx]	3.1	11 May 2017
Notice of Substantial Amendment (non-CTIMP)	1	11 April 2017
Other [Response card.docx]	1	05 April 2014
Summary, synopsis or diagram (flowchart) of protocol in non technical language [A13-Figure 1 Proposed schedule of interactions with participants.docx]	2	11 April 2017
Response to Ethics Committee May 2017		

Membership of the Committee

The members of the Committee who took part in the review are listed on the attached sheet.

Working with NHS Care Organisations

Sponsors should ensure that they notify the R&D office for the relevant NHS care organisation of this amendment in line with the terms detailed in the categorisation email issued by the lead nation for the study.

Statement of compliance

The Committee is constituted in accordance with the Governance Arrangements for Research Ethics Committees and complies fully with the Standard Operating Procedures for Research Ethics Committees in the UK.

We are pleased to welcome researchers and R & D staff at our Research Ethics Committee members' training days – see details at http://www.hra.nhs.uk/hra-training/

16/WM/0424:	Please quote this number on all correspondence

Yours sincerely

Professor Jane Appleton Chair

E-mail: NRESCommittee.WestMidlands-CoventryandWarwick@nhs.net

Enclosures: List of names and professions of members who took part in the review

Copy to: Ms. Caroline Potts, Northumbria NHS Foundation Trust
*   Professor John C Mathers*

West Midlands - Coventry & Warwickshire Research Ethics Committee

Attendance at Sub-Committee of the REC meeting on 08 May 2017

Committee Members:

Name	Profession	Present
Professor Jane Appleton (Chair)	Nurse	Yes
Mrs Louise Harmer	Undergraduate Medical Education Manager, Technology Enhanced Learning and Clinical Skills and Resuscitation Tutor	Yes

West Midlands - Coventry & Warwickshire Research Ethics Committee

The Old Chapel

Royal Standard Place

Nottingham

NG1 6FS

 Please note: This is the favourable opinion implemented   at NHS sites in England until the outcome of the HRA assessment has been confirmed. of the REC only and does not allow the amendment to be

15 December 2017

Abraham Joel

Teaching and Research Fellow

Wansbeck General Hospital

Education Department

Wansbeck General Hospital

Ashington

NE63 9JJ

Dear Abraham Joel

Study title:	Mucosal biomarkers of bowel cancer risk: 10 year follow-up of BORICC Study
REC reference:	16/WM/0424
Amendment number:	2
Amendment date:	17 November 2017
IRAS project ID:	207081

The above amendment was reviewed by the Sub-Committee in correspondence.

Ethical opinion

The members of the Committee taking part in the review gave a favourable ethical opinion of the amendment on the basis described in the notice of amendment form and supporting documentation.

The sub-committee had some queries for the applicant of the amendment. The queries were presented to the applicant by email on 11 December 2017. The applicant responded 12th
December in reply to the email and the responses by the applicant are represented here in italics.

i)   **Has the applicant checked that the non-respondent is still alive? If so, how do they do this?**

Yes. Clinical members of our team (Abraham Joel & Khalil El Gendy) have checked that participants are still alive using Single View software on NHS Northumbria Trust computers. We make no attempt to contact any participants who have passed away or their families.

ii)   **How will the applicant be sure that they really are talking to the person they want?**

When calling, the administrative member of staff making the phone calls (Yasmin Ibrahim) will ask for the participant stating their full name. Should there be any question about the participant in question being on the telephone (for example if there is more than one household member with the same name), Yasmin will have access to the participant's date of birth.

iii) What happens if the person who answers the phone asks for more detail before giving any information?

The administrative member of staff (Yasmin Ibrahim) will have a script including a short paragraph about the BORICC Study at baseline (e.g. where and when it took place and what it investigated). Should the person on the telephone ask for more details or ask any questions about the study, Yasmin will ask that person if they are happy to be contacted by a member of the research team.

iv) How will the applicant know if the person they want still has capacity?

Similar to the situation (i), prior to contacting any potential participants, Single View has been used to check whether participants meet any of our exclusion criteria (e.g. are unable to provide informed written consent due to having a mental illness or dementia).

Regarding those that only want one visit, how will the applicant activity monitor? The subcommittee state there isn't much information about it in the PIS.

The physical activity monitor is sent to participants by post as a component of the study pack, together with instructions for its use. Participants return the monitor when they come to the hospital for their study visit.

There is some information on this in the PIS, such as: Wear a physical activity monitor (a small wrist-worn device) for one week

The above questionnaires, physical activity monitor and sample collection pots will be posted to you in advance. We will then ask you bring these along with you to your hospital appointment. And if you are willing to participate, we will arrange your study visit at the hospital and send you a consent form (to be signed and brought to the hospital study visit), the questionnaires to be completed, together with the sample collection pots and a physical activity monitor.

The sub-committee agreed that although the REC committee would normally advise against phone calls, especially when two written invites have already

been sent which could add pressure to the participant it was agreed the robust answers from the applicant do not present any ethical issue as long as the researchers are very careful to stick to the criteria.

Approved documents

The documents reviewed and approved at the meeting were:

Document	Version	Date
Notice of Substantial Amendment (non-CTIMP)	2	17 November 2017
Other [Telephone call script.docx]	1	17 November 2017
Participant information sheet (PIS) [BORICC Follow Up Study Participant Information Sheet- no biopsies.docx]	1	17 November 2017
Research protocol or project proposal [BORICC Follow Up Study Project Protocol_track changes.docx]	2.0	05 December 2017

Membership of the Committee

The members of the Committee who took part in the review are listed on the attached sheet.

Working with NHS Care Organisations

Sponsors should ensure that they notify the R&D office for the relevant NHS care organisation of this amendment in line with the terms detailed in the categorisation email issued by the lead nation for the study.

Statement of compliance

The Committee is constituted in accordance with the Governance Arrangements for Research Ethics Committees and complies fully with the Standard Operating Procedures for Research Ethics Committees in the UK.

We are pleased to welcome researchers and R & D staff at our Research Ethics Committee members' training days – see details at http://www.hra.nhs.uk/hra-training/

16/WM/0424:	Please quote this number on all correspondence

Yours sincerely

pp Adam Gannett

Dr Helen Brittain (Chair)
Chair

E-mail: NRESCommittee.WestMidlands-CoventryandWarwick@nhs.net

Enclosures: *List of names and professions of members who took part in the review*

Copy to: *Ms. Caroline Potts, Northumbria NHS Foundation Trust Mr. Abraham Joel, Wansbeck General Hospital*

West Midlands - Coventry & Warwickshire Research Ethics Committee

Attendance at Sub-Committee of the REC meeting

Committee Members:

Name	Profession	Present
Dr Helen Brittain (Chair)	Clinical Psychologist Retired	Yes
Mrs Louise Harmer	Undergraduate Medical Education Manager, Technology Enhanced Learning and Clinical Skills and Resuscitation Tutor	Yes

Also in attendance:

Name	Position (or reason for attending)
Mr Adam Garretty	REC Assistant

Dept of Surgery

Woodhorn Lane

Wansbeck Hospital

Dear

Thank you very much for your participation in the BORICC Study several years ago. We are writing to inform you that we are conducting a follow-up study to investigate the effects of ageing (12+ years) and lifestyle factors on changes in biomarkers (a biological marker) of bowel cancer risk.

We have organised three showcase events at North Tyneside General Hospital for participants from the original BORICC Study to provide you with information on the findings from the study 12+ years ago and on what we plan to do in the follow-up study. It will also be an opportunity for you to see the equipment that we will be using, to try out some of our tests, such as hand grip strength, and to ask questions about the new project. Light refreshments will be provided.

We would like to invite you to participate in one of these showcase events which have been organised at different times of the week to try to accommodate everyone. The following are the event dates:

- *Saturday 21st April at 11am*
- *Monday 30th April at 11am*
- *Monday 30th April at 4pm*

If you would like to attend, please confirm your attendance by returning the enclosed card or by contacting the research team (details below). In addition, please let us know if these dates are unsuitable for you and you are interested in attending a future event. If you are interested in taking part in the study but would prefer not to attend a showcase event, please indicate this on the card.

Dr. Fiona Malcomson

Human Nutrition Research Centre

Room 147, 1ˢᵗ Floor William Leech Building

Institute of Cellular Medicine

Medical School

Newcastle University

Framlington Place

Newcastle upon Tyne

NE2 4HH

Telephone: 0191 2081141 (please ask for Fiona or another member of the BFU Study team) *Mobile:* 07791642754

Email: fiona.malcomson@newcastle.ac.uk

Thank you for your cooperation which is very much appreciated.

Yours sincerely

Mike Bradburn

Consultant Surgeon

Wansbeck Hospital

On behalf of the Newcastle University research team: Prof. John Mathers, Dr. Laura Greaves,   Dr. Fiona Malcomson, Mr. Abraham Joel, Mrs. Stella Breininger, Mrs. Thilanka Ranathunga and Mr. Khalil El Gendy

PARTICIPANT INFORMATION SHEET

1.   Invitation

You are being invited to take part in a research follow-up study conducted by Northumbria NHS Foundation Trust and Newcastle University. Before you decide whether you would like to take part, please take time to read the following information carefully. You may wish to discuss the study with relatives, friends and your GP. Please contact the research team if there is anything that is not clear to you, if you have any questions or would like more information.

Your decision will not affect any other aspect of the care that you may be receiving, or may receive in the future, at the hospital. If you do decide to participate, we will ask for your permission to inform your GP, so that they are aware of your participation in the study. Thank you very much for taking the time to read this.

2.   Why is this study being performed?

Bowel problems are common and lifestyle factors, such as diet and physical activity, are known to be important in the development of certain diseases of the large bowel (colon). Ageing is also a strong contributor to changes in the large bowel and disease development. In the original BORICC Study, we found that diet affects certain proteins and genes in the cells of the large bowel. In this follow-up study, we would like to investigate the effects of ageing (over a period of about 10 years) on cells in the large bowel and to what extent these changes are affected by lifestyle factors. We hope that this study will give us a better understanding of the relationship between ageing, diet and physical activity and the health of the bowel.

3.   Why have I been asked to participate in the study?

You have been invited to participate in this follow-up study because you took part in the original BORICC Study about 10 years ago. As we are taking follow-up measurements, we will recruit the

original participants from the BORICC Study so that we can compare the data from 10 years ago with data collected in this later study.

4.   Do I have to take part?

It is for you to decide whether you wish to take part. If you decide to participate in this study, you will be asked to sign a consent form. Even if you do decide to take part in this study, you can withdraw at any time. If you decide to withdraw from the study, you will not have to tell us why and it will not affect your treatment in any way.

5.   What will I have to do as a volunteer?

As mentioned above, if you decide that you wish to volunteer, then you will be invited to sign a consent form.

We would like to collect the following information and samples during a clinic appointment at North Tyneside General Hospital, which will last around 1 hour:

- Medical history
- Height, weight, waist and hip measurements
- Body fat percentage measured using bioimpedance weighing scales with footplates
- Blood samples (seven 5ml tubes, equating to no more than 35ml)
- Sigmoidoscopy and collection of 10 rectal biopsies (please see below)
- One inner cheek swab
- Musculoskeletal function tests (timed up and go, hand grip strength and heel ultrasound tests)

We would also like you to do the following at home:

- Complete a food frequency questionnaire (this will take approximately 30 minutes)
- Complete a lifestyle questionnaire (this will take approximately 5 minutes)
- Complete a sunlight exposure questionnaire (this will take approximately 10 minutes)
- Collect two urine samples and one stool sample - we will provide you with instructions and pots for sample collection
- Wear a physical activity monitor (a small wrist-worn device) for one week The above questionnaires, physical activity monitor and sample collection pots will be posted to you in advance. We will then ask you bring these along with you to your hospital appointment.

6.   Does the study involve any invasive tests?

To obtain small samples of tissue (biopsies) from the bowel wall we will need to perform a short camera examination of your bowel called a sigmoidoscopy. We plan to take ten pinch biopsies from the bowel wall at a distance of 10cm (4 inches) from the back passage. This will be performed by a clinician trained in this endoscopic examination who will examine for any conditions which may cause pain, such as fissures or haemorrhoids, before proceeding.

The procedure is associated with some discomfort but this is usually mild. The procedure should not be painful and is normally carried out without the need for anaesthetic or sedation. If you were to find the procedure too uncomfortable then you would, of course, be able to ask the clinician to stop. In our previous study, we completed 81 similar procedures and did not encounter anybody who found the procedure too uncomfortable to ask the doctor to stop. You should not experience any pain during the taking of biopsies from the bowel wall.

7.   How does the follow-up study differ from the original BORICC Study?

The sigmoidoscopy used to collect the bowel wall samples is a less invasive procedure than that used in the original BORICC study. In the original study, bowel wall biopsies were collected during colonoscopy or flexible sigmoidoscopy procedures which require bowel preparations (such as enemas, suppositories or strong laxatives). In contrast, a sigmoidoscopy does not require you to take any bowel preparation and the camera does not have to go through the bends in the bowel. The procedure should take only approximately 15 minutes.

We will also be taking some additional information from you in this follow-up study which we did not collect in the original BORICC Study:

- Physical activity data collected by a physical activity monitor worn on your wrist for one week
- Sunlight exposure data (to measure vitamin D) collected from a questionnaire
- Physical capability data collected from two muscle function tests (the 'timed stand up and go test' the 'hand grip strength' test and the heel ultrasound test). The 'timed stand up and go' test involves sitting on a chair, standing up, walking to a cone and returning to sit back down on the chair. The handgrip strength involves sitting and resting your arm on an armchair, then gripping and squeezing a dynamometer (a small device that measures force) as hard as you can. The heel ultrasound test involves placing your foot in the heel ultrasound machine's

footwell and sitting still for approximately 10 seconds whilst the device makes the measurements.

- Buccal (inner cheek) samples collected with a swab by rubbing the inner cheek of the mouth.

8. What are the risks of sigmoidoscopy examination and biopsies?

Some people may experience some bloating, cramping, abdominal discomfort and excess wind after the procedure. This is usually from the air that we puff in to the bowel in order to expand it during the examination, which we try to minimise. If these side effects do occur, they are unlikely to last for more than 24 hours and usually resolve without the need for any treatment.

The sigmoidoscopy examination is generally considered a safe procedure, but it does carry a very small risk of complications. It is important that you understand this before deciding whether or not to participate. There is a very small chance (1 in 65,000) of a perforation (a puncture) of the bowel. Although very rare, a perforation will usually require surgery. Significant bleeding is also a rare (1 in 10,000) potential complication. The risk of bleeding or perforation is higher with each biopsy that is being taken. There are no other known lasting adverse effects of this test. If you were to suffer any of the following symptoms within 48 hours after a sigmoidoscopy, you are advised to consult a doctor immediately:

- Severe abdominal pain
- Significant rectal bleeding
- Fever

9. What happens if anything goes wrong?

If, in the very unlikely event, taking part in this study causes any harm to you, there are no special compensation arrangements, but you will still be entitled to complain through the usual hospital procedures. If you are harmed due to someone's negligence or wrongdoing then you may have grounds for legal action, but you may have to pay for it. You may withdraw from the study at any time without explaining why and this will not affect any future care that you may receive.

10. Will my information be confidential?

Yes, all of the information we will collect from you during the study will be strictly confidential. This information will be kept securely while the study is taking place. Only the research team will have

access to the study data. Furthermore, your information and data will be anonymised and you will be given a specific study ID number. Specific details, which could identify you, will only be available to the research team. Your GP will be informed that you are taking part in this study.

11.   What will happen to the samples collected in this study?

The samples that are collected will be examined at laboratories in Newcastle University. All samples will be stored securely. We will perform tests to look for various markers of cell and metabolic activity. We will try to link these changes with your habitual diet, based on the information you gave us in the food frequency questionnaire, and physical activity levels, based on your lifestyle questionnaire and physical activity monitor data.

After the study has finished, the samples will be stored in our laboratory freezers in accordance with government regulations. Your name and details will not be recorded on the samples. All of the samples will be anonymised, meaning that the data resulting from your samples cannot be traced to yourself.

We will keep the samples so that we can do further testing if new techniques or markers are discovered, without having to collect any new samples. We may send samples to collaborating research institutes for additional analyses but this will not be for financial gain.

12.   How often will I need to visit the hospital if I decide to volunteer for the study?

You will be asked to attend the hospital for approximately 1 hour on one occasion only. We will reimburse any travel expenses incurred.

13.   What benefits will I get from the study?

You will not directly benefit from volunteering to participate in this study. However, we will give you feedback on your diet and lifestyle which you may find useful. The research may well help us understand how ageing and lifestyle factors, such as diet and physical activity, affect large bowel health and consequently the development of diseases of the large bowel, such as bowel cancer. This may lead to the development of prevention and/or treatment strategies. Once the study is completed, a summary of the findings can be made available to you upon request.

14.   Do I need to take a day off work?

We understand that people lead busy lives. If appointments during usual working hours do not suit your lifestyle, then we may be able to work flexibly in order to accommodate you. You can discuss this in more detail with one of the members of the research team.

15.   Who has reviewed the study?

The West Midlands – Coventry & Warwickshire Research Ethics Committee has reviewed the study (REC reference 16/WM/0424).

16.   Who is performing the research?

- Professor John Mathers is Professor of Human Nutrition and Director of the Human Nutrition Research Centre (HNRC) at Newcastle University
- Mr. Mike Bradburn is a consultant surgeon at Wansbeck General Hospital
- Dr. Laura Greaves is a Research Fellow at Newcastle University
- Dr. Fiona Malcomson is a Research Associate at Newcastle University
- Mr. Abraham Joel is a Teaching and Research Fellow at Northumbria NHS Foundation Trust and will be conducting this research as part of his PhD project
- Mrs. Stella Breininger is a PhD student at Newcastle University and will be conducting this research as part of her PhD project
- Mrs. Thilanka Ranathunga is a PhD student at Newcastle University and will be conducting this research as part of her PhD project
- Mr. Khalil El Gendy is a MD student at Newcastle University and will be conducting this research as part of his PhD project

17.   Who should I contact if I have questions or would like additional information?

Dr. Fiona Malcomson

Human Nutrition Research Centre

Room 147, 1st Floor William Leech Building

Institute of Cellular Medicine

Medical School

Newcastle University

Framlington Place

Newcastle upon Tyne

NE2 4HH

Telephone: 0191 2081141 (please ask for Fiona or another member of the BFU Study research team)

Mobile: 07791642754

Email: fiona.malcomson@newcastle.ac.uk

In addition, you may contact the Patient Advice Liaison Service (PALS) for confidential advice, support and information on health-related matters.

Patient advice and liaison services: Wansbeck General Hospital

Woodhorn Lane

Ashington

Northumberland

NE63 9JJ

Telephone: 0800 0320202

Email: northoftynepals@nhct.nhs.uk

18.   What should I do next if I would like to volunteer?

If you think that you would like to volunteer in this study, we invite you to contact the research team in writing or by telephone, when we will provide more information about the study and answer any further questions. If you are willing to participate, we will arrange your study visit at the hospital and send you a consent form (to be signed and brought to the hospital study visit), the questionnaires to be completed, together with the sample collection pots and a physical activity monitor.

Please contact us if you have any questions or would like any additional information.

Study coordinator,

Dr. Fiona Malcomson

Research Associate

Human Nutrition Research Centre

Newcastle University

The BFU Study Showcase Event

Discover the results from the BORICC Study at baseline
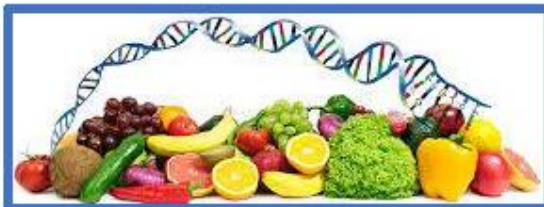
Find out what we are planning to do in the BORICC Follow-Up (BFU) Study

Experience some of the measurements we will be making in the BFU Study

Events will be held at North Tyneside General Hospital on:
- Saturday 21st April at 11am
- Monday 30th April at 11am
- Monday 30th April at 4pm

H. BFU Study response card

Response card

Name: _____

☐ Yes, I am interested in attending the BFU Study
Showcase event on _____
(please specify event date)

☐ Yes, I am interested in attending the BFU Study
Showcase event however these dates are not suitable
for me

☐ Yes, I am interested in taking part in the BFU Study but
I prefer not to attend a showcase event.

☐ No, I am not interested in taking part in the BFU Study
and I do not wish to be contacted again by the research
team.

Please return the response card in the attached pre-paid, addressed envelope. Alternatively, please contact the research team by telephone or email with your response.

Version 1.0
Date 05/04/2017

I. Nextera XT DNA Library Prep Kit (illumina®) Protocol

Nextera XT DNA Library Prep Kit

Reference Guide

For Research Use Only. Not for use in diagnostic procedures.

Agilent RNA 6000 Pico Kit

Table 1	Agilent RNA 6000 Pico Kit (reorder number 5067-1513)
Agilent RNA 6000 Pico Chips	
25 RNA Pico Chips	
3 Electrode Cleaners	
Agilent RNA 6000 Pico Reagents (reorder number 5067-1514)	
● (blue) RNA 6000 Pico Dye Concentrate[1]	
● (green) RNA 6000 Pico Marker (4 vials)	
○ (white) RNA 6000 Pico Conditioning Solution	
● (red) RNA 6000 Pico Gel Matrix (2 vials)	
● (yellow) RNA 6000 Pico Ladder (reorder number 5067-1535) (1 vial, 10x concentrate).	
4 Spin Filters	
Tubes for Gel-Dye Mix	
30 Safe-Lock Eppendorf Tubes PCR clean (DNase/RNase free) for gel-dye mix	
Syringe Kit	
1 Syringe	

[1] "This product is provided under a license by Life Technologies Corporation to Agilent Technologies. The purchase of this product conveys to the buyer the non-transferable right to use the purchased amount of the product and components of the product only as described in accompanying product literature. The sale of this product is expressly conditioned on the buyer not using the product or its components (1) in manufacturing; (2) to provide a service, information, or data to an unaffiliated third party for payment; (3) for therapeutic, diagnostic or prophylactic purposes; (4) to resell, sell or otherwise transfer this product or its components to any third party, or use for any use other than use in the subfields of research and development, quality control, forensics, environmental analysis, biodefense or food safety testing. For information on purchasing a license to this product for purposes other than described above contact Life Technologies Corporation, Cell Analysis Business Unit, Business Development, 29851 Willow Creek Road, Eugene, OR 97402, Tel: (541) 465-8300. Fax: (541) 335-0354."

248

Table 2   Physical Specifications

Type	Specification
Analysis time	30 min
Samples per chip	11
Sample volume	1 μL
Kit stability	= 4 months at 4 °C
Kit size	25 chips 11 samples/chip = 275 samples/kit

Table 3   Analytical Specifications

Specification	Total RNA Assay	mRNA Assay
Qualitative range	50 – 5000 pg/μL in water	250 – 5000 pg/μL in water
Sensitivity (S/N>3)	50 pg/μL in water or 200 pg/μL in TE	250 pg/μL in water or 500 pg/μL in TE
Quantitation reproducibility (within a chip)	20 % CV	20 % CV
Quantitation accuracy	30 %	-
Maximum sample buffer strength	50 mM Tris 0.1 mM EDTA or 50 mM NaCl 15 mM MgCl$_2$	50 mM Tris 0.1 mM EDTA or 50 mM NaCl 15 mM MgCl$_2$

Required Equipment for RNA 6000 Pico Assay

Equipment Supplied with the Agilent 2100 Bioanalyzer

- Chip priming station (reorder number 5065-4401)
- IKA vortex mixer

Additional Material Required (Not Supplied)

- RNaseZAP® recommended for electrode decontamination (Ambion, Inc. cat. no. 9780)
- RNase-free water
- Pipettes (10 µL and 1000 µL) with compatible tips (RNase-free, no filter tips, no autoclaved tips)
- 0.5 mL microcentrifuge tubes (RNase-free).Eppendorf Safe-lock PCR clean or Eppendorf DNA LoBind microcentrifuge tubes are highly recommended.
- Microcentrifuge (≥13000 g)
- Heating block or water bath for ladder/sample preparation
- Mandatory: bayonet electrode cartridge (reorder number 5065-4413)

Check the Agilent Lab-on-a-Chip webpage for details on assays:
www.agilent.com/chem/labonachip.

Setting up the Assay Equipment and Bioanalyzer

Before beginning the chip preparation protocol, ensure that the chip priming station and the bioanalyzer are set up and ready to use.

You have to

- replace the syringe at the chip priming station with each new kit
- adjust the base plate of the chip priming station
- adjust the syringe clip at the chip priming station
- set up the vortex mixer
- finally, make sure that you start the software before you load the chip.

> **NOTE** The RNA 6000 Pico assay is a high sensitivity assay. Please read this guide carefully and follow all instructions to guarantee satisfactory results.

251

Setting up the Chip Priming Station

Replace the syringe with each new reagent kit.

1 Replace the syringe:

   a Unscrew the old syringe from the lid of the chip priming station.

   b Release the old syringe from the clip. Discard the old syringe.

   c Remove the plastic cap of the new syringe and insert it into the clip.

   d Slide it into the hole of the luer lock adapter and screw it tightly to the chip priming station.

2 Adjust the base plate:

   a Open the chip priming station by pulling the latch.

   b Using a screwdriver, open the screw at the underside of the base plate.

   c Lift the base plate and insert it again in position C. Retighten the screw.
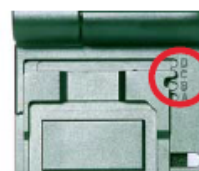
3 Adjust the syringe clip:

   a Release the lever of the clip and slide it up to the top position.

252

Setting up the Bioanalyzer

1 Open the lid of the bioanalyzer and make sure that the electrode cartridge is inserted in the instrument. If not, open the latch and insert the electrode cartridge.
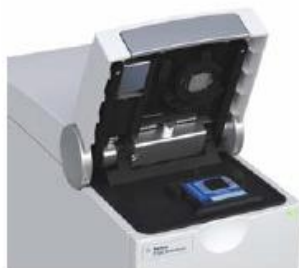
Figure 1   Electrode cartridge inserted in the instrument (graphic shows an example).

2 Remove any remaining chip.

Vortex Mixer

IKA - Model MS3

1 To set up the vortex mixer, adjust the speed knob to 2400 rpm.

Starting the 2100 Expert Software

To start the software:

1 Go to your desktop and double-click the following icon.

The screen of the software appears in the **Instrument** context. The icon in the upper part of the screen represents the current instrument/PC communication status:
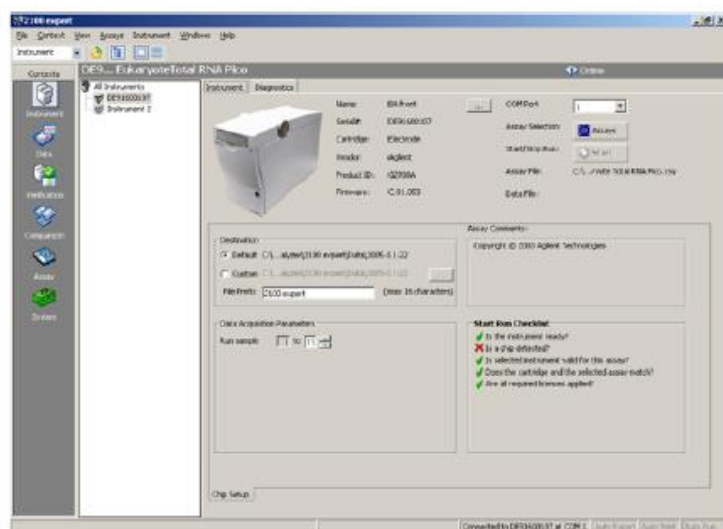
Lid closed, no chip or chip empty

Lid open

Dimmed icon: no communication

Lid closed, chip inserted, RNA or demo assay selected

2 If more than one instrument is connected to your PC, select the instrument you want to use in the tree view.

254

Essential Measurement Practices

- Handle and store all reagents according to the instructions on the label of the individual box.

- Avoid sources of dust or other contaminants. Foreign matter in reagents and samples or in the wells of the chip will interfere with assay results.

- Allow all reagents to equilibrate to room temperature for 30 min before use. Thaw samples on ice.

- Protect dye and dye mixtures from light. Remove light covers only when pipetting. The dye decomposes when exposed to light and this reduces the signal intensity.

- Always insert the pipette tip to the bottom of the well when dispensing the liquid. Placing the pipette at the edge of the well may lead to poor results.
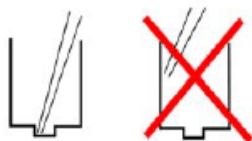
- Always wear gloves when handling RNA and use RNase-free tips, microcentrifuge tubes and water.

- It is recommended to heat denature all RNA samples and RNA ladder before use for 2 min and 70 °C (once) and keep them on ice.

- Do not touch the Agilent 2100 Bioanalyzer instrument during analysis and never place it on vibrating surface.

- Always vortex the dye concentrate for 10 s before preparing the gel-dye mix and spin down afterwards.

- Use a new syringe and electrode cleaners with each new kit.

- Use loaded chips within 5 min after preparation. Reagents might evaporate, leading to poor results.

- To prevent contamination (e.g. RNase), it is strongly recommended to use a dedicated electrode cartridge for RNA assays. For running the RNA 6000 Pico assay, the 16 pin bayonet cartridge is mandatory.

Preparing the RNA Ladder after Arrival

For proper handling of the ladder, following steps are necessary:

CAUTION To avoid RNase contamination and repetitive freeze/thaw cycles, the RNA ladder must be aliquoted in RNase-free vials.

→ Tests have shown that some plastic vial types can bind RNA on their surface. This can have an effect on RNA ladder concentration which affects the ladder identification and the quantitation of the sample. Eppendorf Safe-Lock PCR clean and Eppendorf DNA LoBind 0.5ml Microcentrifuge tubes were successfully tested for RNA ladder aliquoting.

1 After reagent kit arrival, spin ladder down. The ladder can be ordered separately (reorder number 5067-1535).

NOTE In case that the ladder vial type is not compatible with your heating block, transfer the entire volume (10 µl) to a recommended RNase-free vial.

2 Heat denature the ladder for 2 min at 70 °C.

3 Immediately cool the vial on ice.

4 Add 90 µL of RNase-free water and mix thoroughly.

5 Prepare aliquots in recommended 0.5 mL RNase-free vials with the required amount for typical daily use.

6 Store aliquots at -70 °C.

7 Before use, thaw ladder aliquots and keep them on ice (avoid extensive warming upon thawing process).

Agilent RNA 6000 Pico Assay Protocol

Agilent RNA 6000 Pico Assay Protocol

After completing the initial steps in "Setting up the Assay Equipment and Bioanalyzer" on page 7, you can prepare the assay, load the chip, and run the assay, as described in the following procedures.

> **NOTE** If you use the RNA 6000 Pico kit for the first time, you must read these detailed instructions. If you have some experience, you might want to use the *Agilent RNA 6000 Pico Quick Start Guide*.

Cleaning the Electrodes before Running Assays

To avoid decomposition of your RNA sample, follow this electrode cleaning procedure on a daily basis before running any RNA Pico assays.

> **NOTE** To prevent contamination problems, it is strongly recommended to use a dedicated electrode cartridge for RNA assays.

1 Slowly fill one of the wells of the electrode cleaner with 350 µl of fresh RNase-free water.

2 Open the lid and place the electrode cleaner in the Agilent 2100 Bioanalyzer instrument.

3 Close the lid and leave it closed for 5 minutes.

4 Open the lid and remove the electrode cleaner. Label the electrode cleaner and keep it for future use.

5 Wait another 30 seconds to allow the water on the electrodes to evaporate before closing the lid.

257

Preparing the Gel

1 Allow all reagents to equilibrate to room temperature for 30 minutes before use.

2 Place 550 µl of RNA 6000 Pico gel matrix (red ●) into the top receptacle of a spin filter.

NOTE Always use RNase-free microcentrifuge tubes, pipette tips and water.

3 Place the spin filter in a microcentrifuge and spin for 10 minutes at 1500 g ± 20 % (for Eppendorf microcentrifuge, this corresponds to 4000 rpm).

4 Aliquot 65 µl filtered gel into 0.5 ml RNase-free microcentrifuge tubes that are included in the kit. Store the aliquots at 4 °C and use them within one month of preparation.

Preparing the Gel-Dye Mix

| **WARNING** | **Handling DMSO** |

Kit components contain DMSO. Because the dye binds to nucleic acids, it should be treated as a potential mutagen and used with appropriate care.

→ Wear hand and eye protection and follow good laboratory practices when preparing and handling reagents and samples.

→ Handle solutions with particular caution as DMSO is known to facilitate the entry of organic molecules into tissues.

1 Allow all reagents to equilibrate to room temperature for 30 minutes before use. Protect the dye concentrate from light while bringing it to room temperature.

2 Vortex RNA 6000 Pico dye concentrate (blue ●) for 10 seconds and spin down.

3 Add 1 μl of RNA 6000 Pico dye concentrate (blue ●) to a 65 μl aliquot of filtered gel (prepared as described in "Preparing the Gel" on page 15).

Gel-dye mix

1 μl dye
65 μl filtered gel

4 Cap the tube, vortex thoroughly and visually inspect proper mixing of gel and dye. Store the dye concentrate at 4 °C in the dark again.

5 Spin tube for 10 minutes at room temperature at 13000 g (for Eppendorf microcentrifuge, this corresponds to 14000 rpm). Use prepared gel-dye mix within one day.

| **NOTE** | A larger volume of gel-dye mix can be prepared in multiples of the 65+1 ratio, if more than one chip will be used within one day. Always re-spin the gel-dye mix at 13000 g for 10 minutes before each use. |

259

Loading the Gel-Dye Mix

1 Allow the gel-dye mix to equilibrate to room temperature for 30 minutes before use. Protect the gel-dye mix from light during this time.

2 Take a new RNA chip out of its sealed bag.

3 Place the chip on the chip priming station.

4 Pipette 9.0 μl of the gel-dye mix at the bottom of the well marked Ⓖ and dispense the gel-dye mix.

9 μl gel-dye

NOTE When pipetting the gel-dye mix, make sure not to draw up particles that may sit at the bottom of the gel-dye mix vial. Insert the tip of the pipette to the bottom of the chip well when dispensing. This prevents a large air bubble forming under the gel-dye mix. Placing the pipette at the edge of the well may lead to poor results.
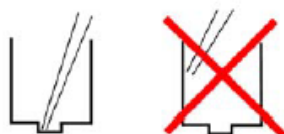
5 Set the timer to 30 seconds, make sure that the plunger is positioned at 1 ml and then close the chip priming station. The lock of the latch will click when the chip priming station is closed correctly.

6 Press the plunger of the syringe down until it is held by the clip.

7 Wait for exactly 30 seconds and then release the plunger with the clip release mechanism.

8 Visually inspect that the plunger moves back at least to the 0.3 ml mark.

9 Wait for 5 seconds, then slowly pull back the plunger to the 1 ml position.

pressurize

10 Open the chip priming station.

11 Pipette 9.0 µl of the gel-dye mix in each of the wells marked **G**

9 µl gel-dye
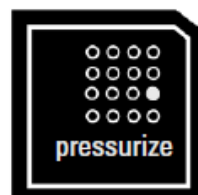
| NOTE | Please discard the remaining vial with gel-dye mix. |

Loading the RNA 6000 Pico Conditioning Solution and Marker

1 Pipette 9 µl of the RNA 6000 Pico conditioning solution (white ⟲) into the well marked CS.

9 µl RNA Cond Solution

2 Pipette 5 µL of the RNA 6000 Pico marker (green ●) into the well marked with a ladder (symbol ✔) and each of the 11 sample wells.

5 µl marker
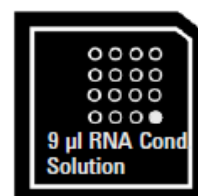
| NOTE | Do not leave any wells empty or the chip will not run properly. Add 5 µL of the RNA marker (green ●) plus 1 µL of deionized water to each unused sample well. |

Loading the Diluted Ladder and Samples

NOTE	Always use RNase-free microcentrifuge tubes, pipette tips and water.

1 To minimize secondary structure, you may heat denature (70 °C, 2 minutes) the samples before loading on the chip.

2 Before use, thaw ladder aliquots and keep them on ice (avoid extensive warming upon thawing process).

1 µl sample
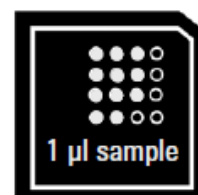
NOTE	Do not heat the diluted ladder. Use the defrosted diluted ladder within one day.

3 Pipette 1 µl of the diluted RNA 6000 Pico ladder (prepared as described in "Preparing the RNA Ladder after Arrival" on page 13) into the well marked with the ladder symbol

4 Pipette 1 µl of each sample into each of the 11 sample wells.

5 Place the chip horizontally in the adapter of the IKA vortex mixer and make sure not to damage the buldge that fixes the chip during vortexing.
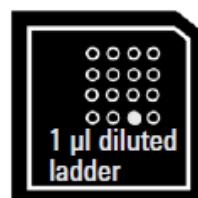
If there is liquid spill at the top of the chip, carefully remove it with a tissue.

1 µl diluted ladder

CAUTION	**Wrong vortexing speed**

If the vortexing speed is too high, liquid spill that disturbs the analysis may occur for samples generated with detergent containing buffers.

→ Reduce vortexing speed to 2000 rpm!

6 Vortex for 60 seconds at 2400 rpm.

7 Refer to the next topic on how to insert the chip in the Agilent 2100 Bioanalyzer instrument. Make sure that the run is started within 5 minutes.

NOTE	Depending on the RNA isolation protocol, varying results can be expected. Known dependencies include: salt content, cell fixation method and tissue stain. Best results are achieved for RNA samples which are dissolved in deionized and RNase-free water. Avoid genomic DNA contamination by including DNase treatment in the preparation protocol.

Inserting a Chip in the Agilent 2100 Bioanalyzer

1 Open the lid of the Agilent 2100 Bioanalyzer instrument.

2 Check that the electrode cartridge is inserted properly. Refer to "Setting up the Bioanalyzer" on page 9 for details.

3 Place the chip carefully into the receptacle. The chip fits only one way.

CAUTION	Sensitive electrodes and liquid spills Forced closing of the lid may damage the electrodes and dropping the lid may cause liquid spills resulting in bad results. → Do not use force to close the lid and do not drop the lid onto the inserted chip.

4 Carefully close the lid. The electrodes in the cartridge fit into the wells of the chip.

5 The 2100 Expert Software screen shows that you have inserted a chip and closed the lid by displaying the chip icon at the top left of the *Instrument* context.
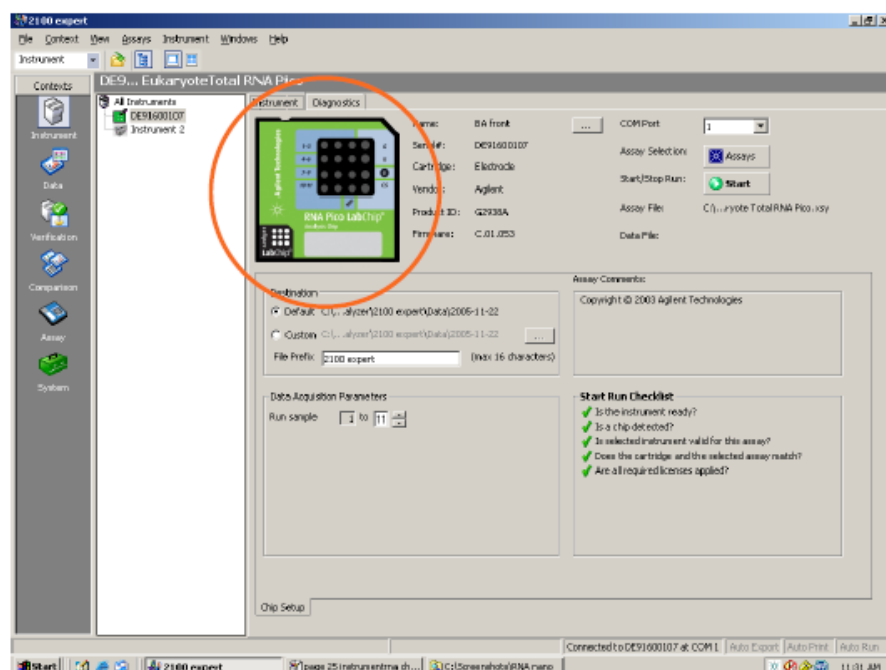
Starting the Chip Run

NOTE	Please note that the order of executing the chip run may change if the Agilent Security Pack software (only applicable for Agilent 2100 Expert Software Revision B.02.02 and higher) is installed. For more details please read the 'User's Guide' which is part of the Online Help of your 2100 Expert Software.

1   In the **Instrument** context, select the appropriate assay from the Assay menu.
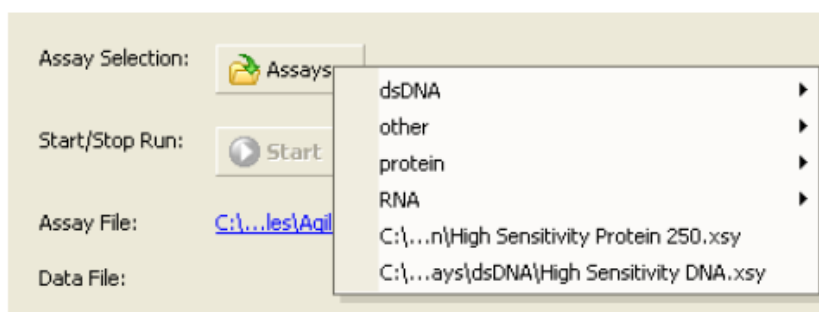
2   Accept the current **File Prefix** or modify it.

NOTE	Run sample numbers can vary between assays.
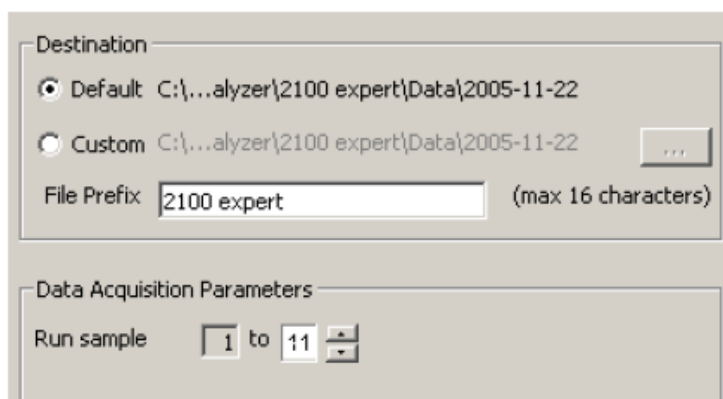
Data will be saved automatically to a file with a name using the prefix you have just entered. At this time you can also customize the file storage location and the number of samples that will be analyzed.

3 To enter sample information like sample names and comments, complete the sample name table.

	Sample Name	Sample Comment	Status	Observation	Result Label	Result Color
▶	Sample 1					
2	Sample 2					
3	Sample 3					
4	Sample 4					
5	Sample 5					
6	Sample 6					
7	Sample 7					
8	Sample 8					
9	Sample 9					
10	Sample 10					
11	Sample 11					
12	Sample 12					

Chip Lot #	Reagent Kit Lot #

Chip Comments :

Sample Information | Study Information

Import... | Export...

4 Click the **Start** button in the upper right of the window to start the chip run. The incoming raw signals are displayed in the **Instrument** context.

▶ **Start**

CAUTION Contamination of electrodes

Leaving the chip for a period longer than 1 hour (e.g. over night) in the Bioanalyzer may cause contamination of the electrodes.

→ Immediately remove the chip after a run.

5 After the chip run is finished, remove the chip from the receptacle of the bioanalyzer and dispose of it according to good laboratory practices.

Revision History

Document	Date	Description of Change
Document # 15031942 v04	January 2019	Added information on reviewing sequencing workflows to ensure compatibility with library prep methods.
Document # 15031942 v03	February 2018	Updated the normalize libraries procedure to indicate that shaking samples after the five-minute elution is necessary only if samples are not resuspended. Reorganized kit contents information, including renaming some sections to match kit labeling and identify storage temperature. Corrected the diagram that shows how the Nextera XT assay works to clarify each transposome dimer has two of the same adapter color.
Document # 15031942 v02	April 2017	Added the following information: • Supported genome size of < 5 Mb. • The ratio of absorbance that indicates contaminants. • Recommendations for PCR amplicons. • AMPure XP bead recommendations for runs ≥ 2 × 250 cycles. • Reagent and library volumes in the PCR plate after the tagmentation and amplification steps. • Beckman Coulter Genomics item # A63880 for Agencourt AMPure XP, 5 ml. • Illumina catalog # PE-121-1003 and # FC-121-1003 for the TruSeq Dual Index Sequencing Primer Box. Added the following technical notes to the list of additional resources: • BestPracticesforStandardandBead-BasedNormalizationin NexteraXT DNA LibraryPreparationKits(Pub.No.470-2016-007) • NexteraXT LibraryPrep: TipsandTroubleshooting(Pub.No.770-2015-015) Consolidated steps in the pool libraries procedure. Identified the NaOH consumable as molecular biology grade. Specified the use of molecular-grade water or 10 mM Tris-HCl, pH 7.5–8.5 to dilute starting material for DNA quality assessment. Specified proceeding immediately when tagmentation is complete so that neutralization occurs while the transposome is active. Specified a thaw time of 20 minutes for NPM (Nextera PCR Master Mix). Updated the normalize libraries procedure to apply to various sample numbers, not only 96. Updated TCY plate to Hard-Shell 96-well PCR plate, skirted. Updated magnetic stand supplier to Thermo Fisher Scientific. Corrected the catalog numbers for Nextera kits provided in the introduction. Corrected the illustration showing how the Nextera assay works.

Document	Date	Description of Change

Document # 15031942 v01	January 2016	Updated design of workflow diagram.
		Renamed and combined some procedures as needed to improve continuity.
		Simplified consumables information at the beginning of each section.
		Revised step-by-step instructions to be more succinct.
		Removed reference to obsolete Experienced User Cards and added reference to the Custom Protocol Selector.
		Clarified AMPure XP bead recommendation for nonamplicon applications. See Clean Up Libraries.
		Added information about normalizing low yield libraries. See Normalize Libraries.
		Corrected index adapter labels on the assay diagram.
15031942 Rev. E	January 2015	Corrected kit contents for Nextera XT DNA Library Preparation Index Kit v2 Set A (FC-131-2001) to include index N715.
15031942 Rev. D	September 2014	Added info for new index kits that enable preparation of up to 384 indexed paired-end libraries.
		Updated DNA Input Recommendations for diluting starting material and the potential results of incomplete tagmentation.
		Added new Nextera XT Quality Metrics with new information on how to troubleshoot fluctuations in cluster density.
		Removed Dual Indexing Principle and Low Plexity Pooling Guidelines sections. This information can be found in the Nextera Low-Plex Pooling Guidelines Tech Note on the Nextera XT DNA Library Prep Kit support page.
		References to read lengths on the MiSeq were updated for v3 chemistry.
		Added instructions for alternate tip if processing fewer than 24 samples while transferring LNB1 beads in Library Normalization.
		Added NaOH 1N pH > 12.5 to the Consumables and Equipment list as a user-supplied consumable.
		Removed Tween 20 from Consumables and Equipment list.
		Consumable not used in protocol.
15031942 Rev. C	October 2012	Modifications were added in PCRClean-Upfor 2x300 runs on the MiSeq.
		New section for clustering samples on the HiSeq, HiScanSQ, and GAIIx. See Clustering Samples for HiSeq, HiScanSQ, and GAIIx. The DualIndexingPrinciple section listed incorrect catalog numbers for the Nextera XT Index kits. The correct catalog numbers are now listed.
		Emphasized making sure the NT (Neutralize Tagment Buffer) and LNS1 (Library Normalization Storage Buffer 1) reagents are at room temperature before use in the protocol.
		Removed reference to Tris-Cl 10 mM, pH8.5 with 0.1% Tween 20 from the User-Supplied Consumables table because it is not used in this library preparation.
Document	Date	Description of Change

267

15031942 Rev. B	July 2012	Emphasized making sure the NT (Neutralize Tagment Buffer) and LNS1 (Library Normalization Storage Buffer 1) reagents are at room temperature before use in the protocol. Removed reference to Tris-Cl 10 mM, pH8.5 with 0.1% Tween 20 from the User-Supplied Consumables table because it is not used in this library preparation.
15031942 Rev. A	May 2012	Initial release.

Table of Contents

Chapter 1 Overview

Introduction

This protocol explains how to prepare up to 384 indexed paired-end libraries from DNA for subsequent sequencing on Illumina® sequencing systems. Reagents provided in the Nextera™ XT Library Prep Kit and Nextera XT Index Kit are used to fragment DNA and add adapter sequences onto the DNA template.

The kit has the following features:

▶ Uses tagmentation, an enzymatic reaction, to fragment DNA and add partial adapter sequences in only 5 minutes.

▶ Master mixed reagents reduce reagent containers, pipetting, and hands-on time. ▶ Only 1 ng input DNA is needed.

▶ Nextera XT typically supports genomes that are < 5 Mb while Nextera DNA typically supports genomes that are > 5 Mb.

Table 1   Example Applications for Nextera Kits

Nextera XT (FC-131-1024, FC-131-1096)	Nextera DNA (FC-121-1030, FC-121-1031)
Small genomes, amplicons, plasmids	Large or complex genomes
PCR amplicons (> 300 bp)*	Human genomes
Plasmids	Nonhuman mammalian genomes (eg, mouse, rat, bovine)
Microbial genomes (eg, Prokaryotes, archaea)	Plant genomes (eg, Arabidopsis, maize, rice)
Concatenated amplicons	Invertebrate genomes (eg, Drosophila)
Double-stranded cDNA	
Single-cell RNA-Seq	

* Using a > 300 bp amplicon size ensures even coverage across the length of the DNA fragment. For more information, see PCRAmpliconson page 2.

DNA Input Recommendations

The Nextera XT protocol is optimized for 1 ng of input DNA.Quantify the starting material before preparing libraries. Dilute starting material in molecular-grade water or 10 mM Tris HCl, pH 7.5–8.5.

Input DNA Quantification

The enzymatic DNA fragmentation used for this protocol is more sensitive to DNA input compared to mechanical fragmentation. Success depends on accurate quantification of input DNA.

Use a fluorometric-based method to quantify input DNA. For example, if you use the Qubit dsDNA BR Assay system, use 2 μl of each DNA sample with 198 μl of the Qubit working solution. Avoid methods that measure total nucleic acid, such as NanoDrop or other UV absorbance methods.

Assess DNA Quality

UV absorbance is a common method for assessing the quality of a DNA sample. The ratio of absorbance at 260 nm to absorbance at 280 nm is used as an indication of sample purity. This protocol is optimized for DNA with absorbance ratio values of 1.8–2.0, which indicates a pure DNA sample. Target a 260/230 ratio of 2.0– 2.2. Values outside this range indicate the presence of contaminants. For a complete list of contaminants,
including sources, avoidance, and effects on the library, see NexteraXT LibraryPrep: Tipsand Troubleshooting(Pub.No.770-2015-015).

Dilute the starting material in molecular-grade water or 10 mM Tris-HCl, pH 7.5–8.5. Incomplete tagmentation can cause library preparation failure, poor clustering, or an unexpectedly high scaffold number.

PCR Amplicons

The PCR amplicon must be > 300 bp. Shorter amplicons can be lost during the library cleanup step.

Tagmentation cannot add an adapter directly to the distal end of a fragment, so a drop in sequencing coverage of ~50 bp from each distal end is expected. To ensure sufficient coverage of the amplicon target region, design primers to extend beyond the target region by 50 bp per end.

Additional Resources

Visit the Nextera XT DNA Library Prep Kit support page on the Illumina website for documentation, software downloads, training resources, and information about compatible Illumina products.

The following documentation is available for download from the Illumina website.

The following documentation is available for download from the Illumina website.

Resource	Description
Custom Protocol Selector	support.illumina.com/custom-protocol-selector.html
	A wizard for generating customized end-to-end documentation that is tailored to the
	library prep method, run parameters, and analysis method used for the sequencing run.
NexteraXTDNALibraryPrepKit Checklist(document# 1000000006566)	Provides a checklist of the protocol steps. The checklist is intended for experienced users.

NexteraLow-PlexPooling Guidelines(Pub.No.770-2011-044)	Provides pooling guidelines and dual indexing strategies for Nextera XT library prep.
BestPracticesforStandardand Bead-BasedNormalizationin NexteraXT DNA Library PreparationKits(Pub.No.470-2016-007)	Provides best practices for bead-based normalization of Nextera XT libraries.
NexteraXT LibraryPrep: Tipsand Troubleshooting(Pub.No.770-2015-015)	Provides best practices for addressing undertagmentation, sample contaminants, and other problems that can occur when preparing Nextera XT libraries.

Chapter 2 Protocol

Introduction

This chapter describes the Nextera XT DNA Library Prep Kit protocol.

▶ Review Best Practices before proceeding. See AdditionalResourceson page 2 for information on accessing Best Practices on the Illumina website.

▶ Before proceeding, confirm kit contents and make sure that you have the required equipment and consumables. See SupportingInformationon page 14.

▶ Review the complete sequencing workflow, from sample through analysis, to ensure compatibility of products and experiment parameters. ▶ Follow the protocols in the order shown, using the specified volumes and incubation parameters.

Prepare for Pooling

If you plan to pool libraries, record information about your samples before beginning library prep. For more information, see the NexteraXTDNALibraryPrepKitsupportpage.

Review NexteraLow-PlexPoolingGuidelines(Pub.No.770-2011-044)when preparing libraries for Illumina sequencing systems that require balanced index combinations.

Tips and Techniques

Unless a safe stopping point is specified in the protocol, proceed immediately to the next step.

Avoiding Cross-Contamination ▶ When adding or transferring samples, change tips between eachsample. ▶ When adding adapters or primers, change tips between eachrowand eachcolumn.

▶ Remove unused index adapter tubes from the working area.

Sealing the Plate

▶ Always seal the 96-well plate before the following steps in the protocol:

▶ Shaking steps ▶ Vortexing steps ▶ Centrifuge steps ▶ Thermal cycling steps

▶ Apply the adhesive seal to cover the plate, and seal with a rubber roller. ▶ Microseal 'B' adhesive seals are effective at -40°C to 110°C, and suitable for skirted or semiskirted PCR plates. Use Microseal 'B' for shaking, centrifuging, and long-term storage. ▶ Microseal 'A' adhesive film is used for thermal cycling steps to prevent evaporation.

Plate Transfers

▶ When transferring volumes between plates, transfer the specified volume from each well of a plate to the corresponding well of the other plate.

Centrifugation

▶ Centrifuge at any step in the procedure to consolidate liquid or beads in the bottom of the well, and to prevent sample loss.

Handling Beads ▶ Do not freeze beads. ▶ Pipette bead suspensions slowly. ▶ Before use, allow the beads to come to room temperature.

▶ Immediately before use, vortex the beads until they are well dispersed. The color of the liquid must appear homogeneous. Vortex throughout protocol as necessary to keep homogenous.

▶ If beads are aspirated into pipette tips, dispense back to the plate on the magnetic stand, and wait until the liquid is clear (~2 minutes). ▶ When washing beads:

▶ Use the specified magnetic stand for the plate. ▶ Dispense liquid so that beads on the side of the wells are wetted. ▶ Keep the plate on the magnetic stand until the instructions specify to remove it. ▶ Do not agitate the plate while it is on the magnetic stand. Do not disturb the bead pellet.

Library Prep Workflow

The following diagram illustrates the workflow using a Nextera XT DNA Library Prep Kit for eight samples. Safe stopping points are marked between steps.

Figure 1   Nextera XT Workflow

Tagment Genomic DNA

This step uses the Nextera transposome to tagment gDNA, which is a process that fragments DNA and then tags the DNA with adapter sequences in a single step.

Consumables ▶ ATM (Amplicon

Tagment Mix) ▶ TD (Tagment DNA

Buffer) ▶ NT (Neutralize Tagment

Buffer) ▶ gDNA (0.2 ng/µl per sample)

▶ Hard-Shell 96-well PCR plate, skirted

▶ Microseal 'B' adhesive seals

Preparation

1 Prepare the following consumables:

Item	Storage	Instructions
gDNA	-25°C to -15°C	Thaw on ice. Invert the thawed tubes 3–5 times, and then centrifuge briefly.
ATM	-25°C to -15°C	Thaw on ice. Invert the thawed tubes 3–5 times, and then centrifuge briefly.
TD	-25°C to -15°C	Thaw on ice. Invert the thawed tubes 3–5 times, and then centrifuge briefly.
NT	15°C to 30°C	Check for precipitates. If present, vortex until all particulates are resuspended.

2 Save the following tagmentation program on the thermal cycler: ▶ Choose the preheat lid option ▶ 55°C for 5 minutes ▶ Hold at 10°C

Procedure

1 Add the following volumes in the order listed to each well of a new Hard-Shell skirted PCR plate. Pipette to mix.

▶ TD (10 µl)

▶ Normalized gDNA (5 µl)

2 Add 5 µl ATM to each well. Pipette to mix. 3 Centrifuge at 280 × g at 20°C for 1 minute.

4 Place on the preprogrammed thermal cycler and run the tagmentation program. When the sample reaches 10°C, immediatelyproceed to step 5 because the transposome is still active.

5 Add 5 µl NT to each well. Pipette to mix.

6 Centrifuge at 280 × g at 20°C for 1 minute.

7 Incubate at room temperature for 5 minutes.

The PCR plate contains 25 µl tagmented and neutralized gDNA, all of which is used in the next step.

Amplify Libraries

This step amplifies the tagmented DNA using a limited-cycle PCR program. PCR adds the Index 1 (i7), Index 2 (i5), and full adapter sequences to the tagmented DNA from the previous step. The index adapters and Nextera PCR Master Mix are added directly to the 25 µl of tagmented gDNA from the previous step.

The adapters and sequences are required for cluster formation. Use the full amount of recommended input DNA and the specified number of PCR cycles, which helps ensure high-quality sequencing results.

When planning the index scheme for libraries, use the same index Index 1 (i7) index in each column of the PCR plate. This scheme allows use of a multichannel pipette to transfer indexes from the tubes to the plate. See AdditionalResourceson page 2 for information on accessing the tech note on low-plex pooling.

Consumables ▶ NPM (Nextera

PCR Master Mix) ▶ Index 1

adapters (N7XX) ▶ Index 2

adapters (S5XX) ▶ TruSeq™ Index

Plate Fixture ▶ Microseal 'A' film

Preparation

1 Prepare the following consumables:

Item	Storage	Instructions
Index adapters (i5 and i7)	-25°C to -15°C	Only prepare adapters being used. Thaw at room temperature for 20 minutes. Invert each tube to mix. Centrifuge briefly.
NPM	-25°C to -15°C	Thaw on ice for 20 minutes.

2 Save the following program on the thermal cycler:

   ▶   Choose the preheat lid

option.

   ▶   72°C for 3 minutes
   ▶ 95°C for 30 seconds
   ▶ 12 cycles of:
   ▶   95°C for 10 seconds
   ▶ 55°C for 30 seconds
   ▶ 72°C for 30 seconds

▶ 72°C for 5 minutes

▶ Hold at 10°C

Procedure

1   [24 libraries] Arrange the index adapters in the TruSeq Index Plate Fixture as follows. ▶ Arrange Index 1 (i7) adapters in columns 1–6 of the TruSeq Index Plate Fixture. ▶ Arrange Index 2 (i5) adapter in rows A–D of the TruSeq Index Plate Fixture.

Figure 2   TruSeq Index Plate Fixture Setup for 24 Libraries
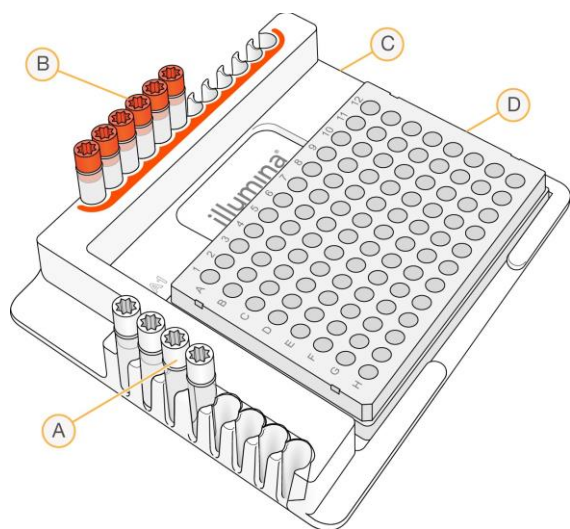
A   Rows A–D: Index 2(i5) adapters (white caps)

B   Columns 1–6: Index 1(i7) adapters (orange caps)

C   TruSeq Index Plate Fixture D Hard-ShellPCR plate

2   [96 libraries] Arrange the index adapters in the TruSeq Index Plate Fixture as follows. ▶ Arrange Index 1 (i7) adapters in columns 1–12 of the TruSeq Index Plate Fixture. ▶ Arrange Index 2 (i5) adapter in rows A–H of the TruSeq Index Plate Fixture.

Figure 3   TruSeq Index Plate Fixture Setup for 96 Libraries
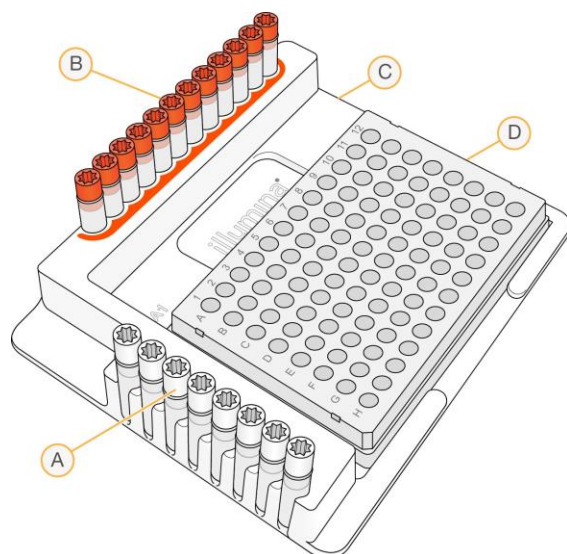
A   Rows A–H: Index 2(i5) adapters (white caps)

B   Columns 1–12: Index 1(i7) adapters (orange caps)

C   TruSeq Index Plate Fixture

D   Hard-ShellPCR plate

3   Using a multichannel pipette, add 5 µl of each Index 1 (i7) adapter down each column. Replace the cap on each i7 adapter tube with a new orange cap.

4   Using a multichannel pipette, add 5 µl of each Index 2 (i5) adapter across each row. Replace the cap on each i5 adapter tube with a new white cap.

5   Add 15 µl NPM to each well containing index adapters. Pipette to mix.

6   Centrifuge at 280 × g at 20°C for 1 minute.

7   Place on the preprogrammed thermal cycler and run the PCR program. The volume is 50 µl.

SAFE STOPPING POINT

If you are stopping, seal the plate and store at 2°C to 8°C for up to 2 days. Alternatively, leave on the thermal cycler overnight.

Clean Up Libraries

This step uses AMPure XP beads to purify the library DNA and remove short library fragments.

Consumables ▶ RSB

(Resuspension Buffer)

▶ AMPure XP beads

▶ Freshly prepared 80% ethanol (EtOH) ▶ 96-well midi plate

▶ Hard-Shell 96-well PCR plate, skirted

About Reagents ▶ The AMPure XP beads are a user-supplied consumable. ▶ Vortex

AMPure XP beads before each use. ▶ Vortex AMPure XP beads frequently to make

sure that beads are evenly distributed.

▶ Always prepare fresh 80% ethanol for wash steps. Ethanol can absorb water from the air, impacting your

results.

Preparation

1 Prepare the following consumables:

Item	Storage	Instructions
RSB	-25°C to -15°C	Thaw at room temperature.
		RSB can be stored at 2°C to 8°C after the initial thaw.
AMPure XP Beads	2°C to 8°C	Let stand on the benchtop for 30 minutes to bring to room temperature.

2 Prepare fresh 80% ethanol from absolute ethanol.

Procedure

1 Centrifuge at 280 × g at 20°C for 1 minute.

2 Transfer 50 µl PCR product from each well of the PCR plate to corresponding wells of a new midi plate.

 NOTE

The ratioofPCR product tovolume ofbeads is3:2. For example, 50 µlPCR product to30 µlAMPure. If you

pulllessthan 50 µlofPCR product, adjust your ratioofAMPure beads accordingly.

3 Add 30 µl AMPure XP beads to each well.

Smaller amplicons in Nextera XT library preps typically yield smaller insert size ranges. To maximize

recovery of smaller fragments from the bead cleanup step, use the following conditions.

Input Size (bp)	AMPure XP Recommendation	AMPure XP Volume (µl)
300–500	1.8x AMPure XP	90
> 500	0.6x AMPure XP (0.5x AMPure XP for ≥ 2 x 250 cycles)*	30 (25 µl for ≥ 2 x 250 cycles)*
gDNA or other genomic input	0.6x AMPure XP	30

*Applicable only to the MiSeq™ or HiSeq™ 2500 using HiSeq Rapid v2 reagents.

4   Shake at 1800 rpm for 2 minutes.

5   Incubate at room temperature for 5 minutes.

6   Place on a magnetic stand and wait until the liquid is clear (~2 minutes).

7   Remove and discard all supernatant from each well.

8   Wash 2 times as follows.

a Add 200 µl fresh 80% EtOH to each well. b

Incubate on the magnetic stand for 30 seconds.

c   Remove and discard all supernatant from each well.

9   Using a 20 µl pipette, remove residual 80% EtOH from each well.

10 Air-dry on the magnetic stand for 15 minutes.

11 Remove from the magnetic stand.

12 Add 52.5 µl RSB to each well.

13 Shake at 1800 rpm for 2 minutes.

14 Incubate at room temperature for 2 minutes.

15 Place on a magnetic stand and wait until the liquid is clear (~2 minutes).

16 Transfer 50 µl supernatant from the midi plate to a new Hard-Shell PCR plate.

SAFE STOPPING POINT

If you are stopping, seal the plate and store at -25°C to -15°C for up to seven days.

Check Libraries

1 Run 1 μl of undiluted library on an Agilent Technology 2100 Bioanalyzer using a High Sensitivity DNA chip.

   The following figure shows example traces of libraries successfully sequenced on a HiSeq 2500 system. Typical libraries show a broad size distribution of ~250–1000 bp, as shown in the top panel. Various libraries can be sequenced with average fragment sizes as small as 250 bp or as large as 1500 bp.

Figure 4   Library Size Distributions of Control gDNA
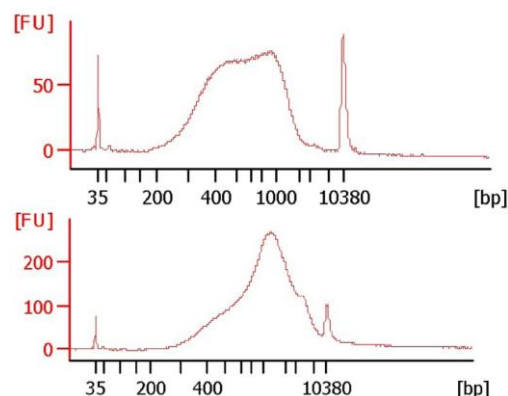
Normalize Libraries

This process normalizes the quantity of each library to ensure more equal library representation in the pooled library.

 NOTE

Manually normalize libraries when the finallibrary yield islessthan 10–15nM. Bead-based normalization on low yield libraries can result in overly diluted samples and low sequencing yields. For more information, see

   BestPracticesforStandardandBead-BasedNormalizationinNexteraXT DNA LibraryPreparationKits (Pub.No.470-2016-007).

Before proceeding, see the documentation for your sequencing system to make sure that normalization methods are compatible. Do not use a bead-based normalization method on libraries being sequenced on a system with onboard denaturation.

Consumables

▶ LNA1 (Library Normalization Additives 1) ▶ LNB1
(Library Normalization Beads 1) ▶ LNW1 (Library
Normalization Wash 1) ▶ LNS1 (Library Normalization
Storage Buffer 1) ▶ 0.1 N NaOH (fewer than 7 days old) (3
ml per 96 samples) ▶ 96-well midi plate ▶ Hard-Shell 96-
well PCR plate, skirted ▶ 15 ml conical tube ▶ Microseal
'B' adhesive seals

About Reagents

▶ Vortex LNA1 vigorously to make sure that all precipitates have dissolved. Inspect in front of a light.

▶ Vortex LNB1 vigorously, with intermittent inversion (at least 1 minute). Repeat until all beads are resuspended and no beads are present at the bottom of the tube when it is inverted.

▶ Always use a wide-bore pipette tip for LNA1.

▶ Mix only the required amounts of LNA1 and LNB1 for the current experiment. Store the remaining LNA1 and LNB1 separately at the recommended temperatures. ▶ Aspirate and dispense beads slowly due to the viscosity of the solution.

WARNING

Thisset ofreagents contains potentially hazardous chemicals. Personalinjury can occur through inhalation, ingestion, skin contact, and eye contact. Wear protective equipment, including eye protection, gloves, and laboratory coat appropriate for risk ofexposure. Handle used reagents aschemicalwaste and discard in accordance with applicable regional, national, and locallawsand regulations. For additionalenvironmental, health, and safety information, see the SDS at support.illumina.com/sds.html.

Preparation

1 Prepare the following consumables:

Item	Storage	Instructions
LNA1	-25°C to -15°C	Prepare under a fume hood.
		Bring to room temperature. Use a 20°C to 25°C water bath as needed.
LNB1	2°C to 8°C	Bring to room temperature. Use a 20°C to 25°C water bath as needed.

LNW1	2°C to 8°C	Bring to room temperature. Use a 20°C to 25°C water bath as needed.
LNS1	Room temperature	Bring to room temperature.

Procedure

1 Transfer 20 µl supernatant from the Hard-Shell PCR plate to a new midi plate.

2 Add 44 µl LNA1 per sample to a new 15 ml conical tube. Calculate about 5% extra sample to account for sample loss due to pipetting.

   For example: for 96 samples, add 4.4 ml LNA1 to the tube (100 samples × 44 µl = 4.4 ml).

3 Thoroughly resuspend LNB1. Pipette to mix.

4 Transfer 8 µl LNB1 per sample (including the 5% extra) to the 15 ml conical tube containing LNA1. Invert to mix.

   For example: for 96 samples, transfer 800 µl LNB1 to the tube of LNA1 (100 samples × 8 µl = 800 µl).

5 Pour the bead mixture into a trough.

6 Add 45 µl combined LNA1 and LNB1 to each well containing libraries.

7 Shake at 1800 rpm for 30 minutes.

8 Place on a magnetic stand and wait until the liquid is clear (~2 minutes).

9 Remove and discard all supernatant from each well.

10 Wash two times as follows.

   a Add 45 µl LNW1 to each well. b Shake at 1800 rpm for 5 minutes. c Place on a magnetic stand and wait until the liquid is clear (~2 minutes). d Remove and discard all supernatant from each well.

11 Add 30 µl 0.1 N NaOH to each well.

12 Shake at 1800 rpm for 5 minutes.

13 During the 5 minute elution, label a new 96-well PCR plate SGP for storage plate.

14 Add 30 µl LNS1 to each well of the SGP plate. Set aside.

15 After the 5 minute elution, make sure that all samples in the midi plate are resuspended. If they are not, resuspend as follows.

 a Pipette to mix or lightly tap the plate on the bench. b Shake at 1800 rpm for 5 minutes.

16 Place on a magnetic stand and wait until the liquid is clear (~2 minutes).

17 Transfer the supernatant from the midi plate to the SGP plate.

18 Centrifuge at 1000 × g for 1 minute.

NOTE

After denaturation, the libraries are single-stranded DNA, which resolves poorly on an agarose gelor Bioanalyzer chip. For quality control, use the double-stranded DNA saved from step 16ofthe cleanup procedure.

SAFE STOPPING POINT

If you are stopping, seal the plate and store at -25°C to -15°C for up to seven days.

Pool Libraries

Pooling libraries combines equal volumes of normalized libraries in a single tube. After pooling, dilute and heat-denature the library pool before loading libraries for the sequencing run.

Consumables ▶ Adhesive PCR foil seal
▶ Eppendorf LoBind microcentrifuge tubes
▶ PCR eight-tube strip

Preparation

1 To prepare for the sequencing run, begin thawing reagents according to the instructions for your instrument.

If the SGP plate was stored frozen at -25°C to -15°C, thaw at room temperature. Pipette to mix.

Procedure

1   Centrifuge at 1000 × g at 20°C for 1 minute.

2   Label a new Eppendorf tube PAL.

3   Transfer 5 µl of each library from the SGP plate to the PAL tube. Invert to mix.

4   Dilute pooled libraries to the loading concentration for your sequencing system. For instructions, see the denature and dilute libraries guide for your system.

5   Store unused pooled libraries in the PAL tube and SGP plate at -25°C to -15°C for up to 7 days.

Appendix A Supporting Information

Supporting Information

Introduction

The protocol described in this guide assumes that you have reviewed the contents of this section, confirmed workflow contents, and obtained all required consumables and equipment.

How the Nextera XT Assay Works

The Nextera XT DNA Library Prep Kit uses an engineered transposome to tagment genomic DNA, which is a process that fragments DNA and then tags the DNA with adapter sequences in one step. Limited-cycle PCR uses the adapters to amplify the insert DNA. The PCR step also adds index adapter sequences on both ends of the DNA, which enables dual-indexed sequencing of pooled libraries on Illumina sequencing platforms.

Transposomes

Genomic DNA

~ 300 bp

Tagmentation

Reduced-Cycle
PCR Amplification

P5

Index 2

Read 1 Sequencing Primer

Read 2 Sequencing Primer

Index 1

P7

p5 Index2 Rd1 SP

Rd2 SP Index1 p7

Sequencing-Ready Fragment
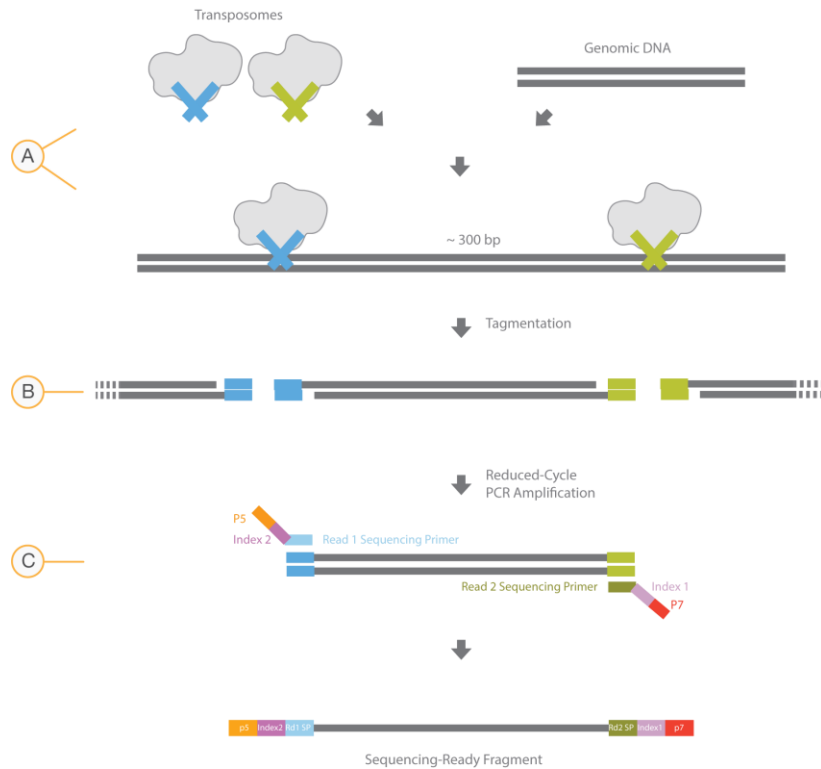
A   Nextera XTtransposome with adapters combined with template DNA

B   Tagmentation tofragment and add adapters

C   Limited-cycle PCR toadd index adapter sequences

Nextera XT Quality Metrics

Two factors can cause cluster density fluctuations in libraries prepared with the Nextera XT DNA Library Prep

Kit: ▶   An average sample size that is too large or too small after

tagmentation.

▶   A final sample concentration that is too low due to a low yield when starting the bead-based

 normalization step.

To troubleshoot fluctuations in cluster density, consider checking library size and library concentration. For more information, see NexteraXT LibraryPrep: TipsandTroubleshooting(Pub.No.770-2015-015).

Check Library Size

Larger molecules cluster less efficiently than smaller molecules. If the fragment size after tagmentation is larger than expected, low cluster numbers are possible. The inverse is also true. The average expected library size after tagmentation is between 400 bp and 1.2 kb.

Check the library size with a high sensitivity Bioanalyzer trace after the PCR cleanup step. Look for a long low plateau. Alternatively, PCR-amplify the library with qPCR primers and run the product on an agarose gel. The sequence for these primers is available in the SequencingLibraryqPCR QuantificationGuide(document# 11322363).

▶ Short libraries indicate too little input DNA—Requantify the input DNA with a fluorometric method. Start with 10%–25% more input DNA. If the library peak is below 400 bp and you want to continue with this library, dilute the library further.

▶ Long libraries indicate too much input DNA or the presence of inhibitors—Start with less input DNA, make sure that the input DNA is free from inhibitors, and repeat the quantification step.

For more information on library dilution, see the denature and dilute libraries guide for your sequencing system.

Check Library Concentration

Bead-based normalization is most efficient when the library yield after amplification is 10–15 nM, or higher. Measure library concentration using high sensitivity dsDNA Qubit after library cleanup, and measure library size with a Bioanalyzer to calculate molarity.

If you are starting with high-quality DNA and see low yield after library cleanup, there are possible issues with AMPure cleanup or the amplification step. If results show either condition, confirm proper storage of the PCR master mix at -25°C to -15°C in a no-frost freezer. Confirm minimal freeze-thaw cycles.

The following resources are available on the Illumina website:

▶ Best practices for bead handling—From the Nextera XT DNA Library Prep Kit support page, select the Best Practices tab and review Handling Magnetic Beads.

▶ Online training module—Review section 2.4 of the TruSeq:SamplePurificationBeadSizeSelectionand BestPractices, which is a short training with guidance on bead handling. To access this training, select the Training tab on the Nextera XT DNA Library Prep Kit support page.

Acronyms

Acronym	Definition
ATM	Amplicon Tagment Mix
CAA	Clean Amplified Plate
CAN	Clean Amplified NTA Plate
LNA1	Library Normalization Additives 1
LNB1	Library Normalization Beads 1
LNS1	Library Normalization Storage Buffer 1
LNW1	Library Normalization Wash 1
LNP	Library Normalization Plate
NT	Neutralize Tagment Buffer
NPM	Nextera PCR Master Mix
NTA	Nextera XT Tagment Amplicon Plate
PAL	Pooled Amplicon Library
RSB	Resuspension Buffer
SGP	Storage Plate
TD	Tagment DNA Buffer

Kit Contents

The Nextera XT DNA Library Prep Kit is available in a 24-sample configuration and a 96-sample configuration. Each kit has a corresponding index kit that contains 24 indexes or 96 indexes. Combining Nextera XT Index Kit v2 Sets A–D achieves 384 unique index combinations.

Kit Name	Catalog #
Nextera XT DNA Library Prep Kit (24 Samples)	FC-131-1024
Nextera XT DNA Library Prep Kit (96 Samples)	FC-131-1096
Nextera XT Index Kit v2 Set A (96 Indexes, 384 Samples)	FC-131-2001
Nextera XT Index Kit v2 Set B (96 Indexes, 384 Samples)	FC-131-2002
Nextera XT Index Kit v2 Set C (96 Indexes, 384 Samples)	FC-131-2003
Nextera XT Index Kit v2 Set D (96 Indexes, 384 Samples)	FC-131-2004
Nextera XT Index Kit (24 Indexes, 96 Samples)	FC-131-1001
Nextera XT Index Kit (96 Indexes, 384 Samples)	FC-131-1002
TruSeq Index Plate Fixture Kit	FC-130-1005

Sequencing primers provided in TruSeq v3 reagent kits are not compatible with Nextera XT libraries. Thus, sequencing Nextera XT libraries on a HiSeq 2500 using TruSeq v3 reagents requires the sequencing primers provided in the Illumina TruSeq Dual Index Sequencing Primer Box. This box is provided in a paired-end (PE121-1003) and single-read (FC-121-1003) version. One box is needed for each run.

Kits are shipped on dry ice unless otherwise specified. Some kit components are stored at a different temperature than the shipping temperature. Make sure that you store kit components at the specified storage temperatures.

DNA Library Prep Kit Contents

(24 Samples) (FC-131-1024)

Box 1

Quantity	Acronym	Reagent Name	Storage Temperature
1	ATM	Amplicon Tagment Mix, 24 rxn	-25°C to -15°C
1	TD	Tagment DNA Buffer	-25°C to -15°C
1	NPM	Nextera PCR Master Mix	-25°C to -15°C
1	RSB	Resuspension Buffer	-25°C to -15°C
1	LNA1	Library Normalization Additives 1	-25°C to -15°C
1	LNW1	Library Normalization Wash 1	2°C to 8°C
1	HT1	Hybridization Buffer	-25°C to -15°C

Box 2

Quantity	Acronym	Reagent Name	Storage Temperature
1	NT	Neutralize Tagment Buffer	Room temperature
1	LNB1	Library Normalization Beads 1	2°C to 8°C
1	LNS1	Library Normalization Storage Buffer 1	Room temperature

Nextera XT DNA Library Prep Kit Contents (96 Samples) (FC-131-1096)

Box 1

Quantity	Acronym	Reagent Name	Storage Temperature

1	ATM	Amplicon Tagment Mix, 96 rxn	-25°C to -15°C
2	TD	Tagment DNA Buffer	-25°C to -15°C
1	NPM	Nextera PCR Master Mix	-25°C to -15°C
4	RSB	Resuspension Buffer	-25°C to -15°C
1	LNA1	Library Normalization Additives 1	-25°C to -15°C
2	LNW1	Library Normalization Wash 1	2°C to 8°C
1	HT1	Hybridization Buffer	-25°C to -15°C

Box 2

Quantity	Acronym	Reagent Name	Storage Temperature
1	NT	Neutralize Tagment Buffer	Room temperature
1	LNB1	Library Normalization Beads 1	2°C to 8°C
1	LNS1	Library Normalization Storage Buffer 1	Room temperature

Index Kit v2 Set A Contents

(96 Indexes, 384 Samples) (FC-131-2001)

Index Adapters, Store at -25°C to -15°C

Quantity	Reagent Name
8 tubes	Index Primers, S502, S503, S505–S508, S510, and S511
12 tubes	Index Primers, N701–N707, N710–N712, N714, and N715

Index Adapter Replacement Caps, Store at 15°C to 30°C

Quantity	Description
1 bag	i7 Index Tube Caps, Orange
1 bag	i5 Index Tube Caps, White

Nextera XT Index Kit v2 Set B Contents (96 Indexes, 384 Samples) (FC-131-2002)

Quantity	Description

Quantity	Description
1 bag	i7 Index Tube Caps, Orange
1 bag	i5 Index Tube Caps, White

Index Adapters, Store at -25°C to -15°C

Quantity	Description
8 tubes	Index Adapters: S502, S503, S505–S508, S510, and S511
12 tubes	Index Adapters: N716, N718–N724, and N726–N729

Index Adapter Replacement Caps, Store at 15°C to 30°C

Quantity	Description
1 bag	i7 Index Tube Caps, Orange
1 bag	i5 Index Tube Caps, White

Nextera XT Index Kit v2 Set C Contents (96 Indexes, 384 Samples) (FC-131-2003)

Index Adapters, Store at -25°C to -15°C

Quantity	Description
8 tubes	Index Adapters: S513, S515–S518, and S520–S522
12 tubes	Index Adapters: N701–N707, N710–N712, N714, and N715

Index Adapter Replacement Caps, Store at 15°C to 30°C Index Kit v2 Set D Contents

(96 Indexes, 384 Samples) (FC-131-2004)

Index Adapters, Store at -25°C to -15°C

Quantity	Description
8 tubes	Index Adapters: S513, S515–S518, and S520–S522
12 tubes	Index Adapters: N716, N718–N724, and N726–N729

Index Adapter Replacement Caps, Store at 15°C to 30°C

Quantity	Description
1 bag	i7 Index Tube Caps, Orange
1 bag	i5 Index Tube Caps, White

Nextera XT Index Kit Contents (24 Indexes, 96 Samples) (FC-131-1001)

Quantity	Description

Quantity	Description
1 bag	i7 Index Tube Caps, Orange
1 bag	i5 Index Tube Caps, White

Index Adapters, Store at -25°C to -15°C

Quantity	Description
4 tubes	Index Adapters: S502–S504 and S517
6 tubes	Index Adapters: N701–N706

Index Adapter Replacement Caps, Store at 15°C to 30°C

Quantity	Description
1 bag	i7 Index Tube Caps, Orange
1 bag	i5 Index Tube Caps, White

Nextera XT Index Kit Contents (96 Indexes, 384 Samples) (FC-131-1002)

Index Adapters, Store at -25°C to -15°C

Quantity	Reagent Name
8 tubes	Index Adapters: S502–S508 and S517
12 tubes	Index Adapters: N701–N712

Index Adapter Replacement Caps, Store at 15°C to 30°C

TruSeq Index Plate Fixture Kit Contents (FC-130-1005)

Each TruSeq Index Plate Fixture Kit contains two fixtures to help arrange index primers before dispensing to a 96-well plate during library amplification. Two fixtures help with arrangement of index primers before dispensing to a 96-well plate during library amplification. The fixture pairs with both the 24-sample kit and 96sample kit.

TruSeq Index Plate Fixture, Store at Room Temperature

Quantity	Description
2	TruSeq Index Plate Fixture

Consumables and Equipment

Confirm that all required user-supplied consumables and equipment are present and available before starting the protocol.

The protocol has been optimized and validated using the items listed. Comparable performance is not guaranteed when using alternate consumables and equipment.

Consumables

Consumable	Supplier
10 µl pipette tips	General lab supplier
10 µl multichannel pipettes	General lab supplier
10 µl single channel pipettes	General lab supplier
1000 µl pipette tips	General lab supplier
1000 µl multichannel pipettes	General lab supplier
1000 µl single channel pipettes	General lab supplier
200 µl pipette tips	General lab supplier
200 µl multichannel pipettes	General lab supplier
200 µl single channel pipettes	General lab supplier
96-well storage plates, round well, 0.8 ml (midi plate)	Fisher Scientific, catalog # AB-0859
Agencourt AMPure XP, 60 ml kit or 5 ml kit	Beckman Coulter Genomics, item # A63881 (60 ml) Beckman Coulter Genomics, item # A63880 (5 ml)
Distilled water	General lab supplier
Ethanol 200 proof (absolute) for molecular biology (500 ml)	Sigma-Aldrich, product # E7023
Microseal 'A' film	Bio-Rad, catalog # MSA-5001
Microseal 'B' adhesive seals	Bio-Rad, catalog # MSB-1001
NaOH 1 N, pH > 12.5, molecular biology grade	General lab supplier
RNase/DNase-free multichannel reagent reservoirs, disposable	VWR, catalog # 89094-658
Ultrapure water	General lab supplier
Hard-Shell 96-well PCR plates	Bio-Rad, catalog # HSP-9601

Equipment

Equipment	Supplier
High-Speed microplate shaker	VWR, catalog # 13500-890 (110 V/120 V) VWR, catalog # 14216-214 (230 V)
Magnetic stand-96	Thermo Fisher Scientific, catalog # AM10027

Microplate centrifuge	General lab supplier
Vortexer	General lab supplier

Thermal Cyclers

Use the following recommended settings for selected thermal cycler models. Before performing library prep, validate any thermal cyclers not listed.

Thermal Cycler	Temp Mode	Lid Temp	Vessel Type
Bio-Rad DNA Engine Tetrad 2	Calculated	Heated, Constant at 100°C	Polypropylene plates and tubes
MJ Research DNA Engine Tetrad	Calculated	Heated	Plate
Eppendorf Mastercycler Pro S	Gradient S, Simulated Tube	Heated	Plate

Technical Assistance

For technical assistance, contact Illumina Technical Support.

Website:	www.illumina.com
Email:	techsupport@illumina.com

Illumina Customer Support Telephone Numbers

Region	Toll Free	Regional
North America	+1.800.809.4566	
Australia	+1.800.775.688	
Austria	+43 800006249	+43 19286540
Belgium	+32 80077160	+32 34002973
China	400.066.5835	
Denmark	+45 80820183	+45 89871156
Finland	+358 800918363	+358 974790110
France	+33 805102193	+33 170770446
Germany	+49 8001014940	+49 8938035677
Hong Kong	800960230	
Ireland	+353 1800936608	+353 016950506
Italy	+39 800985513	+39 236003759
Japan	0800.111.5011	
Netherlands	+31 8000222493	+31 207132960
New Zealand	0800.451.650	
Norway	+47 800 16836	+47 21939693
Singapore	+1.800.579.2745	
Spain	+34 911899417	+34 800300143

Sweden	+46 850619671	+46 200883979
Switzerland	+41 565800000	+41 800200442
Taiwan	00806651752	
United Kingdom	+44 8000126019	+44 2073057197
Other countries	+44.1799.534000	

Safety data sheets (SDSs)—Available on the Illumina website at support.illumina.com/sds.html.

Product documentation—Available for download in PDF from the Illumina website. Go to

support.illumina.com, select a product, then select Documentation & Literature.

K. Characteristics of non-obese Controls: un-pooled data of BOCABS and DISC participants

	Non-obese BOCABS participants	DISC participants
	n=12	n=8
Age (years)	47.3 (3.9)	44 (2.9)
Male	5	3
Female	7	5
British White	12	7
Black African	0	1
BMI (kg/m^2)	25.3 (0.7)	25.6 (0.7)
Body fat (%)	30.3 (0.01)	N/A
Waist (W; cm)	89 (3.5)	87.9 (1.29
Hip (H; cm)	104 (2.0)	100.5 (2.4)
W:H ratio	0.85 (0.02)	0.88 (0.03)

Table 8-2: Characteristics of non-obese Controls recruited to the BOCABS and DISC Study

L. Characteristics of non-obese Controls: un-pooled data of BOCABS and DISC participants

	Non-obese BOCABS participants	DISC participants
	n=9	n=7
Age (years)	45.5 (4.8)	42.9 (3.2)
Male	4	3

Female	5	4
British White	9	6
Black African	0	1
BMI (kg/m^2)	25.4 (1.0)	25.7 (0.8)
Body fat (%)	30.4 (1.5)	N/A
Waist (W; cm)	89.4 (4.4)	88.1 (2.2)
Hip (H; cm)	105.1 (2.4)	100.1 (2.7)
W:H ratio	0.85 (0.03)	0.88 (0.03)

Table 8-3 Characteristics of non-obese Controls recruited to the BOCABS and DISC Study for whom analysis of OXPHOS protein quantification and sequencing of the mtDNA in the colorectal mucosa was conducted.

M. Participant characteristics for each individual of the groups

Group	ID	Age (years)	Gender (Male, Female)	BMI (kg/m2)	Body fat (%)	Waist (W; cm)	Hip (H; cm)	W:H ratio
Pre-surgery	003	51.4	F	35.2	48.0	117.8	125.3	0.94
	007	51.8	M	41.5	41.3	132.0	132.8	0.99
	008	59.4	M	48.3	65.6	150.5	127.6	1.18
	010	55.0	F	49.0	47.8	122.2	139.5	0.88
	011	47.5	F	34.6	43.6	111.0	121.1	0.92
	015	31.7	M	42.7	49.4	121.8	130.9	0.93
	016	49.2	F	42.9	49.7	114.5	125.3	0.91
	017	49.0	F	50.7	51.8	115.5	134.3	0.86
	018	52.5	F	39.4	47.1	118.1	132.6	0.89
	020	43.6	M	41.0	36.4	126.5	81.4	1.03
	022	49.0	F	32.8	46.2	116.5	121.0	0.96
	024	44.3	F	30.2	44.8	106.7	114.6	0.93
	025	65.2	F	40.1	50.5	122.2	133.9	0.91
	026	38.8	F	45.3	53.3	122.0	144.1	0.85
	027	34.1	F	46.6	47.0	112.5	145.2	0.78

	028	50.4	M	46.8	33.8	140.5	126.6	1.11
	029	51.4	F	38.0	50.3	132.8	91.6	1.03
	030	41.3	F	42.5	53.2	132.4	144.3	0.92
	032	46.4	F	37.9	46.8	114.3	124.4	0.92
	033	49.9	M	40.6	47.9	140.3	123.3	1.14
	034	48.0	F	41.0	51.0	122.5	135.3	0.91
	035	37.7	F	48.0	54.6	124.3	148.0	0.84
	037	51.3	F	39.6	52.2	127.0	126.8	1.00
	038	37.3	F	36.6	44.4	96.1	127.6	0.75
	040	43.6	F	35.7	45.3	112.7	131.8	0.86
	043	51.9	M	46.9	44.1	136.5	130.1	1.05
Post-surgery	003	51.4	F	27.3	36.6	95.4	107.7	0.89
	007	51.8	M	32.0	26.3	106.9	114.5	0.93
	008	59.4	M	39.6	48.0	135.7	113.0	1.20
	010	55.0	F	25.7	27.0	79.9	98.6	0.81
	011	47.5	F	31.0	37.0	101.7	110.9	0.92
	015	31.7	M	33.4	32.7	99.8	117.3	0.85
	016	49.2	F	33.4	40.8	96.9	107.0	0.91
	017	49.0	F	35.4	37.5	92.5	113.1	0.82
	018	52.5	F	27.9	34.9	86.9	108.4	0.80

	020	43.6	M	28.4	20.3	92.5	100.1	0.92
	022	49.0	F	25.3	36.4	91.6	104.8	0.87
	024	44.3	F	21.3	27.2	80.6	94.6	0.85
	025	65.2	F	32.8	45.2	107.4	111.4	0.96
	026	38.8	F	40.5	51.9	115.8	125.3	0.92
	027	34.1	F	35.0	40.1	92.5	118.1	0.78
	028	50.4	M	41.3	29.2	126.0	116.1	1.08
	029	51.4	F	26.0	37.0	91.8	103.8	0.88
	030	41.3	F	31.9	41.1	107.0	121.3	0.88
	032	46.4	F	29.2	36.8	95.5	108.8	0.88
	033	49.9	M	30.7	25.2	109.3	113.1	0.97
	034	48.0	F	33.2	41.9	107.8	115.2	0.94
	035	37.7	F	35.7	45.7	100.1	121.1	0.83
	037	51.3	F	29.3	44.2	47.1	53.4	0.88
	038	37.3	F	28.6	32.1	80.8	107.6	0.75
	040	43.6	F	35.7	45.3	112.7	131.8	0.86
	043	51.9	M	33.7	27.5	107.6	110.5	0.97
Non-obese	048	55.3	F	20.1	28.2	75.8	95.2	0.80
Controls	049	41.2	M	25.7	21.2	92.3	106.3	0.87
	051	57.8	F	22.9	29.4	72.1	97.4	0.74

056	59.0	M	29.9	31	106.2	111.6	0.95
057	47.7	M	28.7	27.6	110.3	117.2	0.94
058	55.8	F	25.5	35.1	77.6	100.6	0.77
059	49.0	M	24.2	31.5	89.9	99.5	0.90
062	21.1	F	25.4	33.8	84.6	108.9	0.78
063	23.1	F	26.0	36.2	95.8	109.0	0.88
DISC044	39.0	F	29.6	N/A	89.6	115.8	0.77
DISC089	30.0	F	22.4	N/A	78.1	98.0	0.80
DISC016	40.0	F	25.2	N/A	85.1	100.5	0.85
DISC032	54.0	F	26.1	N/A	89.2	93.9	0.95
DISC073	41.0	M	25.0	N/A	90.3	98.0	0.92
DISC033	43.0	M	25.0	N/A	87.5	96.8	0.90
DISC072	53.0	M	27.0	N/A	97.3	98.2	0.99

Table 8-4: Full characteristic for each participant of the obese pre- and post-surgery group and non-obese Controls for whom analysis of OXPHOS protein quantification and sequencing of the mtDNA in the colorectal mucosa was conducted.

N. Varying levels of complex I and IV deficiency, calculated using z-scores, within and obese pre-surgery participant

O. Coverage map of fragment A and B sequenced in the mitochondrial genome

Figure 8-1: Example coverage map of fragment A (shown in orange) and B (shown in blue) sequenced in an obese pre-surgery participant. The flat blue line illustrates that fragment B was not sequenced.
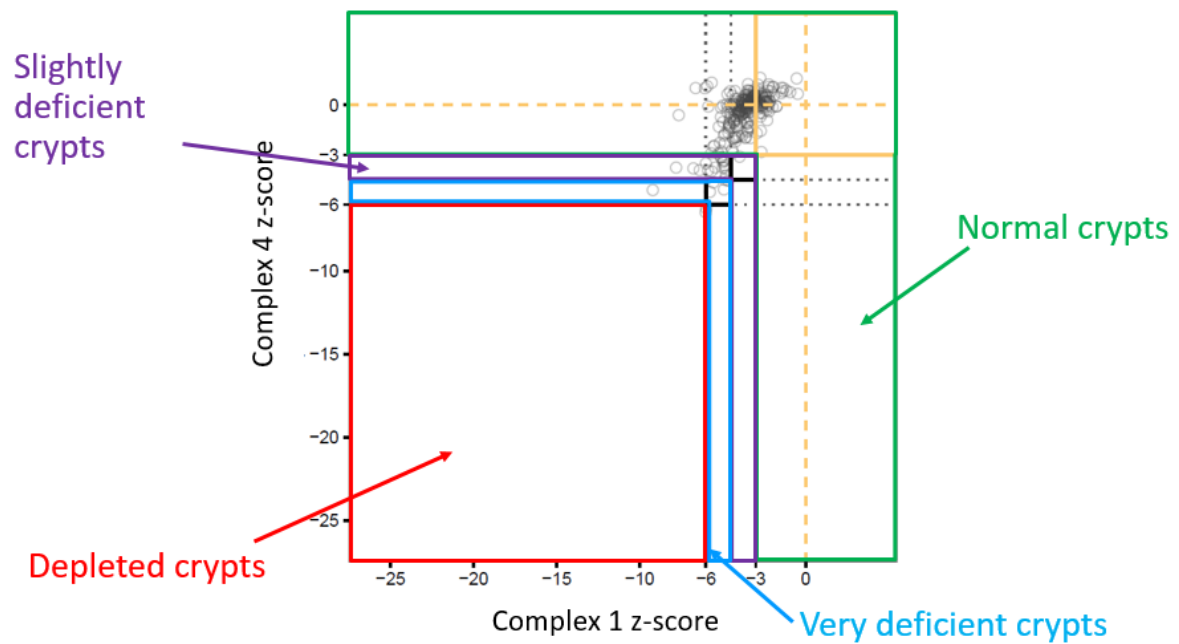
P. Untransformed data of mutation frequency in obese pre-surgery individuals and non-obese Controls
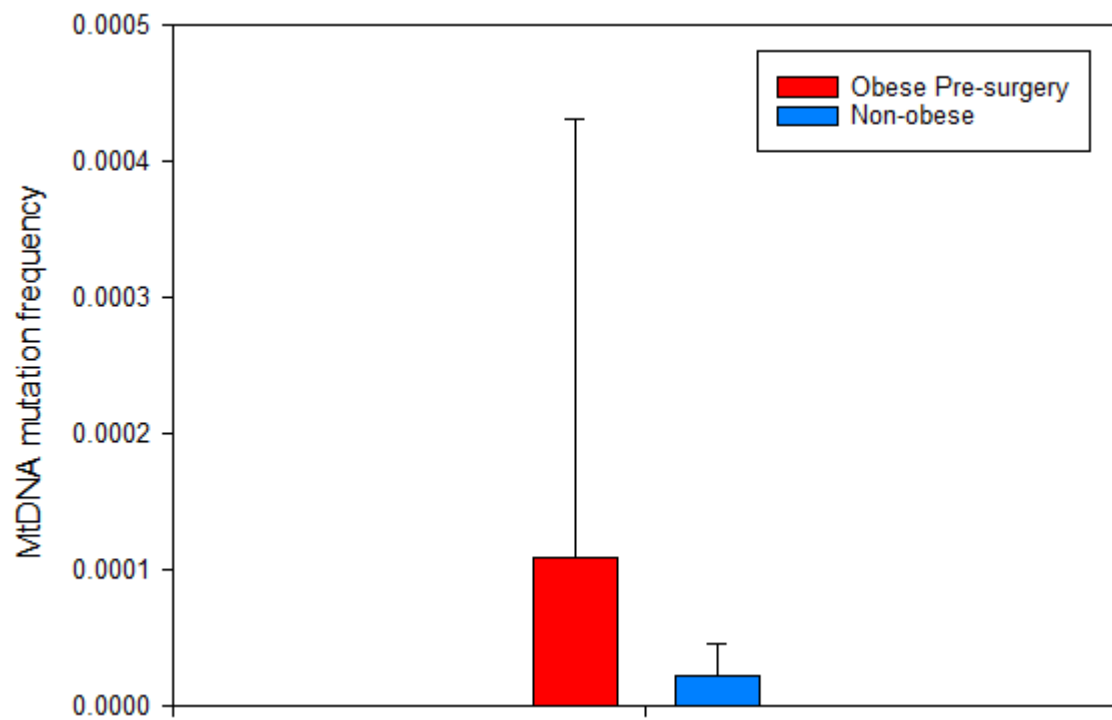
Figure 8-2: Frequency of mtDNA mutations detected by NGS in the colorectal mucosa of obese pre-surgery participants and non-obese Controls (p=0.514 by Mann Whitney U test).

Q. Untransformed data of mutation frequency in pre- and post-surgery individuals
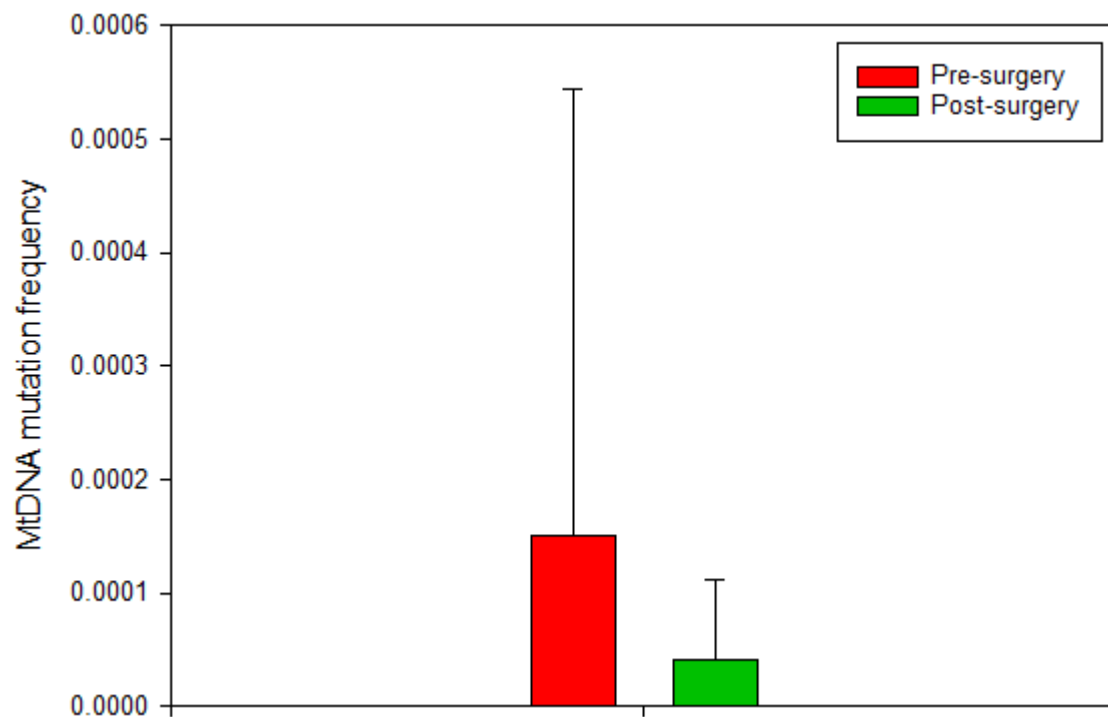
Figure 8-3: Frequency of mtDNA mutations detected by NGS in the colorectal mucosa of obese pre- and post-surgery participants (p=0.213 by Wilcoxon Signed Rank test).

R. Untransformed data of mtDNA mutation frequency across the BMI range in all study groups, BOCABS: pre- and post-surgery and non-obese controls
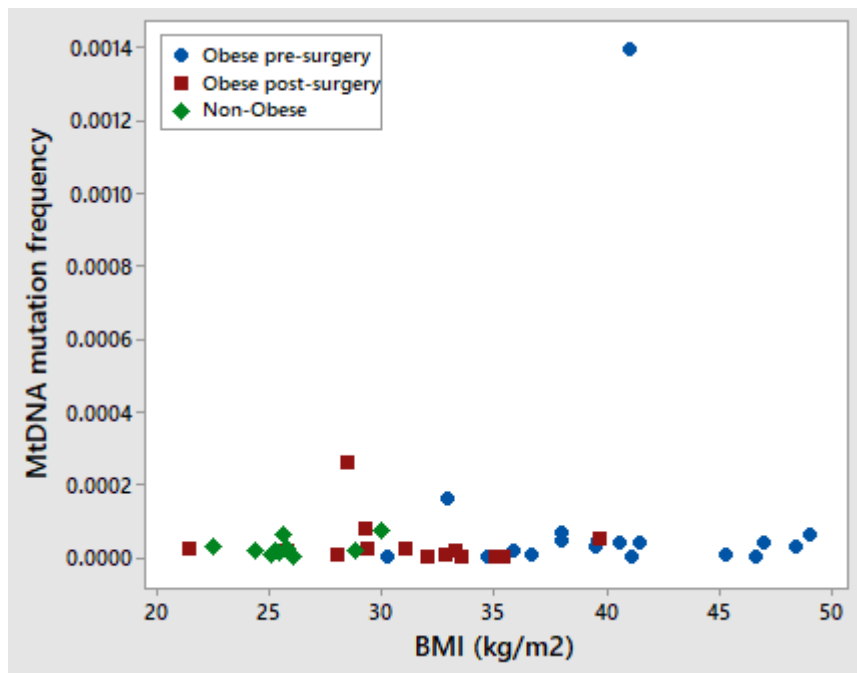
Figure 8-4: MtDNA mutations frequency detected by NGS in the colorectal mucosa across the BMI range for each initially obese pre- and post-surgery and non-obese Control individual.
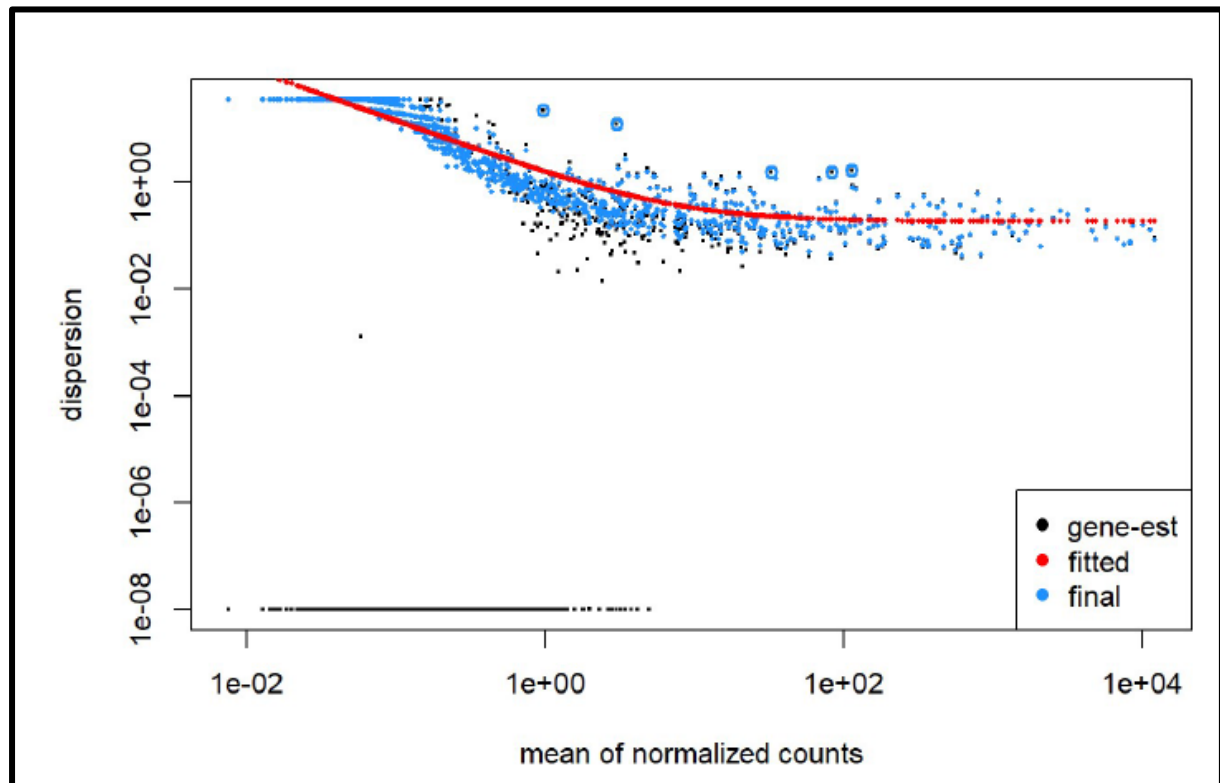
Figure 8-5: Plotted normalised miRNA counts for all participants included in this analysis, gene-est/ black dots: miRNA estimation of the typical relationship between its variance and mean by considering the information for each miRNA separately; fitted/ red dots: fitted dispersion values of miRNA counts dependent on the mean; final/ blue dots: final dispersion value chosen for each miRNA between the 'gene-est' and 'fitted', i.e. miRNAs counts shrunk towards the fitted trend line.

T.   List of total miRNAs (n=1654 in numerical ascending order) identified in Next Generation Sequencing

Mir-1-3p, mir-1-5p, mir-7-5p, mir-7-1-3p, mir-9-5p, mir-9-3p, mir-16-5p, mir-16-2-3p, mir-16-1-3p, mir-17-3p, mir-17-5p, mir-21-5p, mir-21-3p, mir-22-3p, mir-22-5p, mir-24-1-5p, mir-24-3p, mir-24-2-5p, mir-25-5p, mir-25-3p, mir-28-3p, mir-28-5p, mir-31-5p, mir-31-3p, mir-32-5p, mir-32-3p, mir-93-5p, mir-93-3p, mir-95-3p, mir-95-5p, mir-96-5p, mir-96-3p, mir-98-5p, mir-98-3p, mir-100-5p, mir-101-3p, mir-101-5p, mir-105-5p, mir-105-3p, mir-107, mir-122-5p, mir-124-3p, mir-124-5p, mir-126-5p, mir-126-3p, mir-127-5p, mir-127-3p, mir-128-3p, mir-128-2-5p, mir-128-1-5p, mir-129-5p, mir-129-2-3p, mir-129-1-3p, mir-132-3p, mir-132-5p, mir-134-5p, mir-134-3p, mir-136-3p, mir-136-5p, mir-137, mir-138-5p, mir-138-1-3p, mir-

138-2-3p, mir-139-5p, mir-139-3p, mir-140-5p, mir-140-3p, mir-141-5p, mir-141-3p, mir-142-3p, mir-142-5p, mir-143-3p, mir-143-5p, mir-144-5p, mir-144-3p, mir-145-5p, mir-145-3p, mir-149-5p, mir-149-3p, mir-150-3p, mir-150-5p, mir-152-5p, mir-152-3p, mir-153-3p, mir-153-5p, mir-154-5p, mir-154-3p, mir-155-5p, mir-182-5p, mir-182-3p, mir-183-5p, mir-183-3p, mir-184, mir-185-5p, mir-185-3p, mir-186-5p, mir-187-5p, mir-187-3p, mir-188-5p, mir-188-3p, mir-191-5p, mir-191-3p, mir-192-3p, mir-192-5p, mir-194-5p, mir-194-3p, mir-195-5p, mir-195-3p, mir-197-3p, mir-197-5p, mir-202-3p, mir-204-5p, mir-204-3p, mir-205-5p, mir-206, mir-210-3p, mir-210-5p, mir-211-5p, mir-211-3p, mir-212-3p, mir-212-5p, mir-214-5p, mir-214-3p, mir-215-5p, mir-215-3p, mir-217, mir-218-5p, mir-218-1-3p, mir-221-3p, mir-221-5p, mir-222-3p, mir-222-5p, mir-223-3p, mir-223-5p, mir-224-5p, mir-224-3p, mir-296-3p, mir-296-5p, mir-298, mir-299-3p, mir-299-5p, mir-324-5p, mir-324-3p, mir-326, mir-328-3p, mir-329-3p, mir-329-5p, mir-330-5p, mir-330-3p, mir-331-3p, mir-331-5p, mir-335-3p, mir-335-5p, mir-337-3p, mir-337-5p, mir-338-3p, mir-338-5p, mir-339-3p, mir-339-5p, mir-340-5p, mir-340-3p, mir-342-3p, mir-342-5p, mir-345-5p, mir-345-3p, mir-346, mir-361-3p, mir-361-5p, mir-362-5p, mir-363-3p, mir-363-5p, mir-369-5p, mir-369-3p, mir-370-3p, mir-370-5p, mir-372-3p, mir-375, mir-377-5p, mir-377-3p, mir-379-5p, mir-379-3p, mir-381-3p, mir-381-5p, mir-382-5p, mir-382-3p, mir-383-5p, mir-409-5p, mir-409-3p, mir-410-3p, mir-410-5p, mir-411-5p, mir-411-3p, mir-412-5p, mir-412-3p, mir-421, mir-423-3p, mir-423-5p, mir-424-5p, mir-424-3p, mir-425-3p, mir-425-5p, mir-429, mir-431-3p, mir-431-5p, mir-432-5p, mir-433-3p, mir-448, mir-452-5p, mir-452-3p, mir-454-3p, mir-454-5p, mir-455-3p, mir-455-5p, mir-466, mir-483-3p, mir-483-5p, mir-484, mir-485-3p, mir-485-5p, mir-486-3p, mir-486-5p, mir-489-3p, mir-490-3p, mir-490-5p, mir-491-5p, mir-492, mir-493-5p, mir-493-3p, mir-494-3p, mir-494-5p, mir-495-3p, mir-495-5p, mir-496, mir-497-5p, mir-497-3p, mir-501-5p, mir-501-3p, mir-502-3p, mir-502-5p, mir-503-5p, mir-503-3p, mir-504-5p, mir-504-3p, mir-505-3p, mir-505-5p, mir-506-3p, mir-508-5p, mir-508-3p, mir-509-3-5p, mir-509-3p, mir-511-5p, mir-511-3p, mir-521, mir-522-5p, mir-522-3p, mir-532-5p, mir-532-3p, mir-539-5p, mir-539-3p, mir-541-3p, mir-541-5p, mir-542-3p, mir-543, mir-545-5p, mir-552-5p, mir-552-3p, mir-553, mir-555, mir-556-5p, mir-557, mir-558, mir-559, mir-562, mir-564, mir-566, mir-567, mir-571, mir-572, mir-574-3p, mir-574-5p, mir-575, mir-576-5p, mir-576-3p, mir-577, mir-578, mir-579-5p, mir-580-3p, mir-581, mir-582-3p, mir-582-5p, mir-584-5p, mir-584-3p, mir-585-3p, mir-587, mir-588, mir-589-5p, mir-589-3p, mir-590-3p, mir-591, mir-592, mir-595, mir-597-3p, mir-598-3p, mir-598-5p, mir-599, mir-600, mir-601, mir-602, mir-605-3p,

mir-605-5p, mir-607, mir-612, mir-614, mir-615-3p, mir-616-3p, mir-616-5p, mir-618, mir-619-5p, mir-620, mir-621, mir-622, mir-624-3p, mir-624-5p, mir-625-3p, mir-625-5p, mir-627-5p, mir-627-3p, mir-628-3p, mir-628-5p, mir-629-5p, mir-629-3p, mir-632, mir-635, mir-636, mir-638, mir-639, mir-641, mir-643, mir-645, mir-646, mir-647, mir-648, mir-649, mir-650, mir-651-5p, mir-651-3p, mir-652-3p, mir-652-5p, mir-653-5p, mir-653-3p, mir-654-3p, mir-654-5p, mir-655-5p, mir-655-3p, mir-656-5p, mir-656-3p, mir-658, mir-659-5p, mir-660-5p, mir-660-3p, mir-662, mir-665, mir-668-5p, mir-668-3p, mir-670-5p, mir-671-3p, mir-671-5p, mir-675-3p, mir-675-5p, mir-676-3p, mir-676-5p, mir-708-3p, mir-708-5p, mir-744-5p, mir-744-3p, mir-758-3p, mir-760, mir-762, mir-765, mir-766-5p, mir-766-3p, mir-767-5p, mir-769-3p, mir-769-5p, mir-770-5p, mir-802, mir-873-3p, mir-873-5p, mir-874-3p, mir-874-5p, mir-876-3p, mir-877-3p, mir-877-5p, mir-885-5p, mir-887-3p, mir-887-5p, mir-889-5p, mir-889-3p, mir-920, mir-922, mir-924, mir-933, mir-935, mir-937-3p, mir-939-5p, mir-939-3p, mir-940, mir-941, mir-942-5p, mir-942-3p, mir-943, mir-944, mir-1179, mir-1180-3p, mir-1181, mir-1185-1-3p, mir-1185-2-3p, mir-1199-5p, mir-1199-3p, mir-1202, mir-1203, mir-1205, mir-1224-5p, mir-1224-3p, mir-1225-3p, mir-1225-5p, mir-1226-3p, mir-1226-5p, mir-1228-3p, mir-1228-5p, mir-1229-3p, mir-1229-5p, mir-1231, mir-1233-5p, mir-1234-3p, mir-1236-5p, mir-1237-5p, mir-1237-3p, mir-1243, mir-1244, mir-1246, mir-1247-3p, mir-1247-5p, mir-1248, mir-1249-3p, mir-1249-5p, mir-1250-5p, mir-1251-5p, mir-1252-5p, mir-1253, mir-1254, mir-1258, mir-1261, mir-1262, mir-1265, mir-1266-5p, mir-1266-3p, mir-1267, mir-1270, mir-1271-5p, mir-1272, mir-1275, mir-1276, mir-1277-3p, mir-1278, mir-1284, mir-1285-5p, mir-1285-3p, mir-1286, mir-1287-5p, mir-1288-3p, mir-1289, mir-1290, mir-1291, mir-1292-5p, mir-1293, mir-1294, mir-1296-5p, mir-1296-3p, mir-1297, mir-1298-5p, mir-1299, mir-1301-3p, mir-1302, mir-1303, mir-1304-5p, mir-1304-3p, mir-1306-3p, mir-1306-5p, mir-1307-5p, mir-1307-3p, mir-1321, mir-1324, mir-1343-3p, mir-1343-5p, mir-1468-5p, mir-1469, mir-1537-3p, mir-1538, mir-1587, mir-1825, mir-1827, mir-1908-5p, mir-1909-3p, mir-1909-5p, mir-1910-5p, mir-1911-5p, mir-1913 mir-1914-5p, mir-1915-3p, mir-1972, mir-1973, mir-1976, mir-2053, mir-2110, mir-2113, mir-2116-3p, mir-2117, mir-2276-3p, mir-2277-5p, mir-2277-3p, mir-2278, mir-2355-3p, mir-2355-5p, mir-2681-5p, mir-2682-3p, mir-2682-5p, mir-2861, mir-3064-5p, mir-3065-5p, mir-3065-3p, mir-3074-5p, mir-3074-3p, mir-3115, mir-3116, mir-3117-3p, mir-3120-5p, mir-3122, mir-3123, mir-3124-5p, mir-3125, mir-3126-5p, mir-3127-5p, mir-3127-3p, mir-3128, mir-3129-3p, mir-3130-3p, mir-3130-5p, mir-3131, mir-3133, mir-3134, mir-3136-5p, mir-3137, mir-3138, mir-3139, mir-3140-3p, mir-

3144-3p, mir-3146, mir-3147, mir-3149, mir-3151-3p, mir-3152-5p, mir-3152-3p, mir-3154, mir-3157-5p, mir-3157-3p, mir-3158-3p, mir-3158-5p, mir-3159, mir-3160-3p, mir-3161, mir-3162-3p, mir-3162-5p, mir-3164, mir-3166, mir-3167, mir-3168, mir-3170, mir-3173-5p, mir-3173-3p, mir-3174, mir-3176, mir-3177-3p, mir-3177-5p, mir-3178, mir-3179, mir-3180-5p, mir-3180-3p, mir-3181, mir-3182, mir-3183, mir-3185, mir-3187-3p, mir-3187-5p, mir-3188, mir-3190-3p, mir-3190-5p, mir-3191-3p, mir-3191-5p, mir-3192-5p, mir-3193, mir-3194-5p, mir-3194-3p, mir-3195, mir-3196, mir-3198, mir-3199, mir-3200-3p, mir-3200-5p, mir-3202, mir-3529-5p, mir-3591-5p, mir-3605-5p, mir-3605-3p, mir-3606-3p, mir-3607-3p, mir-3607-5p, mir-3609, mir-3610, mir-3611, mir-3613-5p, mir-3613-3p, mir-3614-5p, mir-3614-3p, mir-3615, mir-3617-5p, mir-3619-5p, mir-3619-3p, mir-3620-5p, mir-3620-3p, mir-3646, mir-3648, mir-3651, mir-3652, mir-3653-5p, mir-3653-3p, mir-3654, mir-3655, mir-3656, mir-3658, mir-3659, mir-3660, mir-3661, mir-3663-3p, mir-3663-5p, mir-3664-5p, mir-3664-3p, mir-3665, mir-3667-5p, mir-3667-3p, mir-3674, mir-3675-5p, mir-3675-3p, mir-3678-5p, mir-3679-5p, mir-3679-3p, mir-3681-5p, mir-3684, mir-3687, mir-3688-5p, mir-3688-3p, mir-3690, mir-3691-5p, mir-3691-3p, mir-3907, mir-3908, mir-3909, mir-3910, mir-3911, mir-3912-3p, mir-3913-5p, mir-3915, mir-3916, mir-3917, mir-3918, mir-3922-3p, mir-3925-5p, mir-3925-3p, mir-3928-3p, mir-3929, mir-3934-5p, mir-3934-3p, mir-3936, mir-3938, mir-3939, mir-3940-3p, mir-3940-5p, mir-3941, mir-3944-5p, mir-3944-3p, mir-3960, mir-3974, mir-3976, mir-3977, mir-3978, mir-4251, mir-4258, mir-4259, mir-4265, mir-4266, mir-4267, mir-4269, mir-4273, mir-4274, mir-4277, mir-4279, mir-4283, mir-4284, mir-4286, mir-4289, mir-4291, mir-4292, mir-4295, mir-4296, mir-4301, mir-4304, mir-4306, mir-4309, mir-4311, mir-4313, mir-4314, mir-4317, mir-4318, mir-4319, mir-4321, mir-4322, mir-4323, mir-4324, mir-4325, mir-4326, mir-4328, mir-4330, mir-4417, mir-4418, mir-4421, mir-4422, mir-4423-5p, mir-4425, mir-4426, mir-4429, mir-4430, mir-4431, mir-4437, mir-4440, mir-4442, mir-4443, mir-4444, mir-4446-3p, mir-4447, mir-4448, mir-4449, mir-4450, mir-4452, mir-4453, mir-4454, mir-4456, mir-4458, mir-4459, mir-4460, mir-4461, mir-4463, mir-4466, mir-4467, mir-4469, mir-4472, mir-4473, mir-4474-3p, mir-4478, mir-4479, mir-4482-5p, mir-4482-3p, mir-4484, mir-4485-5p, mir-4485-3p, mir-4487, mir-4488, mir-4489, mir-4491, mir-4492, mir-4496, mir-4497, mir-4498, mir-4500, mir-4502, mir-4504, mir-4505, mir-4506, mir-4507, mir-4508, mir-4510, mir-4511, mir-4512, mir-4515, mir-4516, mir-4517, mir-4518, mir-4519, mir-4520-5p, mir-4520-2-3p, mir-4521, mir-4522, mir-4523, mir-4525, mir-4527, mir-4529-3p, mir-4529-5p, mir-4531, mir-4532, mir-4533, mir-4536-5p, mir-4537, mir-4538, mir-4539, mir-

4632-3p, mir-4634, mir-4635, mir-4636, mir-4637, mir-4638-3p, mir-4638-5p, mir-4639-5p, mir-4640-5p, mir-4640-3p, mir-4642, mir-4645-3p, mir-4646-5p, mir-4646-3p, mir-4647, mir-4648, mir-4649-5p, mir-4650-3p, mir-4651, mir-4654, mir-4656, mir-4657, mir-4660, mir-4661-5p, mir-4664-3p, mir-4664-5p, mir-4665-5p, mir-4667-3p, mir-4667-5p, mir-4668-5p, mir-4669, mir-4671-5p, mir-4672, mir-4673, mir-4674, mir-4675, mir-4676-3p, mir-4676-5p, mir-4677-3p, mir-4680-3p, mir-4680-5p, mir-4681, mir-4683, mir-4684-3p, mir-4684-5p, mir-4685-3p, mir-4686, mir-4687-3p, mir-4687-5p, mir-4688, mir-4689, mir-4690-5p, mir-4690-3p, mir-4697-3p, mir-4698, mir-4700-5p, mir-4701-5p, mir-4701-3p, mir-4703-3p, mir-4706, mir-4707-5p, mir-4707-3p, mir-4708-3p, mir-4709-5p, mir-4709-3p, mir-4710, mir-4713-5p, mir-4715-3p, mir-4715-5p, mir-4716-3p, mir-4717-3p, mir-4721, mir-4723-5p, mir-4723-3p, mir-4724-5p, mir-4724-3p, mir-4725-5p, mir-4726-5p, mir-4728-3p, mir-4728-5p, mir-4730, mir-4731-3p, mir-4731-5p, mir-4732-3p, mir-4732-5p, mir-4736, mir-4737, mir-4738-3p, mir-4739, mir-4740-5p, mir-4741, mir-4742-3p, mir-4745-5p, mir-4746-5p, mir-4747-3p, mir-4748, mir-4750-5p, mir-4751, mir-4752, mir-4753-3p, mir-4755-5p, mir-4755-3p, mir-4756-3p, mir-4757-3p, mir-4758-5p, mir-4758-3p, mir-4761-3p, mir-4762-3p, mir-4763-5p, mir-4764-5p, mir-4767, mir-4768-5p, mir-4772-3p, mir-4772-5p, mir-4773, mir-4774-5p, mir-4777-3p, mir-4778-5p, mir-4780, mir-4781-3p, mir-4782-5p, mir-4783-5p, mir-4784, mir-4785, mir-4787-5p, mir-4787-3p, mir-4788, mir-4790-3p, mir-4791, mir-4792, mir-4795-3p, mir-4796-5p, mir-4797-3p, mir-4797-5p, mir-4799-5p, mir-4800-3p, mir-4800-5p, mir-4802-5p, mir-4804-5p, mir-4999-5p, mir-5000-3p, mir-5001-3p, mir-5001-5p, mir-5002-3p, mir-5003-3p, mir-5004-3p, mir-5006-3p, mir-5007-5p, mir-5008-3p, mir-5009-3p, mir-5009-5p, mir-5010-3p, mir-5010-5p, mir-5047, mir-5087, mir-5088-3p, mir-5088-5p, mir-5089-3p, mir-5089-5p, mir-5090, mir-5091, mir-5092, mir-5095, mir-5096, mir-5100, mir-5187-5p, mir-5187-3p, mir-5188, mir-5189-5p, mir-5189-3p, mir-5191, mir-5193, mir-5196-3p, mir-5571-3p, mir-5571-5p, mir-5572, mir-5581-3p, mir-5582-3p, mir-5585-3p, mir-5587-3p, mir-5588-5p, mir-5588-3p, mir-5680, mir-5682, mir-5684, mir-5685, mir-5687, mir-5689, mir-5690, mir-5691, mir-5693, mir-5695, mir-5696, mir-5697, mir-5698, mir-5699-3p, mir-5699-5p, mir-5701, mir-5702, mir-5703, mir-5706, mir-5707, mir-5708, mir-5739, mir-5787, mir-6070, mir-6071, mir-6073, mir-6078, mir-6080, mir-6081, mir-6083, mir-6085, mir-6087, mir-6089, mir-6124, mir-6125, mir-6126, mir-6127, mir-6128, mir-6129, mir-6130, mir-6131, mir-6132, mir-6133, mir-6134, mir-6165, mir-6500-3p, mir-6501-5p, mir-6501-3p, mir-6502-5p, mir-6503-3p, mir-6503-5p, mir-6504-5p, mir-6505-5p, mir-6506-5p, mir-6507-5p, mir-6509-5p, mir-

6509-3p, mir-6510-3p, mir-6510-5p, mir-6512-5p, mir-6513-5p, mir-6513-3p, mir-6514-3p, mir-6514-5p, mir-6515-5p, mir-6516-5p, mir-6516-3p, mir-6716-3p, mir-6716-5p, mir-6718-5p, mir-6719-3p, mir-6720-3p, mir-6720-5p, mir-6721-5p, mir-6723-5p, mir-6724-5p, mir-6726-3p, mir-6727-5p, mir-6728-5p, mir-6729-5p, mir-6730-3p, mir-6730-5p, mir-6731-5p, mir-6732-3p, mir-6733-3p, mir-6734-3p, mir-6734-5p, mir-6735-5p, mir-6735, mir-6736-5p, mir-6737-3p, mir-6738-5p, mir-6739-5p, mir-6740-5p, mir-6741-5p, mir-6741-3p, mir-6743-3p, mir-6744-5p, mir-6744-3p, mir-6745, mir-6746-5p, mir-6747-3p, mir-6749-3p, mir-6750-3p, mir-6750-5p, mir-6751-3p, mir-6751-5p, mir-6752-3p, mir-6753-3p, mir-6754-3p, mir-6754-5p, mir-6755-5p, mir-6756-5p, mir-6757-5p, mir-6758-5p, mir-6759-5p, mir-6760-5p, mir-6761-5p, mir-6762-3p, mir-6762-5p, mir-6763-5p, mir-6763-3p, mir-6764-5p, mir-6765-5p, mir-6765-3p, mir-6766-3p, mir-6766-5p, mir-6770-3p, mir-6771-5p, mir-6772-3p, mir-6773-5p, mir-6774-3p, mir-6774-5p, mir-6775-3p, mir-6775-5p, mir-6776-5p, mir-6777-5p, mir-6779-5p, mir-6783-5p, mir-6785-5p, mir-6785-3p, mir-6786-3p, mir-6786-5p, mir-6787-3p, mir-6787-5p, mir-6788-3p, mir-6788-5p, mir-6789-3p, mir-6789-5p, mir-6791-3p, mir-6791-5p, mir-6792-5p, mir-6793-5p, mir-6793-3p, mir-6796-5p, mir-6797-3p, mir-6799-3p, mir-6800-5p, mir-6800-3p, mir-6801-5p, mir-6802-3p, mir-6803-3p, mir-6803-5p, mir-6805-5p, mir-6806-3p, mir-6807-5p, mir-6808-3p, mir-6808-5p, mir-6809-5p, mir-6809-3p, mir-6810-5p, mir-6810-3p, mir-6811-5p, mir-6812-5p, mir-6813-3p, mir-6813-5p, mir-6814-3p, mir-6815-5p, mir-6816-3p, mir-6817-3p, mir-6818-5p, mir-6820-5p, mir-6820-3p, mir-6821-5p, mir-6821-3p, mir-6824-5p, mir-6825-3p, mir-6826-5p, mir-6827-3p, mir-6827-5p, mir-6829-3p, mir-6829-5p, mir-6831-5p, mir-6832-5p, mir-6833-3p, mir-6834-5p, mir-6836-3p, mir-6837-3p, mir-6840-5p, mir-6842-3p, mir-6842-5p, mir-6843-3p, mir-6844, mir-6845-3p, mir-6846-5p, mir-6847-5p, mir-6848-3p, mir-6848-5p, mir-6850-5p, mir-6851-5p, mir-6852-3p, mir-6852-5p, mir-6853-3p, mir-6854-5p, mir-6855-5p, mir-6858-5p, mir-6858-3p, mir-6859-3p, mir-6859-5p, mir-6860, mir-6861-3p, mir-6865-3p, mir-6865-5p, mir-6866-5p, mir-6867-5p, mir-6868-3p, mir-6869-5p, mir-6871-5p, mir-6873-3p, mir-6874-3p, mir-6875-5p, mir-6875-3p, mir-6876-5p, mir-6876-3p, mir-6877-5p, mir-6879-5p, mir-6879-3p, mir-6880-5p, mir-6881-3p, mir-6881-5p, mir-6882-3p, mir-6883-5p, mir-6884-3p, mir-6884-5p, mir-6886-5p, mir-6886-3p, mir-6887-5p, mir-6887-3p, mir-6890-3p, mir-6891-5p, mir-6892-3p, mir-6892-5p, mir-6893-3p, mir-6894-3p, mir-6895-3p, mir-7106-3p, mir-7107-5p, mir-7108-3p, mir-7109-3p, mir-7110-3p, mir-7110-5p, mir-7111-5p, mir-7111-3p, mir-7113-5p, mir-7114-5p, mir-7151-5p, mir-7152-3p, mir-7155-3p, mir-7155-5p, mir-7158-3p, mir-7158-5p,

mir-7515, mir-7641, mir-7702, mir-7703, mir-7704, mir-7705, mir-7706, mir-7844-5p, mir-7845-5p, mir-7846-3p, mir-7847-3p, mir-7848-3p, mir-7849-3p, mir-7850-5p, mir-7851-3p, mir-7853-5p, mir-7854-3p, mir-7974, mir-7975, mir-7976, mir-7977, mir-8052, mir-8053, mir-8057, mir-8059, mir-8065, mir-8071, mir-8072, mir-8077, mir-8079, mir-8083, mir-8086, mir-8485, mir-103a-2-5p, mir-103a-3p, mir-103b, mir-106a-5p, mir-106b-3p, mir-106b-5p, mir-10a-3p, mir-10a-5p, mir-10b-5p, mir-10b-3p, mir-1245a, mir-1245b-3p, mir-1245bp, mir-1255a, mir-1255b-5p, mir-125a-5p, mir-125a-3p, mir-125b-2-3p, mir-125b-5p, mir-125b-1-3p, mir-1260a, mir-1260b, mir-1268a, mir-1268b, mir-1269a, mir-1269b, mir-1273a, mir-1273c, mir-1273d, mir-1273e, mir-1273f, mir-1273g-3p, mir-1273g-5p, mir-1273h-5p, mir-1273h-3p, mir-1295a, mir-130a-3p, mir-130a-5p, mir-130b-3p, mir-130b-5p, mir-133a-3p, mir-133a-5p, mir-133b, mir-135a-5p, mir-135a-3p, mir-135b-5p, mir-135b-3p, mir-146a-5p, mir-146a-3p, mir-146b-5p, mir-146b-3p, mir-147a, mir-147b, mir-148a-5p, mir-148a-3p, mir-148b-3p, mir-148b-5p, mir-151a-5p, mir-151a-3p, mir-151b, mir-15a-5p, mir-15b-5p, mir-15b-3p, mir-181a-3p, mir-181a-5p, mir-181a-2-3p, mir-181b-5p, mir-181b-3p, mir-181c-3p, mir-181c-5p, mir-181d-5p, mir-181d-3p, mir-18a-3p, mir-18a-5p, mir-18b-3p, mir-190a-5p, mir-190a-3p, mir-190b, mir-193a-5p, mir-193a-3p, mir-193b-3p, mir-193b-5p, mir-196a-5p, mir-196a-3p, mir-196b-5p, mir-196b-3p, mir-199a-5p, mir-199a-3p, mir-199b-5p, mir-199b-3p, mir-19a-3p, mir-19a-5p, mir-19b-3p, mir-19b-1-5p, mir-200a-5p, mir-200a-3p, mir-200b-5p, mir-200b-3p, mir-200c-3p, mir-200c-5p, mir-203a-3p, mir-203a-5p, mir-203b-3p, mir-20a-5p, mir-20a-3p, mir-20b-5p, mir-20b-3p, mir-216a-3p, mir-216a-5p, mir-216b-5p, mir-219a-1-3p, mir-219a-5p, mir-219a-2-3p, mir-219b-5p, mir-23a-5p, mir-23a-3p, mir-23b-5p, mir-23b-3p, mir-23c, mir-26a-2-3p, mir-26a-5p, mir-26a-1-3p, mir-26b-5p, mir-26b-3p, mir-27a-5p, mir-27a-3p, mir-27b-3p, mir-27b-5p, mir-29a-3p, mir-29a-5p, mir-29b-3p, mir-29b-2-5p, mir-29b-1-5p, mir-29c-5p, mir-29c-3p, mir-301a-5p, mir-301b-5p, mir-30a-5p, mir-30a-3p, mir-30b-5p, mir-30b-3p, mir-30c-2-3p, mir-30c-1-3p, mir-30c-5p, mir-30d-5p, mir-30d-3p, mir-30e-5p, mir-30e-3p, mir-3135a, mir-3135b, mir-3150a-5p, mir-3150b-3p, mir-3150b-5p, mir-3155a, mir-320a, mir-320b, mir-320c, mir-320d, mir-320e, mir-323a-3p, mir-323a-5p, mir-323b-3p, mir-33a-3p, mir-33a-5p, mir-33b-5p, mir-33b-3p, mir-34a-5p, mir-34a-3p, mir-34b-3p, mir-34c-5p, mir-34c-3p, mir-3622a-5p, mir-3622a-3p, mir-3622b-3p, mir-365a-5p, mir-365b-3p, mir-365b-5p, mir-3689b-5p, mir-3689d, mir-3689e, mir-3689f, mir-371b-5p, mir-374a-5p, mir-374a-3p, mir-374b-5p, mir-374c-3p, mir-374c-5p, mir-376a-3p, mir-376a-2-5p, mir-376a-5p, mir-376c-3p, mir-378a-3p, mir-378a-5p, mir-378b, mir-378c, mir-378d, mir-

378e, mir-378f, mir-378g, mir-378h, mir-378i, mir-378j, mir-422a, mir-4419a, mir-4419b, mir-4433a-5p, mir-4433b-5p, mir-4433b-3p, mir-4436a, mir-4436b-3p, mir-4436b-5p, mir-449a, mir-449c-5p, mir-450a-5p, mir-450a-2, mir-450b-5p, mir-451a, mir-451b, mir-4524a-5p, mir-4524a-3p, mir-4659a-3p, mir-4659b-3p, mir-4662a-5p, mir-4666b, mir-487a-5p, mir-487a-3p, mir-487b-3p, mir-487b-5p, mir-499a-5p, mir-499a-3p, mir-500a-3p, mir-500a-5p, mir-500b-5p, mir-500b-3p, mir-513a-5p, mir-513c-3p, mir-513c-5p, mir-514a-3p, mir-516a-3p, mir-517a-3p, mir-517c-3p, mir-519a-3p, mir-519a-5p, mir-519d-3p, mir-519e-5p, mir-520a-3p, mir-520d-5p, mir-520f-3p, mir-520f-5p, mir-526b-5p, mir-544a, mir-544b, mir-548a-3p, mir-548a-5p, mir-548ac, mir-548ad-5p, mir-548ae-5p, mir-548ag, mir-548ah-3p, mir-548ai, mir-548al, mir-548am-3p, mir-548an, mir-548ap-5p, mir-548aq-3p, mir-548ar-3p, mir-548as-5p, mir-548at-5p, mir-548au-5p, mir-548av-3p, mir-548av-5p, mir-548aw, mir-548ax, mir-548ay-5p, mir-548ay-3p, mir-548az-5p, mir-548b-5p, mir-548ba, mir-548bb-3p, mir-548d-3p, mir-548e-3p, mir-548f-3p, mir-548h-5p, mir-548i, mir-548j-5p, mir-548k, mir-548l, mir-548n, mir-548o-3p, mir-548o-5p, mir-548q, mir-548s, mir-548t-5p, mir-548u, mir-548v, mir-548w, mir-548x-5p, mir-548y, mir-548z, mir-549a, mir-550a-3-5p, mir-550a-5p, mir-550a-3p, mir-550b-2-5p, mir-551a, mir-551b-5p, mir-5681a, mir-5692c, mir-642b-5p, mir-642b-3p, mir-6511a-3p, mir-6511a-5p, mir-6511b-3p, mir-663a, mir-663b, mir-664a-5p, mir-664a-3p, mir-664b-3p, mir-664b-5p, mir-6715a-3p, mir-6715b-3p, mir-6769b-3p, mir-6780a-5p, mir-6780b-3p, mir-6780b-5p, mir-891a-5p, mir-892a, mir-892b, mir-892c-3p, mir-92a-3p, mir-92a-1-5p, mir-92b-3p, mir-92b-5p, mir-99a-5p, mir-99a-3p, mir-99b-5p, mir-99b-3p, let-7a-5p, let-7a-3p, let-7a-2-3p, let-7b-5p, let-7b-3p, let-7c-5p, let-7c-3p, let-7d-5p, let-7d-3p, let-7e-5p, let-7e-3p, let-7f-1-3p, let-7f-5p, let-7f-2-3p, let-7g-5p, let-7g-3p, let-7i-3p and let-7i-5p.

U. Heatmaps of sample to sample correlation of raw miRNA counts

(A)

(B)
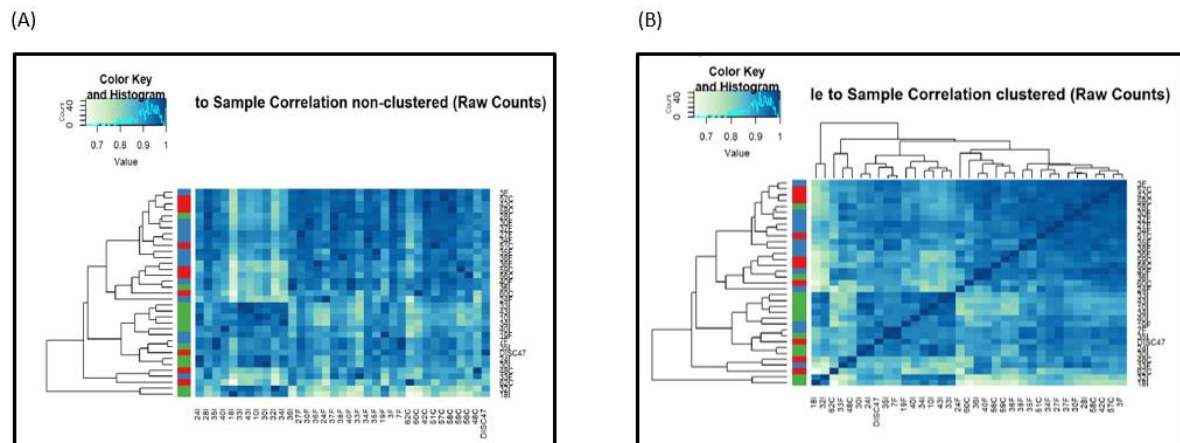
Figure 8-6: (A) Heatmap of non-clustered sample to sample Pearson correlation of raw miRNA counts; (B) Heatmap of clustered sample to sample Pearson correlation of raw miRNA counts (green bars: pre-surgery; blue bars: post-surgery and red bars: non-obese Controls). Clustering is referred to the aggregation of individual participants according to participant group, i.e. pre- and post-surgery and non-obese Controls.

V. Heatmaps of sample to sample correlation of miRNA counts following variance of stabilising transformation (VST) to the miRNA counts

(A)

(B)

Figure 8-7: (A) Heatmap of non-clustered sample to sample Pearson correlation of miRNA count following VST; (B) Heatmap of clustered sample to sample Pearson correlation of miRNA count following VST (green bars: pre-surgery; blue bars: post-surgery and red bars: non-obese Controls). Clustering is referred to the aggregation of individual participants according to participant group, i.e. pre- and post-surgery and non-obese Controls.

W. Heatmaps of sample to sample correlation of miRNA counts after computing the binary logarithms (Log2) to the miRNA counts
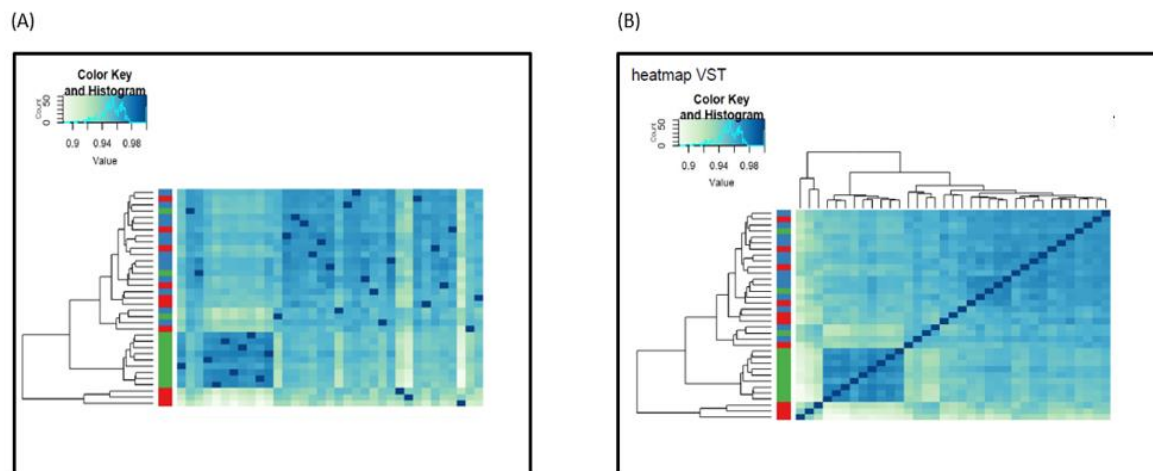

Figure 8-8: (A) Heatmap of clustered sample to sample Pearson correlation of miRNA count after computing Log2; (B) Heatmap of non-clustered sample to sample Pearson correlation of miRNA count after computing Log2 (green bars: pre-surgery; blue bars: post-surgery and red bars: non-obese Controls). Clustering is referred to the aggregation of individual participants according to participant group, i.e. pre- and post-surgery and non-obese Controls.

X. Heatmap of sample to sample correlation of miRNA counts after computing the binary logarithms (Log2) to the miRNA counts
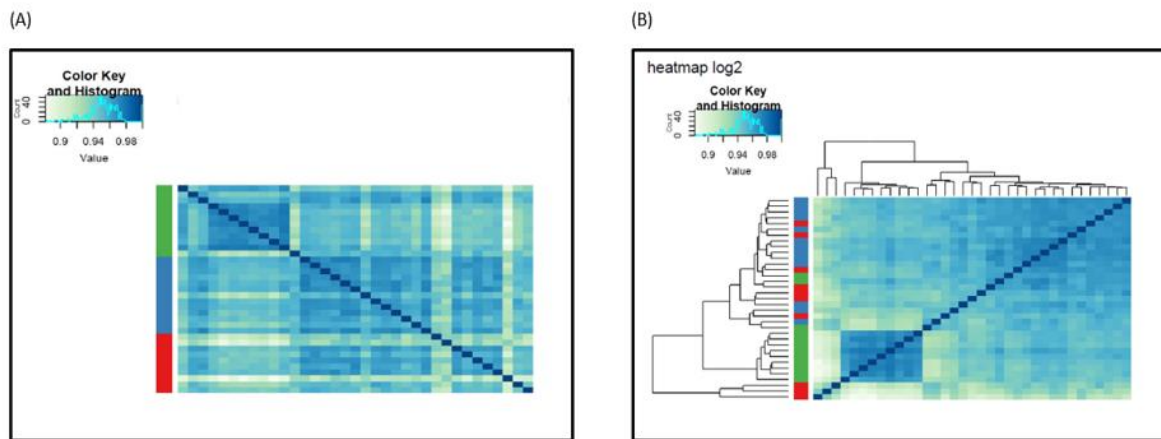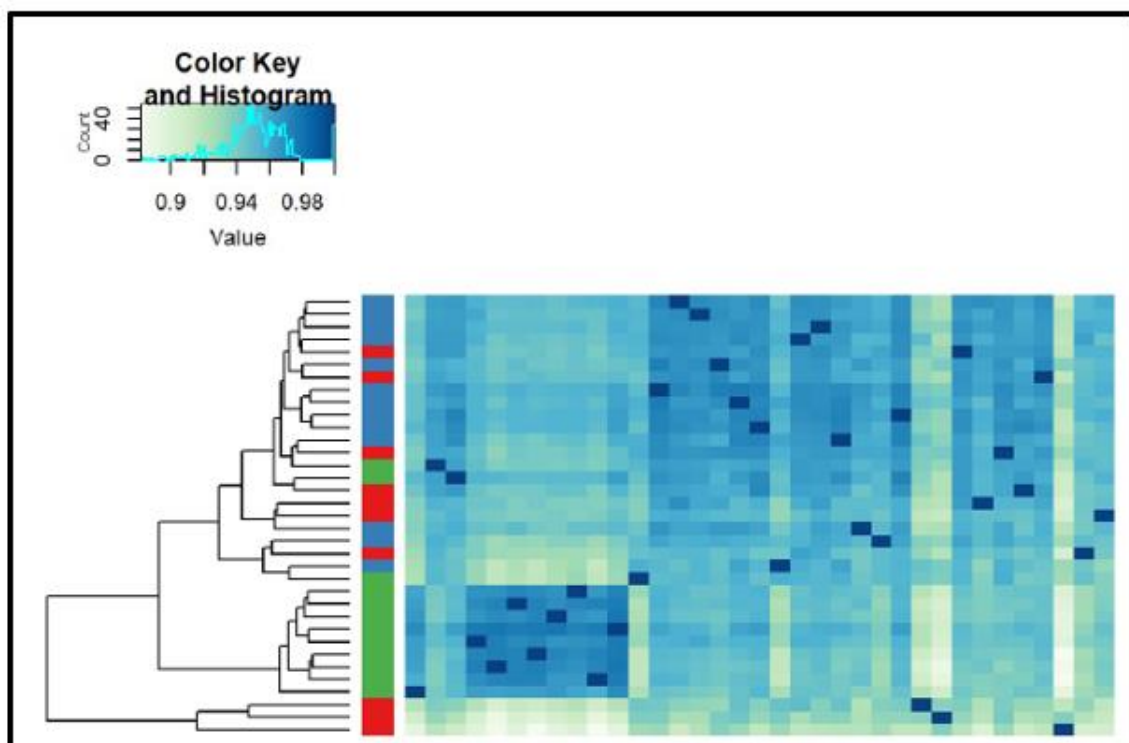

Figure 8-9: Heaptmap of sample to sample Pearson correlation of miRNA count after computing Log2 (green bars: pre-surgery; blue bars: post-surgery and red bars: non-obese Controls).

Y. Heatmaps of top 80 miRNA counts
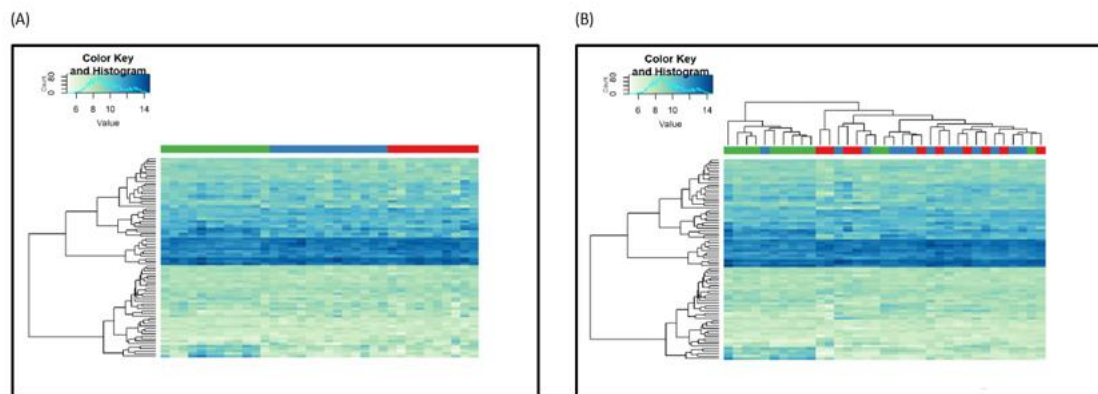
Figure 8-10: (A) Heatmap of top 80 clustered miRNA counts; (B) Heatmap of top 80 non-clustered miRNA counts (green bars: pre-surgery; blue bars: post-surgery and red bars: non-obese Controls) (based on a scoring of values ranging from 4 to 16). Clustering is referred to the aggregation of individual participants according to participant group, i.e. pre- and post-surgery and non-obese Controls.

Z. Heatmaps of top 80 scaled miRNA counts
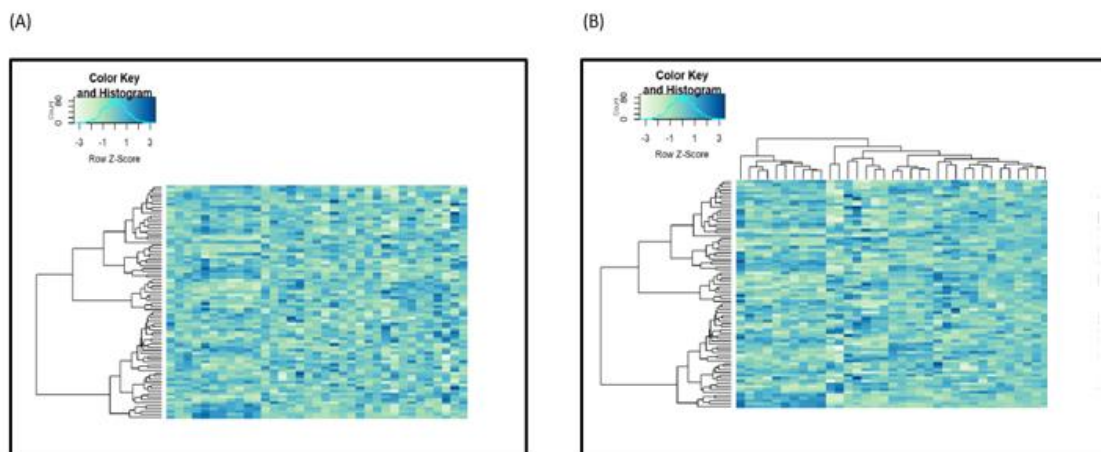
Figure 8-11: (A) Heatmap of top 80 scaled clustered miRNA counts; (B) Heatmap of top 80 scaled and non-clustered miRNA counts (based on a scaled row z-score ranging from -3 to 3). Clustering is referred to the aggregation of individual participants according to participant group, i.e. pre- and post-surgery and non-obese Controls.
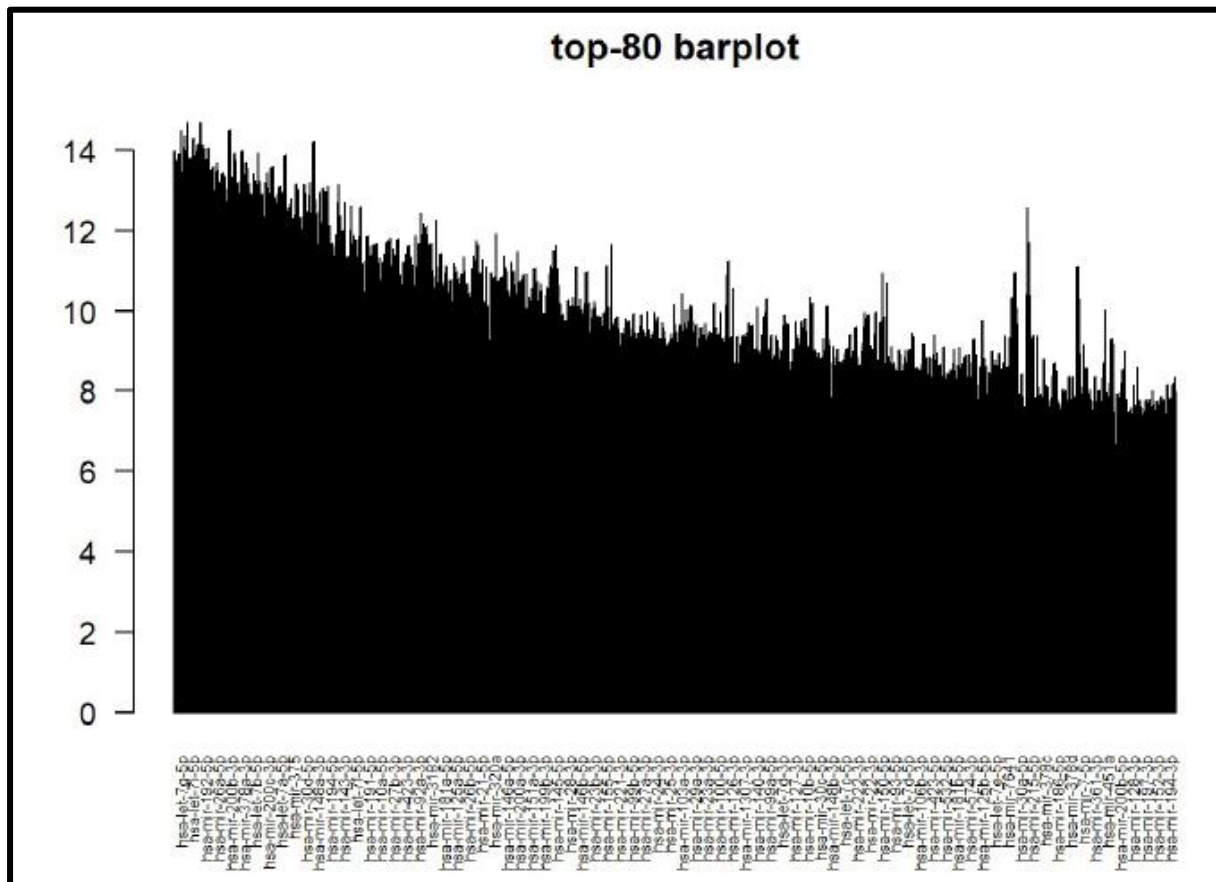
Figure 8-12: Bar plot of the top 80 miRNA counts across pre- and post-RYGB group and non-obese Controls.

BB. List of the miRNAs (n=112 in numerical ascending order) for which abundance differed significantly between the obese pre-RYGB group and the non-obese Controls

Mir-1-3p, mir-7-5p, mir-9-5p, mir-22-3p, mir-24-1, mir-25-5p, mir-28-3p, mir-31-3p, mir-31-5p, mir-126-3p, mir-126-5p, mir-132-3p, mir-140-5p, mir-143-3p, mir-143-5p, mir-145-3p, mir-145-5p, mir-191-5p, mir-194-5p, mir-204-5p, mir-210-3p, mir-210-5p, mir-215-5p-3p, mir-215-3p, mir-223-3p, mir-338-3p, mir-340-5p, mir-342-3p, mir-423-3p, mir-452-5p, mir-455-3p, mir-455-5p, mir-484, mir-486-3p, mir-486-5p, mir-497-5p, mir-543, mir-552-5p, mir-552-3p, mir-566, mir-619-5p, mir-625-3p, mir-652-3p, mir-655-5p, mir-671-3p, mir-671-5p, mir-744-5p, mir-874-3p, mir-887-3p, mir-1247-3p, mir-1247-5p, mir-1248, mir-1253, mir-1262, mir-3127-5p, mir-3196, mir-3648, mir-3656, mir-3665, mir-3960, mir-4284, mir-4429, mir-4446-3p, mir-4459, mir-4473, mir-4497, mir-4516, mir-4709-5p, mir-5096, mir-7851-3p, mir-1268a, mir-1273a, mir-1273c, mir-1273d, mir-1273e, mir-1273f, mir-133a-3p, mir-147b, mir-148a-5p, mir-15b-5p, mir-181a-3p, mir-193b-3p, mir-196a-5p, mir-196b-5p, mir-199b-5p, mir-200a-5p, mir-200b-5p, mir-200b-3p, mir-200c-3p, mir-203a-3p, mir-27b-3p, mir-29a-3p,

mir-29c-5p-5p, mir-29c-3p, mir-30a-5p, mir-30a-3p, mir-30b-5p, mir-30c-2, mir-3135b, mir-3150b-3p, mir-320a, mir-320b, mir-378a-3p, mir-422a, mir-450a-5p, mir-642b-5p, mir-92a-3p, mir-92b-3p, mir-99a-5p, mir-99b-5p, let-7a and let-7d.

CC. Significant miRNA fold change between the pre-RYGB group and the non-obese Controls

Figure 8-13: Volcano plot illustrating significant fold change for the miRNAs (each red dot represents an individual miRNA with its name annotation) which differed in abundance between obese individuals pre-RYGB and non-obese Controls.

DD. Heatmap of clustered significant top 82 miRNAs between the pre-RYGB group and non-obese Controls
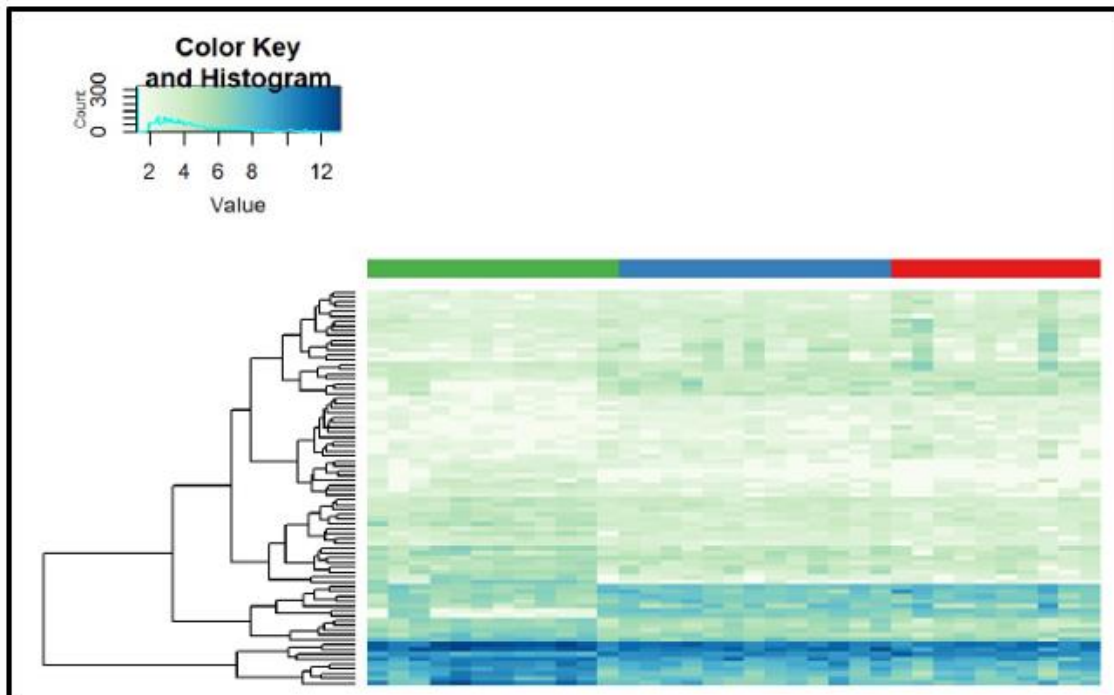
Figure 8-14: Heatmap of the clustered significant top 82 miRNAs between the pre-RYGB group and non-obese Controls for all participants (green bars: pre-surgery; blue bars: post-surgery and red bars: non-obese Controls). Clustering is referred to the aggregation of individual participants according to participant group, i.e. obese pre- and post-RYGB and non-obese Controls.

EE. List of the miRNAs (n=60 in numerical ascending order) for which abundance differed significantly between the initially obese individuals before and after RYGB

Mir-7-5p, mir-9-5p, mir-28-3p, mir-31-5p, mir-31-3p, mir-98-5p, mir-126-5p, mir-126-3p, mir-129-5p, mir-132-3p, mir-185-5p, mir-191-5p, mir-194-5p, mir-204-5p, mir-204-3p, mir-210-3p, mir-215-5p, mir-215-3p, mir-223-3p, mir-335-3p, mir-338-3p, mir-342-3p, mir-421, mir-424-5p, mir-455-3p, mir-552-5p, mir-552-3p, mir-582-5p, mir-652-3p, mir-655-5p, mir-671-3p, mir-671-5p, mir-874-3p, mir-1247-5p, mir-1247-3p, mir-1262, mir-3196, mir-3656, mir-4284, mir-4461, mir-4485-3p, mir-4516, mir-125b-5p, mir-147b, mir-148b-3p, mir-15b-3p, mir-181a-3p, mir-196a-5p, mir-196b-5p, mir-200b-5p, mir-200b-3p, mir-203a-3p, mir-29c-3p, mir-30a-5p, mir-3a-3p, mir-30c-2-3p, mir-3150b-3p, mir-450a-5p, let-7a-3p and mir-892c-3p.

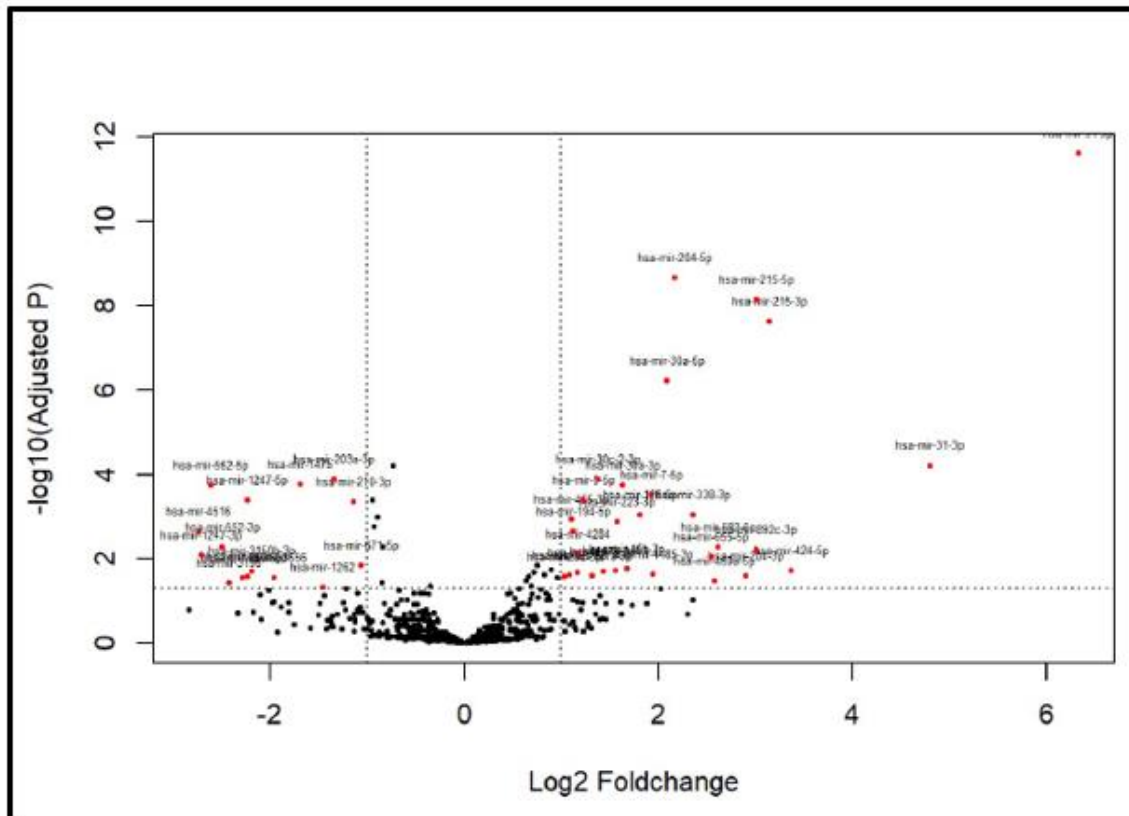*Figure 8-15: Volcano plot illustrating significant fold change for the miRNAs (each red dot represents an individual miRNA with its name annotation) which differed in abundance between obese individuals pre- and post-RYGB.*
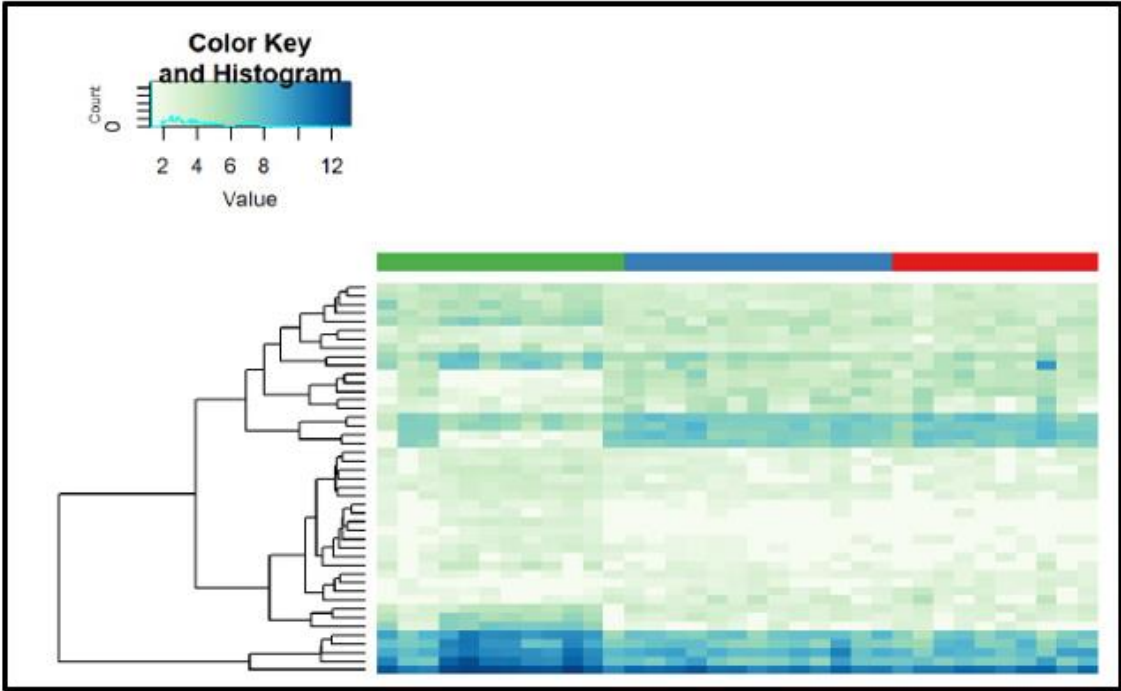
Figure 8-16: Heatmap of the miRNAs, for which expression differed significantly between the obese participants pre- and post-RYGB, for all participants (green bars: obese pre-surgery; blue bars: initially obese post-surgery and red bars: non-obese Controls). Clustering is referred to the aggregation of individual participants according to participant group, i.e. obese pre- and post-RYGB and non-obese Controls.

HH.List of the miRNAs (n=36 in numerical ascending order) for which abundance differed

significantly in both the comparison of i) the obese participants pre-RYGB with non-

obese Controls and ii) the initially obese individuals pre- and post-RYGB and, their

predicted KEGG pathway

Mir-9-5p, mir-31-3p, mir-31-5p, mir-126-5p, mir-126-3p, mir-194-5p, mir-204-5p, mir-210-3p, mir-215-5p, mir-215-3p, mir-223-3p, mir-338-3p, mir-455-3p, mir-552-5p, mir-552-3p, mir-655-5p, mir-671-5p, mir-1247-5p, mir-1247-3p, mir-1262, mir-3196, mir-3656, mir-4284, mir-4516, mir-147b, mir-181a-3p, mir-196a-5p, mir-196b-5p, mir-203a-3p, mir-29c-3p, mir-30a-5p, mir-30a-3p, mir-30c-2-3p, mir-3150b-3p and mir-450a-5p.

The below table shows the predicted KEGG pathways of the identified miRNAs using DIANA Tools by Vlachos (Vlachos, 2015). More specifically, it shows the number of miRNAs (out of the n=36) involved in the specified path way and, the number of genes targeted downstream by those miRNAs. The miRNAs (n=8), which were quantified by qPCR in the current Study were

predicted to be involved in 19 of the 63 pathways shown below, namely: biotin metabolism, bladder cancer, cell cycle, chronic myeloid leukemia, citrate cycle, ECM-receptor interaction, FoxO signaling pathway, glycosaminoglycan biosynthesis - keratan sulfate, hippo signaling pathway, glioma, lysine degradation, melanoma, oocyte meiosis, other types of O-glycan biosynthesis, pantothenate and CoA biosynthesis, p53 signaling pathway, protein processing in endoplasmic reticulum, steroid biosynthesis and 2-Oxocarboxylic acid metabolism.

#	KEGG pathway	p-value	#genes		#miRNAs
1.	ECM-receptor interaction (hsa04512)	9.42769375243e-23	49	see genes	18
2.	Proteoglycans in cancer (hsa05205)	3.23079246328e-15	113	see genes	23
3.	Adherens junction (hsa04520)	1.04332310896e-11	53	see genes	21
4.	Fatty acid biosynthesis (hsa00061)	3.50834950742e-10	7	see genes	10
5.	Viral carcinogenesis (hsa05203)	3.50834950742e-10	106	see genes	21
6.	Pancreatic cancer (hsa05212)	1.63495513009e-09	48	see genes	17
7.	Hepatitis B (hsa05161)	3.61442278537e-09	83	see genes	21
8.	Colorectal cancer (hsa05210)	8.82846605991e-09	46	see genes	18
9.	Chronic myeloid leukemia (hsa05220)	1.76564547642e-08	52	see genes	21
10.	Hippo signaling pathway (hsa04390)	6.15064557973e-08	79	see genes	20
11.	Oocyte meiosis (hsa04114)	9.66240351796e-08	67	see genes	23
12.	Pathways in cancer (hsa05200)	5.53654984813e-07	201	see genes	22
13.	Ubiquitin mediated proteolysis (hsa04120)	8.06434316805e-07	83	see genes	21
14.	Glioma (hsa05214)	1.06188332786e-06	41	see genes	19
15.	Cell cycle (hsa04110)	1.06188332786e-06	75	see genes	21
16.	Protein processing in endoplasmic reticulum (hsa04141)	1.2497854662e-06	96	see genes	23
17.	Renal cell carcinoma (hsa05211)	2.34611807423e-06	45	see genes	17
18.	Lysine degradation (hsa00310)	3.31214930935e-06	28	see genes	17
19.	Small cell lung cancer (hsa05222)	6.5374151537e-06	56	see genes	19
20.	Prostate cancer (hsa05215)	1.16884707304e-05	56	see genes	21
21.	Transcriptional misregulation in cancer (hsa05202)	1.60334039318e-05	92	see genes	22
22.	p53 signaling pathway (hsa04115)	2.21864612468e-05	46	see genes	20
23.	Prion diseases (hsa05020)	3.64886827994e-05	11	see genes	14
24.	Non-small cell lung cancer (hsa05223)	5.71939792774e-05	35	see genes	17
25.	Focal adhesion (hsa04510)	8.06803964235e-05	112	see genes	22
26.	RNA transport (hsa03013)	0.000103571794382	91	see genes	20
27.	Endometrial cancer (hsa05213)	0.000107938665683	34	see genes	19

28.	FoxO signaling pathway (hsa04068)	0.000118529782771	76	see genes	22
29.	Central carbon metabolism in cancer (hsa05230)	0.000328719488368	38	see genes	20
30.	Neurotrophin signaling pathway (hsa04722)	0.000484839271446	68	see genes	19
31.	Steroid biosynthesis (hsa00100)	0.000516318503983	12	see genes	13
32.	Bladder cancer (hsa05219)	0.000561301314104	27	see genes	21
33.	Fatty acid metabolism (hsa01212)	0.000571311844145	20	see genes	15
34.	Sphingolipid signaling pathway (hsa04071)	0.000804642591089	61	see genes	20
35.	HTLV-I infection (hsa05166)	0.000804642591089	133	see genes	23
36.	Thyroid hormone signaling pathway (hsa04919)	0.00086066674884	63	see genes	22
37.	mRNA surveillance pathway (hsa03015)	0.000920882876274	55	see genes	20
38.	Acute myeloid leukemia (hsa05221)	0.0013101884992	34	see genes	18
39.	TGF-beta signaling pathway (hsa04350)	0.00180206005197	40	see genes	19
40.	Progesterone-mediated oocyte maturation (hsa04914)	0.00327186710347	50	see genes	20
41.	TNF signaling pathway (hsa04668)	0.00327949814147	58	see genes	18
42.	Wnt signaling pathway (hsa04310)	0.00402982216188	71	see genes	19
43.	Bacterial invasion of epithelial cells (hsa05100)	0.00402982216188	40	see genes	19
44.	Arrhythmogenic right ventricular cardiomyopathy (ARVC) (hsa05412)	0.00413204970473	33	see genes	20
45.	mTOR signaling pathway (hsa04150)	0.00446568910415	36	see genes	19
46.	Signaling pathways regulating pluripotency of stem cells (hsa04550)	0.00642025659683	67	see genes	20
47.	Nucleotide excision repair (hsa03420)	0.00651081271914	27	see genes	16
48.	Circadian rhythm (hsa04710)	0.00718926231943	20	see genes	19
49.	Epstein-Barr virus infection (hsa05169)	0.00811376950456	101	see genes	21
50.	HIF-1 signaling pathway (hsa04066)	0.0088830863986	55	see genes	20
51.	Apoptosis (hsa04210)	0.00965230477931	47	see genes	19
52.	Toxoplasmosis (hsa05145)	0.0105062110656	61	see genes	20
53.	Melanoma (hsa05218)	0.01986219076	36	see genes	19
54.	Shigellosis (hsa05131)	0.0215086798421	34	see genes	18

55.	Endocytosis (hsa04144)	0.0217756293045	96	see genes	21
56.	Epithelial cell signaling in Helicobacter pylori infection (hsa05120)	0.0228539079365	37	see genes	15
57.	Insulin signaling pathway (hsa04910)	0.0300896435787	70	see genes	22
58.	AMPK signaling pathway (hsa04152)	0.0304188710684	64	see genes	19
59.	Fc gamma R-mediated phagocytosis (hsa04666)	0.0304188710684	47	see genes	19
60.	Regulation of actin cytoskeleton (hsa04810)	0.0304188710684	97	see genes	22
61.	Estrogen signaling pathway (hsa04915)	0.0347651118194	51	see genes	20
62.	Thyroid cancer (hsa05216)	0.0388665857591	17	see genes	17
63.	Vibrio cholerae infection (hsa05110)	0.0417946043738	30	see genes	19

II. CT values for 15 miRNAs obtained using the miRNome array, which showed significant down-regulation with NGS but significant up-regulation using the miRNome array

MiRNA	Ct value pre-surgery	Ct value post-surgery
miR-874-3	27.4	28.4
miR-652-3	26.0	26.9
miR-132-3	26.6	27.4
miR-98-5	26.4	26.9
miR-148b-3	23.2	23.5
miR-129-5	**32.5**	**32.4**
miR-342-3	24.1	24.6
miR-335-3	27.7	28.3
miR-29c-3	20.0	20.4
miR-126-3	21.4	21.9
miR-194-5	18.3	18.5
miR-421	27.6	27.7
miR-9-5	28.8	29.4
miR-181a-3	**31.2**	**31.9**
miR-30c-2-3	**33.2**	**34.0**
let-7a-3	26.5	27.1
miR-223-3	23.5	23.6
miR-30a-3	26.7	27.3
miR-15b-3	27.9	28.2

miR-126-5	21.5	21.8
miR-7-5	23.5	23.7
miR-30a-5	22.3	22.5
miR-204-5	28.8	29.4
miR-338-3	24.4	24.6
miR-450a	**31.5**	**31.5**
miR-582-5	**31.3**	**32.5**
miR-215-5	21.8	22.1
miR-424-5	25.1	25.4
miR-31-5	29.7	**30.0**

Table 8-5: CT values for 15 miRNAs obtained using the miRNome array. These 15 miRNAs were identified by two techniques, the miRNome screening array and NGS, for which a opposite direction for the fold-regulation was observed, i.e. a significant down-regulation with NGS but significant up-regulation using the miRNome array (Afshar, 2016a).